Immunoprofiling of drug-resistant epilepsy with a focus on glutamic acid decarboxylase 65 antibodies

Dr Ronan McGinty

Kellogg College

University of Oxford

Thesis submitted for degree of Doctor of Philosophy

Trinity Term 2021

Department of Clinical Neurosciences

Medical Sciences Division

University of Oxford

Student number 1094596





Abstract

The urgent need to improve therapies for people with drug-resistant epilepsy (DRE) requires improved understanding of the aetiopathophysiology of epilepsy and the mechanisms responsible for pharmacoresistance. Autoantibody-mediated processes may explain DRE in a proportion of cases. Autoantibodies can be detected in people with isolated epilepsy (without encephalitis) but their prevalence rate, associated clinical features and overall clinical significance are unknown. Glutamic acid decarboxylase 65 (GAD65) autoantibodies are the commonest such example described in the literature and GAD65 autoantibody-positive epilepsy is thought to be particularly treatment-resistant. Laboratory techniques for detecting GAD65 autoantibodies are calibrated for the concentrations observed in patients with type 1 diabetes mellitus (T1DM) and it is unclear how well different assays perform at the higher levels of autoantibodies found in autoimmune neurological conditions. It is also unknown whether other immune factors, such as cytokines or lymphocyte subsets, are associated with DRE. Studies of these parameters offer novel potential therapeutic insights.

The aims of this work were to:

- estimate the prevalence of serum autoantibodies in epilepsy, and search for distinguishing clinical and paraclinical features of seropositive patients;
- develop and optimise a novel cell-based assay (CBA) for the detection of GAD65 IgG autoantibodies in neurological conditions;
- apply the novel CBA to cohort screening to identify DRE patients with GAD65 autoantibodies for clinical phenotyping;

- characterise plasma cytokine profiles and immunocellular phenotypes in DRE.

Clinical and experimental data from two large prospective studies of adults with epilepsy are presented. The first focussed on new-onset focal epilepsy (NOFE) and the second on DRE. The observed autoantibody prevalence rate in adult outpatients with epilepsy was 9% (42/479). Neuronal surface-directed autoantibody (NSA) status was best predicted by older age, ictal piloerection, epilepsy risk factors, mood problems, attention domain of the Addenbrooke's Cognitive Examination-Revised (ACE-R) and limbic system changes on MRI.

A fixed and permeabilised CBA was developed to detect GAD65 IgG autoantibodies in serum, plasma, CSF and supernatants of cultured peripheral blood mononuclear cells (PBMCs). Serum from 170 healthy controls tested negative. High endpoint titre GAD65 autoantibodies were present in 7/206 (3.4%) patients with DRE but in none of 213 with NOFE. The CBA demonstrated inter-rater reliability and compared favourably to commercial GAD65 autoantibody radioimmunoprecipitation and enzyme-linked immunosorbent assays. To try and enhance the CBA, molecular cloning techniques for antigen tagging and cell surface expression for use in a live and non-permeabilised CBA were applied. However, antigen surface expression was unsuccessful.

Our novel assay identified seven patients with DRE and high titre GAD65 autoantibodies. All were female and demonstrated continuous GAD65 autoantibody production throughout long-term follow-up. Five of seven had temporal lobe epilepsy, three had T1DM and two

had had bilateral hippocampal sclerosis. Pain was reported as a seizure trigger in three patients, an unusual finding in epilepsy.

Cytokine concentrations measured by a multiplex bead-based immunoassay combined with flow cytometry showed GAD65 autoantibody-positive DRE patient plasmas were enriched for IL1b, IL4, IL10, IL15 and TNFa, consistent with multifaceted immune system involvement. Mass cytometry of PBMCs suggested DRE GAD65 autoantibody-positive patients with high GAD65 autoantibody titres may represent a distinct subgroup.

This work provides valuable insights into potential clinical and immunological aspects of epilepsy, with implications for clinical practice and future epilepsy research.

Acknowledgements

I would like to thank my supervisors, Professor Arjune Sen and Professor Sarosh Irani, for their generous time and expertise in guiding me through this project. I also wish to thank Dr Maria Leite, Professor Beth Lang, Dr Jane Adcock and Dr Patrick Waters for providing constructive feedback.

Many thanks to Selina Thomsen, Dr Antonio Berretta, Catherine Simpson, Dr Emma Sutton, Dr Hannah Fox and Gaëlle Le Friec for providing training in various lab techniques; and to Dr Camilla Pang and Dr Emma Sutton for their mass cytometry pre-processing script.

Thank you to the Oxford Autoimmune Neurology Group and the Oxford Epilepsy Research Group teams – Dr Deniz Akdeniz, Dr Adam Al-Diwani, Dr Bettina Balint, Dr Valentina Damato, Andrew Fower, Dr Adam Handel, Dr Anne-Kathrin Kienzler, Dr Mateusz Makuch, Victor Mgbachi, Dr Sophia Michael, Dr Teresa Moloney, Alba Perez Pons, Dr Melanie Ramberger, Archana Ramesh, Dr Bo Sun, Dr Jakob Theorell, Dr Emma Torzillo, Selina Thomsen, Dr James Varley, Victoria Walker and Dr Mark Woodhall.

Thank you to the Clinical Epilepsy team at the John Radcliffe Hospital, to our industry partners at UCB (including Ray Jupp and Diane Marshal), and to the patients who made this project possible.

Finally, I would like to thank Donan and the rest of my family for their encouragement and support.

Abbreviations

^{125}I, iodine-125;

^{35}S, sulphur-35;

^{3}H, hydrogen-3;

4PL, four-parameter logistic regression curve;

AA, amino acid;

Ab, antibody;

Ab+, antibody-positive;

ABA, astrocyte-based assay;

ACE-R, Addenbrooke's Cognitive Examination-Revised;

AChR, acetylcholine receptor;

ACL, anticardiolipin;

AD, Alzheimer's disease;

AD293, adenovirus-transformed HEK cells;

ADNFLE, autosomal dominant nocturnal frontal lobe epilepsy;

Ag, antigen;

AGE, agarose gel electrophoresis;

AI LE, autoimmune limbic encephalitis;

ai, antibody index;

AI, autoimmune;

AIE, autoimmune encephalitis;

AIN, autoimmune neurology;

ALDH7A1, aldehyde dehydrogenase 7 family member A1 gene;

AMPA-R, alpha-amino-3-hydroxy-5-methyl-4-isoxazolepropionic acid receptor;

ANA, antinuclear antibodies;

ANNA1, anti-neuronal nuclear antibody type 1;

APC-A, allophycocyanin (area);

APC, allophycocyanin;

APE2, Antibody Prevalence in Epilepsy and Encephalopathy;

APL, antiphospholipid;

AQP4, aquaporin-4;

Ara-C, cytosine arabinoside;

ASM, anti-seizure medication;

ASS, acute symptomatic seizures;

AUC, area under the curve;

BBB, blood-brain barrier;

BSA, bovine serum albumin;

C, carboxyl;

CAS, cell acquisition solution;

CASPR2, contactin-associated protein 2;

CBA, cell-based assay;

CBZ, carbamazepine;

CD, cortical dysplasia;

CG, cortical gliosis;

Chr, chromosome;

CHRNA2, cholinergic receptor nicotinic alpha 2 subunit;

CHRNA4, cholinergic receptor nicotinic alpha 4 subunit;

CHRNB2, cholinergic receptor nicotinic beta 2 subunit;

CML, chronic myeloid leukaemia;

CMV, cytomegalovirus;

CNS, central nervous system;

CO_2, carbon dioxide;

COX-2, cyclooxygenase-2;

CPM, counts per minute;

CRMP5, collapsin response-mediator protein 5;

CSF, cerebrospinal fluid;

CSTB, cystatin B gene;

CT, computed tomography;

CyTOF, cytometry by time-of-flight;

D anti-H IgG, Fc-gamma, donkey anti-human IgG, Fc-gamma fragment-specific;

DAPI, 4',6-diamidino-2-phenylindole;

DC, dendritic cells;

DD, demyelinating disease;

DF, dilution factor;

DIV, day in vitro;

DMEM, Dulbecco's modified Eagle's medium;

dnVGKC, double-negative voltage-gated potassium channel complex;

DPPX, dipeptidyl-peptidase-like protein 6;

DR, drug-resistant;

DRE, drug-resistant epilepsy;

dsDNA, double-stranded DNA;

E.coli, Escherichia coli;

ED, emergency department;

EDB, extreme delta brush;

EEG, electroencephalogram;

eGFP, enhanced green fluorescent protein;

ELISA, enzyme-linked immunosorbent assay;

EMU, epilepsy monitoring unit;

EPC, epilepsia partialis continua

EPT, endpoint titre;

ERUK, epilepsy research UK;

ES, epileptic seizure;

FBS, fetal bovine serum;

FCD, focal cortical dysplasia;

FCS, flow cytometry standard;

FCS-A, forward scatter (area);

FL, full length;

FLE, frontal lobe epilepsy;

F:M, female:male;

G anti-H Fab, Fc-gamma, goat anti-human Fab fragment, Fc-gamma fragment-specific;

G anti-H IgG, H&L, goat anti-human IgG, heavy and light chain;

G anti-H IgG, IgM heavy chain, goat anti-human IgG, IgM heavy chain-specific;

G anti-R IgG H&L, goat anti-rabbit IgG, heavy and light chains;

GABA-A-R, gamma-aminobutyric acid receptor type A;

GABA-B-R, gamma-aminobutyric acid receptor type B;

GABA, gamma-aminobutyric acid;

GAD, glutamic acid decarboxylase;

GAD65, glutamic acid decarboxylase 65;

GAD65, glutamic acid decarboxylase 67;

gdT, gamma-delta T cell;

GFAP, glial fibrillary acidic protein;

GGE, genetic generalised epilepsy;

GLUT1, glucose transporter protein type 1;

glycine-R, glycine receptor;

GPR55, G protein-coupled receptor 55;

GTCS, generalised tonic-clonic seizure;

HADS, hospital anxiety and depression score;

HBSS, Hanks' Balanced Salt Solution;

HC, healthy control;

HCN1, hyperpolarisation-activated cyclic nucleotide-gated potassium channel 1

HEK-293T cells, human embryonic kidney 293T cells;

HEPES, hydroxyethylpiperazine ethane sulfonic acid;

HIV, human immunodeficiency virus;

HMGB1, high mobility group box 1;

HS, hippocampal sclerosis;

HT, hypothyroidism;

IB, immunoblot;

ICP-MS-TOF, inductively-coupled plasma mass spectrometry by time-of-flight;

IgD, immunoglobulin D;

IgG H&L, immunoglobulin G heavy and light chains;

IgG, immunoglobulin G;

IL-1R, interleukin-1 receptor

ILAE, International League Against Epilepsy;

IMF, immunofluorescence;

IT, immunotherapy;

ITU, intensive therapy unit;

JME, juvenile myoclonic epilepsy;

JRA, juvenile rheumatoid arthritis;

LB broth, Luria-Bertani broth;

LE, limbic encephalitis;

LEV, levetiracetam;

LGI1, leucine-rich glioma inactivated-1;

LTG, lamotrigine;

Lys, lysine;

MAIT, mucosal-associated invariant T cell;

MAP2, microtubule-associated protein 2

MECP2, methylcytosine-binding protein 2 gene;

MELAS, mitochondrial encephalopathy with lactic acidosis and stroke-like episodes;

MERRF, myoclonic epilepsy with ragged red fibres;

mGluR5, metabotropic glutamate receptor 5;

MOG, myelin oligodendrocyte glycoprotein;

MRC WIMM, Medical Research Council Weatherall Institute of Molecular Medicine;

mRS, modified Rankin Score;

MS, sclerosis;

MTLE, mesial temporal lobe epilepsy;

MTS, mesial temporal sclerosis;

N, amino;

N/A, not applicable;

NBA, neuron-based assay*;*

NF-kB, nuclear factor kappa-light-chain-enhancer of activated B cells

NGS, normal goat serum;

NIBSC, National Institute for Biological Standards and Control;

NK, natural killer cell;

NKT, natural killer T cell;

NMDA-R, N-methyl-D-aspartate receptor;

NMOSD, neuromyelitis optica spectrum disorder;

NOFE, new-onset focal epilepsy;

NORSE, new-onset refractory status epilepticus;

NR, not reported;

NSA, neuronal surface-directed autoantibody;

NSA+, neuronal surface-directed autoantibody-positive;

OANG, Oxford Autoimmune Neurology Group;

OD, optical density;

PA, pernicious anaemia;

PBMC, peripheral blood mononuclear cell;

PBS, phosphate buffered saline;

PC, principal component;

PC, prospective cohort;

PCA-1, Purkinje cell cytoplasmic antibody type 1;

PCA, principal component analysis;

PCR, polymerase chain reaction;

pDC, plasmacytoid dendritic cells;

PE-A, phycoerythrin (area);

PE, phycoerythrin;

PEI, polyethylenimine;

PET, positron emission tomography;

PLP, pyridoxal phosphate;

PN, paraneoplastic;

PNES, psychogenic non-epileptic seizure;

POLG, DNA polymerase gamma catalytic subunit;

PVNH, periventricular nodular heterotopia;

QOLIE-31, quality of life in epilepsy-31;

RA, rheumatoid arthritis;

RBA, radiobinding assay;

RC, retrospective cohort;

RE, restriction endonuclease;

RIA, radioimmunoassay;

RIPA, radioimmunoprecipitation assay;

ROC, receiver operating characteristic;

RPM, revolutions per minute;

RSE, refractory status epilepticus;

RT, room temperature;

SA, streptavidin;

SD, standard deviation;

SE, status epilepticus;

SF, seizure-freedom;

SFE, seizure-free epilepsy;

SLC2A1, solute carrier family 2 member 1 gene;

SN, supernatant;

SPSD, stiff person spectrum disorder

SSC-A, side scatter (area);

ssDNA, single-stranded DNA;

SUDEP, sudden unexpected death in epilepsy;

Sz, seizure;

T1DM, type 1 diabetes mellitus;

T86, truncation at amino acid 96;

T96, truncation at amino acid 96;

TAE, trisaminomethane/acetic acid/EDTA;

TEA, transient epileptic amnesia;

Tfh, follicular helper T cell;

TGF-b transforming growth factor-beta;

Th, helper T cell;

TIME study, the impairment of memory in epilepsy study;

TLE, temporal lobe epilepsy;

TLR, toll-like receptor

TNF-a, tumour necrosis factor-alpha

TPO, thyroid peroxidase;

Treg, regulatory T cell.

TRPV1, transient receptor potential vanilloid 1;

TSC1, tuberous sclerosis 1 gene;

TSC2, tuberous sclerosis 2 gene;

tSNE, t-distributed stochastic neighbour embedding;

TSPO, translocator protein 18 kDa;

vEEG, video-electroencephalogram

VGCC, voltage-gated calcium channel;

VGKCc, voltage-gated potassium channel complex;

VNS, vagus nerve stimulation;

WCC, white cell count;

WHO, World Health Organisation.

Contents

ABSTRACT 2

ACKNOWLEDGEMENTS 5

ABBREVIATIONS 6

CONTENTS 14

LIST OF TABLES 21

LIST OF FIGURES 24

CHAPTER 1 INTRODUCTION 29

1.1 EPILEPSY 29

1.2 ANTI-SEIZURE MEDICATIONS 31

1.3 DRUG-RESISTANT EPILEPSY 31

1.4 IMMUNE DYSREGULATION AND SEIZURES 34

1.5 AUTOANTIBODIES AND SEIZURES 35

1.6 DEFINING AUTOIMMUNE EPILEPSY 35

1.7 RECOGNISING AUTOIMMUNE EPILEPSY 41

1.7.1 CLINICAL AND PARACLINICAL FEATURES 41

1.7.2 SEMIOLOGICAL FEATURES 44

1.8 GAD ANTIGENS AND AUTOANTIBODIES 46

1.8.1 GAD ANTIGEN ISOTYPES 46

1.8.2 GAD ANTIGEN STRUCTURE 47

1.8.3 ROLES OF GAD ISOTYPES 48

1.8.4 ANTIGENICITY OF GAD ISOTYPES 49

1.8.5 CLINICAL ASSOCIATIONS OF GAD65 AUTOANTIBODIES 49

1.9 DETECTION AND MEASUREMENT OF GAD65 AUTOANTIBODIES 50

1.10 MECHANISMS OF AUTOIMMUNE EPILEPSY 54

1.10.1 NEUROINFLAMMATION 54

1.10.2 NEURONAL SURFACE TARGET ANTIGENS 56

1.10.3 INTRANEURONAL TARGET ANTIGENS 56

1.10.4 MODULATION OF IMMUNOLOGICAL FUNCTION FOR SEIZURE CONTROL 58

1.11 EVIDENCE FOR AND AGAINST A PATHOGENIC ROLE OF GAD65 AUTOANTIBODIES 58

1.12 SUMMARY 62

1.13 THESIS AIMS AND HYPOTHESES 64

1.13.1 HYPOTHESES 64

1.13.2 AIMS 64

1.14 THESIS STRUCTURE 65

CHAPTER 2 METHODS 66

2.1 CLINICAL SAMPLES 66

2.1.1 NEW-ONSET FOCAL EPILEPSY IN ADULTS (NOFE) STUDY 66

2.1.2 DRUG-RESISTANT EPILEPSY STUDY 66

2.1.3 TYPE 1 DIABETES MELLITUS (T1DM) AND EPILEPSY STUDY 67

2.1.4 THE IMPAIRMENT OF MEMORY IN EPILEPSY (TIME) PROJECT 67

2.1.5 OXFORD AUTOIMMUNE NEUROLOGY GROUP 67

2.2 ISOLATION OF SERUM, PLASMA AND PBMCS 68

2.2.1 SERUM 68

2.2.2 PLASMA 68

2.2.3 PBMCs 68

2.3 ANTIBODY DETECTION METHODS 70

2.3.1 OPTIMISED PROTOCOL FOR THE NOVEL, FIXED AND PERMEABILISED CELL-BASED ASSAY (CBA) TO DETECT GAD65 IGG ANTIBODIES 70

2.3.2 ADDITIONAL CBA ANTIBODIES 72

2.3.3 LIVE CBA TO DETECT GAD65 IGG ANTIBODIES 73

2.3.4 GAD65 ANTIBODY RADIOIMMUNOPRECIPITATION ASSAY (RIPA) 73

2.3.5 GAD65 ANTIBODY ENZYME-LINKED IMMUNOSORBENT ASSAY (ELISA) 74

2.3.6 PRIMARY CULTURE OF NEURONS 75

2.3.7 NEURON-BASED ASSAY (NBA) 76

2.3.8 ASTROCYTE CULTURES 77

2.3.9 ASTROCYTE-BASED ASSAY (ABA) 79

2.4 MOLECULAR CLONING 79

2.4.1 PRIMER AND GENE FRAGMENT RECONSTITUTION 79

2.4.2 GENE FRAGMENT AMPLIFICATION BY POLYMERASE CHAIN REACTION (PCR) 80

2.4.3 SEPARATION OF PCR PRODUCTS BY AGAROSE GEL ELECTROPHORESIS (AGE) 80

2.4.4 DNA EXTRACTION AND PURIFICATION 81

2.4.5 RESTRICTION ENDONUCLEASE DIGESTION OF PLASMID VECTOR BACKBONE AND GAD65 DNA INSERTS 82

2.4.6 LIGATION OF GAD65 DNA INSERTS AND CUT PLASMID VECTOR BACKBONE BY T4 DNA LIGASE 83

2.4.7 BACTERIAL TRANSFORMATION VIA HEAT SHOCK 83

2.4.8 PREPARATION OF CULTURE PLATES 83

2.4.9 BACTERIAL OUTGROWTH AND EXTRACTION OF PLASMID VECTORS 84

2.4.10 PLASMID MINIPREP 85

2.4.11 CONFIRMATION OF CLONING 85

2.4.12 PLASMID MAXIPREP 86

2.5 CYTOKINE MULTIPLEX IMMUNOASSAY 87

2.6 MASS CYTOMETRY 89

2.6.1 THAWING OF CRYOPRESERVED PERIPHERAL BLOOD MONONUCLEAR CELLS (PBMCS) 89

2.6.2 CISPLATIN STAINING FOR CELL VIABILITY 89

2.6.3 BARCODING FOR SAMPLE MULTIPLEXING 90

2.6.4 ANTIBODY STAINING 90

2.6.5 IRIDIUM STAINING OF DNA FOR IDENTIFICATION OF NUCLEATED CELLS 91

2.6.6 MASS CYTOMETRY SAMPLE ACQUISITION 92

2.6.7 PRE-PROCESSING OF RAW DATA FOR ANALYSIS 92

2.7 CLINICAL PHENOTYPING DATABASE FOR THE DRE STUDY 93

2.8 STATISTICAL ANALYSIS 94

CHAPTER 3 CLINICAL AND SEROLOGICAL OBSERVATIONS 95

3.1 INTRODUCTION 95

3.2 NEW-ONSET FOCAL EPILEPSY AND AUTOANTIBODIES 96

3.3 DRUG-RESISTANT EPILEPSY AND AUTOANTIBODIES 106

3.4 ESTIMATION OF AUTOANTIBODY FREQUENCY IN OUTPATIENTS WITH EPILEPSY 116

3.5 AUTOANTIBODIES IN EPILEPSY OVER TIME 119

3.6 OBSERVED CLINICAL PHENOTYPE OF EPILEPSY PATIENTS WITH HIGH EPT GAD65 AUTOANTIBODIES 126

3.7 SUMMARY 128

CHAPTER 4 DEVELOPMENT OF A NOVEL GAD65 ANTIBODY CELL-BASED ASSAY 130

4.1 INTRODUCTION 130

4.2 OVERVIEW OF THE CBA 131

4.3 ESTABLISHING A POSITIVE SIGNAL FROM THE GAD65 ANTIBODY CBA 133

4.4 OPTIMISATION 139

4.5 APPLICATION OF THE GAD65 CBA 151

4.6 TESTING ELISA AND RIPA CALIBRATORS ON THE GAD65 ANTIBODY CBA 152

4.7 LARGER SCALE TESTING OF PATIENT AND CONTROL SAMPLES ON THE GAD65 ANTIBODY CBA 155

4.8 SENSITIVITY AND SPECIFICITY OF THE GAD65 ANTIBODY CBA 156

4.9 COMPARING GAD65 ANTIBODY CBA ENDPOINT TITRES FOR DIFFERENT PATIENT GROUPS 160

4.10 COMPARISON OF GAD65 ANTIBODY CBA, ELISA AND RIPA 162

4.11 GAD65 ANTIBODY CBA INTERRATER PERFORMANCE 169

4.12 PILOT SCREENING FOR GAD65 IGM AUTOANTIBODIES 170

4.13 ADDITIONAL CHALLENGES WITH READING THE GAD65 ANTIBODY CBA 172

4.14 FURTHER DEVELOPMENT OF THE GAD65 CBA 174

4.15 MODIFICATION OF AN EXISTING LGI1 TRANSFECTION VECTOR 176

4.16 GAD65 INSERTS FOR EXPRESSION CONSTRUCT 178

4.17 LIVE CBA TESTING OF EXPRESSION CONSTRUCTS 186

4.18 SUMMARY 189

CHAPTER 5 CYTOKINES AND LEUKOCYTE PHENOTYPES 190

5.1 INTRODUCTION 190

5.2 MEASUREMENT OF PLASMA CYTOKINES 193

5.3 ANALYSIS OF CYTOKINE MULTIPLEX IMMUNOASSAY 197

5.4 PBMC SAMPLE ACQUISITION BY MASS CYTOMETRY 205

5.5 ACQUISITION AND PRE-ANALYSIS PROCESSING OF MASS CYTOMETRY DATA 211

5.6 BATCH CONTROLS 227

5.7 SUMMARY 231

CHAPTER 6 DISCUSSION 232

6.1 SUMMARY OF KEY FINDINGS **232**

6.1.1 AUTOANTIBODY PREVALENCE IN EPILEPSY 232

6.1.2 AUTOANTIBODIES IN EPILEPSY OVER TIME 232

6.1.3 CLINICAL FEATURES PREDICTIVE OF AUTOANTIBODY STATUS IN NEW-ONSET FOCAL EPILEPSY 233

6.1.4 CLINICAL PHENOTYPE OF GAD65 AUTOANTIBODY-ASSOCIATED EPILEPSY 233

6.1.5 DEVELOPMENT OF A NOVEL GAD65 ANTIBODY CELL-BASED ASSAY 234

6.1.6 PLASMA CYTOKINES IN EPILEPSY 234

6.1.7 IMMUNOCELLULAR PHENOTYPE OF GAD65 AUTOANTIBODY-POSITIVE DRE 234

6.2 INTERPRETATION AND CONTEXT **235**

6.2.1 AUTOANTIBODY PREVALENCE IN EPILEPSY 235

6.2.2 AUTOANTIBODIES IN EPILEPSY OVER TIME 244

6.2.3 CLINICAL FEATURES PREDICTIVE OF AUTOANTIBODY STATUS IN NEW-ONSET FOCAL EPILEPSY 245

6.2.4 CLINICAL PHENOTYPE OF GAD65 AUTOANTIBODY-ASSOCIATED EPILEPSY 246

6.2.5 DEVELOPMENT OF A NOVEL FIXED AND PERMEABILISED GAD65 IGG ANTIBODY CBA 247

6.2.6 PILOT OF GAD65 IGM AUTOANTIBODY DETECTION 249

6.2.7 EXPRESSION CONSTRUCT MODIFICATION FOR GAD65 IGG ANTIBODY LIVE CBA 249

6.2.8 PLASMA CYTOKINES IN EPILEPSY 250

6.2.9 IMMUNOCELLULAR PHENOTYPE OF GAD65 AUTOANTIBODY-POSITIVE DRE 254

6.3 STRENGTHS AND LIMITATIONS **255**

6.3.1 AUTOANTIBODY PREVALENCE IN EPILEPSY 255

6.3.2 AUTOANTIBODIES IN EPILEPSY OVER TIME AND THE CLINICAL PHENOTYPE OF HIGH EPT GAD65 AUTOANTIBODY-ASSOCIATED EPILEPSY 257

6.3.3 CLINICAL FEATURES PREDICTIVE OF AUTOANTIBODY STATUS IN NEW-ONSET FOCAL EPILEPSY 258

6.3.4 DEVELOPMENT OF A NOVEL GAD65 IGG ANTIBODY CELL-BASED ASSAY 259

6.3.5 PILOT OF GAD65 IGM AUTOANTIBODY DETECTION 261

6.3.6 EXPRESSION CONSTRUCT MODIFICATION FOR GAD65 IGG ANTIBODY LIVE CBA 261

6.3.7 PLASMA CYTOKINES IN EPILEPSY AND THE IMMUNOCELLULAR PHENOTYPING OF GAD65 AUTOANTIBODY-POSITIVE DRE 263

6.4 IMPACT OF COVID-19 265

6.5 FUTURE DIRECTIONS 266

6.5.1 HYPOTHESIS: DRE PATIENTS WITH POSITIVE NBA OR ABA RESULTS, BUT LACKING SPECIFIC AUTOANTIBODIES (TO TEN ESTABLISHED ANTIGENS BY CBA), MAY HARBOUR NOVEL NSAS 266

6.5.2 HYPOTHESIS: GAD65 AUTOANTIBODY-POSITIVE DRE REPRESENTS A DISTINCT CLINICAL SUBGROUP 266

6.5.3 HYPOTHESIS: HIGH TITRE GAD65 AUTOANTIBODIES HAVE A PATHOGENIC ROLE IN DRE 267

6.5.4 HYPOTHESIS: AUTOANTIBODY-POSITIVE EPILEPSY AND AUTOANTIBODY-POSITIVE AUTOIMMUNE ENCEPHALITIS ARE PART OF THE SAME DISEASE SPECTRUM 268

6.5.5 HYPOTHESIS: NON-ANTIBODY-MEDIATED AUTOIMMUNE MECHANISMS CONTRIBUTE TO EPILEPSY 269

6.6 CONCLUSIONS 270

APPENDICES 271

APPENDIX A: CLINICAL FEATURES WHICH PREDICT NEURONAL SURFACE AUTOANTIBODIES IN NEW-ONSET FOCAL EPILEPSY – IMPLICATIONS FOR IMMUNOTHERAPIES 271

APPENDIX B: DIAGNOSTIC CRITERIA FOR AUTOIMMUNE ENCEPHALITIS 280

APPENDIX C: CLINICAL PHENOTYPING DATABASE FOR THE DRUG-RESISTANT EPILEPSY STUDY 284

APPENDIX D: COMPARISON OF GAD65 ANTIBODY-POSITIVE DRE AND AUTOIMMUNE NEUROLOGICAL CONDITIONS (EXCLUDING EPILEPSY) 298

REFERENCES 299

List of Tables

Table 1: Epilepsy classification 29

Table 2: Epilepsy aetiology 30

Table 3: Self-described 'autoimmune epilepsy' studies in adults..... 40

Table 4: Neurological disorders associated with GAD65 autoantibodies..... 50

Table 5: RIPA-determined GAD65 autoantibody rates in healthy controls..... 51

Table 6: Studies reporting "high titre" GAD65 autoantibodies in adult epilepsy patients. 53

Table 7: Engel classification of outcomes for resective epilepsy surgery..... 60

Table 8: Phenotypic information captured for participants with new-onset focal epilepsy. 97

Table 9: APE2 score criteria..... 98

Table 10: Patients excluded from the study 99

Table 11: Features of NOFE patients with positive serum autoantibody results 100

Table 12: Clinical phenotyping database – main sections 108

Table 13: Pre-populated responses for the clinical phenotyping database 110

Table 14: Patient demographics..... 111

Table 15: Positive serum autoantibody results for DRE patients..... 112

Table 16: High EPT GAD65 autoantibody-positive DRE patients 113

Table 17: Positive serum autoantibody results for SFE patients and healthy controls 116

Table 18: Assays performed for each patient group 116

Table 19: Frequency of positive autoantibody findings by patient group 117

Table 20: Summary information for 13 NOFE patients later enrolled in DRE/SFE study .. 119

Table 21: Epilepsy patients in sequential studies – characteristics 1 120

Table 22: Epilepsy patients in sequential studies – characteristics 2 121

Table 23: Epilepsy patients in sequential studies – characteristics 3 122

Table 24: Epilepsy patients in sequential studies – characteristics 4 123

Table 25: Epilepsy patients in sequential studies – characteristics 5 124

Table 26: Serial GAD65 autoantibody EPT and seizure frequency 125

Table 27: Association between pre-defined clinical features and autoantibody status 126

Table 28: Exploratory analysis of clinical features and autoantibody status..... 127

Table 29: GAD65 antibody CBA controls..... 133

Table 30: Characteristics of secondary (detector) antibodies trialled for the GAD65 antibody CBA 139

Table 31: Summary of optimisation steps for the novel GAD65 antibody CBA..... 150

Table 32: RIPA and ELISA calibrator scores on the GAD65 antibody CBA..... 154

Table 33: GAD65 antibody CBA screening of 875 patient and control sera..... 155

Table 34: Patients with clinical test results for GAD65 autoantibodies 156

Table 35: Linearity of the GAD65 antibody CBA..... 168

Table 36: Custom primer nucleotide sequences..... 178

Table 37: Workflow for cloning GAD65 expression constructs 180

Table 38: DNA fragment sizes..... 181

Table 39: PCR cycling conditions 181

Table 40: Rationale for cytokines included in testing panel..... 194

Table 41: Plasma samples for cytokine testing..... 196

Table 42: Mass cytometry workflow summary 206

Table 43: PBMCs for acquisition by mass cytometry..... 208

Table 44: Studies screening for multiple autoantibodies in adult epilepsy patients..... 239

Table 45: Studies reporting high-titre GAD65 autoantibodies in adult epilepsy patients 241

Table 46: APE2 score performance in three cohorts. 246

Table 47: Studies of interictal cytokine concentrations in adult epilepsy patients 252

List of Figures

Figure 1: Timeline of ASM introduction and proposed mechanisms of action 33

Figure 2: Timeline of established (non-GAD65) autoantibody-associated autoimmune encephalitides featuring seizures in adults 39

Figure 3: Extreme delta brush 43

Figure 4: Action of glutamic acid decarboxylase 46

Figure 5: GAD65 and GAD67 isoforms 47

Figure 6: GAD dimerisation 48

Figure 7: Intraneuronal target antigens 57

Figure 8: Serum autoantibody detection 98

Figure 9: Dimensionality reduction with multiple factor analysis 102

Figure 10: Multivariate stepwise regression model 103

Figure 11: ROC curves 104

Figure 12: Scatter plots of mRS scores in NSA-positive patients by immunotherapy status over time 105

Figure 13: DRE patient recruitment and follow-up 111

Figure 14: NBA images 114

Figure 15: ABA images 114

Figure 16: Frequency of autoantibody-positive results between groups 118

Figure 17: Permeabilised CBA for GAD65 antibody detection 131

Figure 18: X-ray crystal structure of GAD65 resolved from amino acid 88 132

Figure 19: Control samples for GAD65 antibody CBA 135

Figure 20: Additional commercial GAD65 antibody as a control sample for the CBA 136

Figure 21: Non-GAD65 antigen controls for the GAD65 antibody CBA..... 137

Figure 22: GAD65 CBA performed with and without permeabilisation agent..... 138

Figure 23: Secondary antibody for the GAD65 antibody CBA..... 140

Figure 24: Blocking agent and concentration for the GAD65 antibody CBA 141

Figure 25: Duration of blocking in the GAD65 antibody CBA 142

Figure 26: Number of HEK-293T cells seeded for the GAD65 antibody CBA..... 143

Figure 27: Plasmid DNA concentration for the GAD65 antibody CBA 145

Figure 28: Preabsorption of serum sample prior to GAD65 antibody CBA 146

Figure 29: Temperature for the GAD65 antibody CBA..... 147

Figure 30: Other variables investigated for the GAD65 antibody CBA 148

Figure 31: Microscope objective for reading results of the GAD65 antibody CBA 149

Figure 32: Detection of GAD65 autoantibodies in different sample types..... 151

Figure 33: Selection of an appropriate secondary antibody for testing RIPA and ELISA calibrators on the GAD65 antibody CBA 153

Figure 34: GAD65 antibody results from CBA and RIPA, with mismatches tested on ELISA 158

Figure 35: GAD65 antibody results from RIPA, ELISA and CBA 159

Figure 36: Comparison of GAD65 antibody CBA endpoint titres for different patient groups 161

Figure 37: Overview of GAD65 antibody measurement by RIPA and ELISA 162

Figure 38: Calibration curves for interpolation of serum GAD65 antibody concentrations from raw assay outputs..... 163

Figure 39: Correlation of GAD65 antibody concentrations determined by different assays 165
Figure 40: Interassay variability 166
Figure 41: Intraassay variability 167
Figure 42: CBA samples with discrepant ratings from two raters 169
Figure 43: Provisional screening for GAD65 IgM autoantibodies 171
Figure 44: Non-specific membrane staining on the GAD65 antibody CBA 172
Figure 45: ANA and ANA-related antibody staining on the GAD65 antibody CBA 173
Figure 46: Comparison of fixed/permeabilised and live CBAs 175
Figure 47: Plasmid vector and inserts 177
Figure 48: Gene fragment design for full length GAD65 insert 179
Figure 49: Gene fragment PCR amplification products 182
Figure 50: Restriction digest products for modified FL gene fragment and LCE plasmid 183
Figure 51: Bacterial colonies sampled for PCR 183
Figure 52: PCR products of modified T88 colony screen 184
Figure 53: Restriction digest products for secondary confirmation of modified T96 cloning 185
Figure 54: DNA sequencing chromatogram for the modified GAD65 T96 expression construct 185
Figure 55: Live CBA test of modified GAD65 expression constructs 186
Figure 56: Permeabilised CBA test of modified GAD65 expression constructs 187
Figure 57: Permeabilised CBA test of modified GAD65 expression constructs with reduced DNA at transfection 188

Figure 58: Overview of cytokine multiplex immunoassay 193

Figure 59: Flow cytometry gating..... 198

Figure 60: Boxplots of quantitative cytokine assay results across six patient groups 199

Figure 61: Scree plot 200

Figure 62: Variable correlation plot for PCA dimensions 1 and 2 201

Figure 63: Contributions of variables to principal components 1 and 2 202

Figure 64: Correlation plot 203

Figure 65: Biaxial plot of individual plasma samples in PCA..... 204

Figure 66: Elements used in mass cytometry 205

Figure 67: Comparison of flow cytometry and mass cytometry 206

Figure 68: Mass cytometry overview 207

Figure 69: Antibody panel targeting key leukocyte subpopulations..... 209

Figure 70: Barcoding for sample multiplexing. 210

Figure 71: Rain plot of live detector signal..... 212

Figure 72: Live plot of captured events..... 213

Figure 73: Debarcoding..... 214

Figure 74: Gating strategy for singlets 215

Figure 75: tSNE maps for individuals and patient groups..... 216

Figure 76: Heatmap of median marker expression for PhenoGraph clusters with data from all samples combined 217

Figure 77: tSNE map with data from all samples combined 218

Figure 78: T cell marker expression profiles overlayed on tSNE plot with data from all samples combined..... 219

Figure 79: B cell marker expression profiles overlayed on tSNE plot with data from all samples combined..... 220
Figure 80: Dendritic cell, monocytes and natural killer cell expression profiles overlayed on tSNE plot with data from all samples combined 221
Figure 81: Heatmap showing the abundance of cell subtypes within each PhenoGraph cluster according to 13 individual samples..... 222
Figure 82: Heatmap showing the abundance of cell subtypes within each PhenoGraph cluster according to three patient groups 223
Figure 83: Marker expression histogram for five GAD65 Ab-positive patients 224
Figure 84: Marker expression histogram for five SFE patients 225
Figure 85: Marker expression histogram for three healthy controls 226
Figure 86: tSNE plots for five separate batch control samples 227
Figure 87: Heatmap showing the abundance of cell subtypes within each PhenoGraph cluster according to batch 228
Figure 88: Marker expression histograms for five inter-batch controls 229
Figure 89: tSNE with data from five batch control samples combined 230
Figure 90: Comparison of two previously published CBAs to the novel CBA..... 248

Chapter 1 Introduction

1.1 Epilepsy

A seizure is a paroxysm of abnormally excessive or hypersynchronous neuronal activity within the brain. It can manifest as an array of signs and symptoms.[1] Seizures occur in numerous disorders. Epilepsy, a chronic neurological condition affecting 3.4 million people in Europe[2] and 50 million people worldwide,[3] is characterised by recurrent, unprovoked seizures.

Epilepsy is a heterogeneous disease that can be classified by seizure-onset, epilepsy type, and epilepsy syndrome[4] (**Table 1**). Epilepsy aetiology (**Table 2**) is usually defined alongside classification, although the cause is unknown in 60-70% of individuals.[2,5,6]

Table 1: Epilepsy classification
The current classification system of epilepsy takes a multilevel approach and assumes a definite diagnosis of epilepsy. It may not be possible to establish a diagnosis on all three levels. An epilepsy syndrome comprises features which tend to co-occur, such as seizure type, EEG findings, brain imaging abnormalities, age of onset, seizure triggers, diurnal variation, prognosis and comorbidities.[4] *EEG*, electroencephalogram.

Level of classification	*Categories*	*Comments*
Seizure-onset type	• Focal • Generalised • Unknown	-
Epilepsy type	• Focal • Generalised • Combined focal & generalised • Unknown	• Generalised epilepsy can feature various seizure types including typical absence, atypical absence, myoclonic, atonic, tonic and tonic-clonic • Focal epilepsy includes unifocal and multifocal seizures, with seizures involving up to an entire cerebral hemisphere • Focal seizures can be described as focal aware, focal impaired awareness, focal motor, focal non-motor and focal-to-bilateral tonic-clonic
Epilepsy syndrome	Examples: • Dravet syndrome • Genetic generalised epilepsy • Lennox-Gastaut syndrome • West syndrome	Subtypes of genetic generalised epilepsy: • Childhood Absence Epilepsy • Generalized Tonic–Clonic Seizures Alone • Juvenile Absence Epilepsy • Juvenile Myoclonic Epilepsy

Table 2: Epilepsy aetiology

Some causes of epilepsy may fit well with more than one aetiological category. *Malformations of cortical development include focal cortical dysplasia, grey matter heterotopia, lissencephaly, polymicrogyria and schizencephaly.[7] **Tumours include gangliogliomas and dysembryoplastic neuroepithelial tumours. Gene and chromosome information obtained from Genetics Home Reference (National Institutes of Health).[8] *ADNFLE*, autosomal dominant nocturnal frontal lobe epilepsy; *ALDH7A1*, aldehyde dehydrogenase 7 family member A1 gene; *Chr*, chromosome; *CHRNA2*, cholinergic receptor nicotinic alpha 2 subunit; *CHRNA4*, cholinergic receptor nicotinic alpha 4 subunit; *CHRNB2*, cholinergic receptor nicotinic beta 2 subunit; *CMV*, cytomegalovirus; *CSTB*, cystatin B gene; *GLUT1*, glucose transporter protein type 1; *HIV*, human immunodeficiency virus; *MECP2*, methylcytosine-binding protein 2 gene; *MELAS*, mitochondrial encephalopathy with lactic acidosis and stroke-like episodes; *MERRF*, myoclonic epilepsy with ragged red fibres; *POLG*, DNA polymerase gamma, catalytic subunit; *SLC2A1*, solute carrier family 2 member 1 gene; *TSC1*, tuberous sclerosis 1 gene; and *TSC2*, tuberous sclerosis 2 gene.

Aetiology	*Examples (listed alphabetically)*
Structural	• Hypothalamic hamartoma • Hypoxic-ischaemic injury • Malformations of cortical development***** • Mesial temporal sclerosis • Stroke • Trauma • Tuberous sclerosis • Tumours******
Genetic	• ADNFLE (*CHRNA2 gene, Chr 8; CHRNA4 gene, Chr 20; CHRNB2 gene, Chr 1*) • Dravet syndrome (*SCN1A gene, Chr 2*) • Malformations of cortical development • Rett syndrome (*MECP2 gene, X Chr*) • Ring chromosome 20 • Tuberous sclerosis (*TSC1 gene, Chr 9; TSC2 gene, Chr 16*) • Unverricht-Lundborg syndrome (*CSTB gene, Chr 21*)
Infectious	• Cerebral malaria • Cerebral toxoplasmosis • Congenital CMV infection • Congenital Zika virus infection • HIV • Neurocysticercosis • Subacute sclerosing panencephalitis • Tuberculosis
Metabolic	• Alpers' syndrome (*POLG gene, Chr 15*) • GLUT1 deficiency syndrome (*SLC2A1 gene, Chr 1*) • MELAS (*mitochondrial DNA mutations*) • MERRF (*mitochondrial DNA mutations*) • Pyridoxine (vitamin B6)-dependent epilepsy (*ALDH7A1 gene, Chr 5*)
Immune	• Autoimmune encephalitis • Rasmussen encephalitis
Unknown	-

1.2 Anti-seizure medications

The ultimate aim of epilepsy management is to achieve seizure-freedom without adverse effects.[9] Anti-seizure medications (ASMs) are the mainstay of treatment for most people with epilepsy. ASMs suppress seizures, thereby offering symptomatic relief, but do not modify the underlying causes of epilepsy or alter the long-term course. Many ASMs exert their effects via voltage-gated sodium channel blockade or gamma-aminobutyric acid (GABA) receptor agonism. Additional mechanisms include antagonism of the alpha-amino-3-hydroxy-5-methyl-4-isoxazolepropionic acid (AMPA) and N-methyl-D-aspartate receptor (NMDA) glutamate receptors, and binding of synaptic vesicle glycoprotein 2A (SV2A).[10–12] Despite the development of almost 30 ASMs with differing mechanisms of action (**Figure 1**), advancements have chiefly related to tolerability rather than efficacy.[11]

1.3 Drug-resistant epilepsy

Drug-resistant epilepsy (DRE) is the persistence of seizures despite treatment with ASMs, and is operationally defined as the failure to achieve sustained seizure-freedom following a trial of two appropriately chosen and tolerated drugs.[13] Over one-third of people with epilepsy are drug-resistant[14,15] and this proportion has remained fundamentally unchanged for decades despite additions to the pharmacological armamentarium.[14]

There is, therefore, an urgent need for more effective treatments for people with DRE, who bear a mortality rate 5-10 times higher than that of the general population.[16] Uncontrolled seizures present the greatest risk factor for sudden unexpected death in epilepsy (SUDEP)[17,18] and can cause harm by, for example, injury and drowning.[19,20] Compared to

seizure-free patients, those with DRE experience more ASM-related adverse effects;[21,22] severe mental health and psychological problems;[23,24] isolation and stigma;[25,26] and reduced quality of life.[22,25,27] DRE is responsible for the vast majority of epilepsy-associated healthcare costs.[21,28]

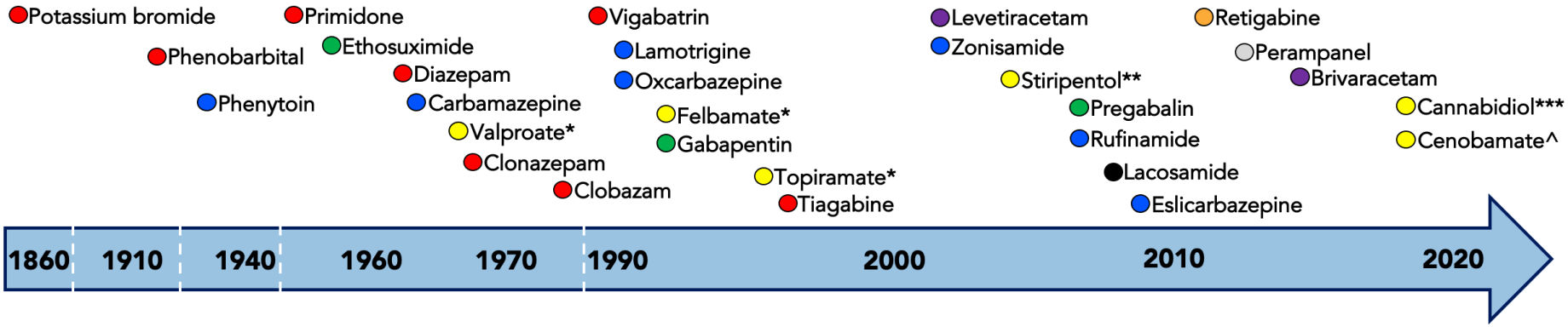
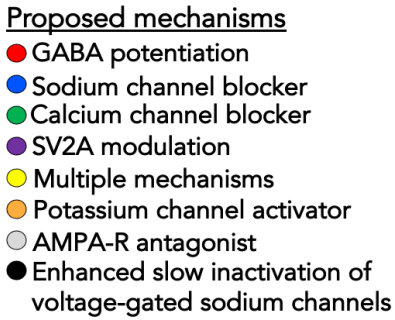


Figure 1: Timeline of ASM introduction and proposed mechanisms of action

GABA potentiation is the most common putative mechanism of ASMs, although multiple other modes of action exist.[10,29] *GABA potentiation, glutamate inhibition, sodium channel blocker and calcium channel blocker. **GABA potentiation and sodium channel blocker. ***TRPV1 desensitisation, GPR55 antagonism and inhibition of adenosine transport.[30] ^Sodium channel blocker (novel binding site) and enhanced presynaptic GABA release (US only).[31] *AMPA-R*, alpha-amino-3-hydroxy-5-methyl-4-isoxazole propionic acid receptor; *ASM*, anti-seizure medication; *GABA*, gamma-aminobutyric acid A receptor; *GPR55*, G protein-coupled receptor-55; *SV2A*, synaptic vesicle protein 2A; and *TRPV1*, transient receptor potential vanilloid-1.



1.4 Immune dysregulation and seizures

Observations suggesting a relationship between aberrant immune function and seizures are well recognised. For example, one-in-five people with epilepsy have a co-existing autoimmune disease, such as type 1 diabetes mellitus (T1DM), autoimmune thyroid disease, rheumatoid arthritis, Grave's disease, myasthenia gravis, inflammatory bowel disease or systemic lupus erythematous.[32–37] Although the causative mechanisms for this are unknown, certain epileptic encephalopathies affecting infants and young children respond to immunotherapy (IT). Steroid therapy, for instance, is used in the treatment of West syndrome, epileptic encephalopathy with continuous spike and wave during sleep, and Landau-Kleffner syndrome.[38,39] A single study also suggested that intravenous immunoglobulin improved seizure control in Lennox-Gastaut Syndrome.[40] Histopathology of brain tissue affected by Rasmussen encephalitis – a unilateral hemispheric syndrome with refractory focal epilepsy, hemiparesis and cognitive impairment – featured predominant T-cell infiltration and microglial activation.[41] Autoantibodies to intracellular paraneoplastic antigens, such as anti-neuronal nuclear antibody type 1 (ANNA1), Ma2, amphiphysin and collapsin response-mediator protein 5 (CRMP5), are often associated with seizures.[42–44] IT may help control seizures in cryptogenic new-onset refractory status epilepticus (NORSE) syndrome.[45,46] Recently, positron emission tomography work has demonstrated the presence of neuroinflammation through increased translocator protein 18 kDa (TSPO) binding in temporal lobe and neocortical epilepsy.[47,48]

1.5 Autoantibodies and seizures

The recognition of paraneoplastic encephalitis with neuronal antinuclear antibodies[49,50] was followed by the discovery of neuronal surface antigen-directed antibodies and anti-glial antibodies in some predominantly non-paraneoplastic forms of autoimmune encephalitis (Figure 2).

The prominence of seizures in these syndromes, the suspected pathogenic role of the autoantibodies and clinical improvement following IT gave rise to the concept of 'autoimmune epilepsy'.

1.6 Defining autoimmune epilepsy

A consensus definition of 'autoimmune epilepsy' does not exist. Understanding is evolving and the International League Against Epilepsy (ILAE) recently addressed the importance of drawing a distinction between acute symptomatic seizures secondary to autoimmune encephalitis and autoimmune-associated epilepsy so as to reflect the different pathophysiological mechanisms, treatments and prognosis.[51]

The term 'autoimmune epilepsy' is often applied to cases that are not, in fact, epilepsy, without regard for the propensity to develop recurrent unprovoked seizures in the long-term. Autoimmune encephalitis, for example, is commonly framed as autoimmune epilepsy, yet generally presents with acute symptomatic seizures that tend to cease along with the resolution of encephalitis and do not require continuing ASM therapy.[52–55]

In the epilepsy literature, 'autoimmune epilepsy' is routinely employed as an umbrella term for a multitude of conditions, such as autoimmune encephalitis with acute symptomatic seizures; autoimmune encephalitis with acute symptomatic seizures plus ensuing epilepsy (which may or may not be associated with an ongoing autoimmune process); paraneoplastic syndromes with acute symptomatic seizures; and 'isolated' epilepsy, ostensibly driven by immune-mediated inflammation of the central nervous system in the absence of autoimmune encephalitis (**Table 3**).

NORSE describes the clinical presentation of refractory status epilepticus (RSE) in patients without a prior history of epilepsy and in whom a clear structural, toxic or metabolic cause cannot be identified.[56] NORSE is sometimes conflated with immune-mediated RSE but has a heterogeneous range of underlying aetiologies.[57,58]

Some of the approaches to experimental design in this area have been unhelpful. Despite previous ILAE guidance stating that provoked/reactive/acute symptomatic seizures should not be considered in a diagnosis of epilepsy,[59] acute symptomatic seizures are routinely grouped with epilepsy as a single entity. Utilising the oxymoron 'acute epilepsy' (e.g. Ganor et al.[60]) and categorising acute symptomatic seizures as unprovoked (e.g. Dubey et al.[61]) is inaccurate but largely unchallenged in this field.

The reported prevalence of autoantibodies in epilepsy fluctuates remarkably between studies, from 3% to 76.5%.[62,63] There are varied reasons for this. Ascertainment bias is a recurrent concern, e.g. Dubey et al. screened participants from acute neurology wards and

intensive care units,[61] which likely enriched the patient cohort for acute symptomatic seizures compared to studies recruiting from outpatient clinics. There is no standard screening panel of 'epilepsy autoantibodies'. Testing for an extensive list of autoantibodies can inflate the apparent rate of seropositivity at the expense of clinical relevance. For example, Dubey et al. assessed subjects for 20 autoantibodies and described a frequency of nearly 35%.[61] However, this included the extraneous findings of antibodies to thyroid peroxidase (TPO),[64] voltage-gated potassium channel complex (VGKC) without leucine-rich glioma inactivated-1(LGI1) or contactin-associated protein-2 (CASPR2) reactivities[65] and glutamic acid decarboxylase-65 (GAD65) at low levels.[66] In contrast, Brenner et al. performed assays for just five autoantibodies, each with some clinical justification, and concluded that 11% of patients were seropositive.[67] The sensitivity and specificity of different antibody assay techniques is important, but infrequently addressed. Meaningful differences between adults and children with regard to the epidemiology of epilepsy[68] and the clinical features of autoimmune neurological conditions[69–71] are sometimes overlooked and these contrasting groups are inappropriately combined, further confounding interpretations.[72]

It is unresolved whether isolated epilepsy (epilepsy without associated encephalitis) can be caused by immune dysregulation. If this were the case, it could potentially explain some cases of resistance to ASMs – which generally do not target the immune system – and provide justification for trialling IT specifically for seizure control. Delineating the immune mechanisms involved could reveal biomarkers for epileptogenesis and autoimmune-

mediated isolated epilepsy. Additionally, potential druggable targets could be identified. These are critical priorities for epilepsy research.[73–75]

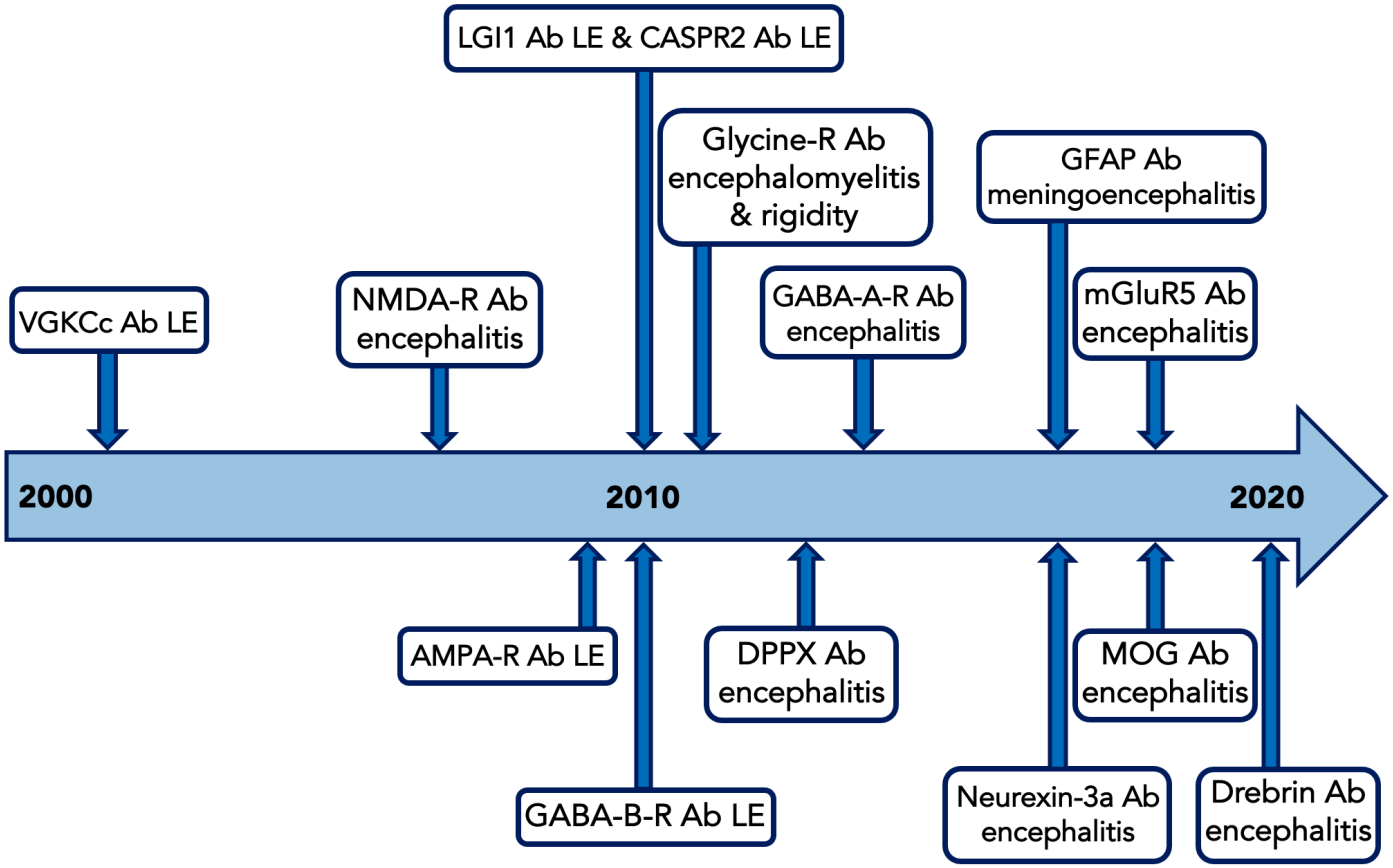


Figure 2: Timeline of established (non-GAD65) autoantibody-associated autoimmune encephalitides featuring seizures in adults

Glial antibody targets: MOG[76] and GFAP.[77] Neuronal antibody targets: drebrin,[78] mGluR5,[79] neurexin-3a,[80] GABA-A-R,[81] GABA-B-R,[82] DPPX,[83] Glycine-R,[84] LGI1,[85] CASPR2,[85] AMPA-R,[86] NMDA-R[87] and VGKCc.[88] *Ab*, antibody; *AMPA-R*, alpha-amino-3-hydroxy-5-methyl-4-isoxazole propionic acid receptor; *CASPR2*, contactin-associated protein-like 2; *DPPX*, dipeptidyl-peptidase-like protein 6; *GABA-A-R*, gamma-aminobutyric acid A receptor; *GABA-B-R*, gamma-aminobutyric acid B receptor; *GFAP*, glial fibrillary acidic protein; *glycine-R*, glycine receptor; *LE*, limbic encephalitis; *LGI1*, leucine-rich glioma inactivated-1; *mGluR5*, metabotropic glutamate receptor 5; *MOG*, myelin oligodendrocyte glycoprotein; *NMDA-R*, N-methyl-D-aspartate receptor; and *VGKCc*, voltage-gated potassium channel complex

Table 3: Self-described 'autoimmune epilepsy' studies in adults

Studies in which the authors apply the term 'autoimmune epilepsy', regardless of how accurately this describes the subjects. Listed chronologically. *Studies that make no distinction between epilepsy and encephalitis with acute symptomatic seizures. *Ab*, antibody; *AI*, autoimmune; *ASS*, acute symptomatic seizures; *CBA*, cell-based assay; *dnVGKC*, double-negative voltage-gated potassium channel complex; *dsDNA*, double-stranded DNA; *ELISA*, enzyme-linked immunosorbent assay; *EMU*, epilepsy monitoring unit; *IB*, immunoblot; *LGI1*, leucine-rich glioma inactivated-1; *MTLE*, mesial temporal lobe epilepsy; *NR*, not reported; *PN*, paraneoplastic; *RIPA*, radioimmunoprecipitation assay; *SPSD*, stiff person spectrum disorder; *Sz*, seizure; *TLE*, temporal lobe epilepsy; *TPO*, thyroid peroxidase and *Y*, yes.

Author	*Subjects*	*PN Abs*	*Clinically irrelevant Abs*	*Assay methods*
Liu 2020[*89]	Adults & children already tested clinically for AI encephalitis-associated Abs who also had a Sz or epilepsy	Y	-	Fixed CBA
Falip 2020[90]	ASS or epilepsy with suggestive clinical features of AI aetiology; subject ages NR.	Y	-	IB, fixed CBA, RIPA
Jesus-Ribeiro 2020[91]	SPSD; adults	-	-	NR
Feyissa 2018[*92]	LGI1 Ab-positive AI encephalitis; subject ages NR	-	-	Fixed CBA
Makhija 2017[*93]	New-onset epilepsy post-leptospiral infection; adults	-	-	Monkey cerebellar capillaries
Varrasi 2017[*94]	AI encephalopathy with ASS; adults	-	TPO	NR
Dubey 2017[*61]	Seizures of unknown cause from clinics, neurology wards, neurology critical care & EMUs; adults	Y	TPO dnVGKCc	Fixed CBA
Steriade 2017[*95]	AI encephalitis; adults	-	-	NR
Feyissa 2017[*96]	AI encephalitis & paraneoplastic disorders with ASS; adults	Y	TPO dnVGKC dsDNA	NR
Dubey 2017[*97]	Adults & children already screened for AI encephalopathy /encephalitis /dementia Ab panels who also had Szs	Y	-	Fixed CBA, ELISA, IB, RIPA
Malter 2016[*98]	AI limbic encephalitis; adults	-	-	IB, fixed CBA
Baysal-Kirac 2016[99]	Antineuronal Ab-positive patients with AI encephalitis or chronic epilepsy; adults	Y	dnVGKCc	IB, live CBA, RIPA
Murata 2015[100]	AI encephalitis; adults	-	-	NR
Dubey 2015[*63]	Adults already diagnosed with encephalitis were then screened for AI limbic encephalitis	Y	TPO dnVGKCc	NR
Miró 2014[101]	MTLE with anti-TPO Abs; adults	-	TPO	RIPA
Toledano 2014[*54]	Adults & children attending AI neurology clinic with Szs	Y	-	NR
Dubey 2014[*102]	AI limbic encephalitis; adults	Y	-	NR
Suleiman 2013[103]	Ab-positive encephalitis, encephalopathy or epilepsy; children	-	dnVGKCc	Live CBA, RIPA
Quek 2012[*104]	Adults & children already diagnosed with AI epilepsy	Y	TPO dnVGKCc	Live CBA RIPA
Ganor 2005[*60]	Epilepsy; children	-	dsDNA	ELISA

1.7 Recognising autoimmune epilepsy

1.7.1 Clinical and paraclinical features

Notwithstanding the absence of data concerning autoimmune-mediated isolated epilepsy, certain features are more prevalent in seizures associated with an autoimmune pathogenic process. Seizure onset is often in adulthood and subacute,[81,105,106] although seizures can manifest as convulsive or non-convulsive status epilepticus.[99,107] A viral prodrome may precede seizures in 20-30% cases.[61,97,108,109] Changes in mood and cognition, with or without encephalitis, occur in up to 90% of anti-neuronal antibody-positive patients with seizures, and psychosis develops in around one-fifth.[61,97,110–113] In epilepsia partialis continua (EPC), up to one-third of patients have an inflammatory aetiology.[114]

Multiple daily seizures typify autoimmune encephalitis with antibodies to LGI1.[104,107,115] High median seizure frequencies of 20 per day are characteristic, reaching 200-300 daily events in some cases.[53,100,115]

Early seizure refractoriness to conventional ASMs is reported in over half of autoantibody-positive patients.[97,101,104,107,116,117] Features of dysautonomia, such as blood pressure instability and cardiac dysrhythmias, are present in 20-40%,[61,97] and in 76% of those with N-methyl-D-aspartate receptor (NMDA-R) autoantibody encephalitis.[118] Amongst LGI1 autoantibody encephalitis patients, allergic cutaneous reactions to ASMs occur in 41%,[53] hyponatraemia is seen in up to two-thirds[105,119,120] and early use of IT correlates with good clinical outcome.[119,121,122]

In recent cohort studies of suspected autoimmune seizures, up to one-third of autoantibody-positive patients had a tumour.[63,97,112] Tumours most commonly associated with antibodies to ANNA-1 (small-cell carcinoma), Ma1 (breast, colon, testicular) and Ma2 (testicular), CRMP-5 (small-cell carcinoma and thymoma) and amphiphysin (small-cell carcinoma and breast adenocarcinoma).[42] Thymoma is observed in approximately 10% of LGI1 autoantibody encephalitis cases;[105,123] 25% of patients with gamma-aminobutyric acid receptor type A (GABA-A-R) autoantibodies; and less than 5% of those with glycine receptor autoantibodies.[123] Half of young women with NMDA-R autoantibody encephalitis have an ovarian teratoma.[124]

Immune-mediated seizures coexist with other autoimmune disorders in up to half of cases, with T1DM, hypothyroidism, coeliac disease and systemic lupus erythematosus determined as most prevalent.[90,116,125]

Electroencephalogram (EEG) features can identify seizures, status epilepticus and encephalopathy but are of limited use in distinguishing between non-autoimmune and autoimmune seizures. Electrographic events without clinical correlates are a common finding with autoantibodies to LGI1[104,107,115,126] and NMDA-R.[127,128] The extreme delta brush (EDB) EEG pattern (**Figure 3**) is generally ascribed to NMDA-R encephalitis,[128–130] although its specificity, sensitivity and prognostic value is not known.[131] EDB has been reported in autoimmune encephalitis with alternative autoantibodies, e.g., glial fibrillary acidic protein (GFAP)[132] or gamma-aminobutyric acid receptor type B (GABA-B-R),[133] and in the setting of ketamine poisoning.[134]

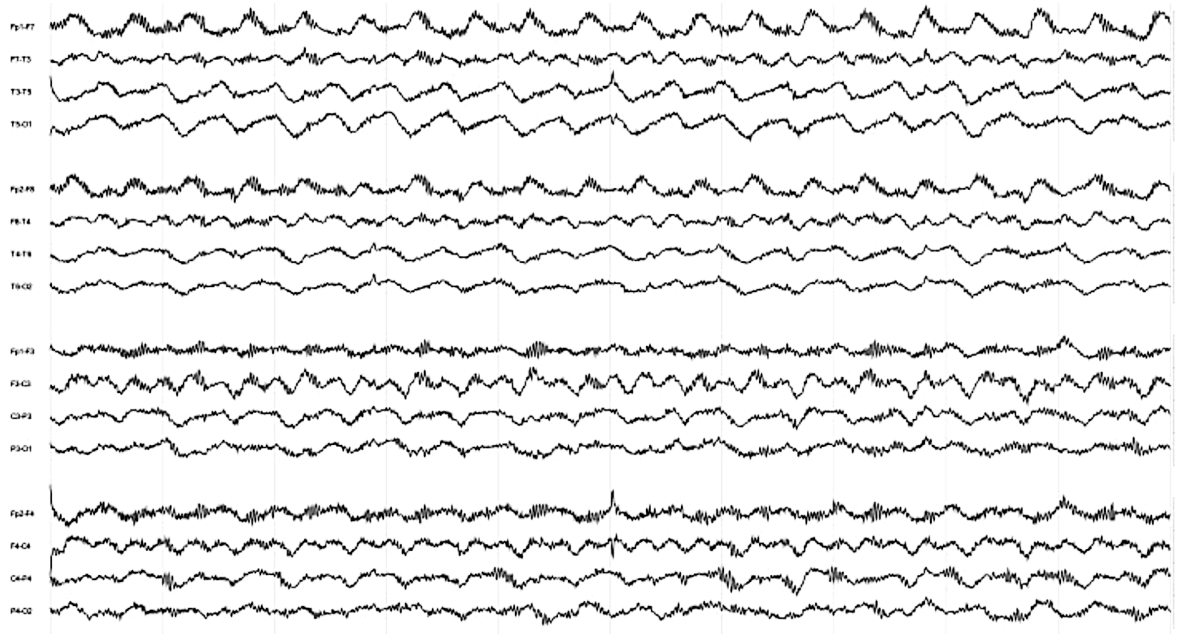


Figure 3: Extreme delta brush
EEG recording from a patient with NMDA-R autoantibody encephalitis showing generalised rhythmic delta activity with superimposed bursts of faster rhythmic beta activity on each delta wave. From Schmitt et al., 2012.[128] (*Copyright Clearance Center Licence Number 4996460397752*). *EEG*, electroencephalogram; and *NMDA-R*, N-methyl-D-aspartate receptor.

Beyond the characteristic MRI appearances of limbic encephalitis (inflammatory lesions of limbic structures with atrophy of the mesial temporal lobes), specific MRI brain changes have not been consistently identified with autoimmune seizures. Brain MRI scans are often unremarkable at seizure onset.[104] Flanaghan et al. determined that T1 hyperintensities of the basal ganglia were associated with LGI1 autoantibody-positive faciobrachial dystonic seizures (FBDS)[135] and Steriade et al. described claustrum fluid-attenuated inversion recovery hyperintensities in patients with suspected autoimmune seizures.[95] A proportion of cases of temporal lobe epilepsy with amygdala enlargement – an electroclinical syndrome distinct from TLE with hippocampal sclerosis – test positive for neuronal antibodies.[98,136,137]

Seizures with an autoimmune aetiology are commonly described as being of temporal lobe origin,[97,99,104,110,138] although extratemporal onset is also recognised.[94,115] Multifocal seizures are known to occur.[81,104,115,120] Bitemporal lobe involvement is reported with antibodies against NMDA,[63] GAD65,[104] GABA-A-R,[81] CASPR2,[113] and LGI1,[105] in addition to some antibody-negative autoimmune patients.[111]

1.7.2 Semiological features

Prompt recognition of autoimmune-mediated seizures is essential. IT may be required for effective seizure control and delays in initiating this can adversely affect clinical outcomes.[119] An accompanying encephalitic phase is likely to prompt consideration of autoimmune aetiology for new-onset seizures. Conversely, identifying the cause of isolated epilepsy may be more challenging. As confirmatory autoantibody results can take weeks to obtain, and IT is not without risks, clinical features that improve diagnostic certainty are widely sought. Unfortunately, most semiological features of autoimmune seizures can appear in non-autoimmune epilepsy too, and there is a paucity of data pertaining to their sensitivity or specificity.

Currently, the only semiology believed to arise exclusively in the context of autoimmunity is FBDS, which are regarded as pathognomonic of LGI1 autoantibody encephalitis.[53,105,139] Of note, FBDS do not present in epilepsy secondary to LGI1 gene mutations.[140,141] LGI1 autoantibody encephalitis patients mostly experience other seizure types in addition, which are not specific to this disorder.[53,92]

According to a small number of cohort studies and case reports, some features that are uncommon among the outpatient epilepsy population are also evident in autoimmune seizures. It is therefore not possible to reliably estimate prevalence rates. Examples of these traits include reflex[90,91,142] and gelastic[143] seizures. Similarly, pilomotor events have been documented with antibodies to LGI1, CASPR2, NMDA, GAD65,[97,104] GABA-A-R,[99] GABA-B-R,[107,144] ANNA-1/Hu,[107,145] and Ma2[144,145] but are also recognised in non-autoimmune epilepsy.[146–150]

Ictal and peri-ictal autonomic changes linked to autoantibodies encompass cardiac dysrhythmias, flushing, salivating, sweating and urinary urge.[90,113,120,121,151] Somatosensory abnormalities, such as hemi-body paraesthesias or pharyngeal tingling, have been observed with autoimmune seizures,[107,115,144,151,152] as have alterations in auditory perception (e.g. dulling[151]) and auditory hallucinations (e.g. buzzing, ticking, hearing music[94,151,153]).

1.8 GAD antigens and autoantibodies

1.8.1 GAD antigen isotypes

The enzyme glutamic acid decarboxylase (GAD) acts on glutamate to produce GABA, the primary inhibitory neurotransmitter in the central nervous system (**Figure 4**). GAD expression is restricted to presynaptic GABAergic neurons of the human brain and spinal cord, pancreatic islet beta-cells, oviduct and testes.[154,155] The two isoforms, GAD65 and GAD67, are named according to their kilodalton molecular weight.[156,157] Both are synthesised in neuronal cytoplasm. GAD65, the more abundant isoform in the brain, is modified and attached to the inner surface of synaptic vesicles at the cytoplasmic side of presynaptic nerve terminals, whereas GAD67 is soluble and distributed throughout the cytoplasm.[158–160] GAD67-synthesised GABA is implicated in synaptogenesis and protection from injury, whereas GAD65 produces GABA for neurotransmission.[161]

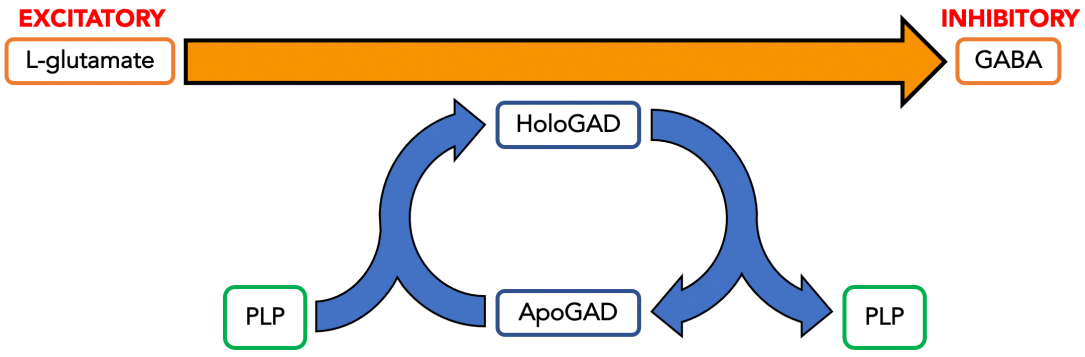


Figure 4: Action of glutamic acid decarboxylase
Decarboxylation of L-glutamate by the GAD enzyme produces the inhibitory neurotransmitter GABA. Pyridoxal phosphate (PLP), the active form of vitamin B6, is a co-enzyme which must couple with GAD to form the functional holoenzyme (holoGAD). Dissociation of this complex forms the inactive apoenzyme (apoGAD). The interconversion of apoGAD and holoGAD is controlled by adenosine triphosphate, phosphate and GABA. CO_2, carbon dioxide; *GABA*, gamma-aminobutyric acid; *GAD*, glutamic acid decarboxylase; and *PLP*, pyridoxal phosphate.

1.8.2 GAD antigen structure

A monomeric GAD unit comprises three functional domains – an amino (N) terminal, a middle pyridoxal phosphate (PLP)-binding domain containing the catalytic site, and a carboxyl (C) terminal (**Figure 5**). There is a high degree of amino acid sequence homology between the isoforms. The N-terminal domain, responsible for anchoring GAD65 in synaptic vesicles, accounts for the major sequence differences.[162,163]

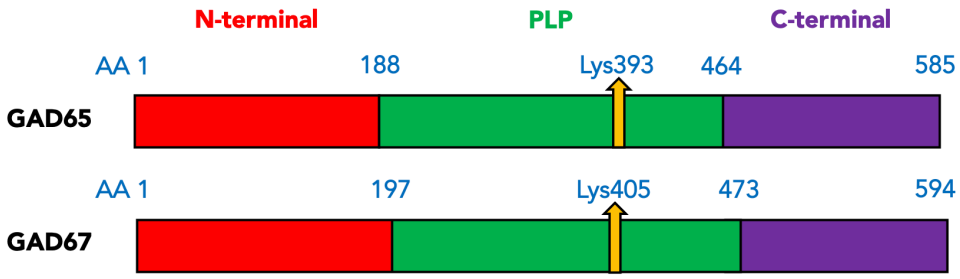


Figure 5: GAD65 and GAD67 isoforms
GAD65 (encoded by the GAD2 gene on chromosome 2) is concentrated at the cytoplasmic side of presynaptic nerve terminals. GAD67 (encoded by GAD1 gene on chromosome 10) is soluble and distributed in abundance throughout the cytoplasm.[162,163] *AA*, amino acid; *GAD*, glutamic acid decarboxylase; *Lys*, lysine; and *PLP*, pyridoxal phosphate.

1.8.3 Roles of GAD isotypes

Both GAD isoforms must form dimers and bind the co-enzyme PLP in order to function (**Figure 6**). GAD67 usually exists as a holoenzyme (PLP-bound) and generates basal GABA production, while GAD65 is predominantly an apoenzyme (not bound to PLP) that becomes activated for pulsatile vesicular GABA release.[160,162,164]

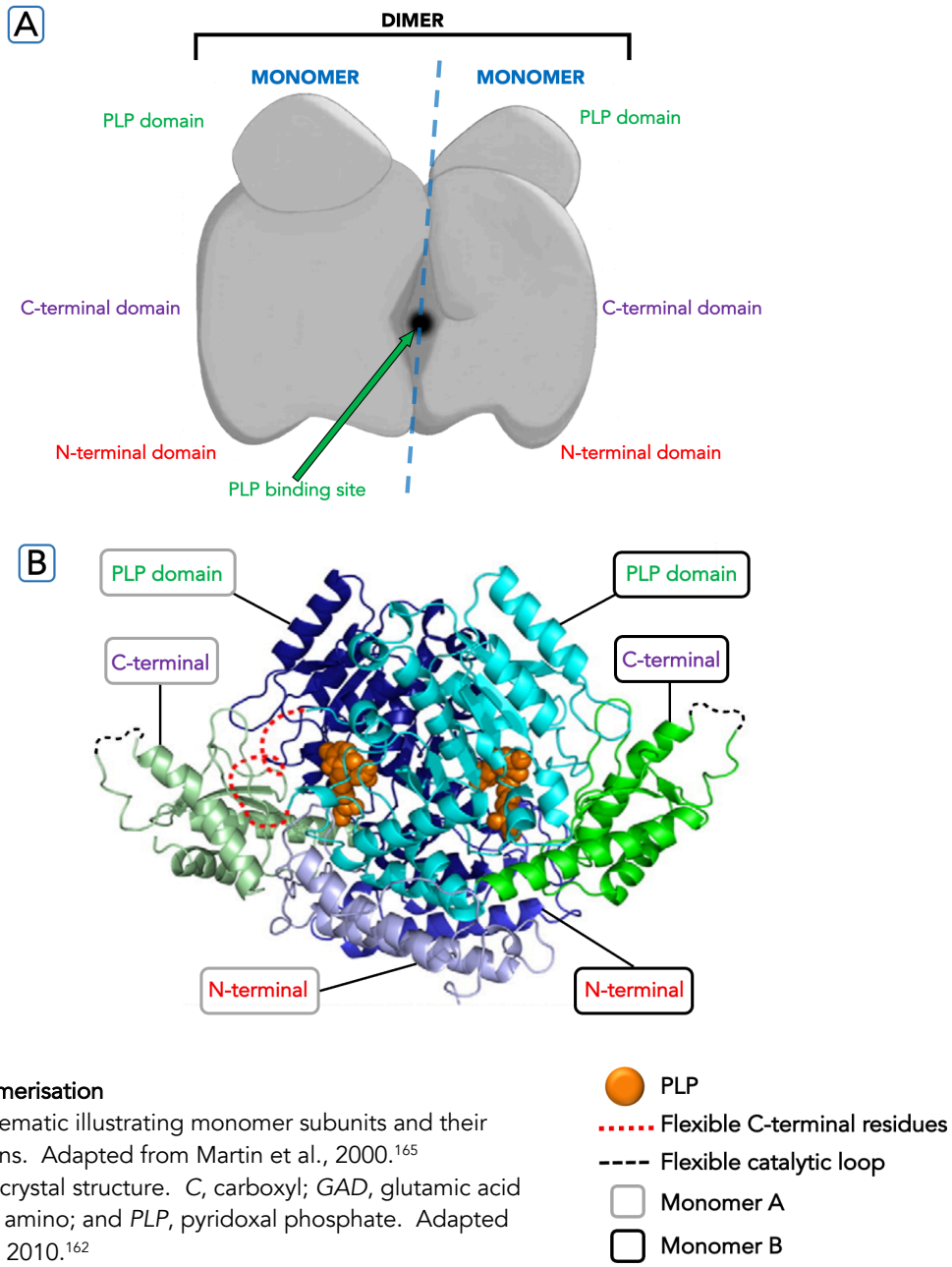


Figure 6: GAD dimerisation
A) GAD dimer schematic illustrating monomer subunits and their constituent domains. Adapted from Martin et al., 2000.[165]
B) GAD dimer 3D crystal structure. *C*, carboxyl; *GAD*, glutamic acid decarboxylase; *N*, amino; and *PLP*, pyridoxal phosphate. Adapted from Fenalti et al., 2010.[162]

1.8.4 Antigenicity of GAD isotypes

Variation in mobility, principally at the C-terminal domain and catalytic loop residue, and electrostatic charge render the GAD65 isoform antigenic.[166] Autoantibodies that primarily react with GAD65 may infrequently cross-react with GAD67 antigen.[164,167] Autoantibodies specific and exclusive to GAD67 are rarely detected,[162,168] and GAD67 is generally accepted as non-antigenic.[166]

1.8.5 Clinical associations of GAD65 autoantibodies

Robust epidemiological investigations into the seroprevalence of GAD65 autoantibodies have not been performed. In people with overt type I diabetes mellitus (T1DM), serum GAD65 autoantibodies are present in 80% at onset,[169,170] and may be detected during a pre-clinical autoimmune phase lasting several years.[66,169–171] Such antibodies tend to decrease or become undetectable over time.[66,172]

GAD65 autoantibodies are also detected in some neurological disorders, such as stiff-person syndrome spectrum disorders[173] (SPSD) and limbic encephalitis,[174] (**Table 4**), where antibody concentrations are orders of magnitude greater than that typically seen in T1DM.[175–177]

Table 4: Neurological disorders associated with GAD65 autoantibodies

GAD65 autoantibody-positive patients may have neurological disorders with or without type 1 diabetes mellitus.[173–175,178–184] Listed alphabetically.

Autonomic neuropathy
Brainstem encephalitis
Cerebellar ataxia
Limbic encephalitis
Myelopathy
Nystagmus and oculomotor dysfunction
Palatal myoclonus
Peripheral neuropathy
Progressive encephalomyelitis with rigidity and myoclonus
Stiff-person syndrome spectrum disorder

The prevalence of GAD65 serum autoantibodies in healthy controls is reported between 0%[169,171] and 8%,[185] with most estimates lying at the lower end of this spectrum[66,186] (Table 5).

GAD65 autoantibody-associated epilepsy is commonly characterised as a chronic, drug-refractory temporal lobe epilepsy syndrome with coexisting systemic autoimmune disease.[174,184,186–189] There are, however, methodological challenges concerning the current GAD65 autoantibody-associated epilepsy literature, meaning that the disease spectrum is not adequately explored, despite approximately 200 published cases.

1.9 Detection and measurement of GAD65 autoantibodies

The most widely used laboratory methods for detecting GAD65 antibodies are immunohistochemistry, radioimmunoprecipitation assay (RIPA), enzyme-linked immunosorbent assay (ELISA) and Western blotting.[190] The traditional 'gold standard' is RIPA. Available data for RIPA-determined GAD65 autoantibody prevalence among healthy controls demonstrate how methodological variations for a single technique can still complicate direct comparison of individual studies – relevant literature uses GAD antigen

from different species, diverse immunoprecipitation methods and units of measurement that cannot be compared (Table 5).

Table 5: RIPA-determined GAD65 autoantibody rates in healthy controls
Estimated GAD65 autoantibody positivity rates among healthy, non-diabetic adults. Studies listed chronologically. Sample sizes range from 42 participants to 4,496. GAD antigen is sourced from human and non-human species. Varying radioactive labels, immunoprecipitation methods and incomparable units of measurement are used. *125I*, iodine-125; *35S*, sulphur-35; *3H*, hydrogen-3; *Ab+*, antibody-positive; *ai*, antibody index; *CPM*, counts per minute; *GAD65*, glutamic acid decarboxylase 65; *NR*, not reported; *RIPA*, radioimmunoprecipitation assay; *RU*, relative units; and *U*, units.

Author	*Number of controls screened*	*Number of GAD65 Ab+*	*GAD antigen species*	*Radioactive label*	*Immune complex isolation*	*Threshold for positive result*
Sørgjerd 2015[66]	4,496	76 (1.7%)	NR	^{3}H leucine	Protein A-Sepharose & protein C-Sepharose	0.06 ai
Liimatainen 2010[86]	200	3 (1.5%)	Human	^{35}S methionine	Protein-A-Sepharose	5.36 RU/ml
Meinck 2001[191]	100	1 (1%)	Human	^{35}S methionine	Protein-A-Sepharose	7 U
Walikonis 1998[85]	117	9 (8%)	Human	^{125}I	Goat anti-human serum IgG & IgM fractions	0.03 nmol/L
Dotta 1997[71]	42	0 (0%)	Human	^{35}S methionine	Protein-A-Sepharose	NR
Niskanen 1995[192]	126	3 (2.4%)	Pig	^{125}I	Protein-A-Sepharose	30 U
Tuomilehto 1994[69]	100	0 (0%)	Pig	NR	NR	18 U
Petersen 1994[193]	100	4 (4%)	Human	^{35}S methionine	Protein-A-Sepharose	750 CPM

In recent years, logistical and safety concerns inherent with radioactivity use in laboratories prompted a fragmented transition towards widespread use of ELISA. There are conflicting accounts regarding the comparability of GAD65 antibody concentrations determined by ELISA and by RIPA.[110,181,189,194–197] Furthermore, both assays are traditionally calibrated to detect GAD65 autoantibodies in T1DM,[198,199] and it is not clear how effectively they perform at the range of antibody concentrations observed in autoimmune neurological conditions.

Highly specific and sensitive cell-based assays (CBA) have been developed for some autoantibodies relevant to immune-mediated disease, such as autoimmune encephalitis,[85] myasthenia gravis[200] and neuromyelitis optica spectrum disorders.[201,202] For detection of autoantibodies by ELISA, antibodies usually must interact with solubilised recombinant protein, which may be derived from non-human species. In contrast, the three-dimensional structure of native antigen is maintained in CBAs, whereby a vector containing human complementary DNA is used to overexpress a single target antigen in mammalian cells.[109,203] As CBAs do not require radioactivity, they do not present the environmental hazards associated with RIPA. The Oxford Autoimmune Neurology Group widely employ CBAs, so developing a CBA for testing GAD65 antibodies allows a single cross-comparison platform, with the potential for multiplexing in future.

There is no standard unit of measurement for GAD65 antibodies and no validated method for converting between units.[61,181] GAD65 antibody concentrations are variably expressed in international units, relative units and units; or as an antibody index or a dilution factor. The selected thresholds for clinical relevance are not always derived with measurements

from non-diabetic healthy controls[167,172,175] and vary widely.[204] Also, key methodological details are often omitted from published work (**Table 6**).

Table 6: Studies reporting "high titre" GAD65 autoantibodies in adult epilepsy patients
Studies listed chronologically. Even when apparently identical units are quoted for ELISA and RIPA results, the units are not equivalent and there is no validated conversion method. *Ab+*, antibody-positive; *Ab*, antibody; *AD*, Alzheimer's disease; *AI*, autoimmune; *CBA*, cell-based assay; *CD*, cortical dysplasia; *CG*, cortical gliosis; *DD*, demyelinating disease; *DF*, dilution factor; *DR*, drug-resistant; *DRE*, drug-resistant epilepsy; *ELISA*, enzyme-linked immunosorbent assay; *F:M*, female:male; *GAD65*, glutamic acid decarboxylase 65; *GGE*, genetic generalised epilepsy; *HC*, healthy control; *HS*, hippocampal sclerosis; *HT*, hypothyroidism; *JME*, juvenile myoclonic epilepsy; *JRA*, juvenile rheumatoid arthritis; *LE*, limbic encephalitis; *MS*, multiple sclerosis; *MTLE*, mesial temporal lobe epilepsy; *MTS*, mesial temporal sclerosis; *NA*, not applicable; *NR*, not reported; *PA*, pernicious anaemia; *PC*, prospective cohort; *RA*, rheumatoid arthritis; *RBA*, radiobinding assay; *RC*, retrospective cohort; *SD*, standard deviation; *SPSD*, stiff person spectrum disorder; and *T1DM*, type 1 diabetes mellitus.

Study	*Number of "high titre" GAD65 Ab+ patients*	*Assay type (result range)*	*Positivity threshold*	*"High titre" threshold*	*Unit*
Tizazu 2020[205]	2/270 (0.7%)	CBA (DF 1:12,800–1:204,800)	NR	NR	NA
Aguiar 2019[206]	5/12 (41.7%)	NR (134.1–312.1)	1	100	IU/ml
Falip 2019[207]	13 (% NR)	ELISA (NR)	NR	2,000	IU/ml
Nóbrega Jr 2018[62]	2/100 (2%)	ELISA (NR)	10	1,000	IU/ml
Ceyhan Dirican 2016[208]	0/54 (0%)	RIPA (NR)	1	NR	U/ml
Moloney 2016[209]	7/25 (28%)	RIPA (9,550–59,200)	10	1,000	U/ml
Lilleker 2014[189]	6/112 (5.4%)	RIPA or ELISA (NR)	RIPA 1 or ELISA 5	RIPA 1,000 or ELISA 50,000	U/ml
Falip 2012[210]	2/42 (4.8%)	RIPA (1,207–87,510)	NR	1,000	IU/ml
Malter 2010[174]	9/53 (17%)	RIPA (1,798 –12,030)	1	NR	U/ml
Liimatainen 2010[186]	7/253 (2.8%)	RIPA (1,680–207,770)	5.36	1,000	RU/ml
Errichiello 2009[188]	6/233 (2.6%)	RIPA (1.93–78.79)	0.9	NR	U/ml
Sokol 2004[211]	1/31 (3.2%)	ELISA (NR)	NR	Control mean + 2 SD	NR
Kwan 2000[212]	4/105 (3.8%)	RIPA (6.3–170.4)	NR	NR	U/ml
Peltola 2000[184]	2/100 (2%)	RIPA (53,000–107,000)	HC mean + 3 SD	NR	RU

1.10 Mechanisms of autoimmune epilepsy

1.10.1 Neuroinflammation

The precise mechanisms leading to epileptogenesis and recurrent seizures remain unknown. Neuroinflammation is thought to contribute to epilepsy pathogenesis through the activation of signalling pathways that modify neuronal and glial cell function and alter synaptic transmission and plasticity, with resultant cell hyperexcitability and excitotoxicity.[213,214]

Oxidative stress secondary to epileptogenic insults (such as status epilepticus, stroke, traumatic brain injury and CNS infection) can trigger neurons and glia to release the 'danger signal', High Mobility Group Box 1 (HMGB1), and the pro-inflammatory cytokine, IL1beta. These molecules initiate interleukin-1 receptor/toll-like receptor (IL1R/TLR) signalling, inducing transcription of nuclear factor kappa-light-chain-enhancer of activated B cells (NF-kB)-regulated inflammatory genes, thereby propagating a 'sterile' neuroinflammatory cascade.[215,216] Activation of the IL1R/TLR4 signalling pathway impedes function of the hyperpolarisation-activated cyclic nucleotide-gated potassium channel 1 (HCN1 channel), producing dysregulation of hippocampal pyramidal cell dendrites.[217]

Cytokines can disrupt neuronal function through receptor modification, e.g., phosphorylation of the AMPA and NMDA receptors' subunits impairs calcium permeability at glutamate receptors.[218] Cytokines also inhibit glial glutamate reuptake and enhance glutamate release by astrocytes, increasing the extracellular glutamate concentration.[219] Data from clinical studies of cytokines in epilepsy are limited and inconclusive.[220,221]

Variations in seizure-to-sampling time and ASM regimens pose challenges when comparing experiments. Kamasak et al.[222] found a correlation between epilepsy severity and serum levels of HMGB1, TLR4, TNF-alpha and IL-1beta measured by ELISA. Tumour necrosis factor-alpha (TNF-a) secretion in astrocytes and neurons in TLE and tuberous sclerosis-related epilepsy is associated with proconvulsant effects,[223,224] as is neuronal upregulation of the enzyme cyclooxygenase-2 (COX2).[214]

Dysfunction of the blood-brain barrier (BBB) permits brain entry to molecules that are capable of eliciting an inflammatory response. The presence of serum albumin in the brain parenchyma, for example, stimulates signalling of transforming growth factor-beta (TGF-b) in astrocytes, with transcription of inflammatory genes and disruption of potassium and glutamate transport. Subsequent inflammation and increased extracellular potassium and glutamate concentrations produce tissue hyperexcitability.[225,226]

Complement system activation has been demonstrated in TLE patients with hippocampal sclerosis.[227] Injection of complement factors C5b6, C7, C8 and C9 into the hippocampi of awake rats was coupled with membrane attack complex formation, seizures and hippocampal neuronal loss,[228] while post-status epilepticus rat hippocampal tissue showed prominent activation of the classical complement pathway with elevated expression of C1q, C3 and C4.[227]

Fabene et al.[229] concluded that multiple chemokines (e.g., CCL2, CCL3, CCL4, and CCL5) were elevated in neurons, glia, endothelial cells and infiltrating leukocytes in brain tissue

samples from DRE patients. In experimental models, neuroinflammation, cell loss, acute seizures, and BBB damage has been observed in response to stimulation of these pathways.[230,231]

1.10.2 Neuronal surface target antigens

Autoantigen-specific B cells – believed to escape the immune tolerance checkpoints that usually prevent autoimmunity – differentiate into the circulating antibody-secreting cells, plasmablasts and long-lived plasma cells.[232] In several subtypes of autoimmune encephalitis, antibodies to neuronal surface-expressed antigens are proposed to access their target epitopes in vivo and, in so doing, exert a direct pathological effect. For instance, in anti-NMDA receptor encephalitis, autoantibodies bind to NMDA receptors and induce receptor internalisation through cross-linking, thereby abolishing the NMDA receptor component of spontaneous excitatory postsynaptic currents.[233] In anti-LGI1 limbic encephalitis, autoantibodies disrupt LGI1 interactions with the receptors, ADAM22 and ADAM23, and produce internalisation of the LGI1-ADAM complex, and down-regulation of presynaptic Kv1.1 channels and postsynaptic AMPA receptors.[234–236]

1.10.3 Intraneuronal target antigens

The significance of autoantibodies against intraneuronal targets is more variable. Archetypal paraneoplastic antibodies target proteins in the neuronal cytoplasm or nucleus which are conjointly expressed by an underlying tumour (**Figure 7**). These antibodies are not thought to have a direct pathogenic role. Instead, antigen-specific cytotoxic T lymphocytes cause neuronal dysfunction.[179,237] Antibodies to amphiphysin, for example, a

presynaptic protein involved in vesicle recycling and neurotransmitter release,[238] have shown evidence of cytotoxic T cell-associated neuronal destruction at post-mortem in SPSD. Amphiphysin autoantibodies may also be capable of entering neurons and disrupting GABA-mediated inhibition.[239,240] Potentially pathogenic mechanisms for autoantibodies against GAD65, another intraneuronal presynaptic protein, have not been definitively demonstrated.

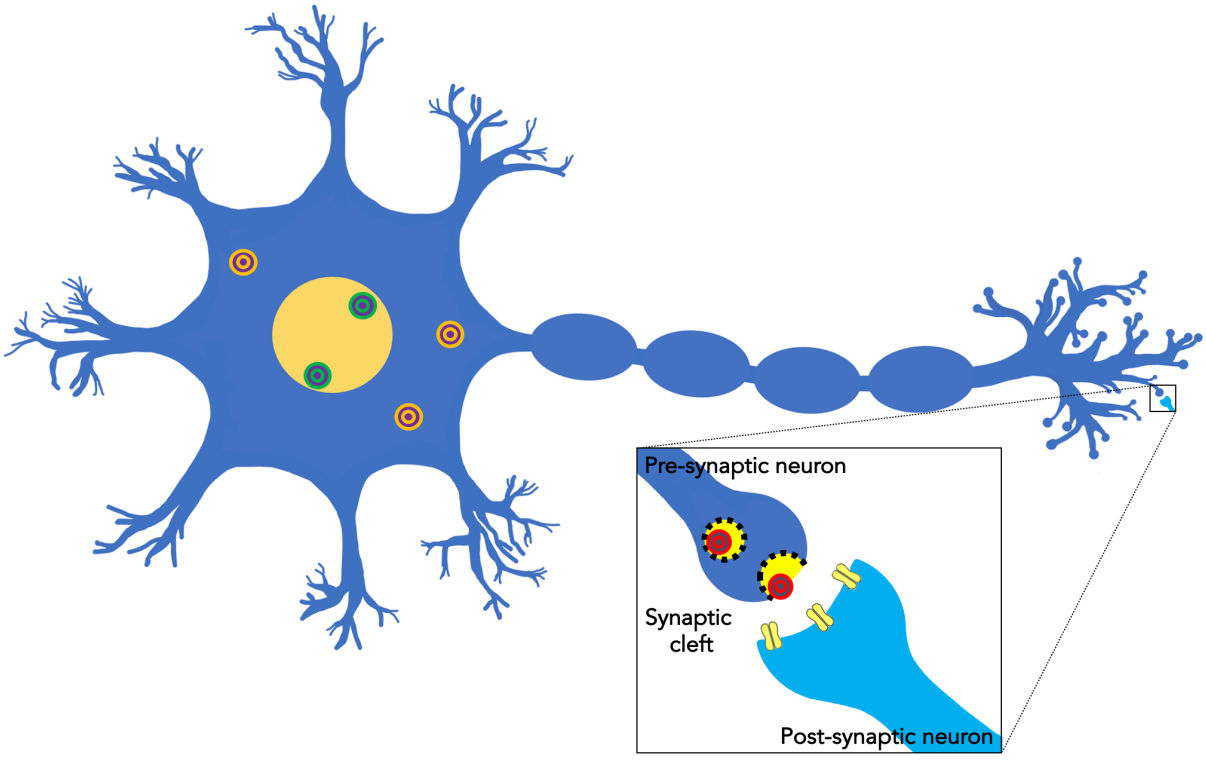


Figure 7: Intraneuronal target antigens
Intraneuronal antigens can be classified as intranuclear (e.g. ANNA1/Hu and Ma2/Ta), cytoplasmic (e.g. PCA-1/Yo) or pre-synaptic (e.g. GAD65 and amphiphysin). *ANNA1*, anti-neuronal nuclear antibody type 1; *GAD65*, glutamic acid decarboxylase 65; and *PCA-1*, Purkinje cell cytoplasmic antibody type 1.

1.10.4 Modulation of immunological function for seizure control

Just as ASMs are effective for some people with epilepsy when the cause is not known, it is possible that broadly acting immunotherapy (e.g., corticosteroids, plasma exchange and intravenous immunoglobulins) may be clinically useful for seizures driven by immunological dysfunction, regardless of aetiology or antibody status, as there may be shared final common pathways for multiple immune mechanisms. More tailored approaches might be required to minimise adverse effects or to improve efficacy – examples could include depletion of a particular lymphocyte subpopulation by targeting its surface receptors with a monoclonal antibody, catabolism of IgG via neonatal Fc receptor antagonism or disruption of a cytokine pathway critical to relevant pathological processes.

1.11 Evidence for and against a pathogenic role of GAD65 autoantibodies

The concentrations of GAD65 autoantibodies found in suspected autoimmune neurological conditions are thought to be considerably higher than the levels observed in T1DM alone.[241,242] Of these neurological syndromes, SPSD has been the most widely researched.[173,191] Intrathecal synthesis of GAD65 autoantibodies in SPSD suggests that they are of clinical significance,[243] as does their presence in this IT-responsive disorder but absence in classically non-immune-mediated neurological conditions.[190,244]

Bjork et al. described that GAD65 autoantibodies isolated from patients with SPSD – but not from subjects with T1DM – could inhibit GAD65 enzymatic activity and reduce GABA synthesis in vitro.[245] Hansen et al. found SPSD-like motor dysfunction was induced in rats following passive transfer of purified SPSD patient IgG into the lateral ventricle or

intrathecal compartment.[246] In a small, randomized, double-blind, placebo-controlled trial, Dalakas et al. reported that intravenous immunoglobulin could be an effective therapy for SPSD with high-titre GAD65 autoantibodies.[243] However, a case report of a woman with SPSD by Nemni et al. illustrated that maternal transfer of GAD65 autoantibodies could occur without any abnormal clinical features[247] – the patient's two singleton babies were born with markedly elevated serum GAD65 autoantibodies that persisted for 24 months. At 8-year follow-up, neither child had developed signs of SPSD or other anti-GAD65-related disease, potentially indicating that SPSD pathogenesis involves factors other than antibodies alone.

The relationship between GAD65 autoantibodies and epilepsy has not been extensively investigated. Studies of GAD65 autoantibody-positive neurological conditions often do not provide sufficiently granular information to enable epilepsy-specific conclusions to be drawn. Comparing separate studies is difficult, as often researchers make no distinction between autoimmune encephalitis with acute symptomatic seizures and isolated epilepsy; provide scant details on antibody assay format and antibody titre; and pool patients with manifold autoantibodies with those who are only seropositive for autoantibodies to GAD65. A study of 106 patients with GAD65 autoantibody-associated neurological syndromes, including 18 with epilepsy, failed to show internalisation of GAD65 antibodies in live rat cerebellar neurons. None of those with epilepsy had DRE or high GAD65 autoantibody concentrations by ELISA, although additional antibodies targeting GABA-A or glycine receptors were present in 5/18.[248] An analysis of 61 high titre GAD65 autoantibody neurology patients recruited just two with isolated DRE.[249] In a cohort of six patients with

GAD65 autoantibody-positive epilepsy, only one had isolated DRE with high GAD65 antibody titres; the commercial GAD65 antibody ELISA kit was changed during the experiment without explanation or validation work to address standardisation.[250]

The critical role of GAD65 in GABA-driven neuronal inhibition provides a rationale for suspecting that seizures might arise if GAD65 antibodies were able to alter GAD65 enzymatic function. This is supported by the observations that mice with genetic deletion of GAD65 develop spontaneous seizures.[251,252] Also, a patient with GAD65 autoantibody-positive isolated DRE and daily seizures became seizure-free following three cycles of plasma exchange, with a parallel reduction in serum antibody titres from 115,900 to 3,970 IU/mL.[253] Carreño et al. described three patients with isolated DRE, unquantified GAD65 serum autoantibodies and unilateral hippocampal sclerosis.[254] They underwent anteromedial temporal lobectomy but none had a good surgical outcome (defined as Engel class I or II; Table 7). Resective epilepsy surgery for people with temporal lobe epilepsy and hippocampal sclerosis can achieve seizure-freedom in up to 80% of cases.[255,256] The surgical failure rate in these GAD65 autoantibody-positive patients is striking – albeit the sample size is small – and could be potentially explained by an ongoing autoimmune substrate for seizures.

Table 7: Engel classification of outcomes for resective epilepsy surgery
Excludes early post-operative seizures. For classes III and IV, consideration of data such as percentage seizure reduction, cognitive function, and quality of life is required.[257]

Engel class	*Description*
I	Free of disabling seizures
II	Rare disabling seizures
III	Worthwhile improvement
IV	No worthwhile improvement

Criteria for defining autoantibody pathogenicity in autoimmune disease have been proposed,[258,259] requiring the demonstration of 1) a circulating autoantibody or cell-mediated immunity, 2) a specific corresponding antigen, 3) an immune response in experimental animal models and 4) essential pathological features of the disease in immunised animals. Experimental evidence pertaining to GAD65 antibodies in isolated epilepsy is minimal and these criteria have not yet been satisfied. Therefore, it remains uncertain if and how GAD65 antibody-antigen interaction occurs in vivo, and by which means the diverse neurological syndromes outlined above can develop. Presynaptic terminals may unselectively permit GAD65 antibodies to gain intracellular access, or GAD65 antigen may be transiently exposed to the extracellular space during vesicle fusion, facilitating antibody-antigen engagement.[260] If not directly pathogenic, GAD65 autoantibodies may coexist with or induce the production of neuronal surface antibodies.[248,261] Alternatively, cytotoxic T-cell damage to GAD65-expressing inhibitory neurons could give rise to extracellular leakage of GAD65 antigen, leading to the generation of GAD65 autoantibodies as an epiphenomenon. Differences in epitope specificities might explain the diversity of GAD65 autoantibody-associated clinical phenotypes but studies claiming to have identified discrete epitope-phenotype patterns have reported conflicting findings,[190,241,262,263] and some authors have uncovered no evidence of epitope differences at all.[248,264]

No published studies have focussed on high-titre GAD65 autoantibodies in isolated DRE, a patient group who could potentially benefit from immunotherapy if robust evidence were obtained to demonstrate and delineate underlying autoimmune mechanisms.

1.12 Summary

The urgent clinical need for more effective treatments for people with DRE is hampered by a limited understanding of the aetiopathophysiology of epilepsy and the mechanisms of pharmacoresistance.

Although acute symptomatic seizures can occur in the setting of autoimmune encephalitis, it is not clear whether isolated autoimmune epilepsy (sans encephalitis) exists. Autoimmunity may explain resistance to conventional anti-seizure medications in a proportion of patients and justify trialling immunotherapy, specifically for seizure control.

The purported prevalence rate of autoantibodies in epilepsy varies substantially, from 3% to 76.5%. Recognising an autoimmune driver to seizures can be challenging without positive antibody results, as discriminating clinical and paraclinical features are seemingly sparse.

The GAD65 enzyme is central to production of the inhibitory neurotransmitter gamma amino butyric acid and is attached to the inner surface of synaptic vesicles at presynaptic nerve terminals. GAD65 autoantibodies, uncommon in healthy controls, are present in 80% of people with T1DM at onset and can be detected at much higher concentrations in an assortment of neurological disorders, including stiff person spectrum disorders, limbic encephalitis and epilepsy. The spectrum of GAD65 autoantibody-associated epilepsy is often described as highly drug-refractory, although the characteristics are not well defined overall.

Many laboratory methods are used for detecting GAD65 autoantibodies. However, the traditional 'gold standard', RIPA, has generally been replaced on logistical grounds by the ELISA, designed to detect autoantibodies at the typically low distribution found in T1DM. There is no standard unit of measurement for GAD65 antibodies, no method of converting between units and no consensus on thresholds for clinical significance. It is not clear how well ELISA performs at the higher GAD65 antibody titres seen in neurological conditions. Detecting and interpreting GAD65 autoantibodies within the sphere of neurology can therefore be particularly challenging.

The precise mechanisms leading to epileptogenesis and recurrent seizures remain unknown. Neuroinflammation may contribute to neuronal hyperexcitability and excitotoxicity. Clinical data on cytokine-related neuroinflammation in epilepsy are limited and inconclusive. In certain subtypes of autoimmune encephalitis, antibodies to neuronal surface-expressed autoantigens are proposed to access target epitopes in vivo and exert a direct pathological effect. The GAD65 antigen is intracellular, and no means of antibody-antigen interaction has been proven. Whether GAD65 autoantibodies are directly pathogenic, therefore, remains a matter of debate.

No published studies have focussed on high titre GAD65 autoantibodies in isolated DRE. The demonstration and delineation of contributory immune pathways in DRE could provide biomarkers for epileptogenesis and autoimmune epilepsy, and identify potential druggable targets – critical priorities for epilepsy research.

1.13 Thesis aims and hypotheses

1.13.1 Hypotheses

- There are immunological contributions to the aetiology of drug-resistant epilepsy (DRE) in a proportion of patients.
- Immunological parameters in people with DRE will align aspects of 'immunophenotype' with clinical and paraclinical features.
- GAD65 autoantibody-positive epilepsy represents a distinct clinical phenotype.
- In some people with DRE, it may be possible to modulate immunological function to ameliorate seizures.

1.13.2 Aims

- To estimate the prevalence of autoantibodies in epilepsy and consider their clinical relevance.
- To identify and clinically phenotype a cohort of DRE patients with high titre GAD65 autoantibodies.
- To define immunological correlates & mechanistic evidence of autoimmunity in DRE.
- To develop a novel cell-based assay for the detection of 'neurologically relevant' GAD65 autoantibodies.

1.14 Thesis structure

- Chapter 2 will detail the materials and methods.
- Chapters 3, 4 and 5 will present results.
- Chapter 6 (discussion) will interpret and contextualise results, reflect on experimental strengths and limitations, acknowledge specific challenges related to the SARS-CoV-2 pandemic, propose directions for future work and draw conclusions.

Chapter 2 Methods

2.1 Clinical samples

All participants provided informed written consent. Ethical approval was granted by the Oxfordshire Regional Ethics Committee (RECA 07/Q160X/28 and REC16/YH/0013). Collaborating laboratory groups also received local ethics consent for participation in this research. Samples were tested blind to clinical information.

2.1.1 New-onset focal epilepsy in adults (NOFE) study

Serum samples from 254 patients were collected in epilepsy clinics between December 2011 and November 2015 at the John Radcliffe Hospital, Oxford; the Great Western Hospital, Swindon; and the Sheffield Teaching Hospital, Sheffield. Samples were stored at -20 °C after collection. 219 patients met inclusion criteria for the NOFE study and underwent screening for a panel of neuronal autoantibodies. 213 samples had sufficient remaining material for repeat GAD65 antibody testing by cell-based assay.

2.1.2 Drug-resistant epilepsy study

Serum, plasma and peripheral blood mononuclear cells (PBMCs) were collected in epilepsy clinics between January 2018 and November 2019 at the John Radcliffe Hospital, Oxford, from 206 patients with DRE and 54 people with epilepsy who were seizure-free. Serum and plasma were stored at -80 °C and PBMCs were stored in cryogenic tanks cooled by liquid nitrogen.

2.1.3 Type 1 diabetes mellitus (T1DM) and epilepsy study

Serum was collected in epilepsy clinics and diabetes clinics between March 2010 and May 2012 at the Sheffield Teaching Hospital, Sheffield, from 25 patients with both T1DM and epilepsy and from 36 patients with T1DM only. Samples were stored at -20 °C. Sufficient remaining material for repeat GAD65 antibody testing by cell-based assay was available for all those with T1DM and epilepsy, and 33 with T1DM only.

2.1.4 The impairment of memory in epilepsy (TIME) project

Serum was collected from 20 subjects with transient epileptic amnesia and 7 with temporal lobe epilepsy by the Exeter University TIME project team between February 2017 and March 2018. Samples were stored at -80 °C.

2.1.5 Oxford autoimmune neurology group

Serum, plasma and PBMCs from 147 patients with a range of autoimmune neurological conditions and from 170 healthy controls were collected between July 2015 and November 2019 at the John Radcliffe Hospital, Oxford (acute neurology in-patient wards, neurosciences intensive care unit, and autoimmune neurology clinics). Serum and plasma were stored at -80 °C and PBMCs were stored in cryogenic tanks cooled by liquid nitrogen.

2.2 Isolation of serum, plasma and PBMCs

2.2.1 Serum

Whole blood collected in serum separating tubes (BD, USA) was centrifuged at 3,000 revolutions per minute (RPM) (Heraeus Megafuge 16; Thermo Fisher Scientific, USA) for 10 minutes at room temperature (RT), acceleration 9 and deceleration 9. Serum was removed by pipette and aliquoted for storage at -80 °C. Prior to each assay, samples were thawed on ice and centrifuged at 12,000 RPM for 5 minutes at RT in a microcentrifuge (Pico 17; Thermo Fisher Scientific, USA).

2.2.2 Plasma

Whole blood collected in sodium heparin-containing blood tubes (BD, USA) was centrifuged at 500 G for 10 minutes at RT (acceleration 9 and deceleration 5). Plasma was removed by pipette and aliquoted for storage at -80 °C. Prior to each assay, samples were thawed on ice and centrifuged for 5 minutes at 12,000 RPM at RT in a microcentrifuge.

2.2.3 PBMCs

Whole blood collected in sodium heparin-containing blood tubes was centrifuged at 500 G for 10 minutes at RT (acceleration 9 and deceleration 5). Extraction of PBMCs was performed within a class 2 biological laminar flow cabinet (Envair, UK). Following removal of the plasma layer, the red blood cell pellets and remaining blood were transferred into 50 ml Falcon conical centrifuge tubes (Thermo Fisher Scientific, USA) and diluted at a ratio of 1:1 (based on the volume of whole blood) with 1% bovine serum albumin (BSA; Thermo Fisher Scientific, USA) in phosphate buffered saline (PBS; Thermo Fisher Scientific, USA),

with a maximum volume of 35 ml diluted blood per tube. The blood/PBS/BSA mixture in each tube was mixed before slow and gentle pipetting onto 15 ml Ficoll (Thermo Fisher Scientific, USA) in another 50 ml Falcon tube, forming two separate layers. The tubes were then centrifuged at 400 G for 30 minutes at RT (acceleration 3, deceleration 0). The resultant interphase layer of PBMCs was then carefully harvested using a sterile polyethylene Pasteur pipette (Camlab, UK). PBMCs were washed by diluting at a ratio of 1:1 with 1% BSA/PBS and centrifuging at 200 G for 10 minutes at RT (acceleration 9, deceleration 7), forming a PBMC pellet at the bottom of the Falcon tube. The supernatant was aspirated (Dymax 8 vacuum aspiration system; Charles Austen Pumps Ltd, UK) and the PBMC pellet was resuspended in 50 ml 1% BSA/PBS for a second wash. A 20 µl sample of the cell solution was added to 20 µl of 0.4% Trypan blue (Thermo Fisher Scientific, USA) for cell counting by microscopy (AE2000; Motic, China) at x100 magnification using a Neubauer haemocytometer chamber (Hawksley, UK). The resuspended pellet was centrifuged at 200 G for 10 minutes at RT (acceleration 7 and deceleration 7). The supernatant was removed and the PBMCs were resuspended at a cell concentration of 20 million cells per ml in 1:1 B cell medium and freezing medium in cryotubes (Hunter Scientific, UK).

A working stock of 100 ml B cell medium was made up of 92.8 ml RPMI 1640 cell medium, 5 ml 5% fetal bovine serum (FBS; Sigma-Aldrich, USA), 1 ml 1% penicillin/streptomycin (Thermo Fisher Scientific, USA), 1 ml 1% GlutaMAX (Thermo Fisher Scientific, USA), 0.1 ml 0.1% beta-mercaptoethanol (Thermo Fisher Scientific, USA) and 0.1 ml 1% IgG-depleted transferrin (Thermo Fisher Scientific, USA). A working stock of 10 ml of freezing medium

comprised 8 ml 80% FCS and 2ml 20% dimethyl sulfoxide (DMSO; Sigma-Aldrich, USA). The cryotubes were placed in a rate-controlled cell-freezing container for cryogenic vials (CoolCell FTS30; BioCision, USA) at -80 °C overnight and transferred to cryogenic storage the following day.

2.3 Antibody detection methods

2.3.1 Optimised protocol for the novel, fixed and permeabilised cell-based assay (CBA) to detect GAD65 IgG antibodies

13mm glass coverslips (VWR, USA) in a 24-well culture plate (Corning Incorporated, USA), were submerged in poly-L-lysine (PLL; Sigma-Aldrich, USA) for 30 minutes. PLL was aspirated and the coverslips were left to dry. HEK293T cells were cultured in Dulbecco's modified Eagle's medium (DMEM) supplemented with 10% FBS and 1% penicillin/streptomycin/amphotericin (Thermo Fisher Scientific, USA). Cells were counted and 100,000 were seeded per well in 1 ml of supplemented DMEM. Plates were transferred to a humidified incubator at 37 °C, 5% carbon dioxide (MC0; PHCbi, Netherlands) for 24 hours.

The DNA transfection mix was prepared with 10.5 µg of DNA (92% GAD65 and 8% eGFP), 350 µl of unsupplemented DMEM and 10.5 µl of polyethylenimine (PEI; Sigma-Aldrich, USA) per plate, made up to a volume of 12 ml with supplemented DMEM. Cells were transiently co-transfected with plasmids encoding GAD65 and enhanced green fluorescent protein (eGFP) by adding 0.5 ml of DNA transfection mix per well. Cells were returned to

the incubator for five hours. The transfection mix was then aspirated and replaced by 1 ml of fresh supplemented DMEM per well.

Twenty-four hours after transfection, the culture medium was aspirated from the cover slips and cells were washed with 0.5 ml PBS before fixation with 250 µl 4% formaldehyde (Sigma-Aldrich, USA) for ten minutes at RT. After three washes with PBS, (using 1ml, 0.5ml and 0.5 ml, respectively), cells were permeabilised with 250 µl 0.3% Triton X-100 detergent (Sigma-Aldrich, USA) in PBS for ten minutes at RT. Non-specific binding was blocked with 250 µl 10% normal goat serum (NGS; Vector Laboratories, USA) in 0.1% Triton X-100/PBS for 60 minutes at 4 °C. Cells were washed another three times with 0.5 mls of PBS.

Two hundred and fifty µl serum sample (primary antibody) diluted 1:100 in 1% NGS/0.1% Triton X-100/PBS was added per well and plates were incubated at RT for 60 minutes with gentle agitation on a see-saw rocker (SSL4; Stuart Equipment, UK). Cover slips were washed with 0.5 ml of PBS three times.

To detect binding of the primary antibody to HEK293 cell-expressed GAD65, 250 µl Alexa Fluor 594-conjugated donkey anti-human IgG Fc-gamma fragment-specific secondary antibody (Jackson Immuno Research Laboratories, USA) was added at a dilution of 1:500 for 45 minutes at RT with gentle agitation under light-protection. The cover slips were washed three times with 250 µl PBS and mounted on glass microscope slides (VWR, USA) with mounting medium (Thermo Fisher Scientific, USA) containing 1:1,000 diamidino-2-phenylindole (DAPI; Thermo Fisher Scientific, USA) for nuclear staining. Cover slips were

visualised on a fluorescence microscope (DM1000; Leica Microsystems, Germany). Antibody binding was assessed using a semi-quantitative scoring system ranging from 0 to 4 (negative if 0, positive if equal to or greater than 1). Photographs were taken with a Rolera-XR digital camera (QImaging Corporation, Canada) and QCapture Pro 6.0 software (QImaging Corporation, Canada).

2.3.2 Additional CBA antibodies

Other secondary antibodies trialled were Alexa Flour 568-conjugated goat anti-human IgG, heavy and light chain (Thermo Fisher Scientific, USA) and Alexa Flour 594-conjugated goat anti-human Fab fragment, Fc-gamma fragment-specific (Jackson Immuno Research Laboratories, USA).

CBAs with RIPA and ELISA calibrators made use of Alexa Fluor 488-conjugated goat anti-rabbit IgG, Fc fragment specific secondary antibody (Jackson Immuno Research Laboratories, USA).

IgM GAD65 antibody screening employed Alexa Fluor 594-conjugated whole IgG goat anti-human polyclonal antibody targeting IgM heavy chain (Invitrogen, USA).

Two different commercial GAD65 antibodies were used as controls – a B96 human monoclonal (Advanced Targeting Systems, Inc, USA) and a rabbit anti-human polyclonal (Invitrogen, USA).

2.3.3 Live CBA to detect GAD65 IgG antibodies

Culture medium was aspirated from HEK293T cells at 24 hours post-transfection. Serum samples (primary antibody) were diluted in DMEM/hydroxyethylpiperazine ethane sulfonic acid (HEPES; Sigma-Aldrich, USA) /1% bovine serum albumin (BSA; Sigma-Aldrich, USA) and 250 µl diluted serum was added per well prior to incubation on a see-saw rocker for 1 hour at RT. The supernatant was discarded, and the cells were washed three times with 250 µl DMEM/HEPES. Cells were fixed with 250 µl 4% formaldehyde (Sigma-Aldrich, USA) in PBS per well for 10 minutes at room temperature. Following further washes (one with 500 µl PBS and two with 500 µl DMEM/HEPES), Alexa Fluor 594-conjugated donkey anti-human IgG Fc-gamma fragment-specific secondary antibody diluted 1:500 in DMEM/HEPES/1%BSA was added at a volume of 250 µl per well and incubated on a see-saw rocker for 45 minutes at RT. After three washes with 250 µl DMEM/HEPES and a wash with 250 µl PBS, cover slips were mounted with 1:1,000 DAPI/mounting media and visualised on fluorescence microscopy.

2.3.4 GAD65 antibody radioimmunoprecipitation assay (RIPA)

A commercial GAD65 antibody RIPA kit (RSR Limited, UK) was used as per the manufacturer's instructions. In brief, freshly reconstituted ^{125}I-labelled GAD65 antigen was added to 5 µl of patient serum and 45 µl of PTX buffer (20 mM phosphate buffer, pH 7.4, 0.1% Triton X-100) at a volume equating to 20,000 counts per minute (CPM). The total sample volume was made up to 100 µl with PTX buffer and then incubated overnight at 4°C.

Radiolabelled GAD65 antigen-GAD65 antibody complexes were then precipitated over 90 minutes at RT with 50 µl sheep anti-human IgG. The precipitate was centrifuged at 13,000 RPM for five minutes at RT to form a pellet. Unbound ^{125}I-labelled GAD65 antigen was removed by aspiration of the supernatant and the pellet was washed with PTX buffer.

Radioactivity emitted from the pellet was counted for two minutes by a gamma scintillation counter (Wallac Wizard 1470; PerkinElmer Inc, USA) and the percentage binding was determined. The level of radioactivity (in CPM) was inversely proportional to the concentration of GAD65 antibodies in the sample. A spline curve was constructed using a set of calibrators of known GAD65 antibody concentrations ranging from 1-300 arbitrary units/ml. GAD65 antibody titres for patient samples were interpolated from the spline curve.

2.3.5 GAD65 antibody enzyme-linked immunosorbent assay (ELISA)

A commercial GAD65 antibody ELISA kit (RSR Limited, UK) was used in accordance with the manufacturer's instructions. Twenty-five µl serum samples, kit calibrators (5-2000 arbitrary units) and controls were added in duplicate to GAD65 antigen-coated wells in a 96-well plate which was incubated for 60 minutes at RT. When sample dilution was required, healthy control serum from the same donor was used as the diluent. Wells were washed with 250 µl wash solution before adding freshly reconstituted GAD65-biotin and incubating for 60 minutes at RT. Following a repeat wash, wells were incubated with streptavidin peroxidase for 20 minutes at RT. Tetramethylbenzidine (peroxidase substrate) was added and left to incubate in the dark for 20 minutes at RT before the reaction was quenched with

sulphuric acid (stop solution). Absorbance at 450 nm was read within 15 minutes on an ELISA plate reader (Infinite; Tecan, Switzerland). Four-parameter logistic regression was used to construct a standard curve using kit calibrator readings, from which GAD65 antibody titres in test samples were then interpolated.

2.3.6 Primary culture of neurons

Plate coating solution was prepared with 95 ml sterile water, 1 ml PLL and 4 ml gelatin (Thermo Fisher Scientific, USA). Omitting the outer wells and those in the seventh row, 54 wells on each 96-well plate (Corning Incorporated, USA) were filled with 50 µl coating solution. The plates were placed in a humidified incubator at 37°C, 5% carbon dioxide (C150; Binder, Germany) for three hours. The coating solution was then aspirated and wells were washed twice with 100 µl sterile water before being left to dry, covered in foil and stored at room temperate until ready for use.

Wistar rat pups were sacrificed on embryonic day 18 by decapitation. Forceps were used to strip away the skin on the skull. The brain was disconnected from the underlying tissue and placed in a 35 mm petri dish (Corning Inc, USA) on ice which contained HEPES medium. Using a dissecting microscope (S9; Leica Microsystems, Germany) and fine-tipped forceps (Thermo Fisher Scientific, USA), one brain at a time was placed in a 35mm petri dish with Hanks' Balanced Salt Solution (HBSS; Thermo Fisher Scientific, USA)-HEPES for stripping of the meninges and removal of the midbrain and thalamus. The hippocampus and cortex were dissected out and handled separately (see primary culture of astrocytes). Tissue was washed with HBSS-HEPES and treated with 1% trypsin (Thermo Fisher Scientific,

USA) in HBSS for 10 minutes in a humidified incubator at 37°C, 5% carbon dioxide. Trypsin was aspirated and the tissue was washed with HBSS-HEPES before resuspension in neurobasal medium (supplemented with 2% B27, 1% GlutaMAX and 1% polysialic acid; Thermo Fisher Scientific, USA) and trituration by gentle pipetting action until no remaining clumps of tissue were visible. Cell density was determined with a haemocytometer. Using only the central wells of a PLL-coated 96-well plate, 12,000 cells in 60 µl medium were seeded per well. To reduce evaporative losses, the outer wells were filled with PBS and plates were wrapped in cling film before being placed in an incubator at 37°C, 5% carbon dioxide. On the fourth day in vitro (DIV), the supplemented neurobasal medium was replaced with fresh medium.

2.3.7 Neuron-based assay (NBA)

Immunocytochemistry was performed at DIV 14. The volume of medium in each well was first corrected to 40 µl. To produce a dilution of 1:100, 0.4 µl neat serum sample was added directly to each well and incubated for 30 minutes at 37°C, 5% carbon dioxide. Cells were washed with 60 µl ice-cold 2% sucrose (Sigma-Aldrich, USA)/PBS using filter-free plastic pipette tips attached to a glass aspirator. Cells were fixed for ten minutes using 60 µl 4% sucrose/4% formaldehyde at RT. After fixation, cells were washed twice in 60 µl PBS. Forty µl Alexa Fluor 488-conjugated goat-anti human IgG heavy and light chain secondary antibody (Thermo Fisher Scientific, USA) was added (1:750 in PBS) and incubated for 45 minutes at RT. Cells were washed twice more with 60 µl PBS.

Mouse monoclonal antibody against the neuronal marker, microtubule-associated protein 2 (MAP2; Sigma-Aldrich, USA) was used to distinguish neurons from other cell types. As this is an intracellular marker, cell permeabilisation was first required and was achieved by adding 40 µl 0.1% triton per well for ten minutes at RT. Then 40 µl anti-MAP2 (1:2,000 in PBS) was added and incubated for 45 minutes at RT. Following two washes with 60 µl PBS, cells were incubated in 40 µl 1:750 Alexa Fluor 568-conjugated goat anti-mouse IgG heavy and light chain secondary antibody (Thermo Fisher Scientific, USA) for 45 minutes at RT. Cells were washed with 60 µl PBS and 30 µl mounting medium containing 1:1,000 DAPI/PBS was added to the bottom of each well for ten minutes at RT. The cells were then washed once more with 150 µl PBS before visualisation at x40 and x20 objectives with a fluorescence microscope (CKX53, Olympus Corporation, Japan). Photographs were taken with a Rolera-XR digital camera and Volocity 6.6 software (Quorum Technologies, Canada), and with a confocal microscope (MRC 1024; Bio-Rad Laboratories, USA) and LaserSharp 2000 software (Bio-Rad Laboratories, USA).

2.3.8 Astrocyte cultures

Meninges-free cortices were treated in a 50 ml tube (Thermo Fisher Scientific, USA) with 5mls 1:10 trypsin/HBSS for 15 minutes in an incubator at 37°C, 5% carbon dioxide. After rinsing twice with DMEM/15% FBS, 1 ml fresh DMEM/15% FBS was added and the tissue was dissociated by gently pipetting up and down. Debris clumps were carefully removed. Additional medium was added (5 ml per brain), then 7.5 ml of cell suspension was transferred to each 25 ml culture flask (Thermo Fisher Scientific, USA) and flasks were placed in the incubator. After three days, astrocytes were firmly attached to the culture

flask surface. The side of the flasks were firmly hit with the palm of a hand to dislodge any loosely attached cells and microglia. The medium was aspirated and replaced with 30 ml of fresh DMEM/10% FBS. Medium changes were repeated on DIV 6 and 9.

Once cells in the primary culture reached confluence (DIV 9-11), a secondary subculture was prepared to reduce the proportion of contaminating cells, such as microglia, and to enrich the culture for astrocytes. Flasks were centrifuged at 200 G for four minutes, then swirled to remove loosely attached cells. The medium was aspirated, and cells were washed twice with 20 ml sterile PBS. Four ml 1:10 trypsin/HBSS was added and flasks were placed in the incubator for three minutes. The sides of the flasks were then tapped to encourage cell separation. 15 ml DMEM/10%FBS was added to each flask and the contents were transferred to a 50 ml tube. A further 5 ml DMEM/10%FBS was used to rinse remaining cells from the flask and added to the 50 ml tube. Cells were centrifuged at 200 G for four minutes, the supernatant was removed, and cells were resuspended in 3 ml fresh DMEM/Nutrient Mixture F-12 (Thermo Fisher Scientific, USA) with 10% FBS. After counting, a solution of 200 cells per µl (0.2 million cells per ml) was prepared. Twelve thousand cells were plated per well in 96-well plates and these were placed in the incubator. The medium was replaced with DMEM/10%FBS on DIV 3. On DIV 6, when the culture was 95% confluent, the medium was replaced with DMEM/5%FBS and 10 µM cytosine arabinoside (ara-C; Thermo Fisher Scientific, USA) to reduce contaminating cells. Cells were maintained for the next 1-2 weeks by medium changes (DMEM/5% FBS and 10 µM ara-C) every 3-4 days. Three days prior to the astrocyte-based assay, the medium was replaced with DMEM/0.5% FBS and 10 µM ara-C.

2.3.9 Astrocyte-based assay (ABA)

Medium was aspirated from the cells and 50 µl diluted test serum (1:100 in 0.5% BSA/DMEM) was added per well. Plates were placed in the incubator for 30 minutes, then washed twice with 100 µl 4% sucrose/PBS prior to fixation with 50 µl 4% PFA in 4%sucrose/PBS for ten minutes at RT. Following two washes with 110 µl PBS, 50 µl 1:750 goat anti-human IgG (Fc-specific) secondary antibody (Sigma-Aldrich, USA) was added to each well and incubated for 45 minutes at RT. Cells were washed twice with 100 µl PBS and incubated in 50 µl 1:750 Alexa Fluor 488-conjugated rabbit anti-goat IgG heavy and light chain tertiary antibody (Invitrogen, USA) for 45 minutes at RT. Cells were then washed twice with 100 µl PBS per well and permeabilised with 50 µl 0.1% triton for ten minutes at RT. Next, 50 µl 1:1,000 mouse anti-human IgG antibody targeting the intracellular astrocyte marker glial fibrillary acid protein (GFAP; BioLegend, USA) was added for 45 minutes at RT before washing twice with 100 µl PBS. Fifty µl 1:750 Alexa Fluor 568-conjugated donkey anti-mouse IgG heavy and light chain secondary antibody (Invitrogen, USA) was added for 45 minutes at RT. Cells were washed a final two times with 100 µl PBS before visualisation at x10 objective with a fluorescence microscope. Photographs were taken with a Rolera-XR digital camera and Volocity 6.6 software.

2.4 Molecular cloning

2.4.1 Primer and gene fragment reconstitution

Custom lyophilised primers (Invitrogen, USA) and custom GAD65 gene fragments (Integrated DNA Technologies Inc, USA) were centrifuged at 13,000 G for one minute

(Microcentrifuge 5415D; Eppendorf, Germany). Nuclease-free water (Promega Corporation, USA) was used to reconstitute primers to 100 µM and gene fragments to 50 ng/µl. Reagents were then stored at -20 °C.

2.4.2 Gene fragment amplification by polymerase chain reaction (PCR)

PCR reaction volumes of 20 µl were prepared in a 96-well semi-skirted PCR plate with straight edges (Star Lab, USA) and comprised 10 µl Go-Taq Green Master Mix (containing Taq DNA polymerase, deoxynucleoside triphosphates, magnesium chloride, reaction buffers and electrophoresis gel dyes; Promega Corporation, USA), 1 µl 1:20 5^1 forward primer, 1 µl 1:20 3^1 reverse primer, 1 µl double-stranded DNA template and 7 µl of nuclease-free water. Samples were spaced to avoid contamination between adjacent wells and to reduce evaporative losses at plate edges. The PCR plate was sealed with adhesive sealing sheets (Thermo Fisher Scientific, USA) and pulsed in a centrifuge to ensure reagents were at the bottom of wells prior to placement in the PCR instrument (T100 thermal cycler; Bio-Rad Laboratories Inc, USA) for amplification. PCR conditions are stated in chapter 4.

2.4.3 Separation of PCR products by agarose gel electrophoresis (AGE)

Fresh 1x trisaminomethane/acetic acid/EDTA (TAE) buffer (40:20:1) was prepared by adding 20 ml of 50x TAE buffer (Thermo Fisher Scientific, USA) to 980ml of deionised water. Agarose gel (0.8%) was prepared by adding 0.4g of agarose powder (UltraPure agarose; Invitrogen, USA) to 50 ml 1x TAE buffer in a 250 ml conical flask. The solution was heated in a microwave oven until all of the agarose crystals dissolved. The flask was intermittently swirled at RT while the contents cooled to approximately 50 °C, before adding 5 µL DNA

stain (GelGreen Nucleic Acid Gel Stain; New England BioLabs Inc, USA). The solution was poured into a casting tray fitted with combs and casting dams (Cleaver Scientific, UK), with care taken to avoid forming bubbles, and allowed to set as a gel. Combs were removed and the gel was placed into an electrophoresis tank (MultiSUB Midi DUO horizontal electrophoresis unit; Cleaver Scientific, UK) filled with 1x TAE buffer. Then 20 µl of each PCR product and a 1kb DNA ladder (Promega Corporation, USA) was loaded into a separate well by pipette. The tank was connected to a power supply unit (PowerPac Basic; Bio-Rad Laboratories Inc, USA) run at 80 V for 40 minutes. The gel was visualised on a transilluminator (BluPAD Dual LED Blue/White Light Transilluminator; Bio-Helix Co. Ltd., Taiwan). Photographs were captured using the transilluminator's smartphone camera adaptor and a smartphone (iPhone X; Apple, USA).

2.4.4 DNA extraction and purification

Gel slices containing DNA fragments of interest, approximately 100 µl in size, were excised from the agarose gel on the transilluminator using surgical blades (Swann-Morton, UK). A Monarch DNA gel extraction kit (New England BioLabs Inc, USA) was used in accordance with the manufacturer's protocol and all centrifugation steps were performed using a microcentrifuge at 16,000 G for one minute. In brief, gel fragments were added to 400 µl gel dissolving buffer and heated in a 55 °C water bath until dissolved (JB Aqua 12; Grant Instruments, UK). The solution was transferred to a column nested within a collection tube, and centrifuged. The flow-through waste liquid in the collection tube was discarded. Two washes were performed by adding 200 µl DNA wash buffer to the columns followed by centrifugation. Further centrifugation was performed without wash buffer prior to

transferring the column to a clean 1.5 ml tube. A final centrifugation step with 12 µl nuclease-free water eluted the DNA. DNA concentration was measured with a spectrophotometer (NanoDrop 1000; Thermo Fisher Scientific, USA) according to the manufacturer's protocol.

2.4.5 Restriction endonuclease digestion of plasmid vector backbone and GAD65 DNA inserts

For the GAD65 insert digests, 30 µl reactions volumes were prepared in 0.5 ml RNase-free PCR tubes (Thermo Fisher Scientific, USA) with a total DNA content of 200 ng, 1.5 µl NHE1-HF (New England BioLabs Inc, USA), 1.5 µl XH01 (New England BioLabs Inc, USA) and 3 µl CutSmart buffer (New England BioLabs Inc, USA). Volume was adjusted with nuclease-free water (Qiagen, Germany).

The LCE plasmid digest 50 µl reaction volume comprised 2,000 ng DNA, 2.5 µl NHE1-HF, 2.5 µl XH01, 5 µl CutSmart buffer and volume was adjusted with nuclease-free water. The reaction mixes were placed on a heatblock (Digital Heating Shaking Drybath; Thermo Fisher Scientific, USA) at 37 °C for three hours, and then centrifuged at 16,000 G for one minute.

Electrophoresis gel dye (Purple Gel Loading Dye (x6); New England BioLabs Inc, USA) was added (6 µl to 30 µl reactions and 10 µl to 50 µl reactions) and the digest products were separated by AGE before DNA gel extraction and purification, as described above.

2.4.6 Ligation of GAD65 DNA inserts and cut plasmid vector backbone by T4 DNA ligase

Reaction volumes of 10 µl were prepared with 50 ng cut LCE plasmid backbone, 10 ng cut GAD65 DNA inserts, 0.6 µl T4 DNA ligase (New England BioLabs Inc, USA) and 1 µl T4 DNA ligase buffer (New England BioLabs Inc, USA). Volume was adjusted with nuclease-free water. The reaction mixes were incubated in a PCR instrument at 16 °C overnight, then stored at -20 °C.

2.4.7 Bacterial transformation via heat shock

Chemically competent *E. coli* cells (DH5alpha-derivative 5-alpha Competent *E. coli* (High Efficiency; New England BioLabs Inc, USA) were thawed on ice. Ligation products were diluted to 1,000 ng/µl. Transfection mixes made up of 5 µl diluted ligation product and 25 µl *E. coli* cells were incubated on ice for 30 minutes, heat shocked for 45 seconds in a water bath at 42 °C and then returned to ice for five minutes.

2.4.8 Preparation of culture plates

Luria-Bertani (LB) broth was prepared by adding 10 g tryptone (Thermo Fisher Scientific, USA), 5 g yeast (Thermo Fisher Scientific, USA), 5 g sodium chloride (Sigma-Aldrich, USA) and 1 l deionised water. Subsequently, LB-agar was produced by combining 500 ml LB broth and 7.5 g agar (Sigma-Aldrich, USA).

On a dedicated microbiology bench and under a flame, ampicillin 100 mg/ml (Sigma-Aldrich, USA) was added to autoclaved LB-agar (1:1,000 dilution). The mixture was poured onto plastic culture plates (Sigma-Aldrich, USA), and left to set and dry for 30 minutes.

2.4.9 Bacterial outgrowth and extraction of plasmid vectors

Each transformed cell suspension was mixed with 475 µl nutrient-rich medium (SOC Outgrowth Medium; New England BioLabs Inc, USA) before incubation in a heat shaker (Certomat BS-T shaking incubation cabinet; Sartorius, Germany) for one hour, 250 RPM at 37 °C. Samples were then centrifuged for one minute at 5,000 G. The supernatant was replaced with 200 µl fresh nutrient-rich medium. Cells were resuspended by flicking the tubes. One hundred and twenty µl of transformed cells were spread across agar culture plates, which were placed upside down in an incubator at 37 °C overnight.

Multiple colonies were selected for bacterial outgrowth. Five ml LB broth medium with 1:1,000 ampicillin was added to 50 ml polypropylene conical centrifuge tubes (Falcon 50 ml tube; Corning Incorporated, USA). A sterile pipette tip was lightly scratched through each colony and dropped into medium. Tubes were placed in a shaking incubator for 12 hours at 37 °C.

Glycerol stocks of each culture were made by adding 800 µl colony culture to 200 µl glycerol (Sigma-Aldrich, USA). The mixture was vortexed and stored at -20 °C.

2.4.10 Plasmid miniprep

Miniprep extraction and purification of the plasmid vectors containing the GAD65 inserts was performed using a plasmid miniprep kit (Qiagen, Germany) as per the manufacturer's instructions. Briefly, 5 ml of each bacterial culture were pelleted by centrifugation at 8,000 RPM for three minutes at RT. Pellets were resuspended in 250 µl Buffer P1 and transferred to a microcentrifuge tube. The same volume of Buffer P2 was added, and the mixture was inverted until cell lysis was indicated by the solution turning blue. Three hundred and fifty µl Buffer N3 was added, and the mixture was inverted until it turned colourless. Mixtures were centrifuged for ten minutes at 13,000 RPM and 800 µl supernatant was transferred by pipette to a spin column and attached to a vacuum manifold (QIAvac 24 Plus Vacuum Manifold; Qiagen, Germany) until drawn through the spin column. The spin columns were then washed by drawing 0.5 ml Buffer PB through them. The spin columns were attached to collection tubes and centrifuged for one minute at 13,000 RPM to remove residual wash buffer. Spin columns were moved to clean 1.5 ml tubes, and DNA was eluted by adding 50 µl Buffer EB (10 mM TrisCl, pH 8.5) and centrifuging at 13,000 RPM for one minute. DNA concentration was measured by spectrophotometer (NanoDrop 1000; Thermo Fisher Scientific, USA). Samples were diluted to 300 mg/µl with nuclease-free water and frozen at -20 °C.

2.4.11 Confirmation of cloning

Colony PCR reaction mixtures were prepared by adding 0.5 µl forward primer, 0.5 µl reverse primer (both 1:20), 5 µl GoTaqGreen and 4 µl nuclease-free water directly into a well on a 96-well PCR plate. A sterile pipette tip was used to gently scratch a colony and

transfer it to a PCR well. PCR for annealing was undertaken at 67 °C (no gradient). PCR products were separated on AGE, as described above, to indicate which bacterial colonies produced GAD65 insert-containing plasmids. Restriction digest and AGE, as described above, were performed on colony PCR products to indicate which plasmids contained inserts of the anticipated size.

Results of the colony PCR and restriction digest informed selection of samples to send for Sanger sequencing (Sequencing Facility at the Medical Research Council Weatherall Institute of Molecular Medicine) to confirm that the GAD65 inserts were successfully cloned in the correct orientation.

2.4.12 Plasmid maxiprep

To produce sufficient stocks of plasmids for use in experiments, larger scale cultures were performed. Starter cultures were prepared by adding 100 µl glycerol stock to 2 ml LB broth/ampicillin (1:1,000) and placed in a shaking incubator for four hours.

All of the starter culture was poured into a 2-litre conical flask containing 400 ml LB broth/ampicillin (1:1,000). Flasks were covered in tinfoil and placed in a shaking incubator overnight.

Cultures were transferred to large centrifuge buckets and centrifuged at 5,000 RPM (Avanti JE Centrifuge; Beckman Coulter Inc, USA). Supernatants were discarded and pelleted cells containing plasmids were retained.

Plasmids were isolated and purified using a plasmid maxiprep kit (Qiagen, Germany) according to the manufacturer's instructions. Briefly, each bacterial cell pellet was resuspended in 8 ml Buffer P1 and then 8 ml Buffer P2 was added. The suspension was mixed until homogeneously coloured blue and incubated at RT for five minutes. Then 8 ml Buffer P3 was added and mixed until the suspension became colourless. The cell lysate was transferred to a filter cartridge, incubated at RT for ten minutes and filtered into a new tube. Five ml Buffer BB was added and mixed. The lysate was then transferred to a spin column and attached to a vacuum manifold until completely drawn through the column. To wash the DNA, 0.7 ml Buffer ETR was added and drawn through the column. Then 0.7 ml Buffer PE was added and drawn through. To remove residual wash buffer, spin columns were placed into 2 ml collection tubes and centrifuged at 10,000 G for one minute. Spin columns were moved to clean 2 ml tubes. DNA was eluted by adding 400 μl Buffer EB and centrifuging for one minute. DNA concentration was measured by spectrophotometer and samples were frozen at -20 °C.

2.5 Cytokine multiplex immunoassay

Target cytokines were human IL1b, IL2, IL4, IL6, IL10, IL15, IL17A, IL23, TNFa, IFNg, CXCL10 (IP10), soluble CD25 and soluble CD40L. All plasma samples had been kept frozen at -80 °C since collection and were previously unthawed. A custom LegendPlex multi-analyte flow assay kit (BioLegend, USA) with a v-bottom 96-well plate was used according to the manufacturer's instructions. In brief, 25 μl of assay buffer and 25 μl diluted plasma samples (1:1 in assay buffer) was added to sample wells; 25 μl kit standards and 25 μl matrix

were added to standard wells; and 25 µl mixed beads were added to each well. The plate was sealed and covered in aluminium foil to protect it from light while incubated at RT for two hours before being centrifuged at 1,050 RPM for 5 minutes. The supernatant was then discarded by inverting the plate and blotting it on clean paper towels. Wells were washed twice with 200 µl washing buffer per well and the plate was centrifuged at 800 RPM. Twenty-five µl detection antibodies were added to each well. The plate was again sealed and covered in aluminium foil, incubated at room temperature for 30 minutes before being centrifuged at 1,050 RPM for 5 minutes. The supernatant was discarded and 150 µl wash buffer was added to each well. Beads were resuspended by pipetting.

Flow cytometry was performed using a FACSCanto II instrument with an automated high throughput plate sampler (BD, USA), BD FACSDiva version 9.0 software (BD, USA) and an acquisition template provided with the LegendPlex kit. The phycoerythrin channel was selected for reporter and the allophycocyanin channel for bead classification. Samples were automatically acquired from the 96-well plate. Loader settings were as follows: sample flow rate 1.5 µl/sec, sample volume 110 µl, mixing volume 70 µl, mixing speed 180 µl/sec, two mixes and wash volume 400 µl. Ten thousand beads were acquired per plate. Data output was in flow cytometry standard (FCS) format which was processed by LegendPlex data analysis software version 1.0 (BioLegend, USA) to determine concentrations of the 13 cytokines in each well.

2.6 Mass cytometry

2.6.1 Thawing of cryopreserved peripheral blood mononuclear cells (PBMCs)

PBMCs were thawed in a 37 °C water bath and transferred to 15 ml Falcon tubes (Thermo Fisher Scientific, USA) containing 1 ml of pre-warmed RPMI media (Thermo Fisher Scientific, USA) using a plastic Pasteur pipette (Thermo Fisher Scientific, USA). A further 10 ml pre-warmed RPMI media was added to each sample, drop-by-drop. Cells were centrifuged at 400 G for 15 minutes (acceleration 9, deceleration 7). The supernatant was aspirated and cell pellets were resuspended in 1 ml RPMI media with DNase (5 µl/ml) and incubated for ten minutes in a 37 °C water bath. One ml of RPMI media with EDTA (1:100, 0.5 mM) was added to make a total volume of 2 ml. A 20 µl sample was taken for cell counting. Another 8 ml of RPMI/EDTA was added to make a total volume of approximately 10 ml, which was centrifuged at 400 G for 15 minutes. During centrifugation, live cells were counted using a haemocytometer. After centrifugation, the supernatant was aspirated and cells were resuspended in Maxpar cell staining buffer (Fluidigm, USA) at a concentration of 3 million cells/0.5 ml. The centrifugation step was repeated, the supernatant was aspirated and cells were resuspended in 500 µl Maxpar PBS (Fluidigm, USA).

2.6.2 Cisplatin staining for cell viability

A working solution of 3 M Cell-ID cisplatin (Fluidigm, USA) was prepared by adding 6 µl 5 mM cisplatin stock to 10 ml Maxpar PBS. A final cisplatin concentration of 1.5 µM was obtained by mixing 0.5 ml cisplatin solution and 0.5 ml cell suspension. This was incubated for five minutes at RT and then cisplatin staining was quenched by 5 ml Maxpar cell staining

buffer. Cells were centrifuged at 400 G for five minutes and resuspended completely in 1 ml 1x Fix Buffer (Fluidigm, USA) before incubation on ice for 15 minutes.

2.6.3 Barcoding for sample multiplexing

The palladium isotope barcoding kit (Fluidigm, USA) was thawed in a fridge at 4 °C and each barcode was resuspended in 100 µl 1x barcode permeabilisation buffer immediately prior to use.

Cells were washed in 1 ml 1x barcode permeabilisation buffer with centrifugation at 400 G for five minutes. The supernatant was aspirated, and the wash and centrifugation were repeated. Each PBMC sample was resuspended in 800 µl 1x barcode permeabilisation buffer and mixed with a distinct barcode before incubation on ice for 30 minutes, with gentle tapping of tubes at 15 minutes. Samples were washed in 2 ml cell staining buffer and centrifuged at 400 G for five minutes. The supernatant was removed and the cell pellet was resuspended in 50 µl cell staining buffer. All barcoded PBMC samples were then combined in a single 15 ml Falcon tube.

2.6.4 Antibody staining

The Maxpar Human Immune Monitoring Panel kit (Fluidigm, USA) contains 29 different antibodies pre-optimised for mass cytometry. An antibody/cell staining buffer cocktail was prepared by adding 22 µl of each antibody to 308 µl cell staining buffer on ice.

In order to block unwanted Fc receptor staining, 100 µl Human Trustain FcX (BioLegend, USA) was added to the multiplexed samples and incubated for ten minutes at RT. Nine hundred µl antibody/cell staining buffer cocktail was added and incubated for 15 minutes at RT. Following a gentle vortex (LP Vortex Mixer; Thermo Fisher Scientific, USA), there was another 15-minute incubation. Cells were washed in 5 ml cell staining buffer, centrifuged at 800 G for five minutes and the supernatant was aspirated. Fresh 4% formaldehyde in PBS/EDTA (1:100) was prepared by mixing 2.5 ml 16% formaldehyde (Thermo Fisher Scientific, USA) 7.5 ml Maxpar PBS and 100 µl 0.5 M EDTA (Thermo Fisher Scientific, USA). The 4% formaldehyde solution was added to the cells, gently vortexed and incubated for ten minutes at RT, with intermittent vortexing. Cells were centrifuged at 800 G for ten minutes (acceleration 9, deceleration 9), the supernatant was aspirated, and cells were resuspended in 5 ml freezing media (90% FBS/10% DMSO) and split among five 1 ml aliquots in 1.8 ml cryotubes. The cryotubes were placed in a rate-controlled cell-freezing container at -80 °C overnight and transferred to cryogenic storage the following day.

2.6.5 Iridium staining of DNA for identification of nucleated cells

On the day of mass cytometry, an aliquot of barcoded and stained cells was thawed in a 37 °C water bath. One ml of warm RPMI media was added before transferring to a 15 ml Falcon tube and centrifugation at 800 G for five minutes. A working solution of iridium was prepared by adding 5 µl 500 µM stock (Fluidigm, USA) to 20 ml fix & perm buffer (Fluidigm, USA). After aspiration of the supernatant, the cell pellet was resuspended in 2 ml of iridium solution and incubated for one hour at RT.

2.6.6 Mass cytometry sample acquisition

Cells in iridium solution were centrifuged at 800 G for five minutes and the supernatant was aspirated. The pellet was washed twice in 4 ml of cell acquisition solution (CAS; Fluidigm, USA) with centrifugation at 800 G for eight minutes. Cells were resuspended in CAS to a target concentration of one million cells/ml and kept on ice. Immediately before sample acquisition, EQ four element calibration beads (Fluidigm, USA) containing 140Ce were added to the cell solution at a ratio of 1:5. The cell/CAS/EQ bead solution was passed through a 35 μm cell-strainer into a 5 ml polypropylene tube (Thermo Fisher Scientific, USA) and placed in the sample loader of the mass cytometry instrument (Helios system; Fluidigm, USA) equipped with a wide-bore autoinjector and CyTOF software version 7.0 (Fluidigm, USA). A mass cytometry channel template provided with the Maxpar Human Immune Monitoring Panel kit (Fluidigm, USA) was selected, as well as palladium isotype channels for barcoding. After instrument calibration and tuning, bead sensitivity testing and system preconditioning with CAS, sample acquisition was undertaken at a rate of 250-500 events per second until completion (i.e., no pre-defined event limit). Instrument recalibration and retuning were repeated every four hours. Data output was in FCS format.

2.6.7 Pre-processing of raw data for analysis

CyTOF software was used to normalise raw data to the calibration beads, concatenate files and debarcode using palladium isotope intensities to assign individual cells to their respective samples of origin. A density-driven automated gating script written by Dr Camilla Pang and adapted by Dr Emma Sutton was run in RStudio Version 1.2.1335 (RStudio PBC, USA) to ArcSinh-transform data, perform clean-up with Gaussian parameters

(width, offset, centre and residual) and to gate out debris, doublets and dead cells. DNA/CD45 and CD3/CD19 were used to gate immune cells and singlets, respectively. Live intact single cells were taken forward for analysis – CD19-positive/CD3-negative cells (B cells), CD19-negative/CD3-positive cells (T cells), and CD19-negative/CD3-negative cells (other immune cells).

2.7 Clinical phenotyping database for the DRE study

I designed the database in Microsoft Excel 2019 for Mac (Microsoft Corporation, USA), with data fields and pre-populated responses selected to create a comprehensive range of likely possibilities, informed by clinical guidelines[265,266] and literature relating to epilepsy aetiology,[267–269] classification,[270–272] seizure semiology,[273–275] magnetic resonance imaging in epilepsy,[276,277] and other relevant clinical information.[278,279] In the live database, the response lists were presented in drop-down menus and an administrator could add extra options if required. The database was constructed using MySQL (Oracle Corporation, USA) and PHP scripting language version 7.4.0 (PHP Group, USA) by Archana Ramesh and hosted on a Drupal content management platform version 7.0 (Drupal Association, USA) to create a website-based user interface. Drupal coding and website maintenance was undertaken by Mohammad Yaqub.

2.8 Statistical analysis

Statistical analysis was performed in Microsoft Excel 2019 for Mac (Microsoft Corporation, USA), Prism version 8.4.3 for Mac (GraphPad, USA) and RStudio version 1.2.1335 (RStudio PBC, USA). Further details are described in the appropriate sections.

Definition of sensitivity = number of true positive results /(number of true positive results plus number of false positive results).

Definition of specificity = number of true negative results/(number of false positive results plus number of true negative results).

Chapter 3 Clinical and serological observations

3.1 Introduction

Neuronal surface-directed autoantibodies (NSAs), such as those directed against leucine-rich glioma inactivated-1 (LGI1), are considered pathogenic in autoimmune encephalitis (AIE), which often features prominent seizures and responds preferentially to immunotherapy compared to anti-seizure medications (ASMs).[53,122,239,280] NSAs or high levels of autoantibodies targeting glutamic acid decarboxylase-65 (GAD65), an intraneuronal enzyme, can be detected in the serum of people with more isolated forms of epilepsy who lack core AIE features.[51,111,281] The reported frequency, associated clinical features and overall clinical significance of autoantibodies in people with isolated epilepsy are, though, unclear, particularly in the context of GAD65 autoantibodies. Improved understanding of the role of autoantibodies in epilepsy could help to identify cases with an underlying immune aetiological component, which are currently considered to be of unknown origin. This could permit the use of existing immunotherapy agents and the development of novel therapies to improve epilepsy management.

The aims of the work in this chapter are to:

- estimate the prevalence of autoantibodies in epilepsy and to consider their clinical relevance;
- identify clinical features associated with autoantibody status;
- report the observed clinical features of epilepsy patients with GAD65 autoantibodies.

I will describe two large studies of autoantibodies and epilepsy. The first involves a cohort of adults with new-onset focal epilepsy (NOFE), as this is often how AIE clinically presents. Data from this study has been published (McGinty et al., 2021;[282] see **Appendix A**) and I would particularly like to acknowledge the contribution by Dr Teresa Moloney and Selina Thomsen to the laboratory work. The second focuses on drug-resistant epilepsy (DRE), providing a valuable control group and the potential opportunity to address questions regarding the long-term evolution of autoantibodies. My overarching hypothesis is that a subgroup of DRE patients may have an immune-related mechanism as the basis for drug-resistance.

3.2 New-onset focal epilepsy and autoantibodies

Between 09/12/2011 and 04/11/2015, consecutive adult patients (≥18 years) with a diagnosis of new-onset focal epilepsy and a first seizure within the previous 12 months were prospectively recruited from epilepsy outpatient clinics at the Oxford University Hospitals NHS Foundation Trust. I screened 241 patients for study suitability; clinically phenotyped 150 participants; performed data analysis; and collected long-term follow-up information.

A single serum sampled was obtained from each patient, along with detailed clinical phenotyping data and results of investigations (**Table 8**). An Antibody Prevalence in Epilepsy and Encephalopathy (APE2) score[61,283] (**Table 9**) was calculated and clinical information was assessed for possible or definite autoimmune encephalitis against explicit diagnostic criteria described by Graus et al.[284] **(Appendix B).** Subsequently, one- and three-year modified Rankin Scores (mRS) were ascertained from patients with NSAs.

Table 8: Phenotypic information captured for participants with new-onset focal epilepsy

For all patients, single time-point information was recorded on the day of serum sampling. Autoimmune encephalitis criteria defined by Graus et al.[284] *AIE*, autoimmune encephalitis; *ASM*, anti-seizure medicine; *EEG*, electroencephalogram; and *MRI*, magnetic resonance imaging.

Clinical features
Sex
Autoantibody status
Date of birth
Date of study recruitment
Date of first seizure
Epilepsy risk factors (neonatal, perinatal, focal neurological insults, family history of epilepsy or Alzheimer's disease)
Formal psychiatric disorder prior to epilepsy diagnosis
Personal or family history of autoimmunity
Personal history of malignancy
History of status epilepticus
Self-reported neuropsychiatric changes (memory/psychosis/mood/anxiety)
Number of seizures in 2/6/12/24/36/48 months from onset
Total number, type and duration of ASMs trialled
Non-ASM medications including immunotherapy trials for seizure-control (date/type/route/course length/dose)
Number of seizures in first 3/6/12/24/36/48 months after ASM commenced
Seizure-cessation reached (Yes/No)
Time to seizure-cessation from starting ASM (months)
Adverse effect from ASM
Clinical impression of AIE
Investigations
Serum sodium
MRI result
EEG result
Clinical assessments/scores
Hospital Anxiety and Depression Score (HADS)
Addenbrooke's Cognitive Examination-Revised (ACE-R) score
Quality of Life in Epilepsy-31 (QOLIE-31) score
Antibody Prevalence in Epilepsy and Encephalopathy (APE2) score
Autoimmune encephalitis (clinical diagnosis and as defined by Graus et al.[284])
Modified Rankin Score (mRS)

Table 9: APE2 score criteria.
The maximum APE2 score is 18 points. A total score of 4 or more points is considered suggestive for underlying pathogenic autoantibodies.[283] *APE2*, Antibody Prevalence in Epilepsy and Encephalopathy; *CSF*, cerebrospinal fluid; and *MRI*, magnetic resonance imaging.

Criteria	*Points*
Faciobrachial dystonic seizures	+3
Brain MRI consistent with encephalitis	+2
CSF inflammation	+2
Facial dyskinesias without faciobrachial dystonic seizures	+2
Seizures refractory to at least two anti-seizure medicines	+2
Systemic malignancy within five years of neurological symptom onset	+2
Viral prodrome	+2
Autonomic dysfunction	+1
Neuropsychiatric changes	+1
New-onset, rapidly progressive mental status changes or new-onset seizure activity	+1

For NSAs, sera were tested against autoantigen-expressing live HEK293 cells (live cell-based assays (CBA), **Figure 8**); and for reactivity with the surface of live cultured hippocampal neurons.[85,285] Antibodies to GAD65 were determined using a commercial radioimmunoprecipitation assay (RIPA).[286]

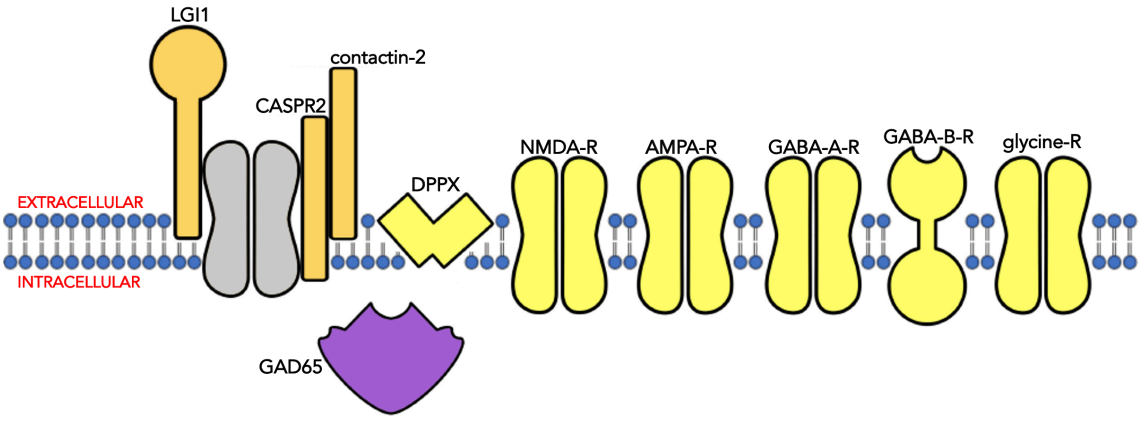


Figure 8: Serum autoantibody detection.
Live CBAs were used to detect serum NSAs to the following specific target antigens: LGI1, CASPR2, contactin-2, DPPX, NMDA-R, AMPA-R, GABA-A-R, GABA-B-R and glycine-R. A radioimmunoprecipitation assay (RIPA) detected antibodies to GAD65. Live neuronal-based assays tested for antibody binding to unspecified neuronal surface antigens. Figure adapted from Varley et al., 2016.[287] The voltage-gated potassium channel is coloured grey, with associated proteins orange. *AMPA-R*, alpha-amino-3-hydroxy-5-methyl-4-isoxazolepropionic acid receptor; *CASPR2*, contactin-associated protein-2; *CBA*, cell-based assay; *DPPX*, dipeptidyl-peptidase-like protein 6; *GABA-A-R*, gamma-amino butyric acid receptor type A; *GABA-B-R*, gamma-amino butyric acid receptor type B; *GAD65*, glutamic acid decarboxylase 65; *glycine-R*, glycine receptor; *LGI1*, leucine-rich glioma inactivated-1; *NMDA-R*, N-methyl-D-aspartate receptor; *NSA*, neuronal surface-directed autoantibody; and *RIPA*, radioimmunoprecipitation assay.

Of 241 recruited patients, I identified 22 who required exclusion from the study (**Table 10**).

Table 10: Patients excluded from the study
Twenty-two patients were excluded.

Reason for exclusion	*Number of patients*
Focal epilepsy diagnosis unconfirmed	9
Epilepsy diagnosis >12months	5
Generalised epilepsy	3
No serum samples received	2
<18 years	1
Duplicate registration	1
Clinical information unavailable	1

One hundred and nine of the remaining 219 (49.8%) participants were female and the median age was 49 years (range 16-91). In 23/219 (10.5%) patients, serum NSAs were detected across candidate and novel autoantigens (**Table 11**). Target antigens were LGI1 (n=3); contactin-associated protein-like 2 (CASPR2, n=4); contactin-2 (n=1); N-methyl-D-aspartate receptor (NMDA-R, n=4); gamma-amino butyric acid type A and B receptors (GABA-A-R, n=2; GABA-B-R, n=2; both n=1); glycine receptor (n=1); and alpha-amino-3-hydroxy-5-methyl-4-isoxazolepropionic acid receptor (AMPA-R, n=1). An additional five patients had antibodies to the surface of live neurons, without an established antigen. No dipeptidyl-peptidase-like protein 6 (DPPX) or high-titre GAD65 antibodies were detected. Overall, from the 23 people with NSAs, nine had a clinical diagnosis of AIE, with 7/9 fulfilling published criteria for this diagnosis.[284] By contrast, none of the 196 without NSAs had a clinical diagnosis of AIE ($p<0.0001$; Fisher's exact test).

Table 11: Features of NOFE patients with positive serum autoantibody results

Positive serum autoantibody results against either established specific antigenic targets or unidentified target antigens with IgG directed against live neurons. Positive APE2 score=≥4.[283] AIE diagnostic criteria outlined by Graus et al.[284] were applied and the clinical impression (according to a consultant epileptologist) was noted. Positive results are shaded in green. All patients were negative for DPPX and GAD65 antibodies. Potentially unidentified target antigens were suggested in five (patients 19-23) with IgG-positivity to the surface of live neurons only. Notable presentations include epilepsia partialis continua affecting the left-side face (patient 13, GABA-A & -B-R Abs); convulsive status epilepticus (patient 15, GABA-B-R Abs); and transient epileptic amnesia (patient 16, AMPA-R Abs). *Ab*, antibody; *AI LE*, autoimmune limbic encephalitis; *AIE*, autoimmune encephalitis; *AMPA-R*, alpha-amino-3-hydroxy-5-methyl-4-isoxazolepropionic acid receptor; *APE2*, Antibody Prevalence in Epilepsy and Encephalopathy; *CASPR2*, contactin-associated protein-2; *DPPX*, dipeptidyl-peptidase-like protein 6; *GABA-A-R*, gamma-amino butyric acid receptor type A; *GABA-B-R*, gamma-amino butyric acid receptor type B; *GAD65*, glutamic acid decarboxylase 65; *glycine-R*, glycine receptor; *IgG*, immunoglobulin G; *LGI1*, leucine-rich glioma inactivated-1; *NMDA-R*, N-methyl-D-aspartate receptor; and *NOFE*, new-onset focal epilepsy.

Patient			Serum antibody									Clinical information		
No.	Age	Sex	LGI1	CASPR2	NMDA-R	GABA-A-R	GABA-B-R	AMPA-R	Contactin-2	Glycine-R	Neurons	APE2 score	Criteria-based AIE diagnosis	Clinical impression of AIE
1	54	M	+								+	6	Possible AIE	Yes
2	59	F	+								+	4	No	Yes
3	61	M	+								+	2	No	No
4	28	M		+								2	No	No
5	41	F		+								2	No	No
6	55	F		+								6	Definite AI LE	Yes
7	79	M		+							+	3	Definite AI LE	Yes
8	18	F			+						+	8	Definite NMDA encephalitis	Yes
9	36	F			+							2	No	No
10	60	F			+							4	Definite NMDA encephalitis	Yes
11	68	F			+	+						1	No	No
12	37	F				+						2	No	No
13	77	F				+	+				+	8	Possible AIE	Yes
14	36	F					+					2	No	No
15	55	F					+				+	9	Definite AI LE	Yes
16	63	M						+			+	2	No	No
17	75	F							+			1	No	No
18	69	F								+		4	No	No
19	37	M									+	2	No	No
20	55	F									+	4	No	No
21	69	M									+	4	No	Yes
22	77	F									+	2	No	No
23	91	M									+	1	No	No

To investigate the relationships between the multiple sets of variables, I collaborated with Dr Adam Handel to perform dimensionality reduction using multiple factor analysis. This showed that the patients were a highly heterogeneous group overall (**Figure 9A**). However, those with NSAs displayed modest clustering, largely driven by those who fulfilled criteria for AIE (**Figure 9B**).

Univariate analysis identified eleven clinical parameters that differed significantly between patients with and without NSAs: age ($p=0.04$), piloerection ($p=0.02$), epilepsy risk factors ($p=0.049$), lesional MRI ($p=0.04$), self-reported mood problems ($p=0.007$), ACE-R attention ($p=0.01$), ACE-R total score ($p=0.04$), QOLIE-31 score ($p=0.02$), formally diagnosed neuropsychiatric abnormalities ($p=0.03$), inflammatory cerebrospinal fluid (CSF) ($p=0.004$), and limbic system changes on MRI ($p=0.0002$). A multivariate stepwise regression model allocated weighted scores to six of these parameters: age ≥54 years = +1, self-reported mood disturbance = +1, limbic system MRI signal changes = +2, ictal piloerection = +2.5, ACE-R attention score ≥16 = -1.5, and epilepsy risk factors = -1.5 (**Figure 10**). The probability of NSA positivity increased with higher scores (Spearman's $\rho=0.99$, $p<0.0001$).

Receiver operating characteristic (ROC) curve analysis confirmed these features were strongly predictive of NSA status (area under the curve (AUC) = 0.83, total score ≥0, sensitivity = 66.7%, specificity = 84.9%; **Figure 11A**). Conversely, the APE2 score performed less well in predicting NSA status (AUC = 0.68, sensitivity = 43.5%, specificity = 79.1%) but more accurately predicted criteria-defined AIE, particularly when associated with NSAs (AUC = 0.94, sensitivity = 85.7%, specificity = 78.8%; **Figure 11B**).

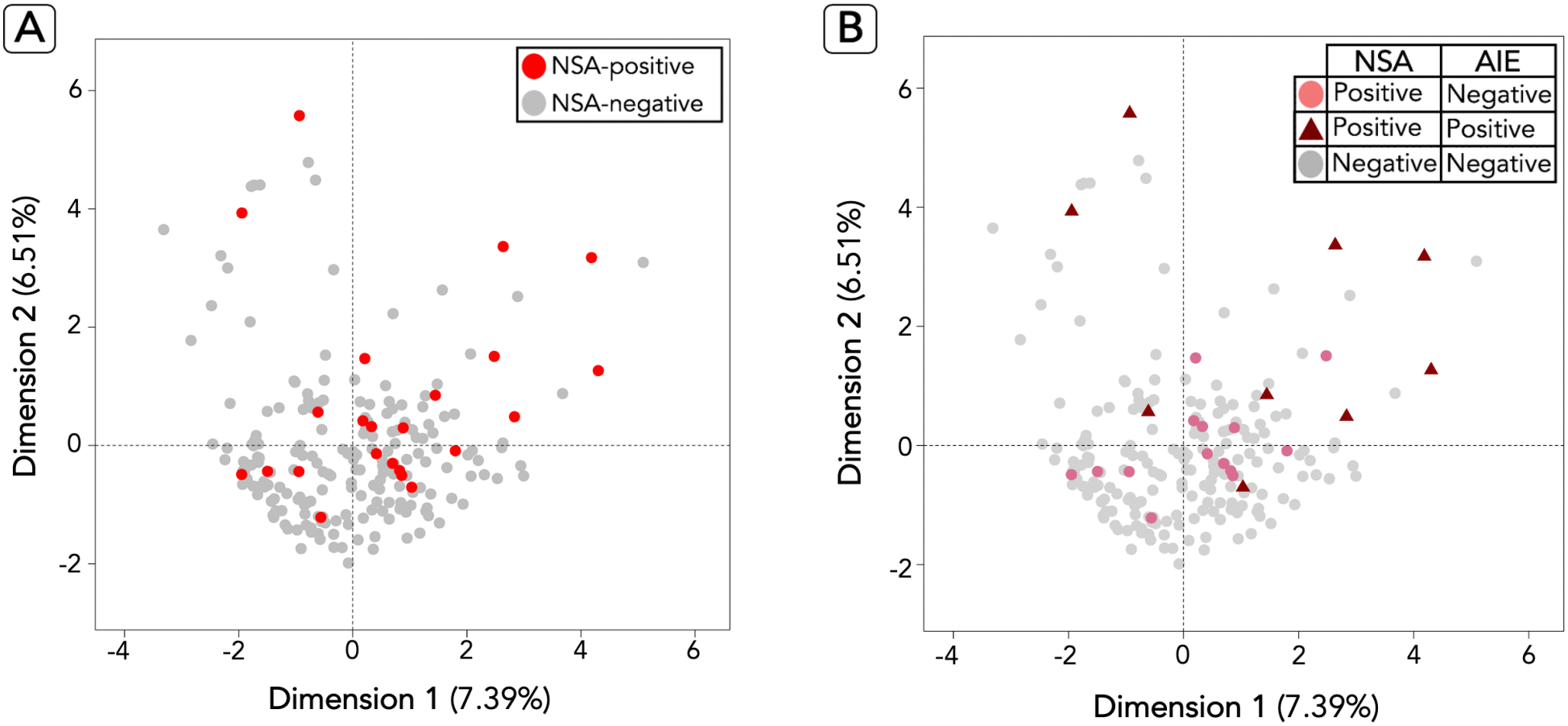


Figure 9: Dimensionality reduction with multiple factor analysis

Multiple factor analysis with the first two dimensions shown. **(A)**: NSA-positive (red circles) and NSA-negative (grey circles). Overall, the cohort is highly heterogeneous. **(B)**: NSA-positive patients without AIE (pink circles), NSA-negative patients without AIE (grey circles) or NSA-positive patients with AIE (brown triangles). NSA-positive patients showed modest clustering, largely driven by those who fulfilled diagnostic criteria for AIE. *AIE*, autoimmune encephalitis; and *NSA*, neuronal surface-directed antibody.

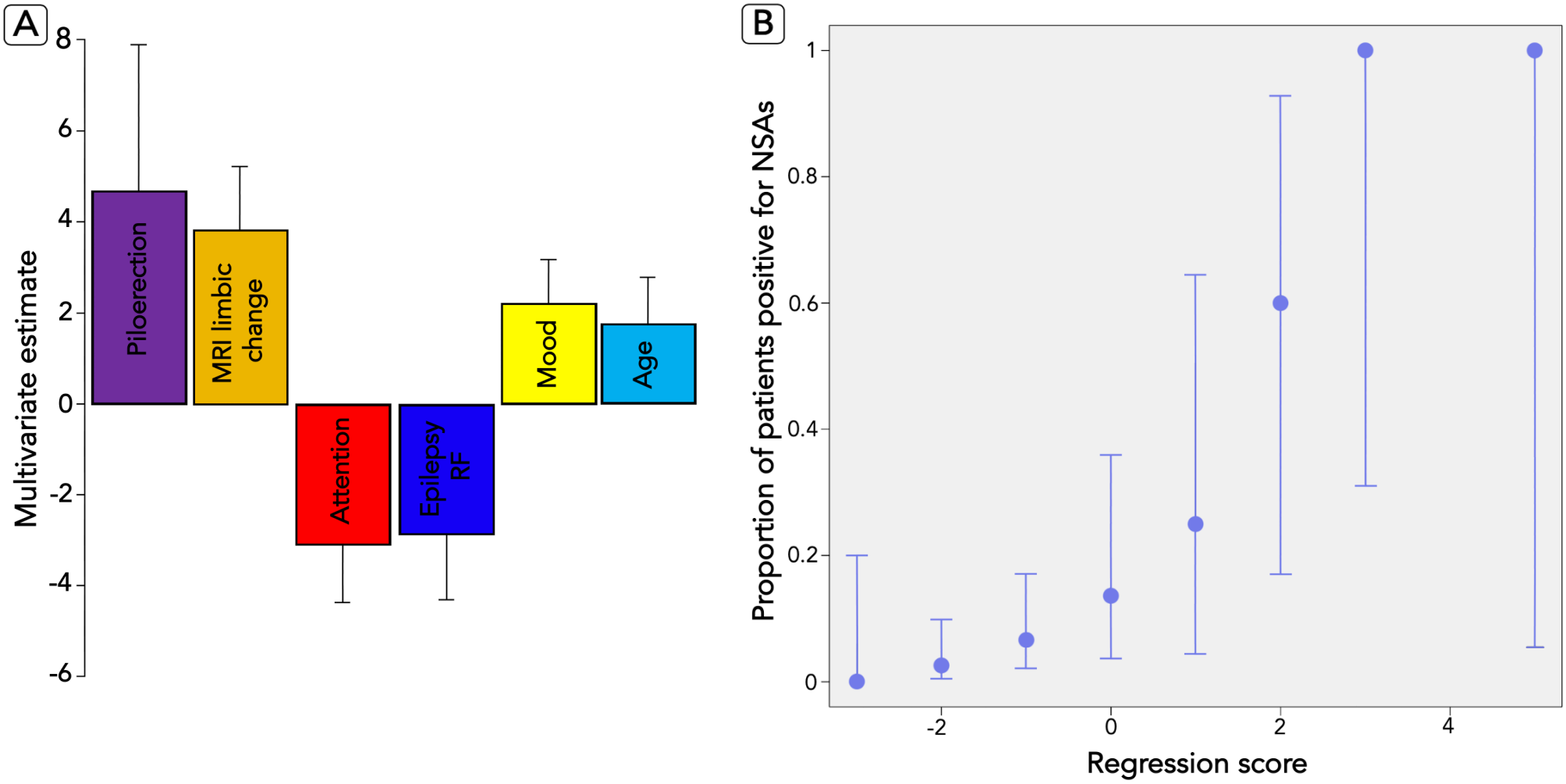


Figure 10: Multivariate stepwise regression model

(A): The weighting and standard error of each factor within the regression model. (B): The proportion of patients with NSAs by regression model total score. Error bars show 95% confidence intervals. *NSA*, neuronal surface-directed antibody; and *RF*, risk factors.

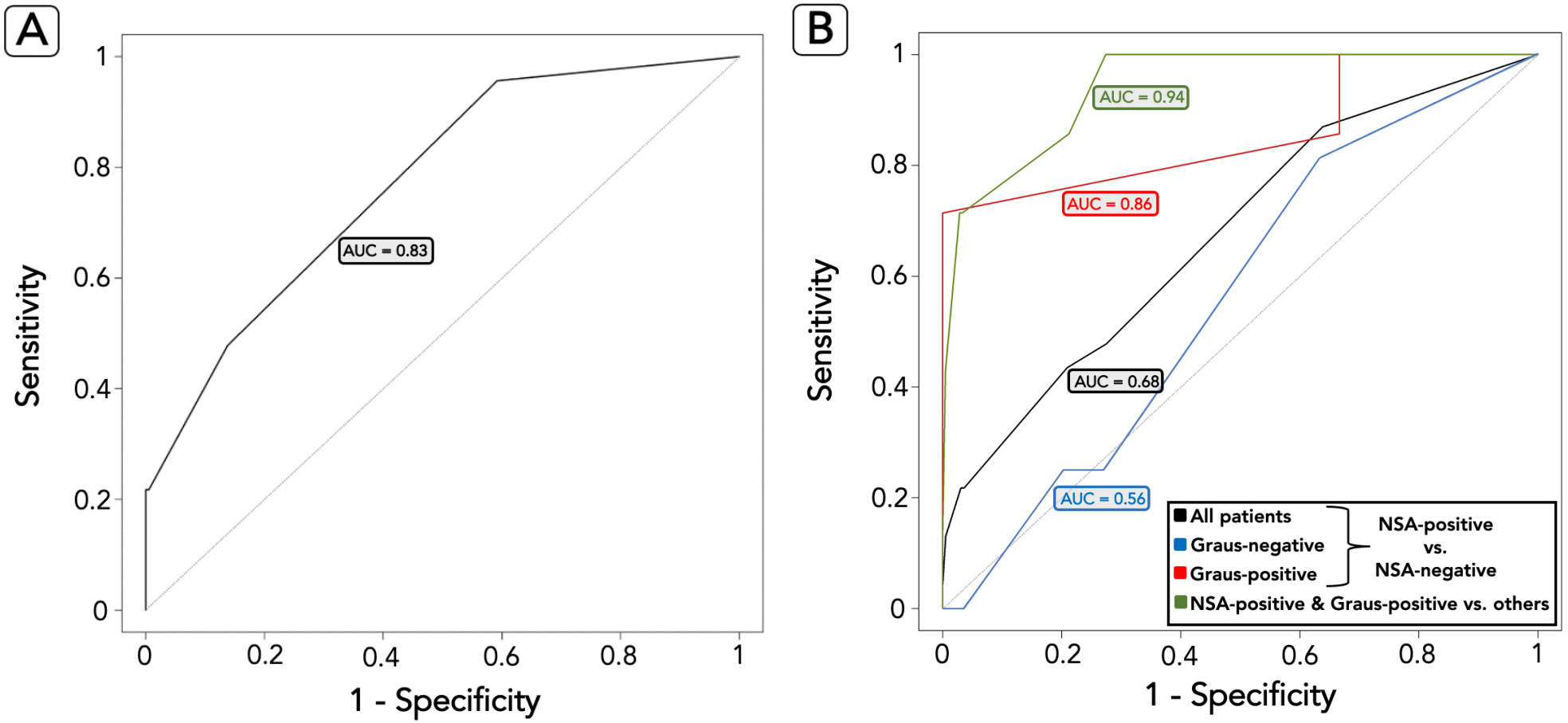


Figure 11: ROC curves

(A): ROC curve of the regression model total score for predicting NSA status across all patients. **(B):** ROC curve of the APE2 score for predicting NSA status across all patients (black), patients without AIE (blue), patients with AIE (red); and predicting NSA-positive AIE across all patients (green). AIE diagnostic criteria defined by Graus et al.[284] *AIE*, autoimmune encephalitis; *APE2*, antibody prevalence in epilepsy and encephalopathy; *AUC*, area under curve; *NSA*, neuronal surface-directed antibody; and *ROC*, receiver operating characteristic.

Immunotherapy was given as part of routine clinical care to 6/7 (85.7%) NSA-positive patients who fulfilled criteria for AIE, versus 1/16 (6.3%) NSA-positive cases without AIE (p=0.0004, Fisher's exact test). Compared to the seven NSA-positive patients who received immunotherapy, those with NSAs but who did not have immunotherapy showed less neurological disability at 1- and 3-year follow-up (p<0.05 for both time points); with 11/16 (68.8%) asymptomatic at 3 years (**Figure 12**).

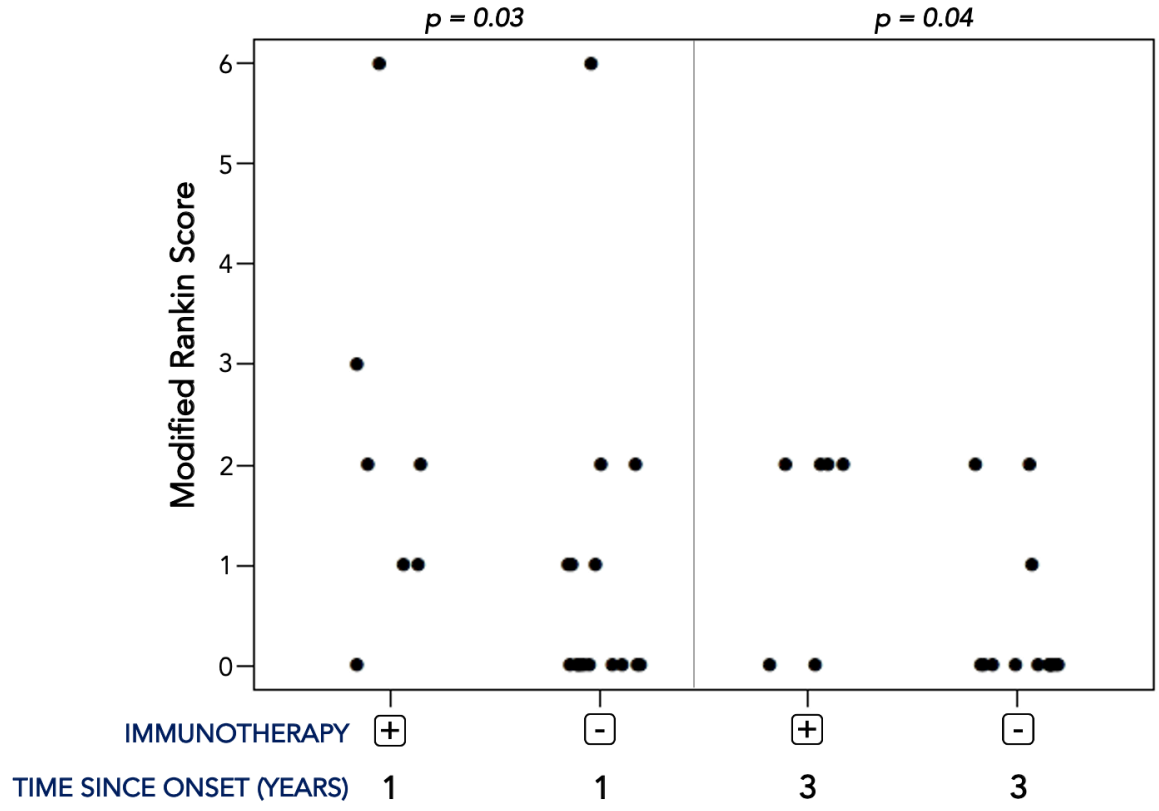


Figure 12: Scatter plots of mRS scores in NSA-positive patients by immunotherapy status over time
Degree of neurological disability (as indicated by the mRS score) among NSA-positive patients by immunotherapy status at 1- and 3-year follow-up assessments (Mann Whitney U test, p-value <0.05). The mRS scale was selected as a clinical outcome measure because it is a widely understood method of communicating levels of neurological disability. Joining data points for each patient to demonstrate improved, static or worse disability at 1 and 3 years would offer useful additional outcome information. However, this was not feasible in practice, as 30/32 scores lay between 0 and 3 points (i.e., there was too much overlap). In future, a measure of functional status with greater granularity could be adopted. *NSA*, neuronal surface-directed antibody; and *mRS*, modified Rankin score.

3.3 Drug-resistant epilepsy and autoantibodies

Having explored autoantibodies in NOFE, I then longitudinally followed-up patients with drug-resistant epilepsy (DRE). For this study, I recruited the first 100 patients, designed the database for in-depth clinical phenotyping, undertook data capture and database entry, clinically reviewed participants at research clinic follow-up visits, and tested patient sera for NSAs. Also, I tested all patient sera for GAD65 autoantibodies using a novel CBA which I developed (described in Chapter 4). In addition, I prepared primary neuron cultures and tested all patient sera for surface reactivity to cultured neurons and astrocytes.

Between January 2018 and November 2019, consecutive people with DRE were recruited from adult epilepsy outpatient clinics at the Oxford University Hospitals NHS Foundation Trust. DRE was defined as "failure of adequate trials of two tolerated and appropriately chosen and used [ASM] schedules (whether as monotherapies or in combination) to achieve sustained seizure freedom".[13] Patients with acute symptomatic seizures only were not eligible for study inclusion. A further five follow-up visits at four-month intervals were planned for each patient. Epilepsy patients who were seizure-free for a minimum of 12 months taking ASM monotherapy were recruited as disease controls and assessed at a single time-point.

Serum samples were provided by patients at each visit for testing against the same panel of ten specific autoantibodies used in the NOFE study, with GAD65 autoantibodies detected by a novel permeabilised CBA rather than RIPA. Screening for surface reactivity to neurons and astrocytes was also performed (methodological details are described in Chapter 2).

Astrocyte-based assays (ABA) were employed to screen for astrocyte surface-directed autoantibodies of potential pathological relevance. There is growing evidence to implicate astrocyte dysfunction in epilepsy[288–290] and seizures can feature in some neurological conditions associated with autoantibodies against astrocyte proteins, such as glial fibrillary acidic protein (GFAP) astrocytopathy[291] and neuromyelitis optica spectrum disorders (NMOSD)[292]. The Oxford Autoimmune Neurology Group (OANG) has an interest in these disorders. My prior involvement in helping to establish a continuous pipeline for astrocyte cultures within the laboratory meant that it was logistically feasible to extend the already broad antibody screening panel to include astrocyte-based assays. The development and optimisation of additional glia cell cultures would not have been possible within the available time, although data do exist for microglial[293] and, less so, oligodendrocyte[294,295] involvement in epilepsy.

A purpose-built clinical phenotyping database (**Table 12**) was used to record a comprehensive and detailed epilepsy history for each study participant. To aid consistency in data capture, I designed the database with extensive lists of pre-populated responses within each field. Researchers selected from these options instead of inputting free-text (**Table 13** and **Appendix C**).

Regrettably, all patient follow-up visits and laboratory work ceased in March 2020 due to the SARS-CoV-2 pandemic. Subsequently, the planned longitudinal data element of the project was incomplete for some participants.

Table 12: Clinical phenotyping database – main sections

The database had 400 data fields organised under the headings below. The components of the database were selected to provide a comprehensive clinical epilepsy review, to take account of the information reported in other large epilepsy/autoimmune epilepsy/autoimmune encephalitis studies, and to focus on autoimmunity and seizure semiology in detail. *ASM*, anti-seizure medicine; *CSF*, cerebrospinal fluid; *CT*, computed tomography; *DRE*, drug-resistant epilepsy; *EEG*, electroencephalogram; *IT*, immunotherapy; *ITU*, intensive therapy unit; *PET*, positron emission tomography; *SE*, status epilepticus; *SF*, seizure-freedom; *SFE*, seizure-free epilepsy; and *VNS*, vagus nerve stimulation.

Key demographics
Normalised date of birth
Biological sex
Ethnic background
Date of/age at enrolment
Social History
Living circumstances
Relationship status
Employment status
Highest level of education
Alcohol intake
Smoking status
Illicit drug use
Driving status
Medical History
Known autoimmune disease(s) prior to study enrolment (with onset date of symptoms)
Mental health history (formal psychiatric diagnosis and onset date; history of detention under the Mental Health Act; history of peri-ictal psychosis)
Current malignancy (diagnosis, date of diagnosis, treatment)
Previous (cured) malignancy (diagnosis, date of diagnosis, treatment, date of last follow-up)
Other medical conditions excluding chronic autoimmune, malignancy and mental health
Current non-epilepsy-related medications
Epilepsy History
Handedness
Presumed epilepsy aetiology
Specific epilepsy syndrome
Known epilepsy risk factor(s)
Total Number of 1st-degree relatives (parent, sibling or child) with epilepsy and cause in each case
Additional relevant family history
Known genetic mutations pre-enrolment
Seizure onset localisation
Date of/age at first afebrile and unprovoked seizure
Date of/age at epilepsy diagnosis
Status epilepticus as first presentation of epilepsy
Status epilepticus after epilepsy onset
Total number of episodes of status epilepticus by subtype (convulsive SE, epilepsia partialis continua, non-convulsive SE, refractory SE (not controlled by 1st/2nd line drugs), super refractory (not controlled by 3rd line anaesthetic agent or continuing for ≥24 hours after anaesthesia started), undefined SE
Encephalitis at epilepsy onset
Total number of generalised tonic-clonic seizures in lifetime
Longest ever period of seizure-freedom
Total no. seizure-related ITU admissions in lifetime
Total no. seizure-related Accident & Emergency Department attendances in lifetime

Seizure-related injuries
Epilepsy Investigations
MRI brain scan key finding
PET-CT brain scan key findings
Neuropsychology assessments (baseline and repeat(s))
EEG key findings
Type(s) of EEG performed (ambulatory, routine, sleep, in-patient video-EEG, intracranial)
Localisation suggested by EEG
Syndrome suggested by EEG
Seizure profile
Seizure facilitating factors/triggers
Reflex epilepsy trait(s)
Seizure type(s), most frequent first: motor or non-motor onset, very first feature(s) experienced at onset (aura), early observed ictal clinical signs, seizure frequency, seizure clusters
Non-pharmacological epilepsy treatments
VNS (active at time of enrolment)
Ketogenic diet
Epilepsy surgery (date and pathology)
Coexisting psychogenic non-epileptic seizures
CSF autoantibody tests prior to study enrolment (autoantibody, date of test, titre)
Serum autoantibody tests prior to study enrolment (autoantibody, date of test, titre)
Immunotherapy
IT agent(s) primarily for seizure control (drug, dose, course description, start date, clinical response)
IT agent(s) primarily for non-seizure-related indication (indication, drug, dose, course description, start date, clinical response)
Clinical assessments/scores (all patients)
Addenbrooke's Cognitive Examination-Revised (ACE-R) score
EpiTrack score
General Anxiety Disorder-7 (GAD-7) score
Hospital Anxiety and Depression Score (HADS)
Montreal Cognitive Assessment (MoCA) score
Neurological Disorders Depression Inventory for Epilepsy (NDDI-E) score
Quality of Life in Epilepsy-31 (QOLIE-31) score
Study visit 1 (for DRE)
Current ASMs (adverse effects, total daily dose (mg))
Current rescue medications (drug, dose, typical frequency of use, adverse effects)
Previously trialled ASMs (max total daily dose (mg) and duration of time at this dose, reason for discontinuation)
Autoantibodies detected on visit 1 serum sample
Study visits 2-6 (for DRE)
Any ASM dose changes
Any ASMs stopped (max total daily dose (mg) and duration of time at this dose, reason for discontinuation)
Any new ASMs
Change in seizure frequency
Likely reason identified for change in seizure frequency?
Autoantibodies detect on visit 2-6 serum samples

For SFE only:

- ASM on which SF was attained (adverse effects, total daily dose (mg))
- estimated date of last seizure and duration of SF
- study enrolment date
- autoantibodies detected on study serum sample
- current ASMs (adverse effects, total daily dose (mg))
- previously trialled ASMs (max total daily dose (mg) and duration of time at this dose, reason for discontinuation)

Table 13: Pre-populated responses for the clinical phenotyping database

Examples of pre-populated responses for the data field labelled 'early observed ictal clinical signs'. In the live database, the options were presented in drop-down boxes and an administrator could create additional choices if required.

Early observed ictal clinical signs		
Atonia	Dystonic posturing – bilateral, symmetric	Non-versive head turn to right
Autonomic signs	Emotional features	Orofacial automatisms
Behaviour arrest	Epileptic spasms	Pallor
Blinking	Eyelid myoclonia	Pilo-erection – bilateral
Bradycardia	Flushing	Pilo-erection – unilateral
Burping	Forced speech	Respiratory function change
Cardiac arrhythmia	Hyperkinetic (including leg pedalling)	Speech disturbance
Choking	Hypersalivation	Tachycardia
Clonus – unilateral	Incontinence	Tonic movements
Clonus – bilateral	Laughter	Tonic-clonic movements
Cognitive (impaired language/other domains))	Manual automatisms	Unsteadiness
Complex motor/hypermotor activity	Miosis	Versive head turn to left
Crying	Mydriasis	Versive head turn to right
Cyanosis	Myoclonic absence	Visual aura - bilateral
Diaphoresis	Myoclonic-atonic movements	Visual aura - unilateral
Drop attack	Myoclonic-tonic-clonic movements	Visual aura - unspecified
Dystonic posturing – unilateral	Myoclonus	Vomiting
Dystonic posturing – bilateral, asymmetric	Non-versive head turn to left	Not known

As of March 2020, 206 DRE patients and 54 seizure-free epilepsy (SFE) patients were recruited (**Figure 13** and **Table 14**), and serum autoantibody screening was completed for samples collected at visit number one.

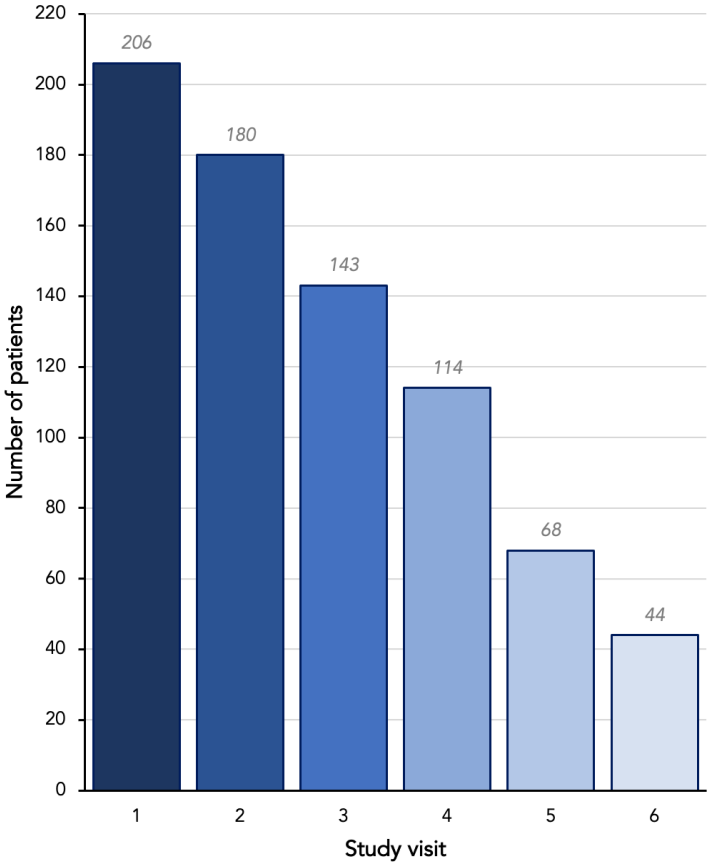


Figure 13: DRE patient recruitment and follow-up
As of March 2020, 206 DRE patients were recruited, 44 of whom had completed a further five follow-up visits. *DRE*, drug-resistant epilepsy.

Table 14: Patient demographics
DRE, drug-resistant epilepsy; and *SFE*, seizure-free epilepsy.

	DRE (n=206)	*SFE (n=54)*
No. female patients	125 (47.9%)	27 (50%)
Median age in years (range)	37 (17-77)	45 (18-79)

Thirteen of 206 (6.3%) DRE patients were found to have specific NSAs: GABA-B-R (n=3), GABA-B-R and glycine-R (n=1), contactin-2 (n=4), GABA-A-R (n=2), NMDA-R (n=2), and DPPX (n=1) (**Table 15**).

Table 15: Positive serum autoantibody results for DRE patients

Seven of eight DRE subjects (patients ***14-21***) who tested positive for GAD65 autoantibodies had high EPT (>1:1,000). Novel antibodies are possible in 22 patients positive solely on NBA (***22-24*** & ***26-29***), ABA (***30-43***) or NBA/ABA (***25***); and in patient ***18*** (NBA-positive & GAD65 antibody-positive). Double positive results were obtained in patient ***4*** (40M, normal brain MRI & non-localising EEG); ***13*** (64F, TLE & unilateral HS, prior encephalitis of unknown cause); ***18*** (32F, TLE & bilateral HS, GAD65 antibody EPT 1:25,600); and ***25*** (56F, FLE & ganglioglioma). *ABA*, astrocyte-based assay; *DPPX*, dipeptidyl-peptidase-like protein 6; *DRE*, drug-resistant epilepsy; *EEG*, electroencephalogram; *EPT*, endpoint titre; *F*, female; *FLE*, frontal lobe epilepsy; *GABA-A-R*, gamma-amino butyric acid receptor type A; *GABA-B-R*, gamma-amino butyric acid receptor type B; *GAD65*, glutamic acid decarboxylase 65; *HS*, hippocampal sclerosis; *M*, male; *NBA*, neuron-based assay; *glycine-R*, glycine receptor; *NMDA-R*, N-methyl-D-aspartate receptor; and *TLE*, temporal lobe epilepsy.

Patient			Serum antibody								
No.	Age	Sex	GABA-B-R	Contactin-2	GABA-A-R	NMDA-R	Glycine-R	DPPX	GAD65	Neurons	Astrocytes
1	20	F	+								
2	46	F	+								
3	20	M	+								
4	40	M	+				+				
5	30	F		+							
6	25	M		+							
7	22	F		+							
8	69	F		+							
9	24	F			+						
10	55	F			+						
11	56	M				+					
12	59	F				+					
13	64	F						+		+	
14	59	F							+		
15	34	F							+		
16	43	F							+		
17	27	F							+		
18	32	F							+	+	
19	47	F							+		
20	23	F							+		
21	70	F							+		
22	40	M								+	
23	57	F								+	
24	32	M								+	
25	56	F								+	+
26	35	F								+	
27	53	F								+	
28	32	F								+	
29	21	M								+	
30	21	M									+
31	62	M									+
32	37	M									+
33	20	F									+
34	40	F									+
35	23	F									+
36	18	F									+
37	34	M									+
38	36	M									+
39	32	M									+
40	48	F									+
41	39	F									+
42	50	M									+
43	62	F									+

In contrast to the NOFE patients, seven DRE patients had GAD65 autoantibodies with high endpoint titres (EPT), defined as above 1:1,000 (**Table 16**). One DRE patient had GAD65 autoantibodies with a lower EPT of 1:200. Taking account of 22 patients who were only found to have potential novel antibodies (i.e., those targeting neurons and/or astrocytes in the absence of a specific NSA), the overall autoantibody frequency in our DRE population was 43/206 (20.9%).

Table 16: High EPT GAD65 autoantibody-positive DRE patients
Seven patients had high EPT titre GAD65 autoantibodies (>1:1,000) detected in serum samples from their first study visit. Clinical CSF samples were obtained for two patients (***3*** & ***5***), both positive for GAD65 autoantibodies. The clinical immunology service assay has a maximum detection limit of 50,000 units/ml. A research CSF sample from patient ***5*** was positive for GAD65 antibodies with high EPT. Note that patient ***5*** is listed in table 15 as patient ***13***. Further research CSF sampling was not possible due to the coronavirus lockdown. *Ab* antibody; *DF*, dilution factor; *DRE*, drug-resistant epilepsy; *EPT*, endpoint titre; *GAD65*, glutamic acid decarboxylase 65; N/A, not available.

DRE patient	*RESEARCH SAMPLES*		*CLINICAL SAMPLES*	
	Serum GAD65 Ab EPT (as DF)	*CSF GAD65 Ab EPT (as DF)*	*Serum GAD65 Ab titre (units/ml)*	*CSF GAD65 Ab titre (units/ml)*
1	3,200	N/A	N/A	N/A
2	3,200	N/A	N/A	N/A
3	6,400	N/A	50,000	647
4	25,600	N/A	N/A	N/A
5	25,600	4,000	50,000	50,000
6	25,600	N/A	N/A	N/A
7	409,600	N/A	N/A	N/A

Three DRE patients had autoimmune encephalitis around the time of seizure-onset, although serum antibodies were only detected in one (GAD65 and neuronal surface-directed). Novel autoantibodies were suggested in DRE patients with surface reactivity to cultured neurons (n=8), astrocytes (n=14) or both (n=1) in the absence of a specific NSA. Images from neuron-based assays (NBA) are shown in **Figure 14** and from ABA in **Figure 15**.

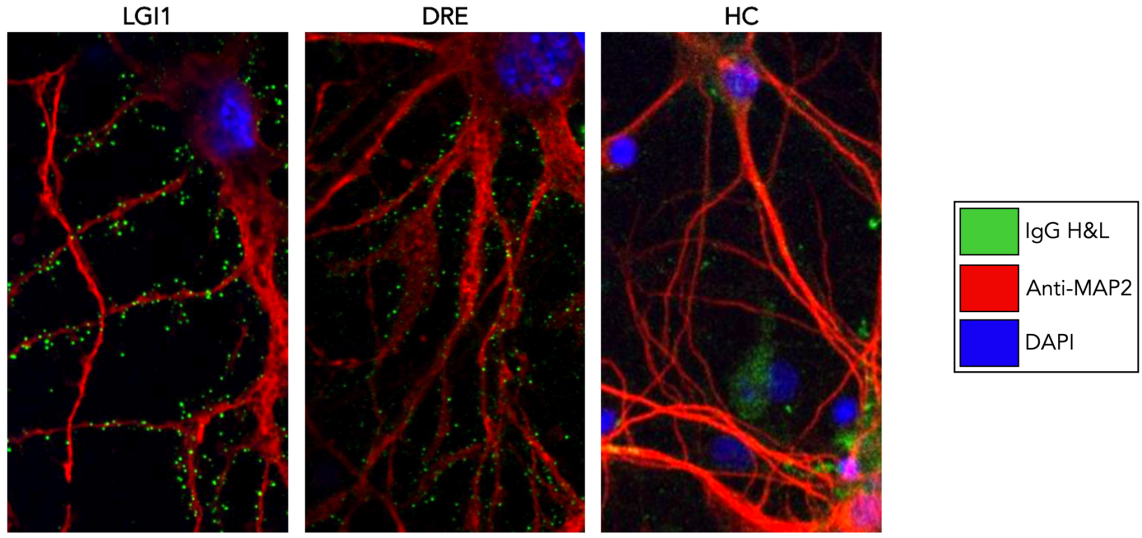


Figure 14: NBA images

Confocal microscopy images, (x63 magnification, oil immersion). Immunohistochemistry performed on day 14 cultured hippocampal neurons (derived from embryonic day 18 rat brain). Following incubation of live neurons with sera, a secondary antibody (IgG H&L) with a fluorescent green tag was added, which bound to human immunoglobulin. The neuronal marker, MAP2, was targeted with a secondary antibody conjugated to a red fluorescent tag. Fluorescence was visualised on microscopy. **Left:** LGI1 antibody-positive control serum gave rise to puncta (green) distributed along the surface of neurons (red). **Middle:** Similar appearances with serum from a DRE patient. **Right:** No puncta with healthy control serum. *DAPI*, 4',6-diamidino-2-phenylindole; *DRE*, drug-resistant epilepsy; *IgG H&L*, immunoglobulin G heavy and light chains; *LGI1*, leucine-rich glioma inactivated-1; *MAP2*, microtubule-associated protein 2; and *NBA*, neuron-based assay.

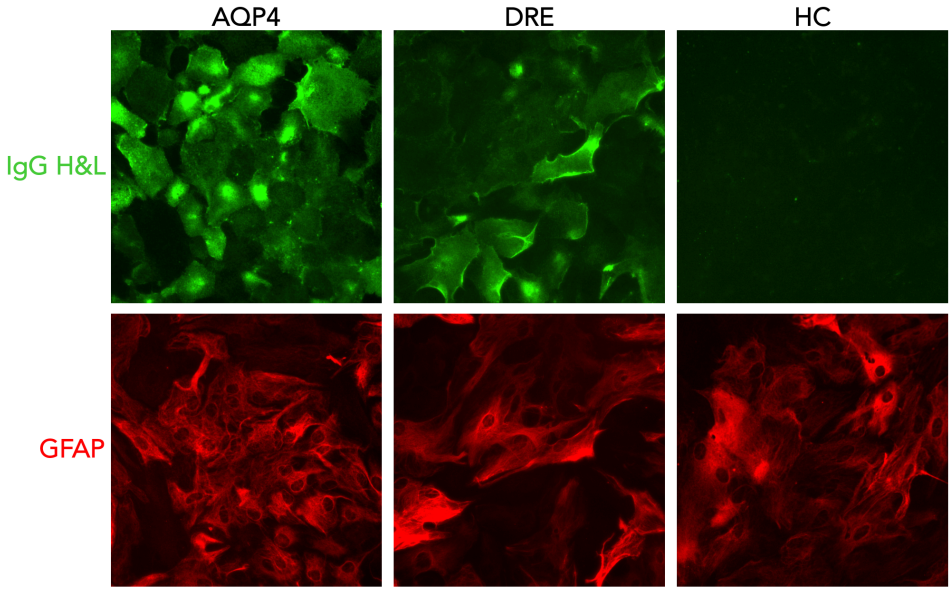


Figure 15: ABA images

Fluorescence microscopy images (x40 magnification). Immunohistochemistry performed on day 10 cultured astrocytes (derived from embryonic day 18 rat brain). After incubation of live astrocytes with sera, a secondary antibody (to human IgG H&L) with a fluorescent green tag was added. The astrocytic marker, GFAP, was targeted with a red fluorescent-tagged secondary antibody. Fluorescence was visualised on microscopy. **Left:** AQP4 antibody-positive control serum gave rise to a cell-surface staining pattern (green) in GFAP-positive cells (red). **Middle:** Similar appearances with serum from a subject with DRE (21-year-old male with temporal lobe epilepsy and unilateral hippocampal sclerosis). **Right:** Absence of the AQP4 antibody staining pattern with healthy control serum. *AQP4*, aquaporin-4; *DRE*, drug-resistant epilepsy; *GFAP*, glial fibrillary acidic protein; and *IgG H&L*, immunoglobulin G heavy and light chains.

To assess whether results of the GAD65 autoantibody tests in the NOFE study (measured by RIPA) were comparable to the results in the DRE study (measured by CBA), all NOFE patient samples were re-tested using CBA. On the RIPA screening originally performed for the NOFE study, none of the 219 samples was identified as highly positive for GAD65 autoantibodies. Given that only highly positive samples would have been re-tested using calibrators to provide an accurate antibody concentration, antibody titres were not produced. Using the new GAD65 antibody CBA to screen the same samples, 218 were negative for GAD65 autoantibodies and one (0.46%) was positive with a low EPT of 1:200.

Among SFE patients, 4/54 (7.4%) had NSAs: GABA-B-R (n=2), GABA-A-R (n=1), and NMDA-R (n=1). An additional five patients had potential novel autoantibodies, bringing the overall autoantibody frequency for this group to 9/54 (16.7%, Table 17A). None had GAD65 autoantibodies.

From 2016 to 2020, OANG obtained serum samples from 110 healthy controls. Due to the COVID-19 pandemic, specific autoantibody testing is outstanding for 55 and none have yet been tested on ABA. Two of the 55 (3.6%) healthy controls tested so far were positive for autoantibodies against GABA-A-R (n=1) and neurons without an associated specific NSA (n=1, Table 17B).

Table 17: Positive serum autoantibody results for SFE patients and healthy controls
(A): SFE patients. **(B)**: Healthy controls. GAD65 antibodies were not detected in SFE patients or healthy controls. *GABA-A-R*, gamma-amino butyric acid receptor type A; *GABA-B-R*, gamma-amino butyric acid receptor type B; *GAD65*, glutamic acid decarboxylase 65; *NMDA-R*, N-methyl-D-aspartate receptor; and *SFE*, seizure-free epilepsy.

A

SFE patients			Serum antibody				
No.	Age	Sex	GABA-B-R	GABA-A-R	NMDA-R	Neurons	Astrocytes
1	41	F	+				
2	34	F	+				
3	26	F		+			
4	25	F			+		
5	58	M				+	+
6	46	M				+	
7	50	F					+
8	53	M					+
9	26	F					+

B

Healthy controls			Serum antibody	
No.	Age	Sex	GABA-A-R	Neurons
1	40	M	+	
2	36	M		+

3.4 Estimation of autoantibody frequency in outpatients with epilepsy

Limiting results by assay type, so that only assays used to screen all four patient groups were included in the analysis (**Table 18**), enabled comparison of autoantibody frequency between groups.

Table 18: Assays performed for each patient group
The same set of ten NSAs was used for all four patient groups. GAD65 antibodies were tested by RIPA for NOFE patients and by CBA for all others. ABAs were only used for testing samples from DRE and SFE patients. *Ab*, antibody; *ABA*, astrocyte-based assay; *DRE*, drug-resistant epilepsy; *GAD65*, glutamic acid decarboxylase 65; *HC*, healthy controls; *NBA*, neuron-based assay; *N*, no; *NOFE*, new-onset focal epilepsy; *NSA*, neuronal surface-directed antibody; *RIPA*, radioimmunoprecipitation assay; *SFE*, seizure-free epilepsy; and *Y*, yes.

Patient group	*Live CBAs for NSAs*	*Novel permeabilised GAD65 Ab CBA*	*NBA*	*ABA*
NOFE	Y	Y	Y	N
DRE	Y	Y	Y	Y
SFE	Y	Y	Y	Y
HC	Y	Y	Y	N

For comparison to the broader epilepsy literature, further restriction to specific autoantibodies (i.e. excluding potential novel antibodies) was required (**Table 19**).

Table 19: Frequency of positive autoantibody findings by patient group

Sera from four groups (NOFE, DRE, SFE and HC) were tested for a panel of ten specific autoantibodies (NSA targets: LGI1, CASPR2, contactin-2, DPPX, NMDA-R, AMPA-R, GABA-A-R, GABA-B-R, and glycine-R; intracellular targets: GAD65). In addition, unidentified target antigens were screened for by NBA (all four groups) and ABA (DRE and SFE groups only due to COVID-19-related laboratory closure). A novel antibody was suggested by a positive NBA or ABA result without an associated specific NSA. Thirty-six participants had NSA and high EPT GAD65 autoantibodies were detected in seven (all DRE). Fourteen patients had multiple positive results – NOFE: one GABA-A/GABA-B-R/NBA, one NMDA-R/GABA-A-R, three LGI1/NBA, two GABA-B-R/NBA, one AMPA-R/NBA, one CASPR2/NBA and one NMDA-R/NBA; DRE: one DPPX/NBA, one GAD65/NBA, one NBA/ABA; and SFE: one NBA/ABA. **(A):** To compare the four patient groups: ABA results are excluded, as these were not performed for NOFE and HC. **(B)**: To compare findings to published clinical epilepsy studies: results from NBA and ABA are excluded, as these are not universally employed. DRE patients had the highest proportion of positive antibody results, regardless of whether potentially novel autoantibodies were included. *****EPT above 1:1,000. *Ab+*, antibody-positive; *ABA*, astrocyte-based assay; *ABA+*, astrocyte-based assay-positive; *AMPA-R*, alpha-amino-3-hydroxy-5-methyl-4-isoxazolepropionic acid receptor; *CASPR2*, contactin-associated protein-2; *CBA*, cell-based assay; *DPPX*, dipeptidyl-peptidase-like protein 6; *DRE*, drug-resistant epilepsy; *EPT*, endpoint titre; *GABA-A-R*, gamma-amino butyric acid receptor type A; *GABA-B-R*, gamma-amino butyric acid receptor type B; *GAD65*, glutamic acid decarboxylase 65; *glycine-R*, glycine receptor; *HC*, healthy control; *LGI1*, leucine-rich glioma inactivated-1; *NBA+*, neuron-based assay-positive; *NMDA-R*, N-methyl-D-aspartate receptor; *NOFE*, new-onset focal epilepsy; *NSA*, neuronal surface-directed antibody; *NSA+*, neuronal surface-directed antibody-positive; *RIPA*, radioimmunoprecipitation assay and *SFE*, seizure-free epilepsy.

					TOTAL NUMBER OF ANTIBODIES (%)		
Patient group (n)	Number of NSA+	Number of high EPT* GAD65 Ab+	Number of NBA+ results without specific NSA	Number of ABA+ results without specific NSA	Specific & suspected novel	(A) Specific & suspected novel excluding ABA	(B) Specific only
NOFE (219)	18	0	5	N/A	23 (*10.5*)	23 (*10.5*)	18 (*8.2*)
DRE (206)	13	7	8	14	42 (*20.4*)	28 (*13.6*)	20 (*9.7*)
SFE (54)	4	0	2	3	9 (*16.7*)	6 (*11.1*)	4 (*7.4*)
HC (55)	1	0	1	N/A	2 (*3.6*)	2 (3.6)	1 (*1.8*)

This approach produced specific autoantibody frequencies of 18/219 (8.2%) for the NOFE group, 20/206 (9.7%) for DRE, 4/54 (7.4%) for SFE and 1/55 (1.8%) for healthy controls (HC). No statistically significant differences in the frequency of specific autoantibodies between patient groups were found (NOFE vs SFE, DRE vs SFE, NOFE vs HC, DRE vs HC, SFE vs HC; **Figure 16**). The specific NSA-positivity rate for all epilepsy patients (42/479) versus healthy controls (1/55) was not significant (p=0.1103, Fisher's exact test). Focussing solely on GAD65 autoantibody positivity, there was a statistically significant difference between DRE and NOFE (p=0.006, Fisher's exact test); but no significant difference between DRE and SFE (p=0.3507) or between DRE and HC (p=0.3510) – most likely due to the small sample sizes of the SFE and HC groups.

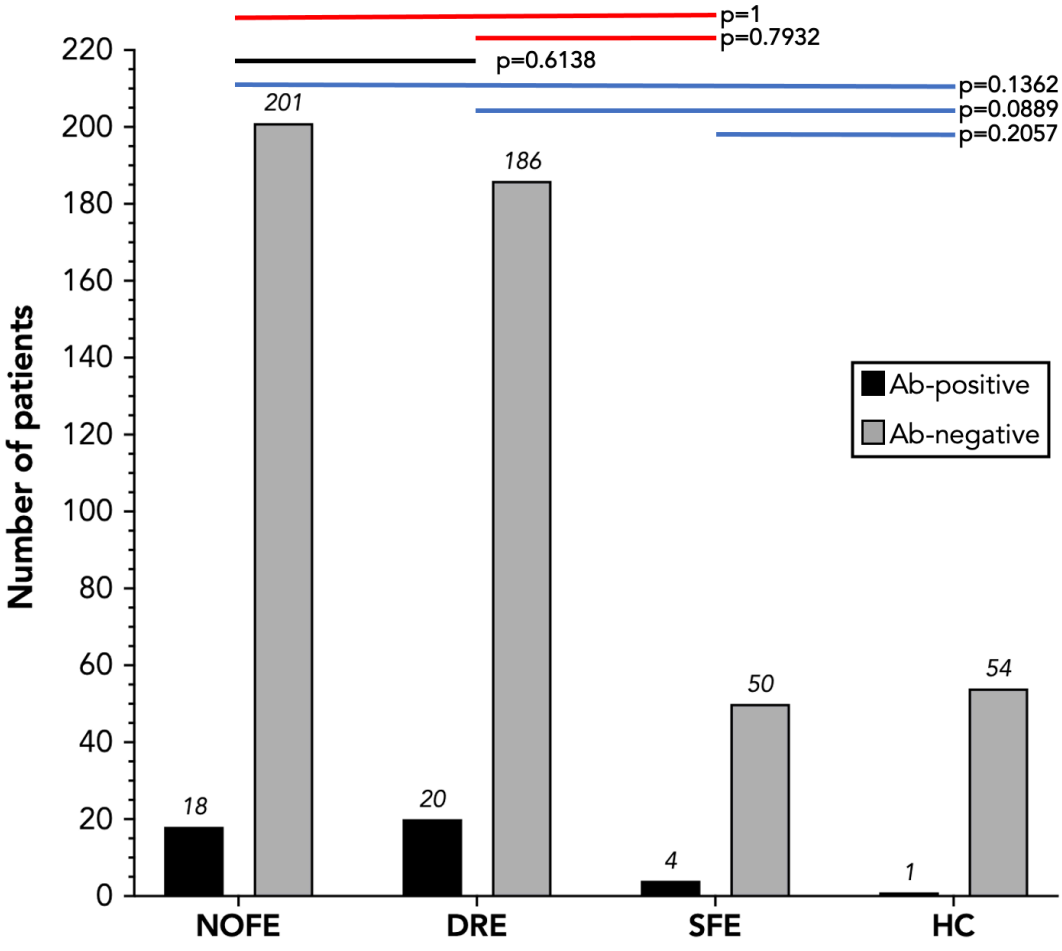


Figure 16: Frequency of autoantibody-positive results between groups
Results are shown for specific autoantibodies only. Fisher's exact test. *Ab*, antibody; *DRE*, drug-resistant epilepsy; *HC*, healthy control; *NOFE*, new-onset focal epilepsy; and *SFE*, seizure-free epilepsy.

3.5 Autoantibodies in epilepsy over time

To assess whether autoantibodies in epilepsy change over time, I evaluated 13 patients who participated in both of the studies described above. By the point of enrolment in the most recent study, six had developed DRE (four female) and seven were SFE controls (three female). Neither age at epilepsy onset nor duration of epilepsy was significantly associated with clinical outcome (i.e. DRE or SFE), (Table 20).

Table 20: Summary information for 13 NOFE patients later enrolled in DRE/SFE study
Median values. *Mann-Whitney U test.

	DRE (n=6)	*SFE (n=7)*	*P-value**
Age at epilepsy onset	40.5 years (range 19-70)	37 years (24-64)	0.9184
Duration of epilepsy by enrolment to 2nd study	46 months (range 31-66)	63 months (range 37-101)	0.2343
Interval between NOFE & DRE/SFE studies	35 months (range 32-45)	37 months (range 24-41)	0.2104

NOFE autoantibody status did not predict clinical outcome (Table 21). Two patients, both now seizure-free, had single positive autoantibody results (GABA-B-R autoantibodies and positive NBA) in the NOFE study. One remained positive for GABA-B-R autoantibodies after 35 months while the other had no autoantibodies detected on repeat testing at 41 months. A seronegative NOFE patient tested positive for GABA-A-R autoantibodies after 32 months, by which time they had developed DRE. None of the 13 people in this cohort had GAD65 autoantibodies detected at any stage. None of the nine NOFE patients with autoimmune encephalitis developed DRE.

Table 21: Epilepsy patients in sequential studies – characteristics 1

Thirteen patients from the NOFE study were recruited to the DRE/SFE study (patients ***7-13*** were SFE controls prescribed lamotrigine monotherapy). One patient remained positive for GABA-B-R serum autoantibodies over 35 months despite becoming seizure-free. One patient tested NBA-positive as a new-onset epilepsy patient but was NBA-negative and seizure-free 41 months later. One patient did not have any serum autoantibodies detected in the first study, yet 32 months later was positive for GABA-A-R autoantibodies. *Ab*, antibody; *DRE*, drug-resistant epilepsy; *GABA-A-R*, gamma-amino butyric acid receptor type A; *GABA-B-R*, gamma-amino butyric acid receptor type B; *NBA*, neuron-based assay; *NOFE*, new-onset focal epilepsy; and *SFE*, seizure-free epilepsy.

Patient	*Sex*	*Age*	*Study 1 group*	*Study 1 Ab result*	*Interval (months)*	*Study 2 group*	*Study 2 Ab result*
1	F	37	NOFE	Negative	35	DRE	Negative
2	M	44	NOFE	Negative	37	DRE	Negative
3	F	20	NOFE	Negative	34	DRE	Negative
4	F	52	NOFE	Negative	32	DRE	GABA-A-R
5	F	19	NOFE	Negative	35	DRE	Negative
6	M	70	NOFE	Negative	45	DRE	Negative
7	F	48	NOFE	Negative	39	SFE	Negative
8	M	37	NOFE	Neurons	41	SFE	Negative
9	M	64	NOFE	Negative	37	SFE	Negative
10	F	35	NOFE	Negative	36	SFE	Negative
11	F	36	NOFE	GABA-B-R	35	SFE	GABA-B-R
12	M	24	NOFE	Negative	36	SFE	Negative
13	M	52	NOFE	Negative	37	SFE	Negative

An exploratory analysis did not find statistically significant correlations between long-term clinical outcome and a range of clinical features, including MRI and EEG abnormalities (**Table 22**); generalised tonic-clonic seizures, status epilepticus, seizure frequency around the time of NOFE and seizure clustering (**Table 23**); known epilepsy risk factors, known epilepsy aetiology and temporal lobe epilepsy (**Table 24**); autoimmune disease, malignancy, memory problems, mood disorders and encephalitis (**Table 25**).

Table 22: Epilepsy patients in sequential studies – characteristics 2

Of the DRE patients with MRI brain studies available at assessment as NOFE, 4/5 were abnormal, compared to 2/7 SFE patients (p=0.2424, Fisher's exact test). NOFE EEG was abnormal in 5/6 patients who went on to develop DRE and 3/7 SFE patients (p 0.2657, Fisher's exact test). SFE (patient numbers 7-13) are highlighted in grey. *DRE*, drug-resistant epilepsy; *EEG*, electroencephalogram; *FCD*, focal cortical dysplasia; *MRI*, magnetic resonance imaging; *N*, no; N/A, not applicable; *NOFE*, new-onset focal epilepsy; *PVNH*, periventricular nodular heterotopia; and *SFE*, seizure-free epilepsy.

Patient	*MRI findings*	*EEG findings*	*Most common seizure type*
1	Normal	Normal	Focal aware seizures
2	Lesional (left high T2 signal & atrophy, dysplasia of left hippocampus & amygdala)	Definite focal epileptiform abnormalities	Focal aware seizures
3	Lesional (bilateral PVNH & FCD, hypoplasia of hippocampi)	Definite focal epileptiform abnormalities	Focal impaired awareness seizures
4	Lesional (bilateral hippocampal atrophy)	Focal slowing	Focal aware seizures
5	Lesional (bilateral hippocampal atrophy & generalised cerebral atrophy)	Definite focal epileptiform abnormalities & generalised slowing	Focal aware seizures
6	N/A	Definite focal epileptiform abnormalities	Focal impaired awareness seizures
7	Normal	Focal slowing	Focal aware seizures
8	Lesional (bilateral cerebral angioma/cavernoma)	Normal	Focal impaired awareness to bilateral tonic-clonic seizures
9	Perinatal insult	Normal	Focal impaired awareness to bilateral tonic-clonic seizures
10	Normal	Normal	Uncharacterised seizures
11	Normal	Definite focal & generalised epileptiform abnormalities	Generalised onset seizures
12	Normal	Normal	Focal impaired awareness seizures
13	Normal	Focal slowing	Focal aware seizures

Table 23: Epilepsy patients in sequential studies – characteristics 3

The seven SFE patients (shaded in grey) all achieved seizure-freedom on lamotrigine monotherapy. Four of six DRE patients and 6/7 SFE patients had a history of GTCS (p= 0.5594, Fisher's exact test). One DRE patient, but no SFE patients, had a history of status epilepticus (p= 0.4615, Fisher's exact test). Seizure frequency of more than two seizures per month was noted in the NOFE study for 2/6 participants who subsequently developed DRE and 5/7 people who became seizure-free (p= 0.2861, Fisher's exact test). Seizure clusters were experienced by 1/6 DRE and 0/7 SFE patients (p= 0.4615, Fisher's exact test). *ES*, epileptic seizure; *GTCS*, generalised tonic-clonic seizure; *N*, no; *N/A*, not applicable; *PNES*, psychogenic non-epileptic seizures; *SE*, status epilepticus; *Sz*, seizure; *vEEG*, video-electroencephalogram; and *Y*, yes.

Patient	*GTCS*	*SE*	*Study 1 Sz frequency/ month*	*Study 2 Sz frequency*	*Sz clusters*	*PNES*	*Epilepsy surgery*
1	N	N	30	30 per year	N	N	N
2	Y	N	1	25 per year	N	N	Left selective amygdalo-hippocampectomy
3	Y	N	1	9 per week	N	Clinical suspicion only	N
4	Y	N	2	1 per day	N	N	N
5	N	Y	1	7 per year	N	N	N
6	Y	N	1	8 per month	Y	vEEG-confirmed; patient can distinguish between ES & PNES	N
7	Y	N	1	N/A	N	N	N
8	Y	N	3	N/A	N	N	N
9	Y	N	3	N/A	N	N	N
10	Y	N	7	N/A	N	N	N
11	N	N	20	N/A	N	N	N
12	Y	N	2	N/A	N	N	N
13	Y	N	1	N/A	N	N	N

Table 24: Epilepsy patients in sequential studies – characteristics 4

Epilepsy risk factors were established for 3/6 DRE and 4/7 SFE patients (p=1, Fisher's exact test). A cause of epilepsy was determined in 5/6 DRE and 2/7 SFE patients (p=0.1026, Fisher's exact test). Of those with a known syndrome, TLE was identified in 2/4 DRE patients compared to 1/1 SFE (p=1, Fisher's exact test). Patients with SFE (no. 7-13) are shaded in grey. *FCD*, focal cortical dysplasia; *FLE*, frontal lobe epilepsy; *HS*, hippocampal sclerosis; *N*, no; and *TLE*, temporal lobe epilepsy.

Patient	*Epilepsy risk factors*	*Genetic mutations*	*Presumed epilepsy aetiology*	*Syndrome*
1	Family history (non-1st degree)	N	Not known	FLE
2	N	N	HS & FCD	TLE
3	Perinatal complication	N	Grey matter heterotopia	Focal, not specified
4	Childhood meningitis; adult encephalitis (unknown cause)	N	Encephalitis (no cause identified)	TLE
5	N	N	Cryptogenic (no cause identified)	Focal, not specified
6	N	N	Cryptogenic (no cause identified)	FLE
7	Family history (1st degree)	N	Not known	TLE
8	N	KRIT1	Cerebral angioma/cavernoma	Focal, not specified
9	Perinatal complication	N	Not known	Focal, not specified
10	Family history (1st degree)	N	Not known	Focal, not specified
11	N	N	Genetic (idiopathic)	Focal & generalised
12	Perinatal complication	N	Not known	Focal, not specified
13	N	N	Not known	Focal, not specified

Table 25: Epilepsy patients in sequential studies – characteristics 5

One DRE patient had chronic myeloid leukaemia but no other patients were known to have malignancies. One DRE patient had encephalitis (cause not known). Autoimmune diseases were noted in 3/6 DRE patients and 2/7 SFE patients (p=0.5921, Fisher's exact test). Memory problems were reported in 5/6 DRE and 2/7 SFE patients (p=0.1026, Fisher's exact test), and mood disorders were present in 4/6 DRE and 2/7 SFE patients (p=0.2861, Fisher's exact test). SFE patients (no. 7-13) are highlighted in grey. *CML*, chronic myeloid leukaemia; *DRE*, drug-resistant epilepsy; *N*, no; *RA*, rheumatoid arthritis; *SFE*, seizure-free epilepsy; and *Y*, yes.

Patient	*Autoimmune disease*	*Neoplasia*	*Memory problems*	*Mood problems*	*Encephalitis*
1	N	N	Y	Y	N
2	N	N	Y	Y	N
3	Coeliac disease	N	N	Y	N
4	Chronic anterior uveitis, RA	N	Y	N	Y (unknown cause)
5	Hypothyroidism	N	Y	N	N
6	N	CML	Y	Y	N
7	N	N	N	Y	N
8	Lichen planus	N	N	Y	N
9	Atopy (asthma, allergic rhinitis, eczema)	N	N	N	N
10	N	N	N	N	N
11	N	N	Y	N	N
12	N	N	Y	N	N
13	N	N	N	N	N

In these 'study crossover' patients, no features of AIE were observed. There were no patterns of semiological features or unusual ictal features (such as piloerection, flushing or diaphoresis), and there was no hyponatraemia at epilepsy onset.

Another opportunity to explore autoantibodies in epilepsy over a shorter time period was provided by the seven DRE patients with high EPT GAD65 autoantibodies. I tested serial serum samples from four-monthly follow-up visits with a new GAD65 antibody CBA (median number of study visits=6, range 3-7). All remained seropositive for GAD65 autoantibodies throughout the period of monitoring. There was some fluctuation in EPTs, although these generally stayed within the same range (Table 26). In 3/5 patients for whom information was available, the trend in change of seizure frequency broadly mirrored EPT variation.

Table 26: Serial GAD65 autoantibody EPT and seizure frequency

Seven DRE patients had GAD65 autoantibodies with high EPTs on their first serum sample. EPTs (expressed as dilution factors) are provided for study follow-up visits and are coloured by EPT range. Visits were approximately four months apart (currently paused due to coronavirus pandemic). Qualitative information regarding changes in seizure frequency relative to the previous study visit (indicated by boxed black arrows) was available for five patients. For most of the subjects, the GAD65 autoantibody EPTs remained at roughly the same order of magnitude over time. *Ab*, antibody; *CBA*, cell-based assay; *DF*, dilution factor; *EPT*, endpoint titre; *GAD65*, glutamic acid decarboxylase 65; and *N/A*, not available.

GAD65 Ab CBA EPT
- 100-1,000
- 1,000-10,000
- 10,000-50,000
- >50,000

Seizure frequency
- ↑ Increased
- ↓ Decreased
- ↔ Unchanged

GAD65 Ab EPT (as DF)	Patient 1	Patient 2	Patient 3	Patient 4	Patient 5	Patient 6	Patient 7
Visit 1	3,200	409,600	25,600	3,200	25,600	25,600	6,400
Visit 2	3,200 ↓	409,600 ↑	25,600 ↔	1,600 ↑	25,600 ↑	25,600 N/A	800 N/A
Visit 3	3,200 ↔	102,400 ↓	25,600 ↑	1,600 ↓	25,600 ↑	25,600 N/A	6,400 N/A
Visit 4	3,200 ↔	102,400 ↔	25,600 ↔	3,200 ↑	25,600 N/A		
Visit 5	3,200 ↔	102,400 ↓	25,600 ↓	3,200 ↔			
Visit 6	3,200 ↔	102,400 ↓	25,600 N/A	400 ↑			
Visit 7	3,200 N/A	25,600 N/A					

3.6 Observed clinical phenotype of epilepsy patients with high EPT GAD65 autoantibodies

All seven of the DRE patients with high EPT GAD65 autoantibodies were female, with a median age at study enrolment of 34 years (range 23-59). Clinical characteristics were compared to those of 14 age- and sex-matched, autoantibody-negative DRE patients.

Pre-defined clinical features (temporal lobe epilepsy, adult-onset epilepsy and type I diabetes mellitus) did not show a statistically significant association with autoantibody status after Bonferroni correction for multiple comparisons (Table 27), nor did clinical features (uncorrected, Table 28). Notwithstanding the statistical findings, reports of acute pain as a seizure trigger are unusual.

Table 27: Association between pre-defined clinical features and autoantibody status
Significance = p>0.0167, Fisher's exact test (Bonferroni correction). The three patients with TIDM had adult-onset epilepsy. *Two non-TLE patients excluded: occipital lobe epilepsy (n=1) and unclassified (n=1). *Ab*, antibody; *DRE*, drug-resistant epilepsy; *EPT*, endpoint titre; *GAD65*, glutamic acid decarboxylase; *TIDM*, type I diabetes mellitus; and *TLE*, temporal lobe epilepsy.

Clinical feature	*High GAD65 Ab EPT DRE (n=7)*	*Ab-negative DRE (n=14)*	*P-value*
TLE	5*	4	0.0498
Adult-onset epilepsy	5	5	0.3972
TIDM	3	0	0.0263

Table 28: Exploratory analysis of clinical features and autoantibody status

Significance = p<0.05, unadjusted. Fisher's exact test unless otherwise indicated. *Mann-Whitney U test. No patients from either group received immunotherapy for seizure control. **High GAD65 Ab EPT DRE**: AI diseases: T1DM, antiphospholipid syndrome, vitiligo & TIDM, and hyperthyroidism & TIDM. TIDM onset occurred before the first seizure in 1/3, whereas epilepsy manifested prior to TIDM in 2/3. Mental health disorders: depression (n=2), depression and psychosis, depression and substance misuse. **Ab-negative DRE**: AI diseases: coeliac disease and alopecia. Mental health disorders: anxiety and depression (n=4), anxiety. Seizure triggers: Patients were asked if they had identified any seizure triggers in general. Pain, a rare seizure trigger in epilepsy, was not specifically asked about but was spontaneously volunteered by these patients. *Ab*, antibody; *AI*, autoimmune; *ASM*, anti-seizure medication; *DRE*, drug-resistant epilepsy; *EEG*, electroencephalogram; *EPT*, endpoint titre; *GAD65*, glutamic acid decarboxylase; *GTCS*, generalised tonic-clonic seizure; *MRI*, magnetic resonance imaging; *SE*, status epilepticus; and *TIDM*, type I diabetes mellitus.

Clinical feature	*High GAD65 Ab EPT DRE (n=7)*	*Ab-negative DRE (n=14)*	*P-value*
Exclusively hippocampal abnormalities on MRI	4	3	0.1564
Bilateral hippocampal sclerosis	2	0	0.1
Focal epileptiform abnormalities on EEG	6	10	0.1827
Recurrent SE (more than one episode)	2	4	>0.9999
Family history of epilepsy (1st-degree relative, non-acquired)	1	1	>0.9999
Known early life risk factors for epilepsy	2	9	0.1827
DRE post-epilepsy surgery	1	2	>0.9999
History of AI encephalitis	2	1	0.2474
Any AI disease	4	2	0.1196
AI disease excluding TIDM	3	2	0.28
Mental health disorders	4	5	0.3972
Seizure frequency greater than 1/week	2	10	0.0873
10 or more GTCS in life	3	6	>0.9999
Pain as a seizure trigger	3	1	0.0877
4 or more ASMs trialled	5	13	0.2474
Duration of epilepsy* (median and range)	18 years (2-55)	20.5 years (3-51)	0.9834
Age at epilepsy onset* (median and range)	20 years (4-30)	9 years (1-37)	0.9203

3.7 Summary

Two large, prospective studies with enrolment of consecutive patients determined an overall frequency of specific serum autoantibodies in epilepsy of 8.8% (42/479); 8.2% (18/219) in NOFE, 9.7% (20/206) in DRE and 7.4% (4/54) in SFE – compared to 1/55 (1.8%) for healthy controls. High EPT GAD65 autoantibodies were detected in 7/206 (3.4%) patients with DRE, but in no subjects with NOFE. In addition, five patients with NOFE and 23 with DRE had potential novel autoantibodies detected with cultured neurons and astrocytes.

Multivariate regression modelling identified that, among adults with NOFE, NSA status was best predicted by older age, ictal piloerection, epilepsy risk factors, mood problems, ACE-R attention sub-score and limbic system change on MRI. Even without immunotherapy, clinical outcomes were very good among individuals with isolated epilepsy who had serum autoantibodies without encephalitis. Our model was more sensitive and specific for predicting NSA-seropositivity in those with isolated epilepsy than the Antibody Prevalence in Epilepsy and Encephalopathy (APE2) score, which largely reflected the more florid features of classical AIE.

Thirteen patients assessed with NOFE were enrolled in the second study following a median interval of 36 months. No patterns of clinical or semiological features were associated with autoantibody status, change in autoantibody status or clinical outcome. All tested GAD65 autoantibody-negative on their first serum sample and none developed GAD65 autoantibodies over time.

Seven DRE patients with high EPT GAD65 autoantibodies remained seropositive over four-monthly serial follow-up visits (median number of visits = 6). Some fluctuation in EPT occurred but these generally remained at the same level of magnitude over time.

Clinical phenotyping of the seven high EPT GAD65 autoantibody-positive patients demonstrated that all had DRE and were female, with a median age at epilepsy onset of 20 years. Five had temporal lobe epilepsy, one had occipital lobe epilepsy and one had unclassified epilepsy. Three subjects had TIDM, all of whom developed adult-onset epilepsy. Two patients had bilateral hippocampal sclerosis. None received immunotherapy. Compared to fourteen age- and sex-matched autoantibody-negative DRE patients, the high EPT GAD65 autoantibody-positive group had similar duration of epilepsy but less frequent seizures, fewer lifetime GTCS and trialled fewer ASMs. Three of the GAD65 autoantibody-positive patients reported pain as a seizure trigger.

These results are contextualised and discussed in Chapter 6.

Chapter 4 Development of a novel GAD65 antibody cell-based assay

4.1 Introduction

Traditionally, the radioimmunoprecipitation assay (RIPA) has been considered the 'gold standard' laboratory method for detecting GAD65 antibodies. However, the inherent logistical constraints of working with radioactivity, compounded by the decreasing availability of commercial GAD65 RIPA kits, prompted a piecemeal transition towards the use of enzyme-linked immunosorbent assay (ELISA) in both diagnostic and research laboratories. There are conflicting reports about the comparability of GAD65 antibody levels determined by ELISA and RIPA.[190,196,197] Although both may yield antibody concentrations measured in units per ml, these units are not equivalent, and there is no consensus on how to convert between them. Both assays were developed principally for detecting GAD65 autoantibodies in type 1 diabetes mellitus (T1DM),[198,199] and it is not clear how they perform at the much higher antibody titres associated with autoimmune neurological conditions.

The work covered in this chapter aimed to:

- develop and optimise a novel cell-based assay (CBA) capable of detecting GAD65 autoantibodies in neurology patients with a suspected immune aetiology;
- explore whether the CBA is a useful test for GAD65 antibodies compared to RIPA and ELISA;
- identify any challenges with using the CBA for high throughput screening.

4.2 Overview of the CBA

The optimised CBA protocol is detailed in Chapter 2. In brief, a DNA sequence encoding GAD65 protein (the target antigen) within a plasmid vector is taken up and transiently expressed intracellularly by human embryonic kidney (HEK)-293T cells. When patient serum containing GAD65 autoantibodies is incubated with permeabilised HEK-293T cells, GAD65 antibodies enter the cells and bind directly to GAD65 protein. A secondary ('detector') antibody then binds to the GAD65 antibody (**Figure 17**).

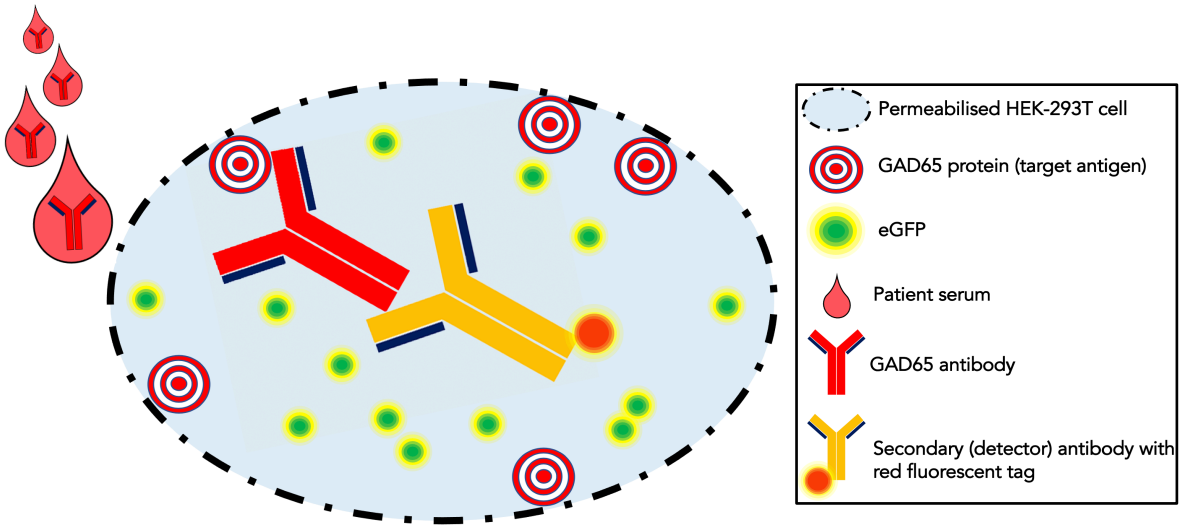


Figure 17: Permeabilised CBA for GAD65 antibody detection
Patient serum is incubated with permeabilised HEK-293T cells expressing GAD65 and eGFP intracellularly. GAD65 autoantibodies present in the serum (primary antibodies) enter the cell and bind to target GAD65 antigen. A secondary ('detector') antibody is then added, which binds to the GAD65 antibody. On fluorescence microscopy, a red fluorescent tag conjugated to the secondary antibody can be visualised, and green signal from cotransfected eGFP confirms that PEI-mediated cell transfection and expression occurred. *CBA*, cell-based assay; *eGFP*, enhanced green fluorescent protein; *GAD65*, glutamic acid decarboxylase 65; *HEK-293T cell*, human embryonic kidney 293T cell; and *PEI*, polyethylenimine.

The crystal structure of GAD65 has been resolved from amino acid 88 onwards,[296] suggesting that a version of the protein truncated at this point might be more stable than the full-length protein (**Figure 18**). In support of this, a GAD65 protein truncated at amino acid 96 was previously reported to reduce the number of false positive GAD65 antibody results when compared to the full-length protein.[297] A pCMV-TNT vector encoding the human GAD65 protein with a truncation at amino acid 96 was recently gifted to the Oxford Autoimmune Neurology Group (by Dr Vito Lampasona, the San Raffaele Scientific Institute, Milan). Based on its immediate availability and the above observations, I opted to use this expression construct.

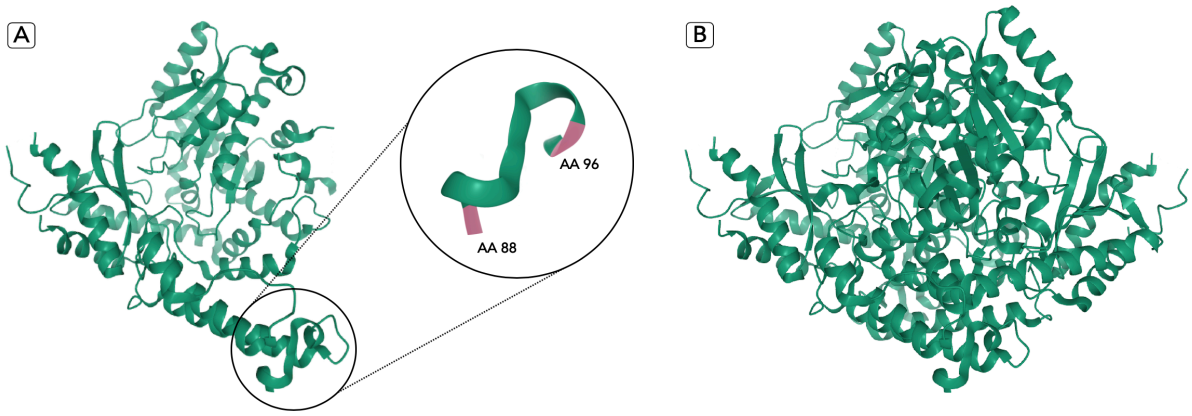


Figure 18: X-ray crystal structure of GAD65 resolved from amino acid 88
(A): GAD65 monomer with potential truncation sites at the N terminus (amino acids 88 and 96) are highlighted in pink. **(B)**: GAD65 functional dimer. Adapted from crystal structure provided by Rose et al./Research Collaboratory for Structural Bioinformatics Protein Data Bank [296]. *GAD65*, glutamic acid decarboxylase 65, *AA*, amino acid.

4.3 Establishing a positive signal from the GAD65 antibody CBA

Experimental controls (Table 29) were selected to demonstrate that the CBA could detect GAD65 antibodies and that the positive signal was specific to GAD65 antibodies.

Table 29: GAD65 antibody CBA controls

A summary table of control samples and their relevance in establishing a novel GAD65 antibody CBA. *Ab*, antibody; *Ab+*, antibody-positive; *AQP4*, aquaporin-4; *CASPR2*, contactin-associated protein-2; *CBA*, cell-based assay; *D anti-H IgG Fc*, donkey anti-human IgG, Fc-gamma fragment-specific; *DAPI*, 4′,6-diamidino-2-phenylindole; *eGFP*, enhanced green fluorescent protein; *ELISA*, enzyme-linked immunosorbent assay; *GAD65*, glutamic acid decarboxylase 65; *GFAP*, glial fibrillary acidic protein; *glycine-R*, glycine receptor; *HEK-293T cells*, human embryonic kidney 293T cells; *IgG*, immunoglobulin G; *LGI1*, leucine-rich glioma inactivated-1; *NMDA-R*, N-methyl-D-aspartate receptor; and *RIPA*, radioimmunoprecipitation assay.

Control	*Rationale/Question*
GAD65 antibodies as primary Ab: Known strongly GAD65 Ab-positive serum Human monoclonal GAD65 (B96) Ab Rabbit polyclonal GAD65 antibody	Can the assay detect GAD65 antibodies? If so, what are the characteristics of a positive signal?
Non-GAD65 primary Ab: No primary Ab (serum-free CBA) Known GAD65 Ab-negative serum Healthy control serum GFAP (intracellular antigen) Ab+ serum NMDA-R Ab+ serum LGI1 Ab+ serum AQP4 Ab+ serum Glycine-R Ab+ serum CASPR2 Ab+ serum	Is the IgG signal specific for GAD65 Ab?
Cell transfection with non-GAD65 antigens Non-transfected HEK-293T cells LGI1 DNA-transfected HEK-293T cells CASPR2 DNA-transfected HEK-293T cells GFAP DNA-transfected HEK-293T cells	Is the IgG signal specific for GAD65 Ab? Non-transfected cells – is there inherent HEK-293T cell GAD65 protein?
Detergent-free (i.e. non-permeabilised) protocol	Is the IgG signal intracellular or extracellular?

Corresponding fluorescence microscopy images are shown in **Figure 19** and **Figure 20**. After permeabilisation of GAD65-transfected cells, a GAD65 antibody-positive sample gives rise to an intracellular, annular, pericytoplasmic IgG staining pattern in a patchy distribution (**Figure 19.A1-4**). This pattern was absent when testing sera from healthy controls (**Figure 19.B1**), GAD65 autoantibody-negative patients (**Figure 19.A5**), and patients with autoantibodies to neuronal surface targets (**Figure 19.B2-6**) or the intracellular antigen, GFAP (**Figure 19.B7**). Replacing sample volume with diluent and running a serum-free CBA did not generate any IgG signal (**Figure 19.A6**).

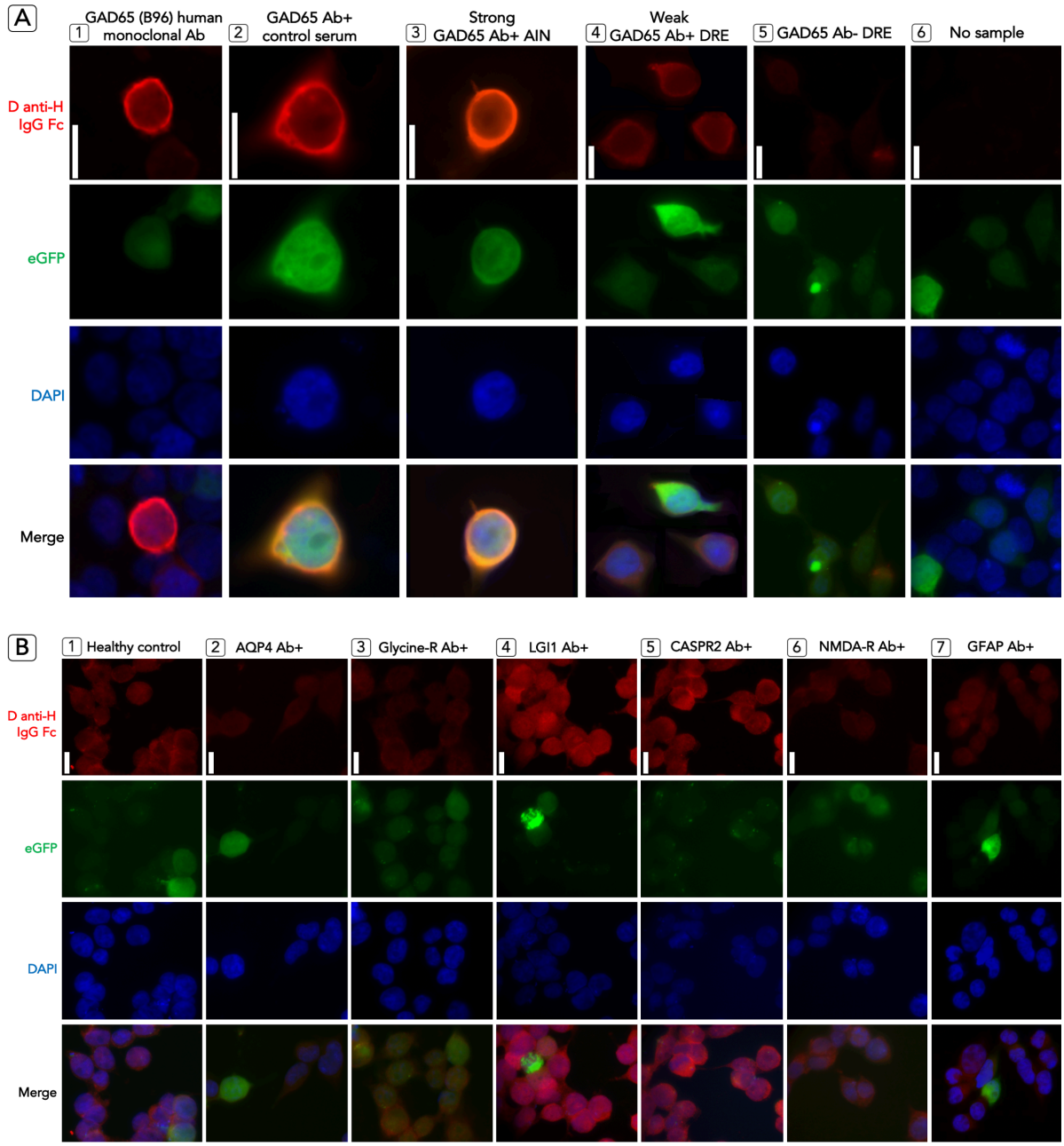


Figure 19: Control samples for GAD65 antibody CBA

Fluorescence microscopy images (photographs taken at x100 magnification, oil immersion; cropped for clarity, vertical white bars indicate scale). Control samples tested on the novel GAD65 antibody CBA at a dilution of 1:100. Green fluorescence from eGFP confirms cell transfection and expression occurred. DAPI-stained nuclei appear blue. Commercial GAD65 B96 human monoclonal antibody **(A1)** and serum from a known GAD65 antibody seropositive patient **(A2)** produced the same patchily distributed intracellular, annular, pericytoplasmic staining pattern (red fluorescence). This pattern was not observed on testing serum from a known GAD65 antibody seronegative patient **(A5)** or when additional diluent replaced serum **(A6)**. The yellow colour on merge photographs reflects GAD65 antibodies binding to cells expressing eGFP and GAD65 **(A1-4)**. No positive IgG signal on testing healthy control serum **(B1)** or sera from patients with a known neuronal surface (AQP4, glycine-R, LGI1, CASPR2, NMDA-R **(B2-6)**). GFAP, like GAD65, is an intracellular antigen. GFAP antibody-positive serum **(B7)** was used as a control for permeabilisation and was negative. *Ab*, antibody; *Ab-*, antibody-negative; *Ab+*, antibody-positive; *AIN*, autoimmune neurology; *AQP4*, aquaporin-4; *CASPR2*, contactin-associated protein-2; *CBA*, cell-based assay; *D anti-H IgG Fc*, donkey anti-human IgG, Fc-gamma fragment-specific; *DAPI*, 4′,6-diamidino-2-phenylindole; *DRE*, drug-resistant epilepsy; *eGFP*, enhanced green fluorescent protein; *GAD65*, glutamic acid decarboxylase 65; *GFAP*, glial fibrillary acidic protein; *glycine-R*, glycine receptor; *IgG*, immunoglobulin G; *LGI1*, leucine-rich glioma inactivated-1; and *NMDA-R*, N-methyl-D-aspartate receptor.

Reassuringly, two different commercial GAD65 antibodies, a B96 human monoclonal (**Figure 19.A1**) and a rabbit polyclonal (**Figure 20.2-4**), produced the same staining pattern as serum from a known GAD65 autoantibody-positive patient (**Figure 19.A2-4** and **Figure 20.1**).

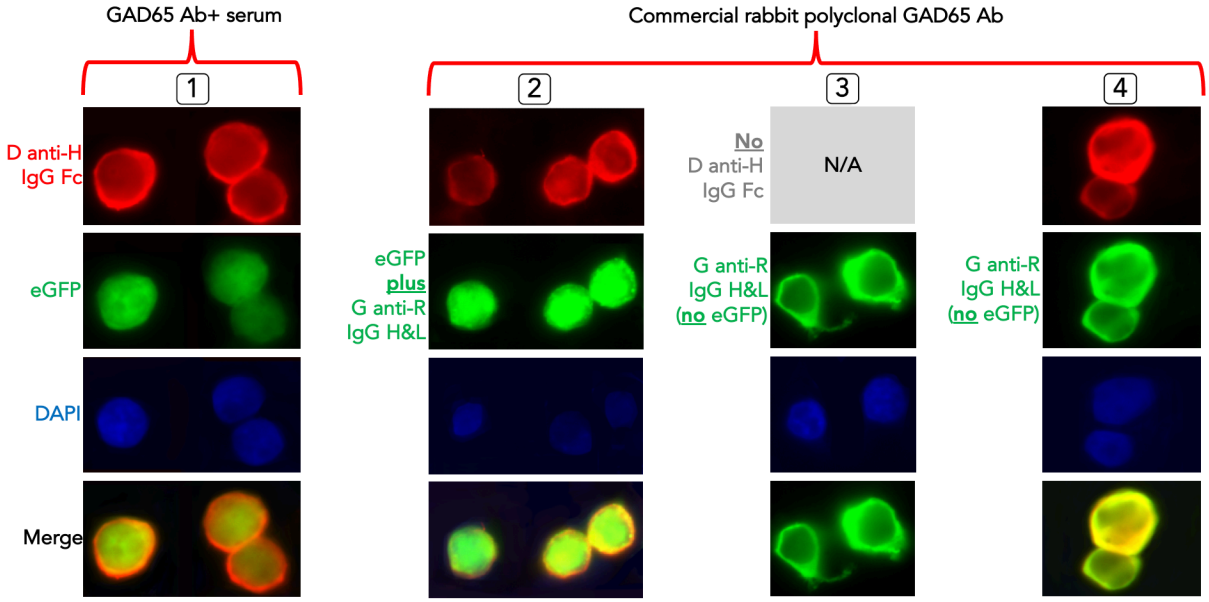


Figure 20: Additional commercial GAD65 antibody as a control sample for the CBA
Fluorescence microscopy images (x100 magnification, oil immersion). Labels to the left side of column 1 apply across each row, unless otherwise stated. GAD65 autoantibody-positive serum **(column 1)** detected with donkey anti-human IgG Fc secondary antibody (red fluorescent tag, 1:100) compared to commercial rabbit polyclonal GAD65 antibody **(columns 2, 3, 4)** detected with a goat anti-rabbit IgG H&L secondary antibody (green fluorescent tag,1:250). **Column 2**: The bright, diffuse intracellular eGFP signal (also green) partly obscures the pericytoplasmic annular signal of the commercial GAD65 antibody. To aid visualisation, the commercial antibody was also tested without eGFP transfection **(columns 3 and 4)**. **Column 4**: Concurrent use of two secondary antibodies (D anti-H IgG Fc 1:1,000 and G anti-R IgG H&L 1:250) gave rise to a red fluorescent IgG signal identical to the green fluorescent IgG signal. *Ab*, antibody; *Ab+*, antibody-positive; *AIN*, autoimmune neurology; *AQP4*, aquaporin-4; *CASPR2*, contactin-associated protein-2; *CBA*, cell-based assay; *D anti-H IgG Fc*, donkey anti-human IgG, Fc-gamma fragment-specific; *DAPI*, 4',6-diamidino-2-phenylindole; *eGFP*, enhanced green fluorescent protein; *GAD65*, glutamic acid decarboxylase 65; *G anti-R IgG H&L*, goat anti-rabbit IgG, heavy and light chains; *IgG*, immunoglobulin G; and *N/A*, not applicable.

No specific positive signal was observed when the CBA was performed with non-transfected (**Figure 21.5**) or non-GAD65 antigen transfected HEK-293T cells (**Figure 21.2-4**).

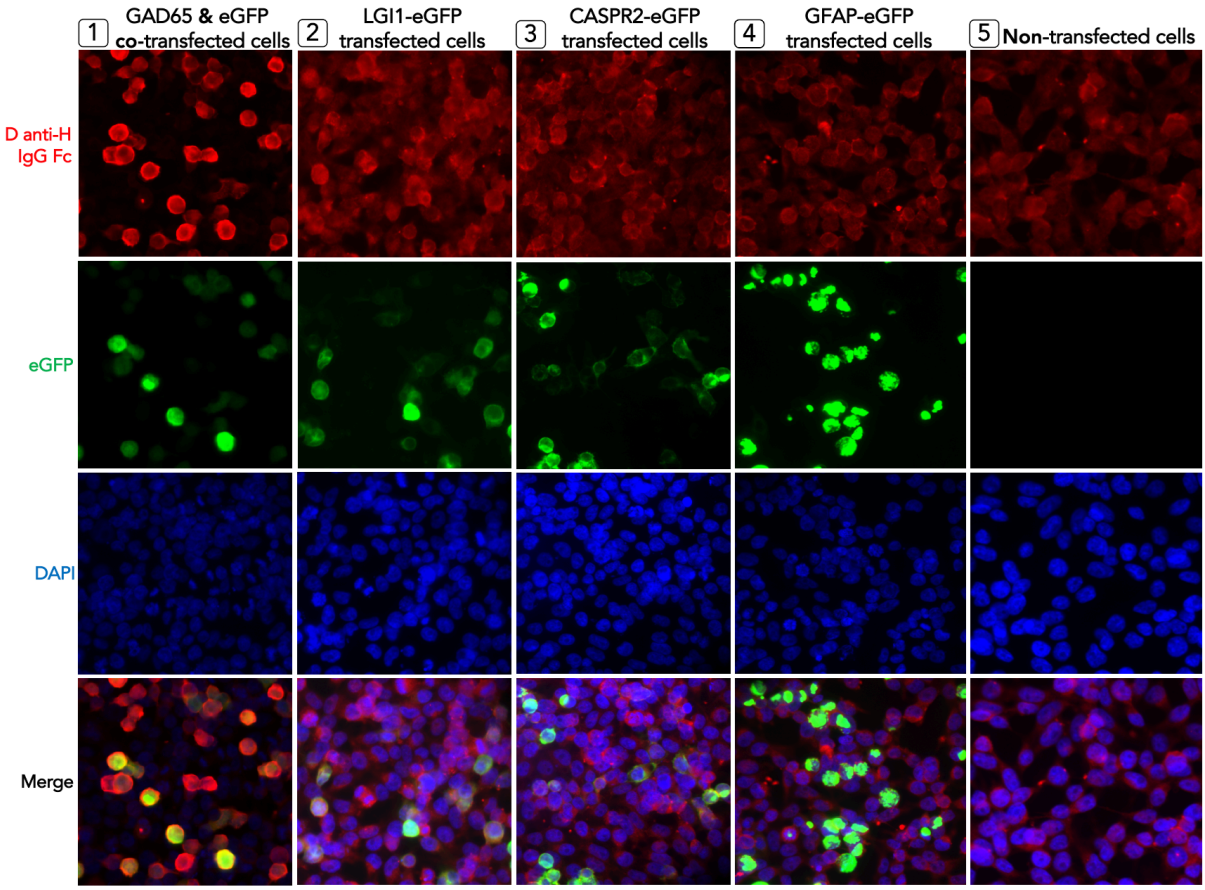


Figure 21: Non-GAD65 antigen controls for the GAD65 antibody CBA
Fluorescent microscopy images (x40 magnification). Each column represents a separate CBA, all performed with serum from the same GAD65 autoantibody-positive autoimmune neurology patient. **Columns 2-4:** HEK-293T cells expressed an antigen other than GAD65. The LGI1, CASPR2 and GFAP expression vectors encode eGFP-tagged antigens. The GAD65 vector lacks eGFP, and so co-transfection with a separate eGFP expression vector was required for the GAD65 antibody CBA. The characteristic patchy staining pattern of GAD65 antibodies was only seen with GAD65-expressing cells **(column 1)**. *CASPR2*, contactin-associated protein-2; *D anti-H IgG Fc*, donkey anti-human IgG, Fc-gamma fragment-specific; *DAPI*, 4',6-diamidino-2-phenylindole; *eGFP*, enhanced green fluorescent protein; *GAD65*, glutamic acid decarboxylase 65; *GFAP*, glial fibrillary acidic protein; *IgG*, immunoglobulin G; and *LGI1*, leucine-rich glioma inactivated-1.

As expected, production of the positive IgG signal was dependent on cell permeabilisation (Figure 22).

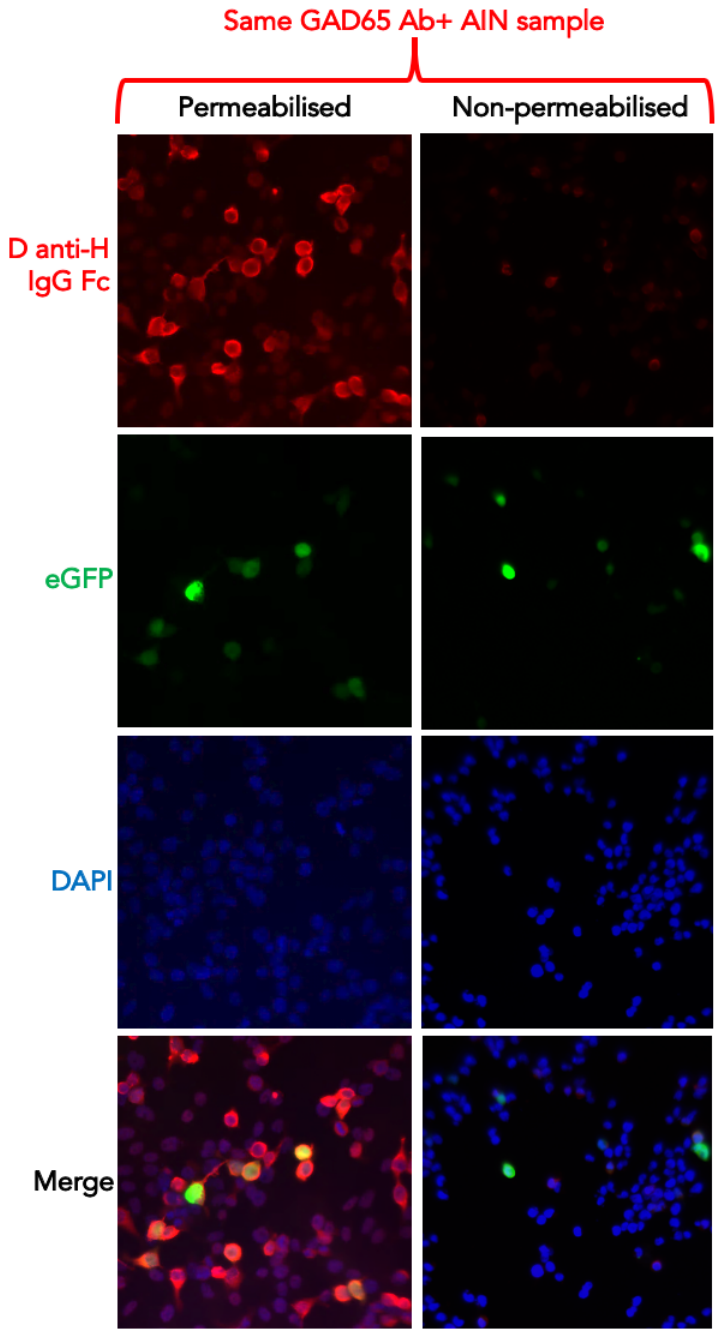


Figure 22: GAD65 CBA performed with and without permeabilisation agent
Fluorescence microscopy images (x40 magnification). The GAD65 antigen is intracellular. Two assays, one with permeabilisation agent and one without, were performed using the same GAD65 Ab+ serum. The positive IgG signal was only seen with cell permeabilisation. *Ab+*, antibody-positive; *AIN*, autoimmune neurology; *D anti-H IgG Fc*, donkey anti-human IgG, Fc-gamma fragment-specific; *DAPI*, 4′,6-diamidino-2-phenylindole; *GAD65*, glutamic acid decarboxylase 65; *GFAP*, glial fibrillary acidic protein; and *IgG*, immunoglobulin G.

4.4 Optimisation

CBAs for detecting antibodies to intracellular antigens typically involve cell fixation and permeabilisation, blocking non-specific antibody binding, primary antibody incubation, secondary antibody incubation, and washing.[118,298–301] The GAD65 antibody CBA was developed in a similar way, with protocol iterations centred on a systematic, rational approach and trialling elements of methodology from appropriate literature.

Three different secondary antibodies were compared (**Table 30** and **Figure 23**) – donkey anti-human IgG targeting the Fc-gamma portion of the primary IgG antibody heavy chain; goat anti-human IgG antibody targeting the heavy and light chains of the primary IgG antibody; and goat anti-human Fab fragment antibody targeting the Fc-gamma portion of the primary IgG antibody heavy chain. The donkey anti-human IgG, Fc-gamma fragment-specific secondary antibody produced the brightest antigen-specific signal with the least background signal.

Table 30: Characteristics of secondary (detector) antibodies trialled for the GAD65 antibody CBA
Three secondary antibodies were tested. The goat anti-human IgG, heavy and light chain antibody was selected because it was the standard secondary antibody used in the Oxford Autoimmune Neurology Group laboratory for CBAs at the time. The goat anti-human Fab fragment, Fc-gamma fragment-specific antibody was readily available in the lab and had an appropriate host/target species profile. The donkey anti-human IgG, Fc-gamma fragment-specific antibody was chosen for variation in antibody format and host species. *CBA*, cell-based assay; *GAD65*, glutamic acid decarboxylase 65; and *IgG*, immunoglobulin G.

Target species	*Host species*	*Antibody format*	*Specificity*	*Conjugate*	*Clonality*	*Purification*
Human	Donkey	Whole IgG	IgG, Fc-gamma fragment-specific	Alexa Fluor® 594	Polyclonal	Affinity-purified
Human	Goat	Whole IgG	IgG, heavy and light chains	Alexa Fluor® 568	Polyclonal	Affinity purified and cross-adsorption against mouse, rabbit and bovine serum
Human	Goat	Fab fragment	IgG, Fc-gamma fragment-specific	Alexa Fluor® 594	Polyclonal	Affinity-purified

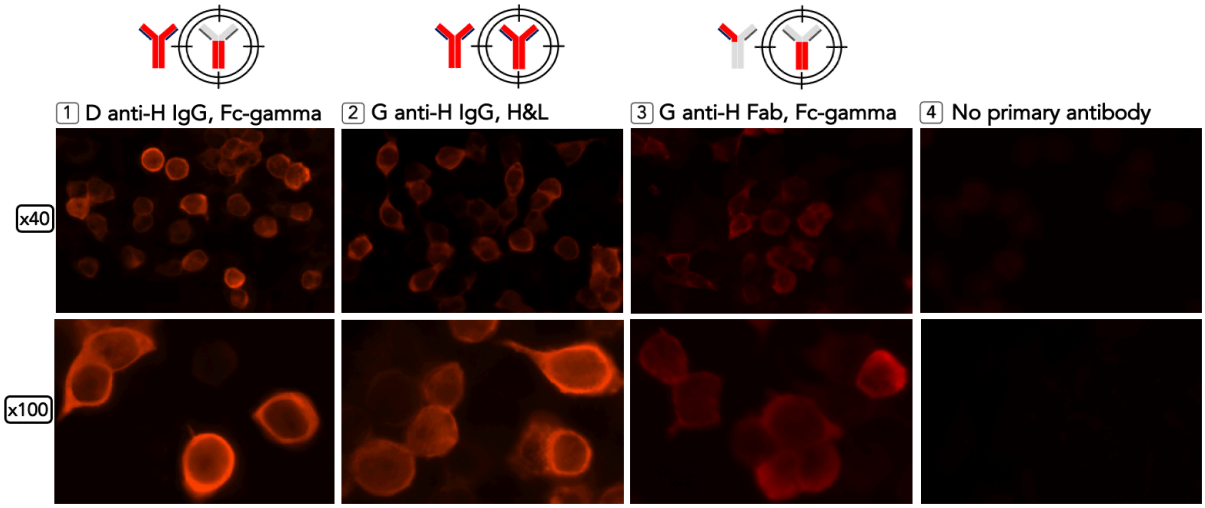


Figure 23: Secondary antibody for the GAD65 antibody CBA
Fluorescence microscopy images (upper row x40 magnification and lower row x100 magnification; same fields) comparing three different IgG secondary (detector) antibodies: **(1)** D anti-H IgG, Fc-gamma (1:500); **(2)** G anti-H IgG, H&L (1:750); and **(3)** G anti-H Fab, Fc-gamma (1:500). The same sample/primary antibody (GAD65 autoantibody-positive patient from the autoimmune neurology clinic) was used each time (1:100). Antigen-specific signal was brightest with D anti-H IgG, Fc-gamma secondary. There was good specific signal with G anti-H IgG, H&L, although more background. Specific signal was weakest with G anti-H Fab, Fc-gamma. **(4)** D anti-H IgG, Fc-gamma (1:500) with no primary antibody. There was no noticeable difference when assays were performed without a primary antibody but with either of the other two secondaries (not shown). *CBA*, cell-based assay; *D anti-H IgG, Fc-gamma*, donkey anti-human IgG, Fc-gamma fragment-specific; *GAD65*, glutamic acid decarboxylase 65; *G anti-H Fab, Fc-gamma*, goat anti-human Fab fragment, Fc-gamma fragment-specific; and *G anti-H IgG, H&L*, goat anti-human IgG, heavy and light chain.

Normal donkey serum, normal goat serum and bovine serum albumin were trialled as blocking agents at concentrations of 1, 5 and 10% (**Figure 24**). At all concentrations, bovine serum albumin was associated with the most significant amount of non-specific background staining. Normal donkey serum and normal goat serum reduced background to a similar degree at 1 and 5% concentrations. At 10% concentration, goat serum performed better and is considerably less expensive than donkey serum.

Serial photographs of blocking agent incubation times (at 30, 60, 90, 120 minutes and overnight) were taken (**Figure 25**). Background staining reduced with increasing blocking time, with the best effect from overnight incubation.

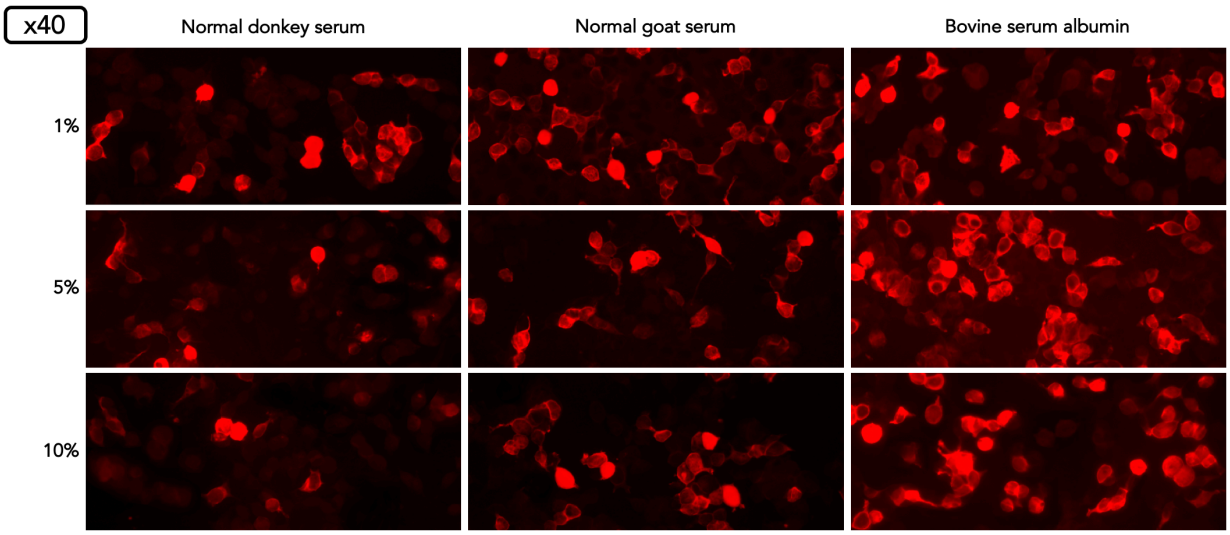


Figure 24: Blocking agent and concentration for the GAD65 antibody CBA
Fluorescence microscopy images (x40 magnification, oil immersion). Intentional overexposure of GAD65 antibody-positive cells to capture background staining as observed by the naked eye through the microscope eyepiece (the limited dynamic range of the camera precluded photographing positive and background staining simultaneously in a representative manner). Comparison of normal donkey serum, normal goat serum and bovine serum albumin as blocking agents at concentrations of 1, 5 and 10%. Serum from the same GAD65 autoantibody-positive autoimmune neurology patient was used for all tests (dilution 1:100). At all concentrations, bovine serum albumin resulted in the most background staining. 1 and 5% concentrations of normal donkey serum and normal goat serum performed similarly to reduce background. At 10% concentration, goat serum performed better. Due to COVID-19-related laboratory restrictions, it was not possible to complete experiments with control serum or non-transfected cells, or to show decreasing non-specific binding without significant change in positive signal. *CBA*, cell-based assay; and *GAD65*, glutamic acid decarboxylase 65.

HEK cells are inevitably lost over the course of a CBA (e.g., due to washes). Too few cells at the point of microscopy can render reading unreliable. Conversely, cells clump at higher densities, making background staining and non-specific membrane staining appear brighter and more difficult to distinguish from a true positive signal. Hence, cells were seeded at 50,000; 80,000; 100,000; and 200,000 cells per well on a 24 well-plate for comparison (**Figure 26**). Plating 100,000 cells per well consistently yielded sufficient cells for reading without excessive clumping.

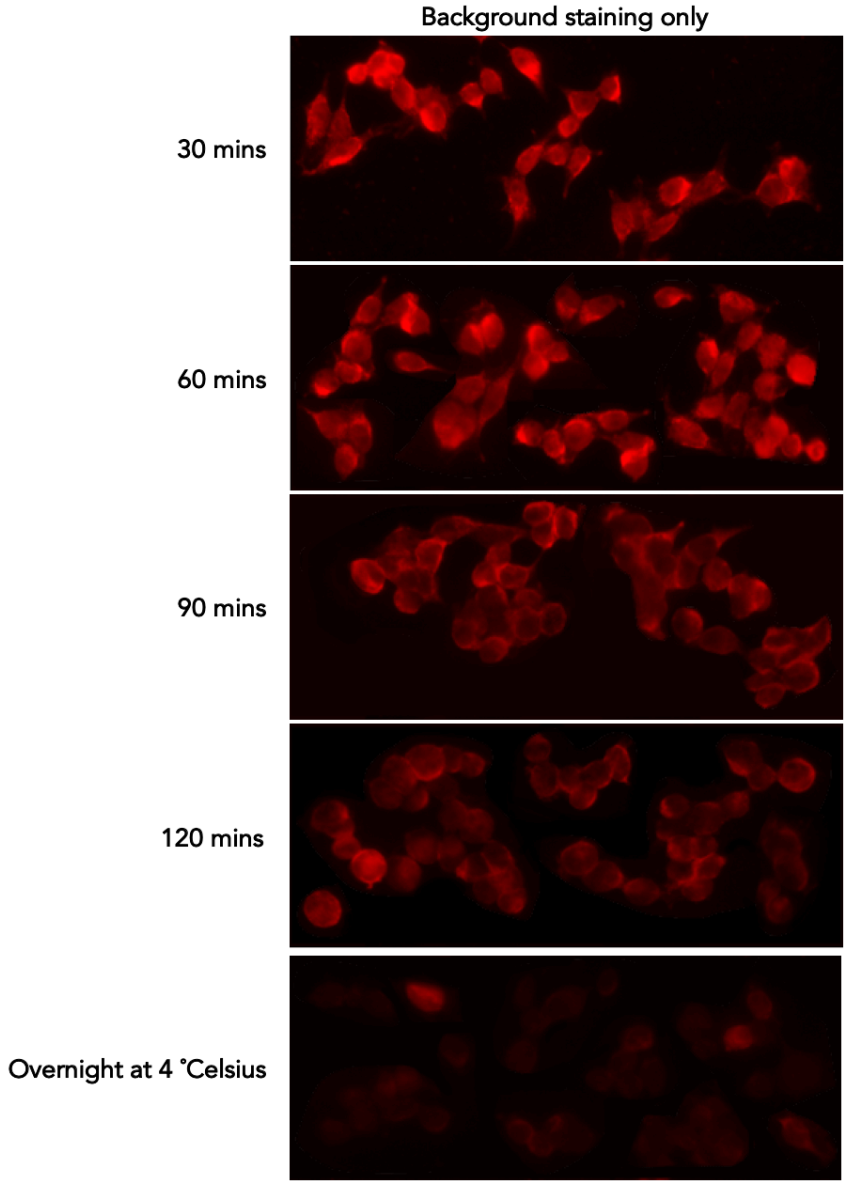


Figure 25: Duration of blocking in the GAD65 antibody CBA

Fluorescence microscopy images (magnification x40). Showing non-specific background staining only. GAD65 antibody-positive cells (not shown) were intentionally overexposed to capture the background staining as observed by the naked eye through the microscope eyepiece (the limited dynamic range of the camera precluded photographing positive and background staining simultaneously in a representative manner). Serum (1:100) from a GAD65 autoantibody-positive autoimmune neurology patient was incubated with blocking agent (10% NGS). Serial photographs were taken with the same exposure length of 25 milliseconds. Incubation of up to 120 minutes was at room temperature; overnight incubation was at 4 °Celsius to prevent bacterial growth in samples. Background staining attenuated with increasing incubation time; best effect with overnight incubation. *CBA*, cell-based assay; *GAD65*, glutamic acid decarboxylase 65; and *NGS*, normal goat serum.

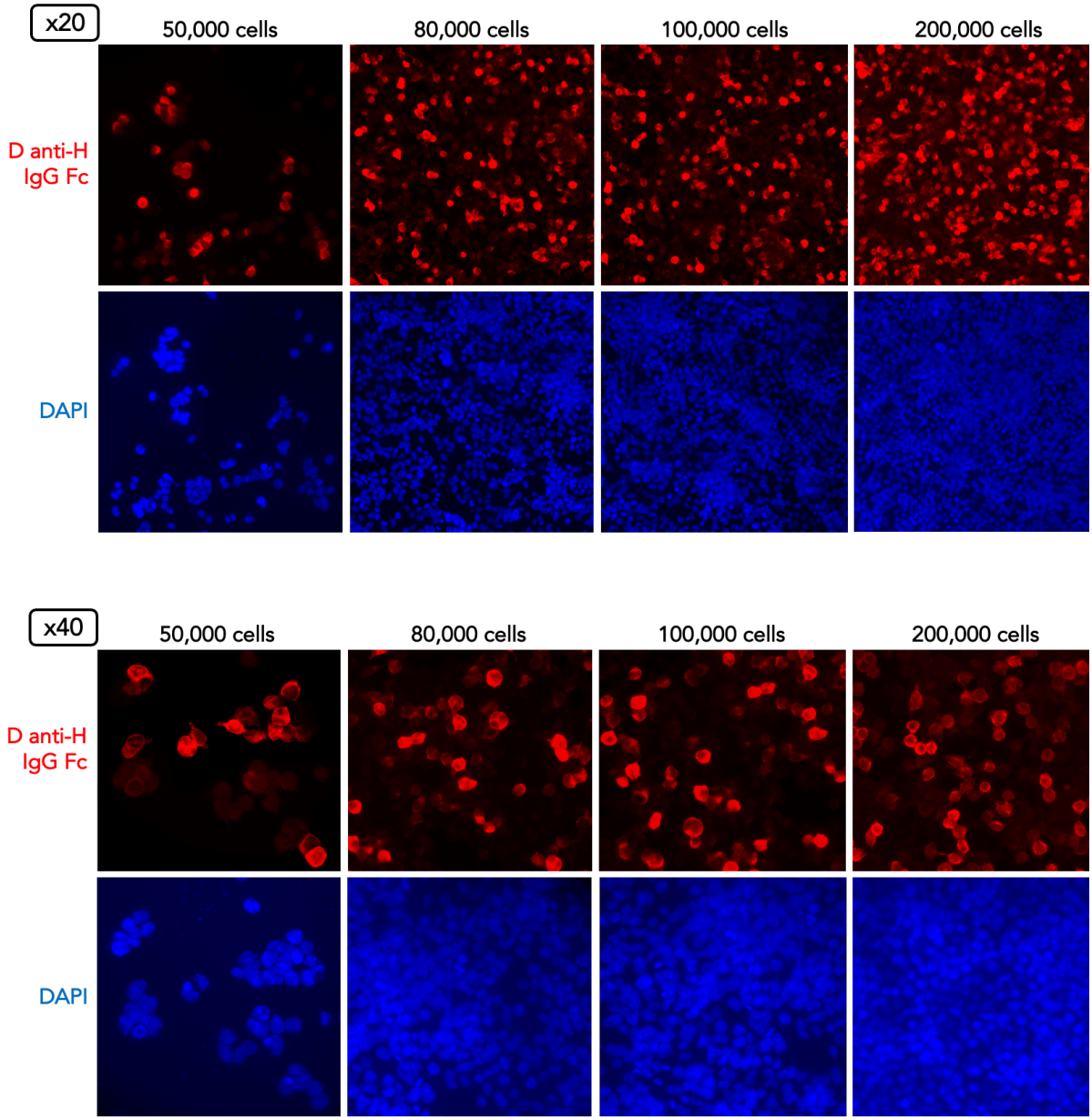
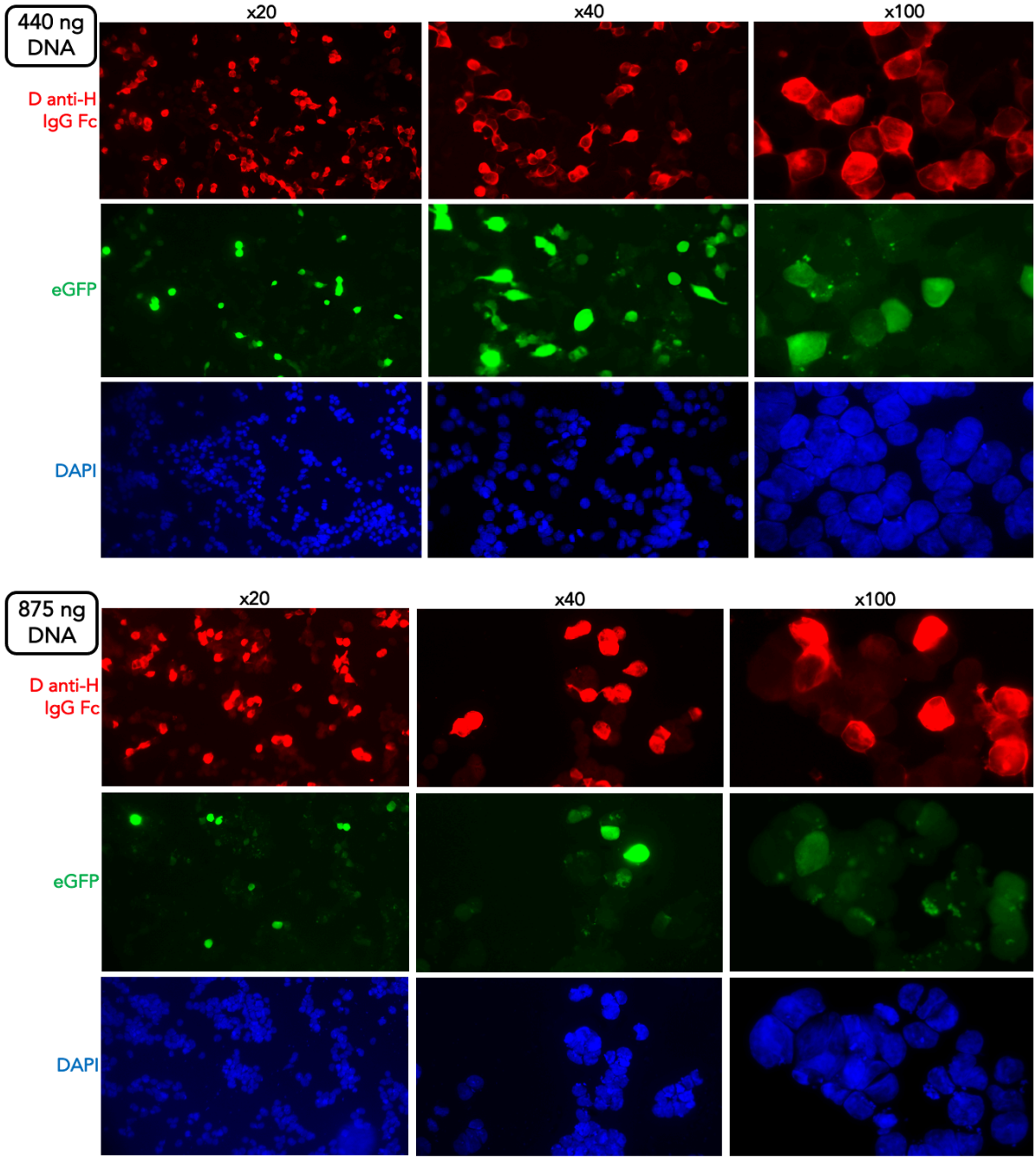


Figure 26: Number of HEK-293T cells seeded for the GAD65 antibody CBA

Fluorescence microscopy images (upper panel magnification x20 and lower panel magnification x40). The number of cells seeded per well (in a 24-well plate) ranged from 50,000 – 200,000. Serum from the same GAD65 autoantibody-positive autoimmune neurology patient was used for all tests (1:100). The best balance between cell loss and cell clumping was achieved with plating 100,000 cells. *CBA*, cell-based assay; *D anti-H IgG Fc*, donkey anti-human IgG Fc-gamma fragment-specific; *DAPI*, 4',6-diamidino-2-phenylindole; *GAD65*, glutamic acid decarboxylase 65; HEK-293T cells, human embryonic kidney 293T cells; and *IgG*, immunoglobulin G.

The CBA protocol routinely used by the Oxford Autoimmune Neurology Group involves transfecting 875 ng of plasmid DNA per well (in a 24 well-plate). To test if cell transfection rates could be improved to aid assay interpretation, the amount of DNA added per well was varied (**Figure 27**). Doubling the amount of DNA to 1,750 ng per well led to a lower transfection rate for GAD65 and eGFP, whereas halving the amount of DNA to 440 ng improved the transfection rate for both.



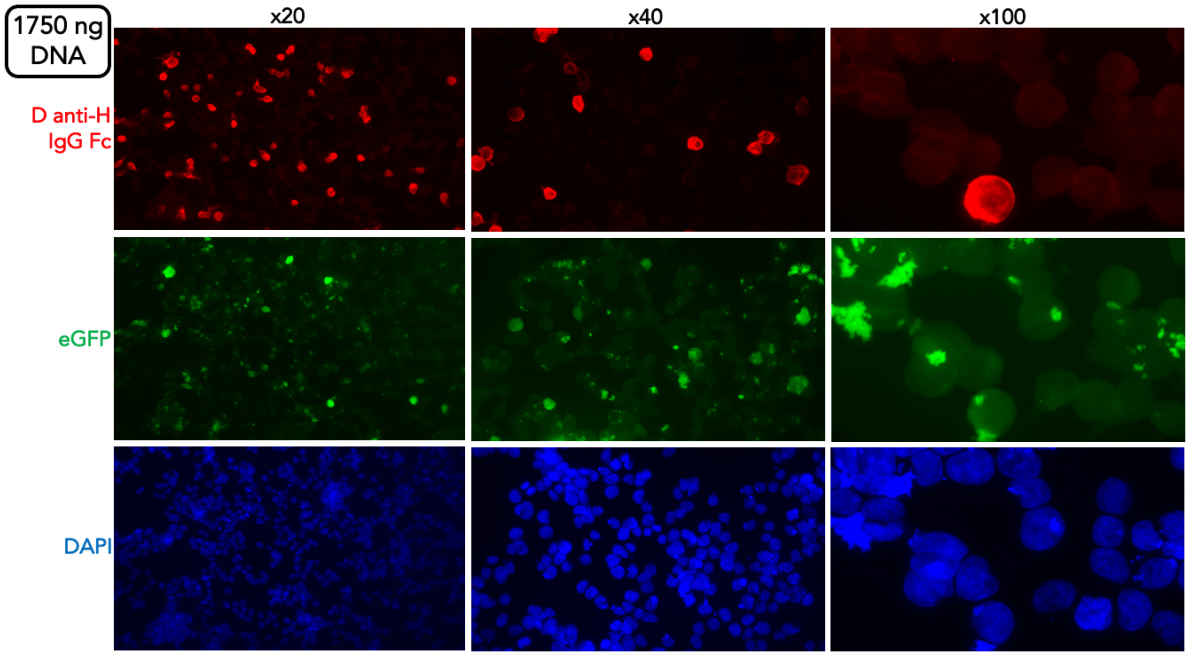


Figure 27: Plasmid DNA concentration for the GAD65 antibody CBA
Fluorescence microscopy images. Each panel shows cells at magnifications x20, x40 and x100 (oil immersion). The amount of plasmid DNA added per well (to 100,000 cells) was varied: 440 ng DNA **(upper panel)**, 875 ng DNA **(middle panel)** and 1750 ng DNA **(lower panel)**. The same GAD65 autoantibody-positive autoimmune neurology patient serum sample was used for all wells (1:100). The highest GAD65 antibody and eGFP signals were with 440 ng DNA per well. The transfection reagent, PEI, is a cytotoxic synthetic polycation. Similarly, plasmid DNA is cytotoxic. Therefore, the addition of more DNA to the cell transfection mix (requiring more PEI) potentially increased cytotoxicity and reduced transfection efficiency. *CBA*, cell-based assay; *D anti-H IgG Fc*, donkey anti-human IgG Fc-gamma fragment-specific; *GAD65*, glutamic acid decarboxylase 65; *DAPI*, 4',6-diamidino-2-phenylindole; *eGFP*, enhanced green fluorescent protein; *IgG*, immunoglobulin G; and *PEI*, polyethylenimine.

A preabsorption step was added to determine whether the assay's signal-to-noise ratio could be improved (**Figure 28**). However, incubating the serum sample with non-transfected HEK-293T cells before the CBA led to increased non-specific signal.

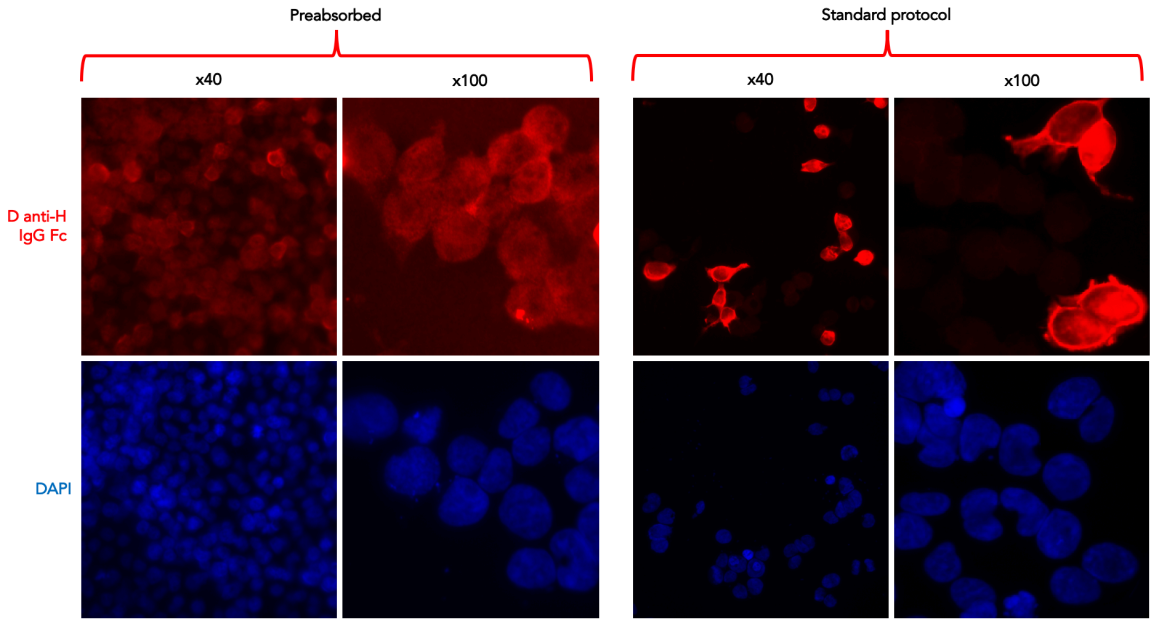


Figure 28: Preabsorption of serum sample prior to GAD65 antibody CBA
Fluorescence microscopy images (magnification x40 and x100, oil immersion). Intentional overexposure of GAD65 antibody-positive cells to capture non-specific background staining as observed by the naked eye through the microscope eyepiece (the limited dynamic range of the camera precluded photographing specific and non-specific staining in a representative manner simultaneously). The same serum sample from a GAD65 autoantibody-positive autoimmune neurology patient was tested using the standard protocol (**right panel**). This was compared to a modified protocol with an added preabsorption step, whereby the sample was incubated with permeabilised, non-transfected HEK-293T cells for 45 minutes immediately before the CBA (**left panel**). The preabsorption step produced more non-specific signal. *CBA*, cell-based assay; *D anti-H IgG Fc*, donkey anti-human IgG Fc-gamma fragment-specific; *DAPI*, 4',6-diamidino-2-phenylindole; *GAD65*, glutamic acid decarboxylase 65; and *IgG*, immunoglobulin G.

Primary and secondary antibody incubations of the same duration were compared at room temperature, 37 °Celsius and 4 °Celsius (**Figure 29**). Specific signal was best at room temperature, decreased at 37 °Celsius and was almost lost at 4 °Celsius.

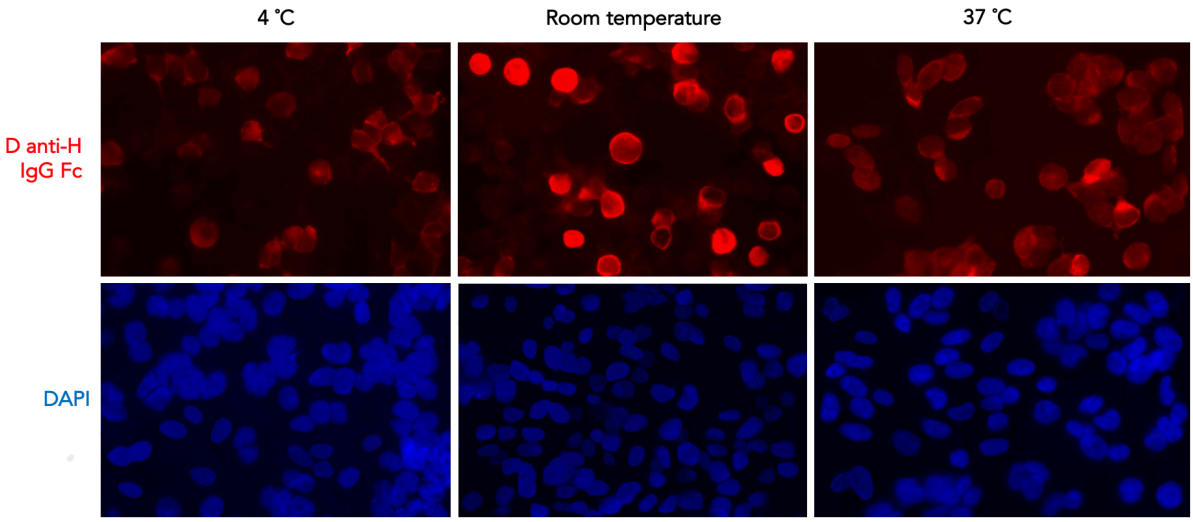


Figure 29: Temperature for the GAD65 antibody CBA
Fluorescence microscopy images (magnification x40). Intentional overexposure of GAD65 antibody-positive cells to capture non-specific background staining as observed by the naked eye through the microscope eyepiece (the limited dynamic range of the camera precluded photographing specific and non-specific staining in a representative manner simultaneously). Primary and secondary antibody incubations were performed at a range of temperatures using serum samples from the same GAD65 autoantibody-positive autoimmune neurology patient. Compared to room temperature (**middle column**), specific signal was decreased at 37 °Celsius (**right column**) and almost completely lost at 4 °Celsius (**left column**). *CBA*, cell-based assay; *D anti-H IgG Fc*, donkey anti-human IgG Fc-gamma fragment-specific; *DAPI*, 4',6-diamidino-2-phenylindole; *GAD65*, glutamic acid decarboxylase 65; and *IgG*, immunoglobulin G.

Other variations in the protocol were selected for investigation (**Figure 30**). Ruiz-García et al.[302] recently developed a CBA for detecting autoantibodies to the intracellular target SOX1 – mirroring this methodology produced a less bright positive signal (**Figure 30.2**). Incubation of the primary antibody overnight at 4 °Celsius (**Figure 30.3**) did not improve the CBA, nor did running the primary incubation at pH 5.5 (intracellular pH) (**Figure 30.4**). Reducing the permeabilisation agent from 0.3 to 0.1% resulted in a patchy and less intense positive signal (**Figure 30.5**).

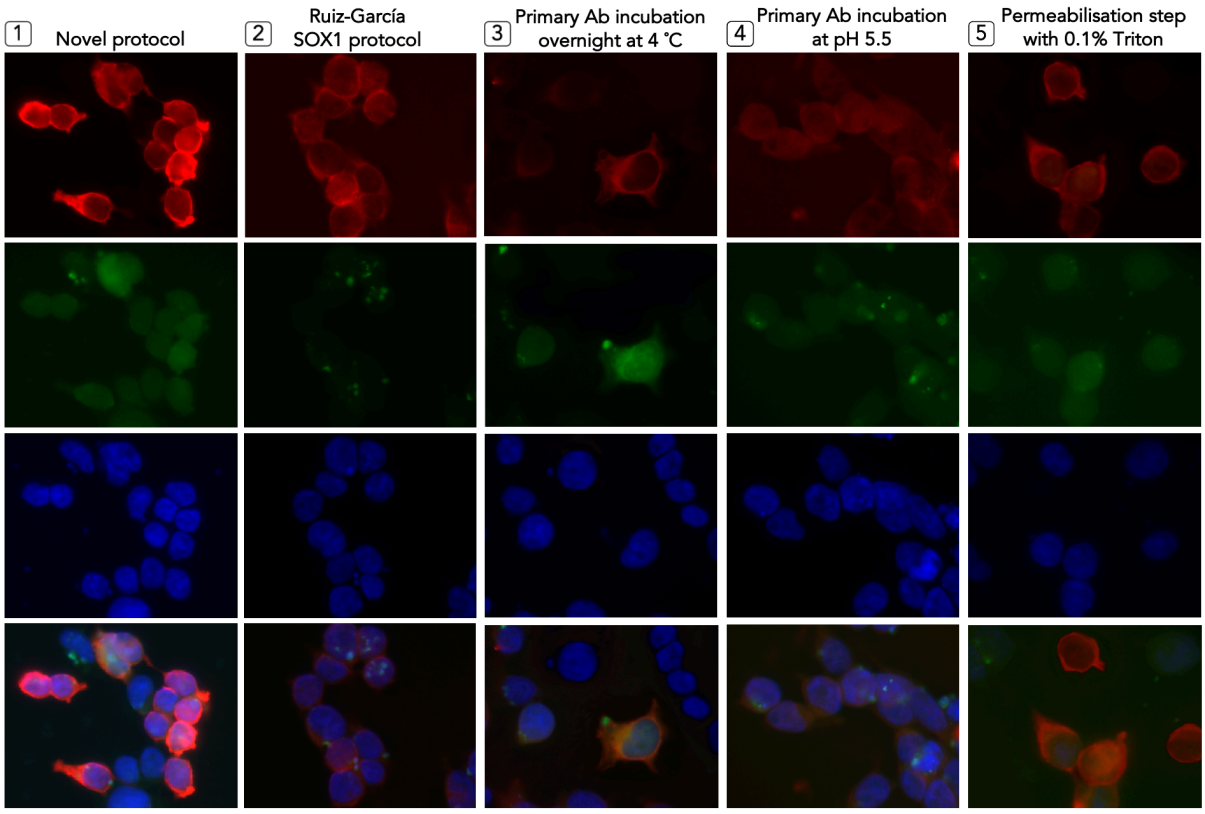


Figure 30: Other variables investigated for the GAD65 antibody CBA
Fluorescence microscopy images (x100 magnification, oil immersion). **(1):** The novel GAD65 antibody CBA protocol in development by this point involved a discrete 10-minute permeabilisation step with 0.3% Triton X-100. In addition, serum is diluted (1:100) in1% normal goat serum in 0.1% Triton X-100/PBS. Primary antibody incubation is for 60 minutes at room temperate and pH 7.4; and 10% normal goat serum is used for blocking. **(2):** The Ruiz-García et al.[302] protocol for detecting autoantibodies to the intracellular target SOX1 utilises a serum dilution of 1:40 in PBS/1%BSA, a 5-minute discrete permeabilisation step with 0.3% Triton X-100 and an otherwise Triton-free protocol, and the primary incubation takes place overnight at 4 °Celsius. Compared to the standard protocol, the Ruiz-García methodology produced a less bright positive signal. **(3):** Incubation of the primary antibody overnight at 4 °Celsius (but otherwise adhering to the standard protocol) did not improve the CBA. **(4):** Running the primary incubation at pH 5.5 did not improve the CBA. **(5):** Reducing the permeabilisation agent from 0.3 to 0.1% resulted in a patchy and less intense positive signal. *Ab*, antibody; *CBA*, cell-based assay; and *GAD65*, glutamic acid decarboxylase 65.

The microscope objective best suited for screening batches of samples was considered (Figure 31). Distinguishing between genuine positive signal and non-specific/background staining was most reliable at x100 objective (oil immersion), although this was much more time-consuming. The best balance between reliability of interpretation of staining patterns and time efficiency was using the x40 objective, with occasional use of x100 (oil immersion) for more difficult-to-interpret samples.

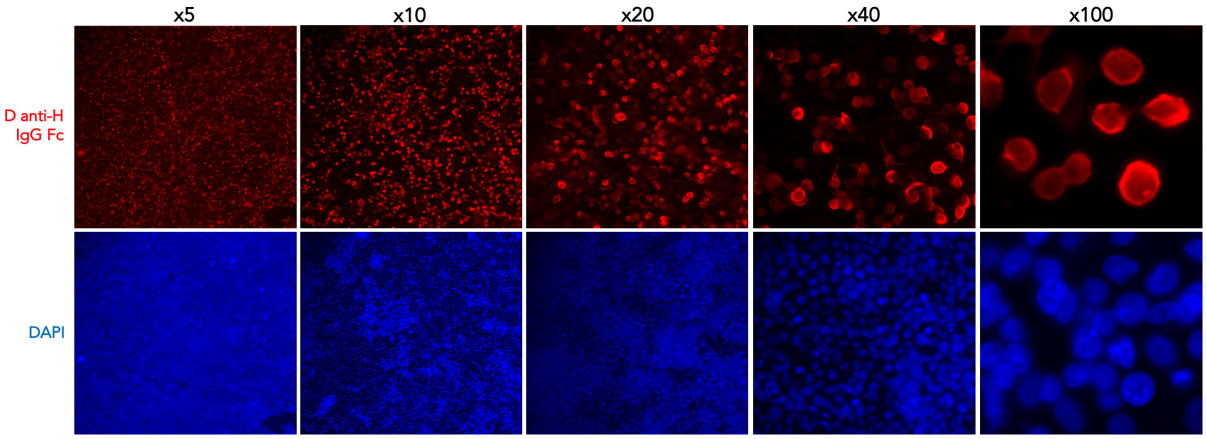


Figure 31: Microscope objective for reading results of the GAD65 antibody CBA
Fluorescence microscopy images of the same serum sample (1:100) from a GAD65 antibody-positive autoimmune neurology patient photographed at a range of magnifications – x5, x10, x20, x40 and x100 (with oil immersion). Distinguishing between real positive samples and non-specific/background staining was most reliable at x100, but this objective was more time consuming for reading. The best balance for interpretation of staining patterns and time efficiency was to use the x40 objective, with occasional use of x100 with oil immersion. *CBA*, cell-based assay *D anti-H IgG Fc*, donkey anti-human IgG Fc-gamma fragment-specific; *DAPI*, 4′,6-diamidino-2-phenylindole; *GAD65*, glutamic acid decarboxylase 65; and *IgG*, immunoglobulin G.

The appropriate serum dilution for screening particular patient groups would be determined later, after testing a broad range of patients and controls. As permeabilised CBAs typically use starting dilutions of serum in the range of 1:500 and above[303,304], 1:100 was selected as a starting point to avoid missing low positive results of interest.

The outcome of the optimisation experiments is summarised in Table 31.

Table 31: Summary of optimisation steps for the novel GAD65 antibody CBA
Outcome of various optimisation steps using 24-well plates. *CBA*, cell-based assay; *eGFP*, enhanced green fluorescent protein; *GAD65*, glutamic acid decarboxylase 65; *HEK-293T cells*, human embryonic kidney 293T cells; *IgG*, immunoglobulin G.

Variables	*Outcome*
Amount of GAD65 and eGFP DNA transfected	440 ng DNA per well improved eGFP transfection rate
Number of HEK-293T cells seeded	100,000 HEK-293T cells per well provide sufficient areas of cell monolayer and mitigate wash-related cell loss
Blocking agent, concentration, and incubation period	Normal goat serum 10% with overnight incubation reduces background signal
Concentration of permeabilisation agent	Triton X-100 0.1% in diluents for sample and secondary antibodies; discrete permeabilisation step with Triton X-100 0.3%
Secondary antibody	Donkey anti-human IgG Fc-specific
Primary antibody incubation pH	pH 7.4
Primary antibody incubation temperature	Room temperature
Preabsorption of patient samples on non-transfected HEK-293T cells before CBA	No preabsorption

4.5 Application of the GAD65 CBA

The CBA which I optimised was able to detect GAD65 antibodies in serum, plasma, CSF and peripheral blood mononuclear cell culture supernatants (**Figure 32**).

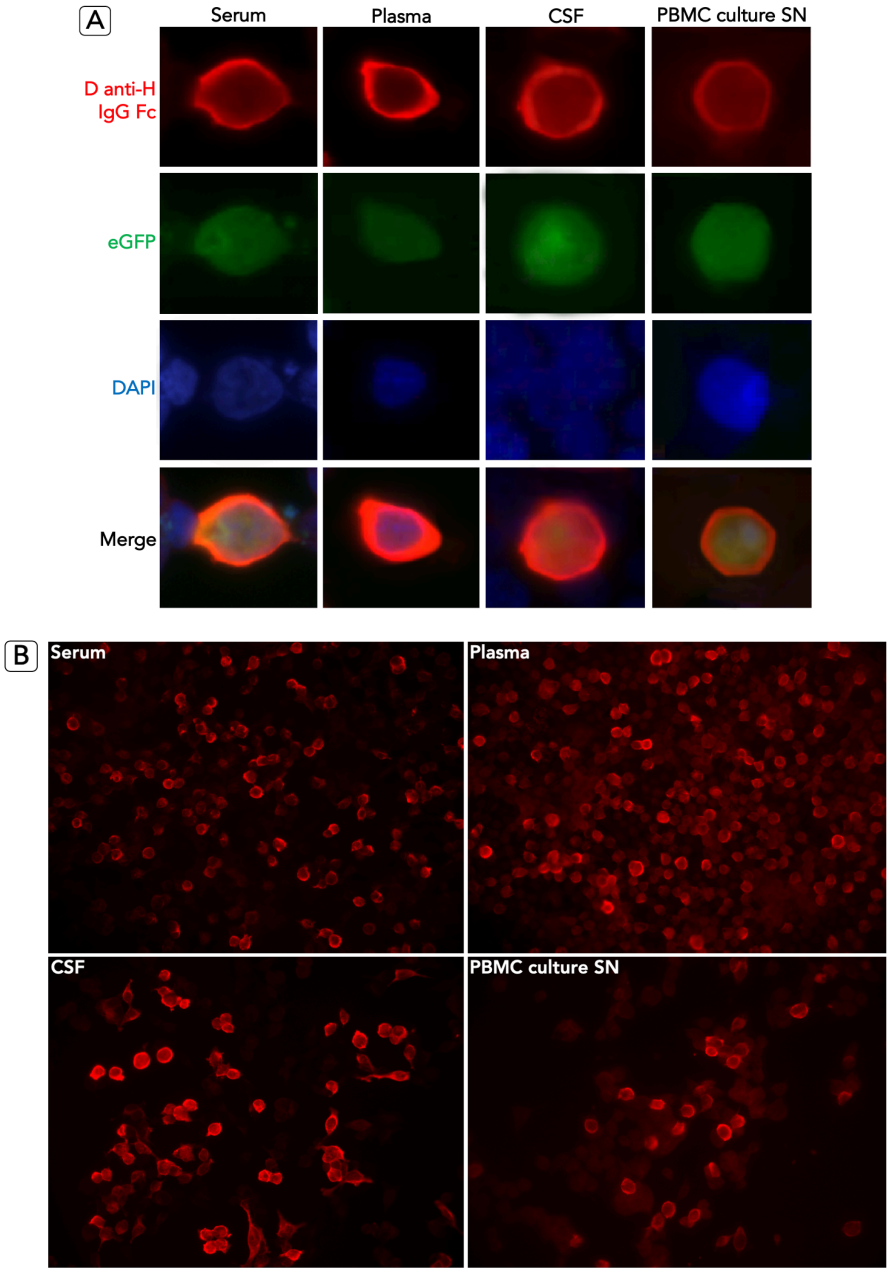


Figure 32: Detection of GAD65 autoantibodies in different sample types
Fluorescence microscopy images. **(A):** magnification x100, oil immersion; single positive-staining cells. GAD65 autoantibodies detected in serum (875 samples tested), plasma (42 samples tested), CSF (16 samples tested) and PBMC culture supernatant (five samples tested) at sample dilutions of 1:100, 1:100, 1:10 and 1:4, respectively. PBMC culture supernatants provided by Dr Adam Al-Diwani, Oxford Autoimmune Neurology Group. **(B):** magnification x40; whole field. Images are representative of other positive samples. *CBA*, cell-based assay; *CSF*, cerebrospinal fluid; *D anti-H IgG Fc*, donkey anti-human IgG Fc-gamma fragment-specific; *DAPI*, 4',6-diamidino-2-phenylindole; *eGFP*, enhanced green fluorescent protein; *GAD65*, glutamic acid decarboxylase 65; *IgG*, immunoglobulin G; *PBMC*, peripheral blood mononuclear cell; and *SN*, supernatant.

4.6 Testing ELISA and RIPA calibrators on the GAD65 antibody CBA

Calibrators (standards) containing pre-determined concentrations of GAD65 antibody are supplied with the ELISA and RIPA kits to form calibration curves for interpolation of autoantibody concentrations in patient samples. The manufacturer, RSR Ltd, reported that the same GAD65 antibody was used for calibrators in both kits but declined to disclose the host species. I planned to test the calibrators as CBA samples to assess whether their stated antibody concentration correlated with CBA score. Firstly, an appropriate secondary antibody had to be selected. Secondary antibodies against rabbit, mouse and goat were trialled but GAD65 antibodies were only detected by goat anti-rabbit IgG (**Figure 33**).

A goat anti-rabbit IgG secondary antibody targeting heavy and light chains produced a positive signal. The results of the subsequent CBA using this secondary antibody are shown in **Table 32**. Overall, the CBA scores increased with calibrator (GAD65 antibody) concentration, for both ELISA and RIPA.

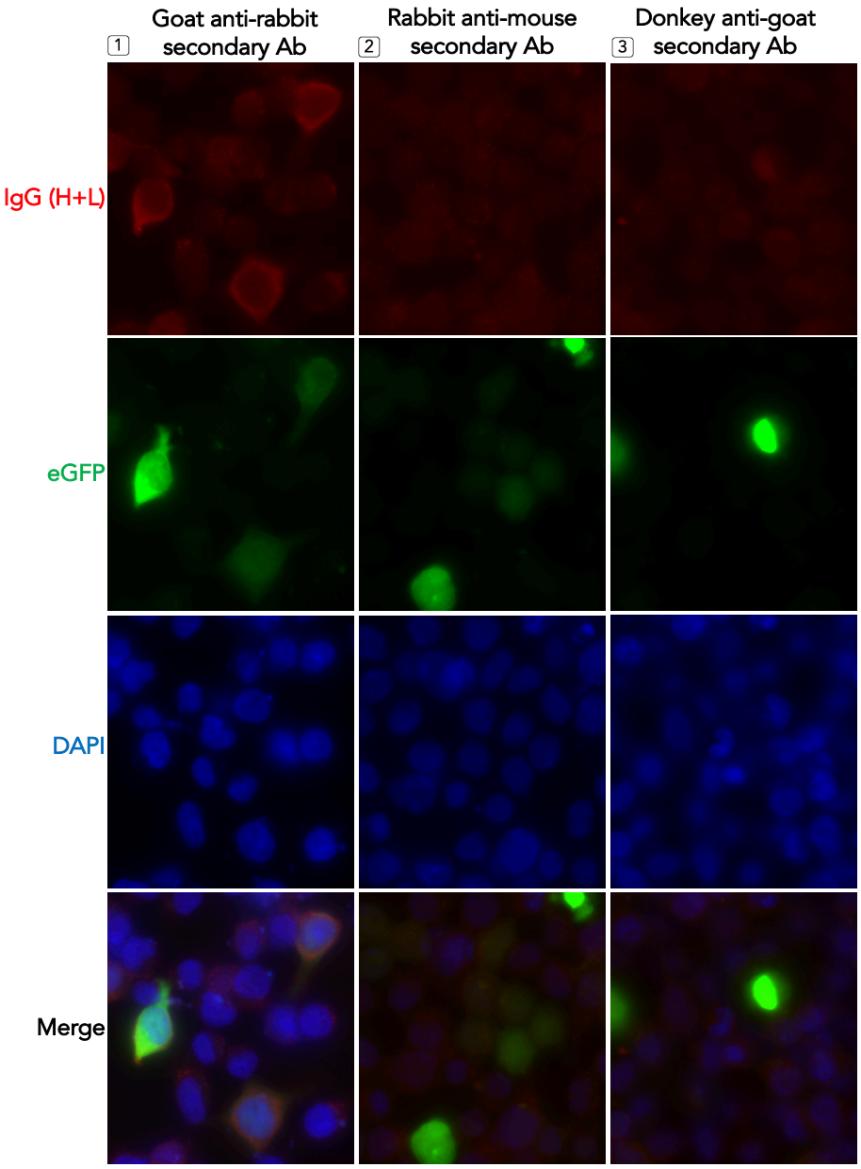


Figure 33: Selection of an appropriate secondary antibody for testing RIPA and ELISA calibrators on the GAD65 antibody CBA

Fluorescence microscopy images (magnification x100, oil immersion). A 2000 units/ml ELISA calibrator (1:100) was tested on the GAD65 antibody CBA using secondary antibodies raised in three different species (rabbit, mouse and goat). All antibodies targeted IgG heavy and light chains, and were diluted 1:750. **(1):** goat anti-rabbit IgG. **(2):** rabbit anti-mouse IgG. **(3):** donkey anti-goat IgG. These antibodies were selected because the species are commonly used in research, and they were readily available in the Oxford Autoimmune Neurology Group lab. GAD65 antibody-positive signal only observed with goat anti-rabbit IgG. *Ab*, antibody; *CBA*, cell-based assay; *DAPI*, 4′,6-diamidino-2-phenylindole; *eGFP*, enhanced green fluorescent protein; *ELISA*, enzyme-linked immunosorbent assay; *GAD65*, glutamic acid decarboxylase 65; *H&L*, heavy and light chains; *IgG*, immunoglobulin; and *RIPA*, radioimmunoprecipitation assay.

Table 32: RIPA and ELISA calibrator scores on the GAD65 antibody CBA

RIPA and ELISA kit calibrators were tested as samples (neat) on the GAD65 antibody CBA using a goat anti-rabbit IgG secondary antibody targeting heavy and light chains. Interpretation of CBA scoring – **0**: negative, **1**: low positive, **2-4**: positive. Units of measurement for RIPA are arbitrary and are not equivalent to the units of measurement for ELISA. The trend for CBA scores to rise in conjunction with increasing calibrator concentration is broadly supportive that higher CBA scores correlate to higher concentrations of GAD65 antibody but there are multiple factors that preclude further interpretation of this data. For example, the calibrators are from non-human species; the calibrators would usually interact with other reagents during RIPA and ELISA experiments which were not present in the CBA; the secondary antibody used to produce the CBA output is usually absent from the commercial assays and is not appropriately species-matched; and the raw RIPA and ELISA outputs (counts per minute and absorbance, respectively) require transformation and interpolation before determining an antibody concentration. *CBA*, cell-based assay; *ELISA*, enzyme-linked immunosorbent assay; *GAD65*, glutamic acid decarboxylase 65; and *RIPA*, radioimmunoprecipitation assay.

Sample	CBA score
RIPA calibrator 1 unit/ml	1.5
RIPA calibrator 3 units/ml	1.5
RIPA calibrator 10 units/ml	2.5
RIPA calibrator 30 units/ml	3.5
RIPA calibrator 120 units/ml	3.5
RIPA calibrator 300 units/ml	4
ELISA calibrator 5 units/ml	1.5
ELISA calibrator 18 units/ml	2
ELISA calibrator 35 units/ml	2
ELISA calibrator 250 units/ml	3.5
ELISA calibrator 2000 units/ml	4
Healthy control serum	0
GAD65 Ab+ control serum	4
No primary sample	0

4.7 Larger scale testing of patient and control samples on the GAD65 antibody CBA

A large selection of unique serum samples was tested for GAD65 antibodies on the new CBA (**Table 33**). GAD65 autoantibodies were detected in patient sera from: 8/206 (3.9%) drug-resistant epilepsy (DRE); 18/33 (54.5%) type 1 diabetes mellitus (T1DM); 17/25 (68%) T1DM with coexisting epilepsy; and 1/133 (0.8%) seropositive for neuronal surface-directed antibodies (NSAs). All 14 autoimmune neurology clinic patients known to have GAD65 autoantibodies tested positive on the CBA, in contrast to none of the healthy controls (n=170).

Table 33: GAD65 antibody CBA screening of 875 patient and control sera

875 unique serum samples were assayed at 1:100 using the GAD65 antibody CBA which I developed and optimised. CBA scores – 0: negative, 1: low positive, 2-4: positive. Endpoint titre (EPT): serial dilution at which a positive sample's CBA score reduces to 1. *****Positive: 7 samples were highly positive (CBA score of 4 at 1:100; EPTs 3,200; 3,200; 6,400; 25,600; 25,600; 25,600 and 409,600) and one was a low positive (CBA score of 1 at 1:100; EPT 200). ******23 of these 170 healthy control samples were also tested on a research ELISA, and all were negative. **^**NSA-positive sera (n=133). Information relating to the serum samples is provided in Chapter 2. *Ab+*, antibody-positive; *AChR*, acetylcholine receptor; *AMPA-R*, alpha-amino-3-hydroxy-5-methyl-4-isoxazolepropionic acid receptor; *AQP4*, aquaporin-4; *CASPR2*, contactin-associated protein-2; *CBA*, cell-based assay; *DRE*, drug-resistant epilepsy; *ELISA*, enzyme-linked immunosorbent assay; *EPT*, endpoint titre; *ERUK*, epilepsy research UK; *GABA-B-R*, gamma-amino butyric acid receptor type B; *GAD65*, glutamic acid decarboxylase 65; *glycine-R*, glycine receptor; *LGI1*, leucine-rich glioma inactivated-1; *NMDA-R*, N-methyl-D-aspartate receptor; *OANG*, Oxford Autoimmune Neurology Group; *TIME study*, the impairment of memory in epilepsy study; and *T1DM*, type 1 diabetes mellitus.

Sample group	*Source*	*Number of samples screened*	*Number of GAD65 Ab+ results*
Drug-resistant epilepsy patients	DRE study	206	8***** (*3.9%*)
Seizure-free epilepsy patients	DRE study	54	0
New-onset focal epilepsy patients	ERUK study	213	1 (*0.5%*)
T1DM patients	Moloney 2016 study	33	18 (*54.5%*)
T1DM & epilepsy patients	Moloney 2016 study	25	17 (*68%*)
Transient epileptic amnesia patients	TIME study	20	2 (*10%*)
Temporal lobe epilepsy patients	TIME study	7	0
AChR Ab+ controls**^** AMPA-R Ab+ controls**^** AQP4 Ab+ controls**^** CASPR2 Ab+ controls**^** GABA-B-R Ab+ controls**^** GAD65 Ab+ controls Glycine-R Ab+ controls**^** LGI1 Ab+ controls**^** NMDA-R Ab+ controls**^**	OANG	*18* *1* *7* *33* *1* 14 *6* *44* *23*	*0* *1 (100%)* *0* *0* *0* 14 (*100%*) *0* *0* *0*
Healthy controls	Various	170******	0
	Total	*875*	*61 (7%)*

4.8 Sensitivity and specificity of the GAD65 antibody CBA

To estimate sensitivity and specificity for the new CBA, clinical results were sought. Sixty-five patients (55 with drug-resistant epilepsy and 10 with seizure-free epilepsy) were selected from the drug-resistant epilepsy study. Electronic medical records were then interrogated for clinical GAD65 antibody tests (i.e., performed by the clinical immunology lab at the Oxford University Hospitals NHS Foundation Trust). Only 9/65 (13.8%) patients had undergone clinical testing for GAD65 autoantibodies and 3/9 were positive (**Table 34**). Based on this small sample, the GAD65 antibody research CBA would have a sensitivity of 100% and a specificity of 100%; and the research ELISA kit sensitivity would be 100%, with 83.33% specificity.

Table 34: Patients with clinical test results for GAD65 autoantibodies
Nine patients with clinical GAD65 antibody tests were identified from searching medical records for 65 randomly selected epilepsy patients (55 DRE and 10 SFE). Research ELISA threshold for positivity: >=5 units/ml. 'Clinical testing' means that the test was performed by the clinical immunology service at the Oxford University Hospitals NHS Foundation Trust. The research and clinical ELISAs make use of the same commercial kit, although the clinical lab team has modified the protocol from that provided by the manufacturer, e.g., samples are diluted in PBS (rather than healthy control serum) and are tested only once (not in duplicate). Patient 4 tested negative by clinical ELISA, negative by research CBA but low positive by research ELISA (both replicates – 11.99 and 11.44 units/ml). It is possible that this patient genuinely harboured GAD65 antibodies at a titre beneath the detection limit of the CBA (at a starting dilution of 1:100) and which was not detected by the clinical ELISA (e.g., due to differences in protocols and intraassay variability). Potential ways to resolve this discrepancy include rat brain immunohistochemistry or recombinant protein-based immunoblot. *Ab*, antibody; *CBA*, cell-based assay; *ELISA*, enzyme-linked immunosorbent assay; *EPT*, endpoint titre; *GAD65*, glutamic acid decarboxylase 65; *N/A*, not applicable; *PBS*, phosphate-buffered saline; *SFE*, seizure-free epilepsy; and *T1DM*, type 1 diabetes mellitus.

Patient number	*Patient group*	*Clinical GAD65 Ab test result*	*Clinical GAD65 Ab titre (units/ml)*	*New research CBA result*	*New research CBA EPT*	*Research ELISA result*	*Research ELISA Ab titre (units/ml)*	*T1DM*
1	DRE	Positive	>50,000	Positive	25,600	Positive	>curve	Yes
2	DRE	Positive	45,208	Positive	3,200	Positive	>curve	No
3	DRE	Positive	>50,000	Positive	25,600	Positive	>curve	Yes
4	DRE	Negative	N/A	Negative	N/A	Positive	11.7	No
5	DRE	Negative	N/A	Negative	N/A	Negative	0	No
6	DRE	Negative	N/A	Negative	N/A	Negative	1.2	No
7	DRE	Negative	N/A	Negative	N/A	Negative	0	No
8	DRE	Negative	N/A	Negative	N/A	Negative	3.9	No
9	DRE	Negative	N/A	Negative	N/A	Negative	0	No

In the absence of a larger sample of DRE patients with clinical GAD65 antibody results, and with the inevitable lack of a gold standard for comparison, I identified samples which had already been tested across multiple assay types and used these results as the basis for additional estimates of the CBA's sensitivity and specificity.

Blind to GAD65 antibody RIPA results from a 2016 study conducted within our lab group, I re-screened 50 serum samples using the new GAD65 antibody CBA (Figure 34A). For 36/50 (72%) samples, the 2016 RIPA and current CBA results were concordant in terms of GAD65 antibody negativity or positivity. I then screened the 14 samples with non-concordant results by ELISA – CBA and ELISA GAD65 antibody results matched for 13 of these 14 (92.9%) samples.

If any combination of two assay types (out of RIPA, CBA and ELISA) produced concordant positive or negative GAD65 antibody results for a given sample, the concordant result was considered accurate. These data produced an estimated GAD65 antibody CBA sensitivity of 100% and a specificity of 95.5% (Figure 34B).

A

Sample number	Patient group	RIPA result	CBA result
1	T1DM		
2	T1DM		
3	T1DM		
4	T1DM		
5	T1DM		
6	T1DM		
7	T1DM		
8	T1DM		
9	T1DM		
10	T1DM		
11	T1DM		
12	T1DM		
13	T1DM		
14	T1DM		
15	T1DM & epilepsy		
16	T1DM & epilepsy		
17	T1DM & epilepsy		
18	T1DM & epilepsy		
19	T1DM & epilepsy		
20	T1DM & epilepsy		
21	T1DM & epilepsy		
22	T1DM & epilepsy		100
23	T1DM		200
24	T1DM		100
25	T1DM		200

Sample number	Patient group	RIPA result	CBA result
26	T1DM		200
27	T1DM		200
28	T1DM		200
29	T1DM		100
30	T1DM		100
31	T1DM		100
32	T1DM		100
33	T1DM		400
34	T1DM & epilepsy		100
35	T1DM & epilepsy		200
36	T1DM	60,000	25,600
37	T1DM	16,500	1,600
38	T1DM	215	400
39	T1DM	13,900	3,200
40	T1DM	637	200
41	T1DM & epilepsy	50	3,200
42	T1DM & epilepsy	59,200	102,400
43	T1DM & epilepsy	17,400	51,200
44	T1DM & epilepsy	10,800	102,400
45	T1DM & epilepsy	750	400
46	T1DM & epilepsy	9,550	25,600
47	T1DM & epilepsy	130	200
48	T1DM & epilepsy	20	200
49	T1DM & epilepsy	13,700	6,400
50	T1DM & epilepsy	10,700	6,400

B

	GAD65 antibodies present		GAD65 antibodies absent	
Positive result	True positive	28	False positive	1
Negative result	False negative	0	True negative	21

C

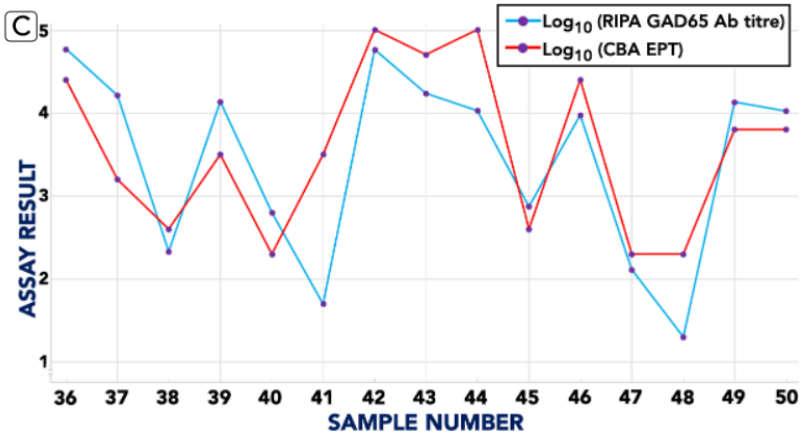
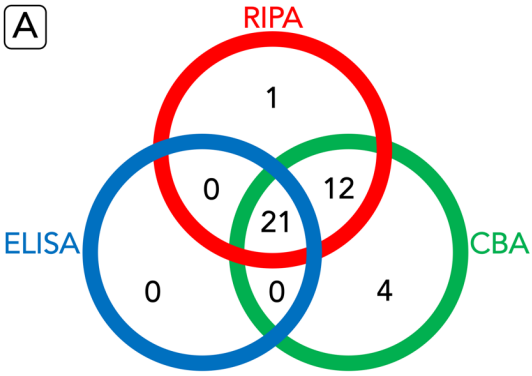


Figure 34: GAD65 antibody results from CBA and RIPA, with mismatches tested on ELISA

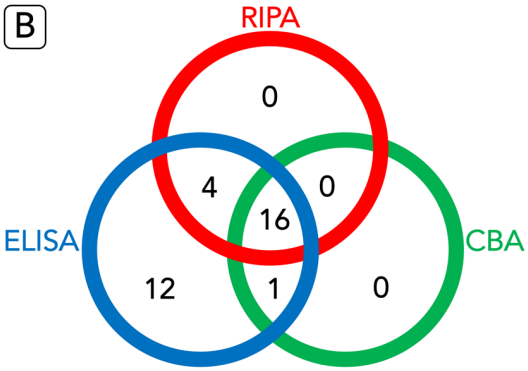
(A): Sera from patients with T1DM (n=30) and T1DM & epilepsy (n=20) tested for GAD65 antibodies by RIPA in 2016 were re-screened (blind to previous results) for GAD65 antibodies using the new CBA. Positive results are shaded in green, negative in grey. RIPA GAD65 antibody titres and CBA EPT (as dilution factors) are stated. 'Concordant' GAD65 antibody results (whether positive or negative) were obtained by RIPA and CBA for 36/50 (72%) samples (sample numbers 1-21 and 36-50). Non-concordant GAD65 antibody results were obtained for 14/50 samples (sample numbers 22-35), which all tested negative by RIPA but positive by CBA. By ELISA, 13 of these 14 samples tested positive for GAD65 antibodies (titres ranging from 8.9 to 8,814.3 units/ml) and sample number 27 tested negative. **(B):** Concordant GAD65 antibody results (positive or negative) from any two assay types (CBA, RIPA or ELISA) were considered accurate for the pragmatic estimation of sensitivity and specificity of the new GAD65 CBA (100% and 95.5%, respectively). The CBA result for patient 27 (CBA score 1 at 1:200) was considered a false positive by this method. It may be that apparent positive signal was generated by non-specific binding. However, if GAD65 antibodies were present (i.e., low positive) but the antibody-antigen interaction was dependent on epitope conformation, the antibodies may not have been detected by ELISA or RIPA (linear GAD epitopes). The estimated sensitivity of the CBA is higher than the specificity – this is likely an artefact of the pragmatic method applied to class results as 'accurate'. **(C):** Plot of positive RIPA (blue line) and CBA (red line) results. *Ab*, antibody; *CBA*, cell-based assay; *ELISA*, enzyme-linked immunosorbent assay; *EPT*, endpoint titre; *GAD65*, glutamic acid decarboxylase 65; *RIPA*, radioimmunoprecipitation assay; and *T1DM*, type 1 diabetes mellitus.

Next, I selected 52 samples already tested for GAD65 antibodies by RIPA, including 16 samples which I had assayed prior to the RIPA kit's withdrawal by the manufacturer and 36 samples tested in 2016. I re-screened all 52 samples using ELISA and the new CBA. Results were considered accurate when at least two assays (from RIPA, ELISA and CBA) produced positive or negative GAD65 antibody results in agreement (**Figure 35A and B**). Based on these data, the ELISA appeared more likely to produce false negative results than the CBA or RIPA; and the CBA had an estimated sensitivity of 89.2% and specificity of 80% (**Figure 35C**).

A



B



C

	GAD65 antibodies present		GAD65 antibodies absent	
Positive result	True positive	33	False positive	4
Negative result	False negative	4	True negative	16

Figure 35: GAD65 antibody results from RIPA, ELISA and CBA
52 samples (30 T1DM, 6 T1DM & epilepsy, 11 GAD65 antibody-positive AIN, and 5 healthy controls) were tested for GAD65 antibodies by RIPA, ELISA and CBA.
(A): 38 GAD65 antibody-positive results: 21/38 (55.3%) by all three assays; 12/38 (31.6%) by RIPA and CBA only; 4/38 (10.5%) by CBA only; and 1/52 (1.9%) by RIPA only. No samples were positive only by ELISA.
(B): 33 GAD65 antibody-negative results: 16/33 (48.5%) by all three assays; 4/33 (12.1%) by RIPA and ELISA only; 1/33 (3%) by ELISA and CBA only; and 12/33 by ELISA only.
(C): When at least two assays produced a result in agreement, this was considered accurate for the pragmatic purposes of estimating sensitivity and specificity of the new GAD65 CBA (89.2% and 80%, respectively). Note that this approach counts some results more than once, so there are 57 results for only 52 samples). *CBA*, cell-based assay; *ELISA*, enzyme-linked immunosorbent assay; *GAD65*, glutamic acid decarboxylase 65; *RIPA*, radio-immunoprecipitation assay; and *T1DM*, type 1 diabetes mellitus.

4.9 Comparing GAD65 antibody CBA endpoint titres for different patient groups

Sixty patient samples which tested positive on the new GAD65 antibody CBA were grouped into TIDM (n=18), epilepsy (n=31), and autoimmune neurology clinic GAD65 antibody-positive subjects without epilepsy (n=11). An endpoint titre (EPT) was established for each sample by serial dilution until the CBA score dropped to 1 (**Figure 36**).

The median GAD65 antibody EPT was highest for the autoimmune neurology (AIN) group. Although there was some overlap in EPT between groups, there were significant differences in EPT between the epilepsy and the TIDM groups, and between the AIN and the TIDM groups (both $p<0.0001$, Mann Whitney). There was also a significant difference in EPT between the epilepsy and the AIN groups ($p<0.0001$, Mann Whitney). The EPT difference for epilepsy patients with T1DM versus subjects with epilepsy alone was non-significant ($p=0.2987$, Mann Whitney).

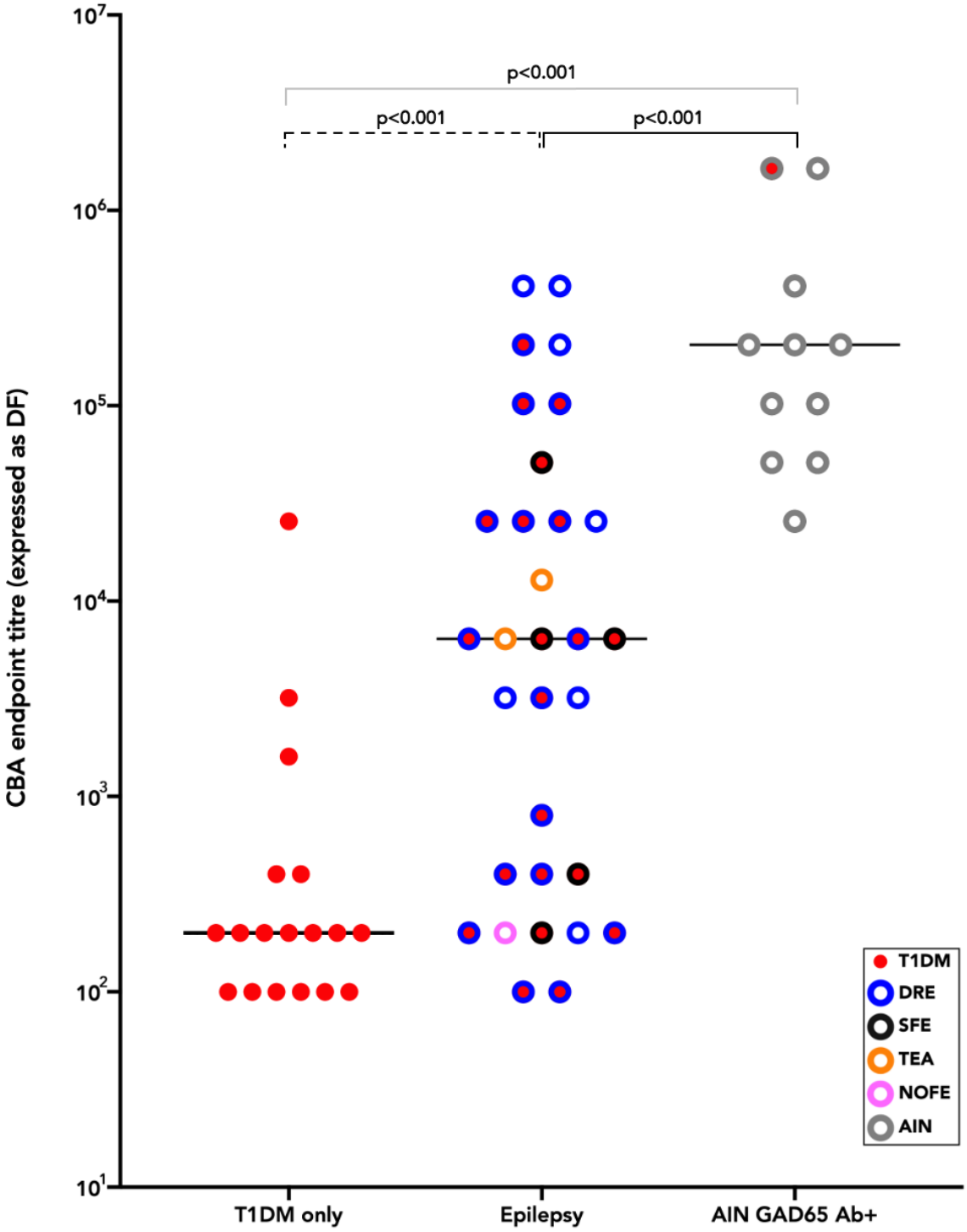


Figure 36: Comparison of GAD65 antibody CBA endpoint titres for different patient groups
GAD65 antibody-positive serum samples were serially diluted (starting at 1:100, with the dilution factor increasing by x2 each time) until endpoint titres (EPT) were established (i.e., when CBA scores dropped to 1). Patients were divided into T1DM only (n=18), epilepsy (n=31) and non-epilepsy AIN GAD65 Ab+ (n=11) groups. Median EPT values (horizontal lines) were 200 (T1DM); 6,400 (epilepsy); and 204,800 (AIN GAD65 Ab+). There was a significant difference in EPT between the epilepsy group and T1DM patients (<0.0001, Mann Whitney), and between the AIN GAD65 Ab+ group and T1DM patients (<0.0001, Mann Whitney). The non-epilepsy AIN GAD65 Ab+ diagnoses were SPSD (n=4), CA (n=2) and unclassified (n=5). *Ab+*, antibody-positive; *AIN*, autoimmune neurology clinic patient (non-epilepsy); *CA*, cerebellar ataxia; *CBA*, cell-based assay; *DF*, dilution factor; *DRE*, drug-resistant epilepsy; *EPT*, endpoint titre; *GAD65*, glutamic acid decarboxylase 65; *NOFE*, new-onset focal epilepsy; *SPSD*, stiff person spectrum disorders; *T1DM*, type I diabetes mellitus; and *TEA*, transient epileptic amnesia.

4.10 Comparison of GAD65 antibody CBA, ELISA and RIPA

I assessed the performance of the novel GAD65 antibody CBA against the RIPA and ELISA.

Figure 37 and **Figure 38** provide an overview of RIPA and ELISA techniques.

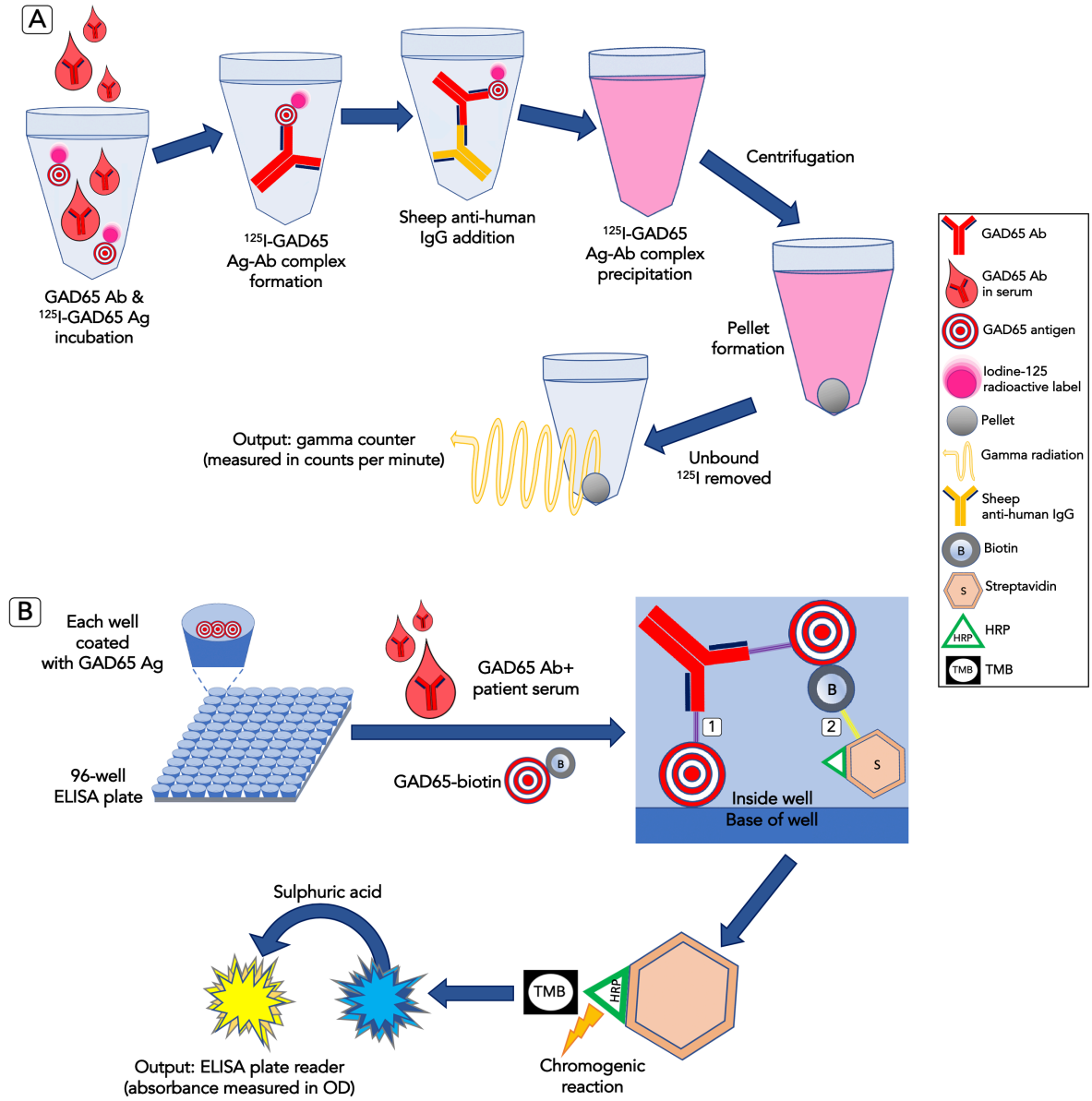


Figure 37: Overview of GAD65 antibody measurement by RIPA and ELISA
(A) RIPA: GAD65 autoantibodies in patient sera are incubated with ^{125}I-labelled GAD65 protein before adding sheep anti-human IgG, which precipitates a ^{125}I-labelled GAD65 antigen-antibody complex. Centrifugation forms a gamma radiation-emitting pellet. A gamma scintillation counter measures radiation to determine the amount of bound ^{125}I, which is proportional to the serum GAD65 antibody concentration. **(B) ELISA:** Plate wells are pre-coated with immobilised GAD65 antigen. Serum GAD65 antibodies form a bridge between GAD65 protein on the plate **(1)** and GAD65-biotin in solution **(2)**. Streptavidin (covalently coupled to HRP) binds to biotin. TMB turns blue in the presence of HRP. Sulphuric acid then stops the reaction and causes a colour change to yellow. A plate reader calculates absorbance (in OD) at 450 nm. *Ab*, antibody; *Ag*, antigen; *ELISA*, enzyme-linked immunosorbent assay; *GAD65*, glutamic acid decarboxylase 65; *HRP*, horseradish peroxidase; ^{125}*I*, iodine-125; *IgG*, immunoglobulin G; *OD*, optical density; *NIBSC*, National Institute for Biological Standards and Control; *RIPA*, radioimmunoprecipitation assay; and *TMB*, tetramethylbenzene.

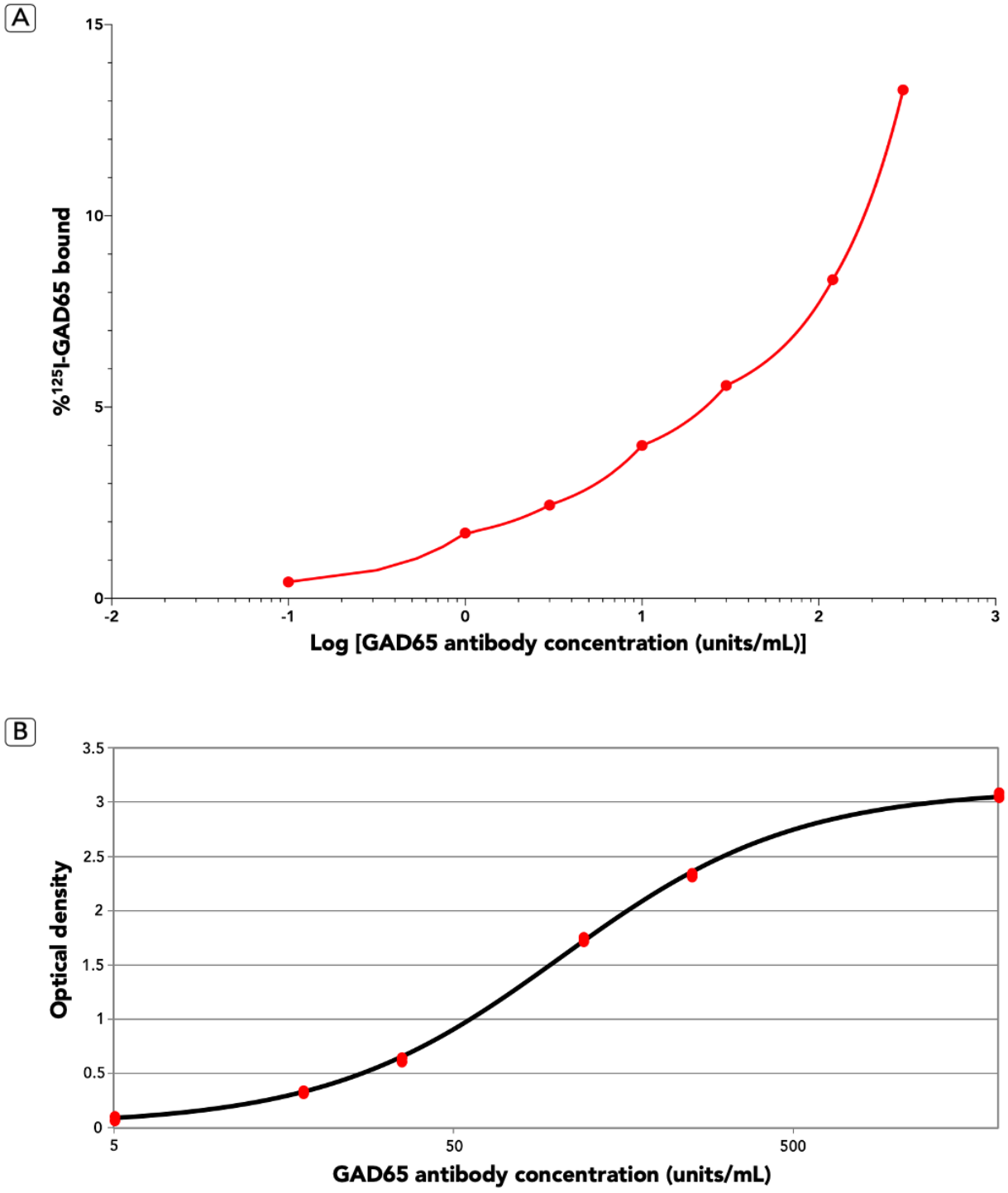


Figure 38: Calibration curves for interpolation of serum GAD65 antibody concentrations from raw assay outputs
(A): RIPA: results for RIPA kit calibrators (0-300 units/ml) were used to produce a spline curve to determine serum GAD65 antibody titres. If results fell outside the measurable range, serial dilutions were tested. **(B):** ELISA: a four-parameter logistic (4PL) regression curve was constructed from analysis of ELISA kit calibrators (0-2,000 units/ml), aligned to the WHO reference preparation NIBSC 97/550[199], to establish serum GAD65 antibody titres. ELISA results were considered technically valid if results from replicates were within 15% and the mean of the replicates lay within the central linear section of the 4PL curve. If results fell outside of this linear section, serial dilutions were tested. *ELISA*, enzyme-linked immunosorbent assay; *GAD65*, glutamic acid decarboxylase 65; ^{125}I, iodine-125; *NIBSC*, National Institute for Biological Standards and Control; *RIPA*, radioimmunoprecipitation assay; and *WHO*, World Health Organisation.

GAD65 antibody titres determined by RIPA and ELISA (when technical parameters for validity were satisfied) correlated very well with each other (Figure 39A, Spearman's rank correlation, $r = 0.9199$; and $p<0.0001$) and with CBA EPTs (Figure 39B). There was a closer fit between RIPA and CBA than with ELISA and CBA.

Interassay variability was investigated using appropriate kit calibrators as samples on four sets of ELISA and RIPA experiments. RIPA yielded more consistent results (Figure 40). Also, the same GAD65 autoantibody-positive serum control was tested among other samples on twenty different CBAs. CBA scoring was performed blind to sample details. The control sample scored 4 each time.

Analysing sample replicates permitted examination of intraassay variability, which was greater with ELISA than with RIPA (Figure 41). The same GAD65 autoantibody-positive serum control was tested four times alongside other samples in each of five CBAs, and always scored 4 (blinded to sample identity).

Sample dilution was directly proportional to the antibody measurement over a range of concentrations (1:10, 1:50, 1:100, 1:500, 1:1,000) by RIPA (linear) but not by ELISA (non-linear). The CBA was non-linear when sample dilutions were correlated with EPTs (Table 35).

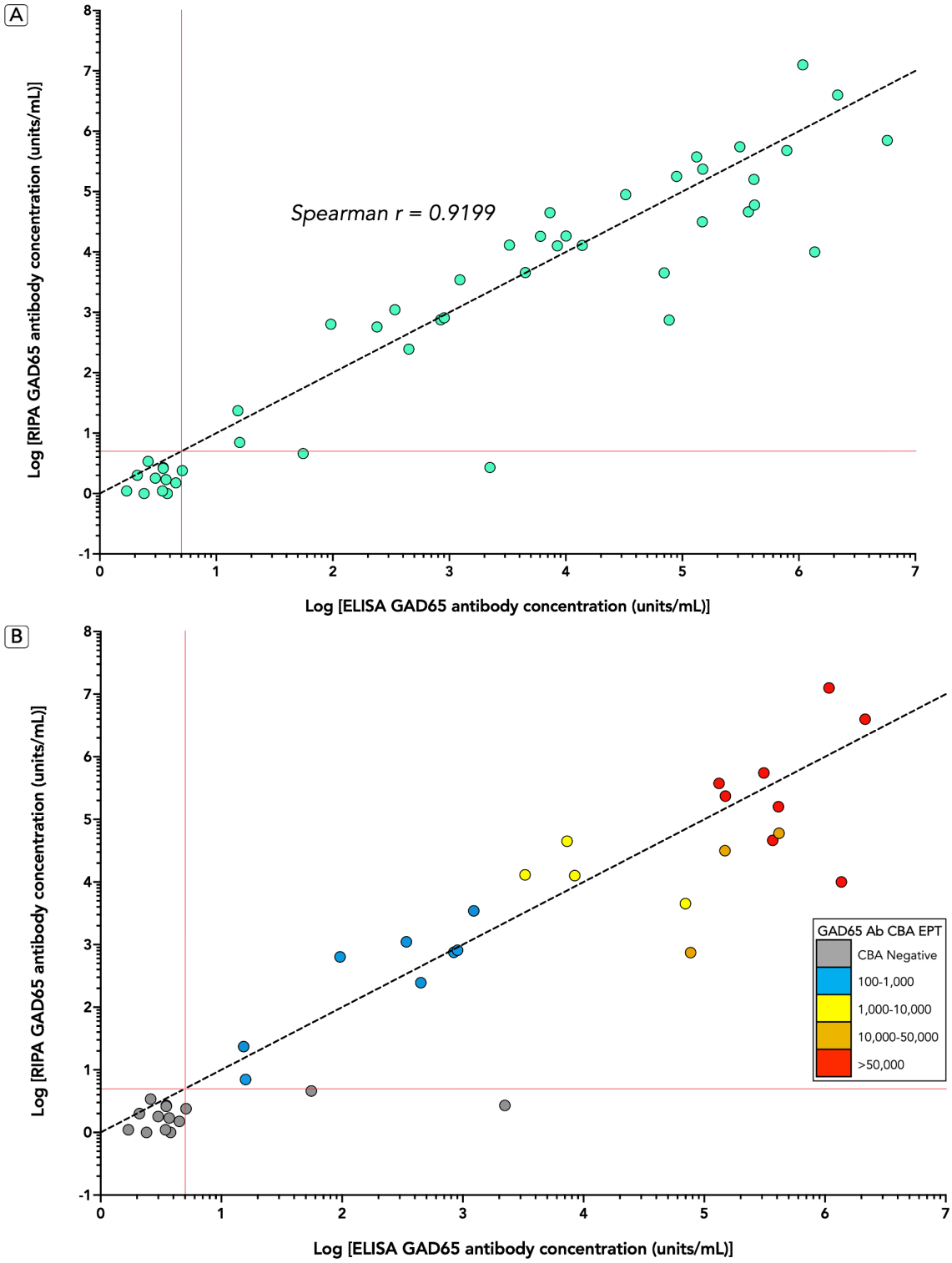


Figure 39: Correlation of GAD65 antibody concentrations determined by different assays

The use of endpoint titres (expressed as dilution factors) allows a greater dynamic range than CBA scores (range of 100–1,638,400 versus range of 1–4, respectively). **(A):** Sera from 40 patients and six healthy controls were tested on both RIPA and ELISA (technically valid results only). **(B):** Sera from 31 patients and six healthy controls were tested on RIPA, ELISA (technically valid results only) and CBA. Red lines indicate thresholds for positivity on RIPA and ELISA. Overall, there was a very good correlation between CBA endpoint titres and antibody titres from RIPA and ELISA, although there appeared to be a better fit between RIPA and CBA. ELISA results were considered technically valid if replicates were within 15% and the mean lay within the central linear section of the 4PL curve. *CBA*, cell-based assay; *ELISA*, enzyme-linked immunosorbent assay; *EPT*, endpoint titre; *GAD65*, glutamic acid decarboxylase 65; and *RIPA*, radioimmunoprecipitation assay.

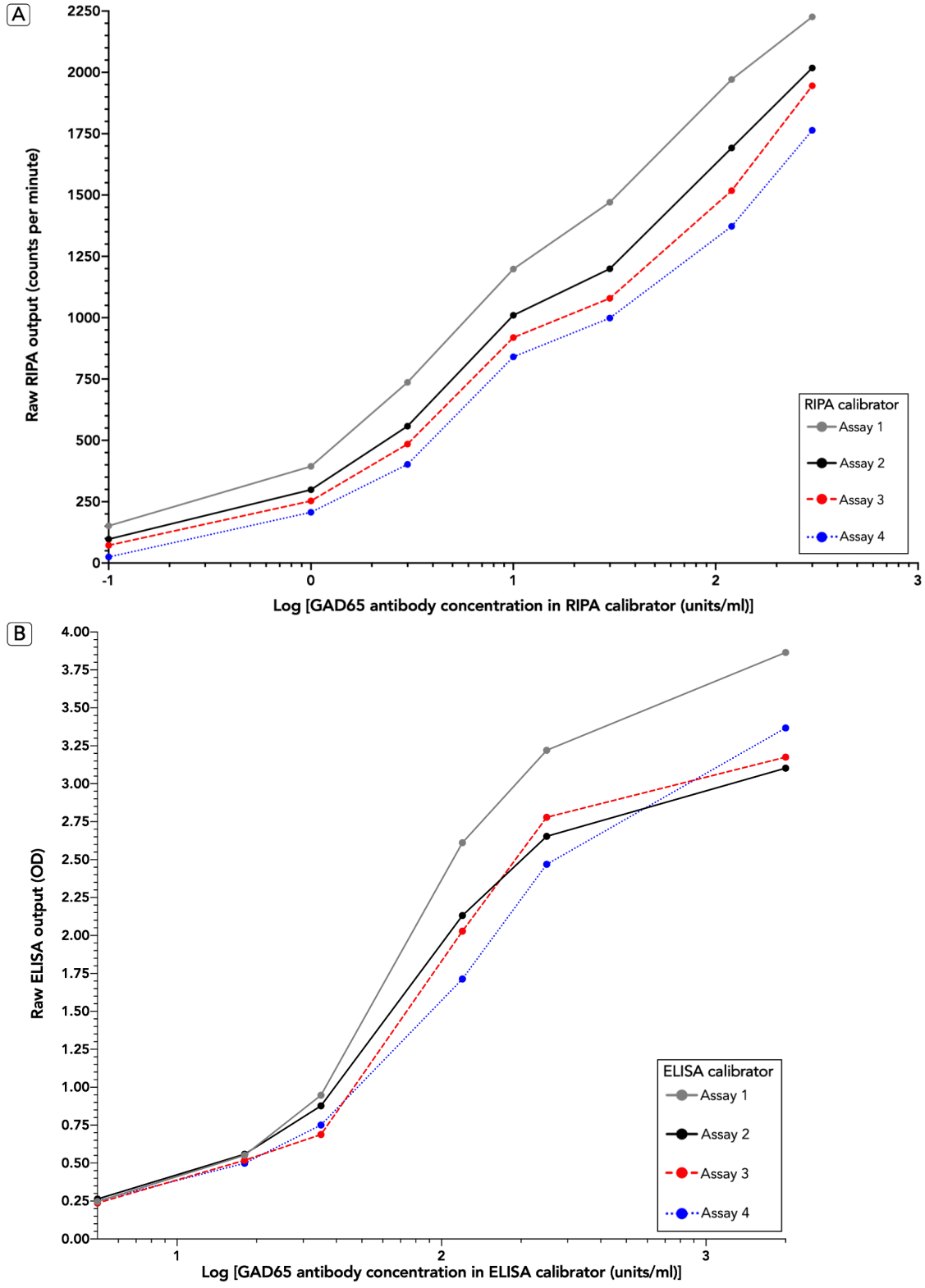
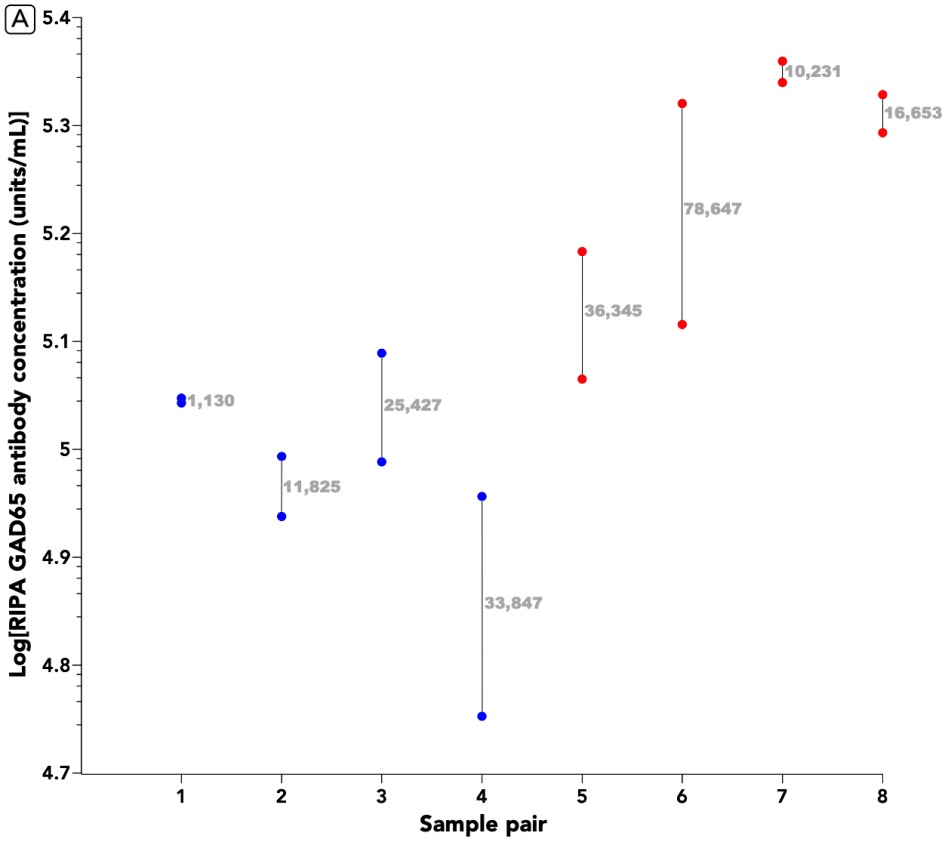


Figure 40: Interassay variability

(A): RIPA kit calibrators were tested on four different RIPA experiments for comparison. Note that radioisotope decay was ongoing between experiments. The shape of the curve was well maintained on each run and the traces did not overlap. **(B):** ELISA kit calibrators were tested on four different ELISA experiments. The shape of the curve was less well preserved compared to RIPA and several of the curves crossed. *ELISA*, enzyme-linked immunosorbent assay; *GAD65*, glutamic acid decarboxylase 65; *OD*, optical density; and *RIPA*, radioimmunoprecipitation assay.



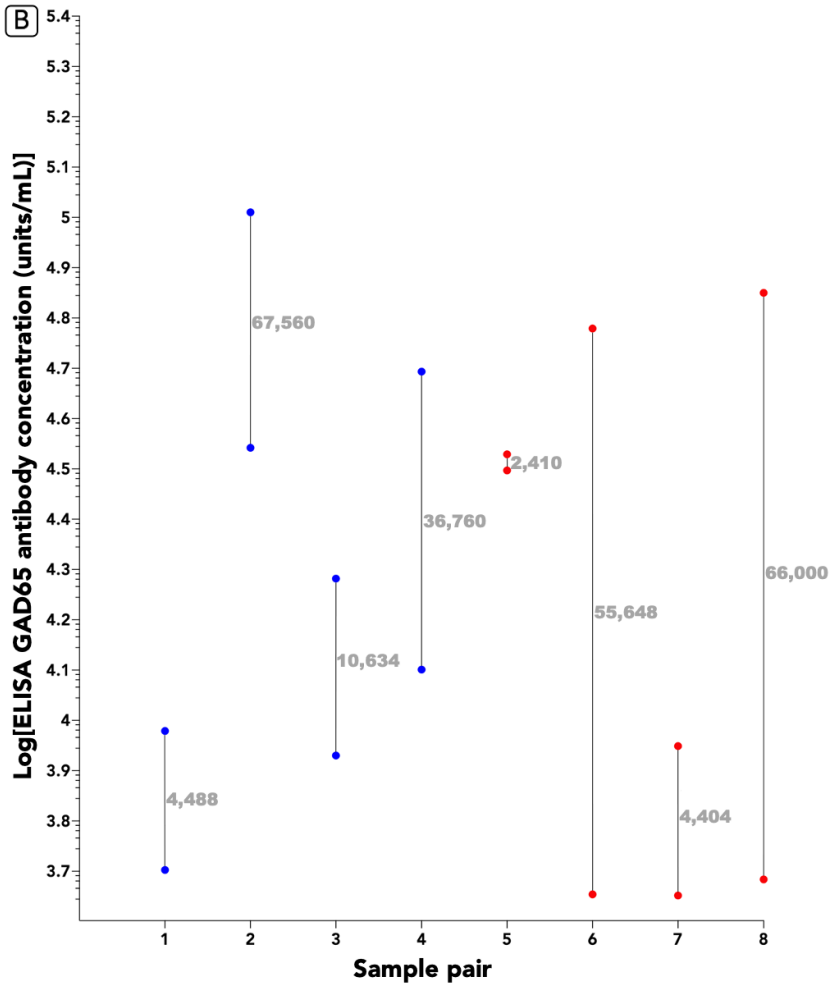


Figure 41: Intraassay variability
Eight samples were tested in duplicate on RIPA **(A)** and another eight samples were tested in duplicate on ELISA **(B)**. Absolute differences between replicates (units/mL) are noted in grey. There was considerably more variation between ELISA replicates regardless of sample dilution. *ELISA*, enzyme-linked immunosorbent assay; *GAD65*, glutamic acid decarboxylase 65; and *RIPA*, radio-immunoprecipitation assay.



Table 35: Linearity of the GAD65 antibody CBA

Fourteen serum samples strongly positive for GAD65 autoantibodies were serially diluted. CBA scores at each dilution factor (DF) were noted. CBA scores – 0: negative, 1: low positive, 2-4: positive. CBA scores of 4 are represented by dark red shading and CBA scores of 0 by dark blue. Endpoint titre: when a CBA score falls to 1. The relationship between CBA score and dilution factor was non-linear. Most of the samples showed a similar rate of decrement in CBA score with increasing dilution factor. *CBA*, cell-based assay; *DF*, dilution factor; and *GAD65*, glutamic acid decarboxylase 65.

	Serum sample													
DF	1	2	3	4	5	6	7	8	9	10	11	12	13	14
50	4	4	4	4	4	4	4	4	4	4	4	4	4	4
100	4	4	4	4	4	4	4	4	4	4	4	4	4	4
200	4	4	4	4	4	4	4	4	4	4	4	4	4	4
400	4	4	4	4	4	4	4	4	4	4	4	4	4	4
800	4	3	4	4	4	4	4	4	4	4	4	4	3.5	3.5
1,600	3	3	4	3.5	3	4	3	4	3	3	3	3	3.5	3
3,200	3	2.5	3	3	3	3	3	4	2	3	3	3	3	2.5
6,400	3	2.5	3	3	2.5	2.5	2	3.5	2	2	2.5	2.5	2.5	2
12,800	2	2	2.5	3	2	2	1	3.5	1.5	2	2.5	2	2.5	2
25,600	2	1	2.5	3	2	2	1	3	1.5	1.5	2	2	2	1.5
51,200	1.5	0	2.5	3	2	1.5	1	2	1	1	2	1	1	1
102,400	1.5	0	2	2	2	1.5	1	2	1	0	1.5	1	1	0
204,800	1	0	1.5	1	1	1	1	1.5	0	0	1	0	1	0
409,600	0	0	1	0	1	0	0	1.5	0	0	0	0	1	0
819,200	0	0	1	0	0	0	0	1.5	0	0	0	0	0	0
1,638,400	0	0	1	0	0	0	0	1	0	0	0	0	0	0
3,276,800	0	0	0	0	0	0	0	0	0	0	0	0	0	0

4.11 GAD65 antibody CBA interrater performance

Microscope slides for one hundred and nineteen serum samples tested on CBA were reviewed separately by two raters (RMcG and HF), both blind to patient details. HF is a postdoctoral researcher with extensive experience of reading various diagnostic assays, and we first agreed on scoring for 20 samples with pre-established GAD65 autoantibody status. When read at x40 magnification, there was inter-rater agreement for 111/119 (93.3%) samples. Inter-rater reliability (Cohen's Kappa, range 0-1) was 0.856. For discrepant results, both raters re-read the relevant samples (still blind to patient details) at x100 magnification (oil immersion) and reached a consensus. **Figure 42** shows examples of difficult-to-read samples.

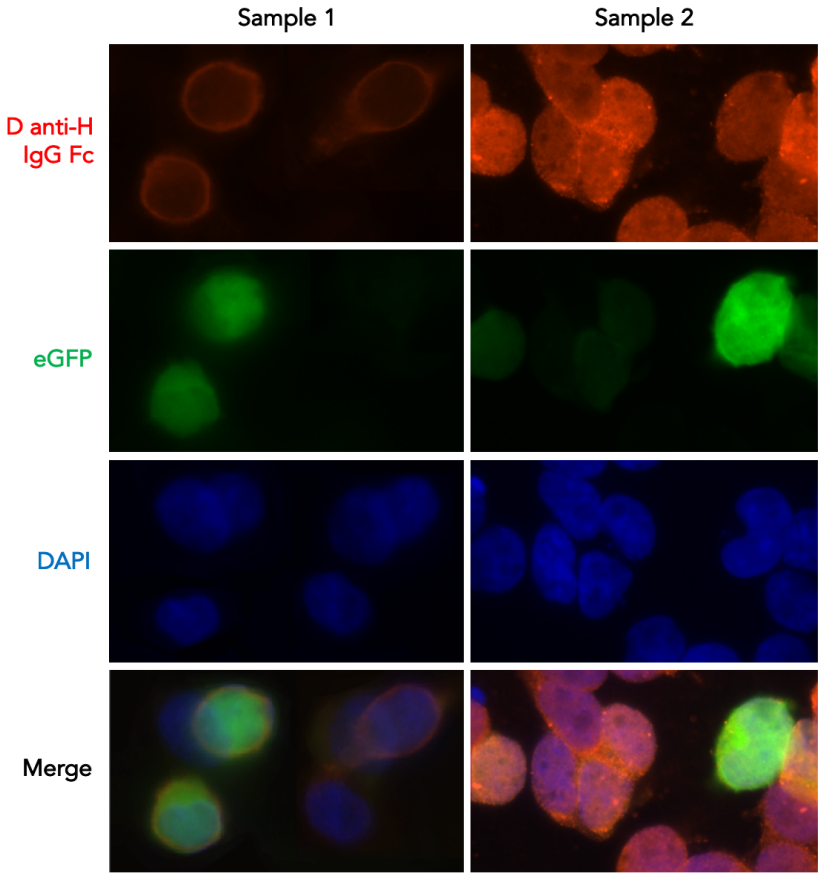


Figure 42: CBA samples with discrepant ratings from two raters
Fluorescence microscopy images (magnification x100, oil immersion). Examples of results from sera which were difficult-to-read at x40. **Sample 1:** GAD65 autoantibody-positive result incorrectly rated as negative by one reader at x40. **Sample 2:** GAD65 autoantibody-negative result with non-specific staining mistakenly called GAD65 autoantibody-positive by one reader at x40. *CBA*, cell-based assay; *D anti-H IgG Fc*, donkey anti-human IgG Fc-gamma fragment-specific; *DAPI*, 4′,6-diamidino-2-phenylindole; *eGFP*, enhanced green fluorescent protein; *GAD65*, glutamic acid decarboxylase 65; and *IgG*, immunoglobulin G.

4.12 Pilot screening for GAD65 IgM autoantibodies

It is not known whether GAD65 autoantibodies of the IgM isotype are present in people with epilepsy. Most pathologically significant antibodies in autoimmune neurological conditions are class-switched IgG and GAD65 IgM is not prominent in the epilepsy literature. There are reports of potentially pathogenic IgM autoantibodies coexisting with IgG autoantibodies targeting NMDA-R[305–307], AQP4[308] and GABA-A-R[309]. Although the mechanisms responsible for the long-term production of GAD65 IgG autoantibodies have yet to be delineated, continuous antigen exposure (with ongoing IgM synthesis) is one potential explanation.

To determine whether the CBA could detect GAD65 IgM autoantibodies, a range of GAD65 IgG antibody-positive samples were assayed using an IgM secondary antibody (Figure 43). None were positive for IgM. Due to the coronavirus pandemic lockdown, it was not possible to try IgG depletion with protein G beads before repeating the IgM CBA – a technique which has been successful in our lab group previously.[310]

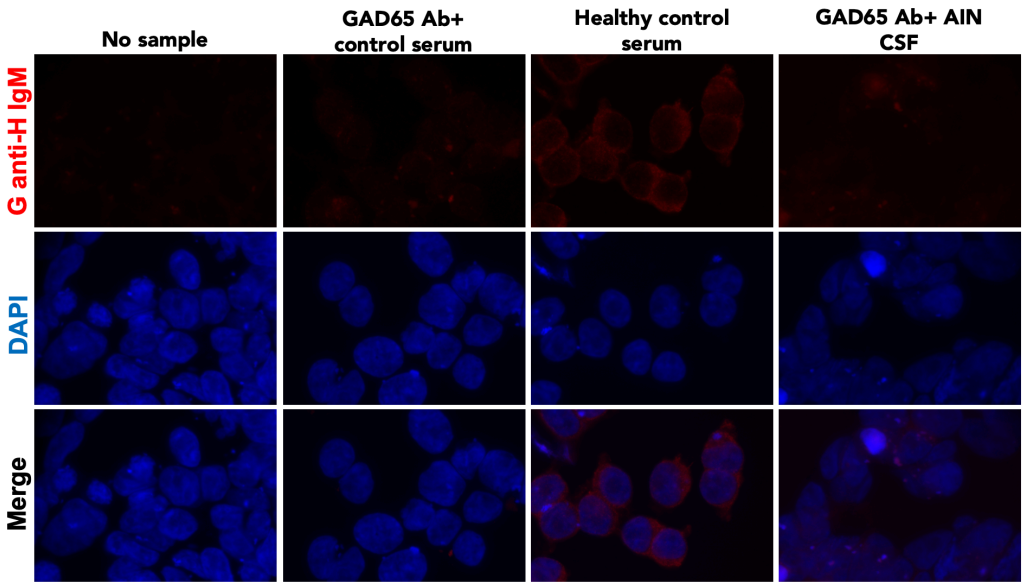


Figure 43: Provisional screening for GAD65 IgM autoantibodies
Fluorescence microscopy images (magnification x100, oil immersion). CBA performed with an anti-IgM secondary antibody (whole IgG goat anti-human polyclonal antibody targeting IgM heavy chain, cross-adsorbed against human IgG and IgA prior to conjugation with Alexa Fluor® 594 at 1:500). 21 serum samples tested in total (LGI1 Ab+; CASPR2 Ab+; GAD65 Ab+ control; healthy control; 3x GAD65 Ab+ DRE; 8x GAD65 Ab+ AIN; 2x GAD65+ TEA; 2x GAD+ T1DM; and 2x T1DM & epilepsy), 2x CSF samples (GAD65 Ab+ DRE) were tested. As a control, the CBA was also performed without a sample. All results were negative. *Ab+*, antibody-positive; *AIN*, autoimmune neurology; *CASPR2*, contactin-associated protein-2; *CBA*, cell-based assay; *CSF*, cerebrospinal fluid; *DAPI*, 4′,6-diamidino-2-phenylindole; *DRE*, drug-resistant epilepsy; *eGFP*, enhanced green fluorescent protein; *GAD65*, glutamic acid decarboxylase 65; *G anti-H,* goat anti-human IgG, IgM heavy chain-specific; *IgG*, immunoglobulin G; *IgM*, immunoglobulin M; *LGI1*, leucine-rich glioma inactivated-1; *TEA*, transient epileptic amnesia; and *T1DM*, type I diabetes mellitus.

4.13 Additional challenges with reading the GAD65 antibody CBA

With increasing experience of reading the GAD65 antibody CBA, I observed non-specific membrane staining plus staining from apparent nuclear and cytoplasmic reactive antibodies which did not appear representative of GAD65 antibody positivity (**Figure 44** and **Figure 45**). Upon recognising this, I repeated the sample screening hitherto completed to ensure accurate results.

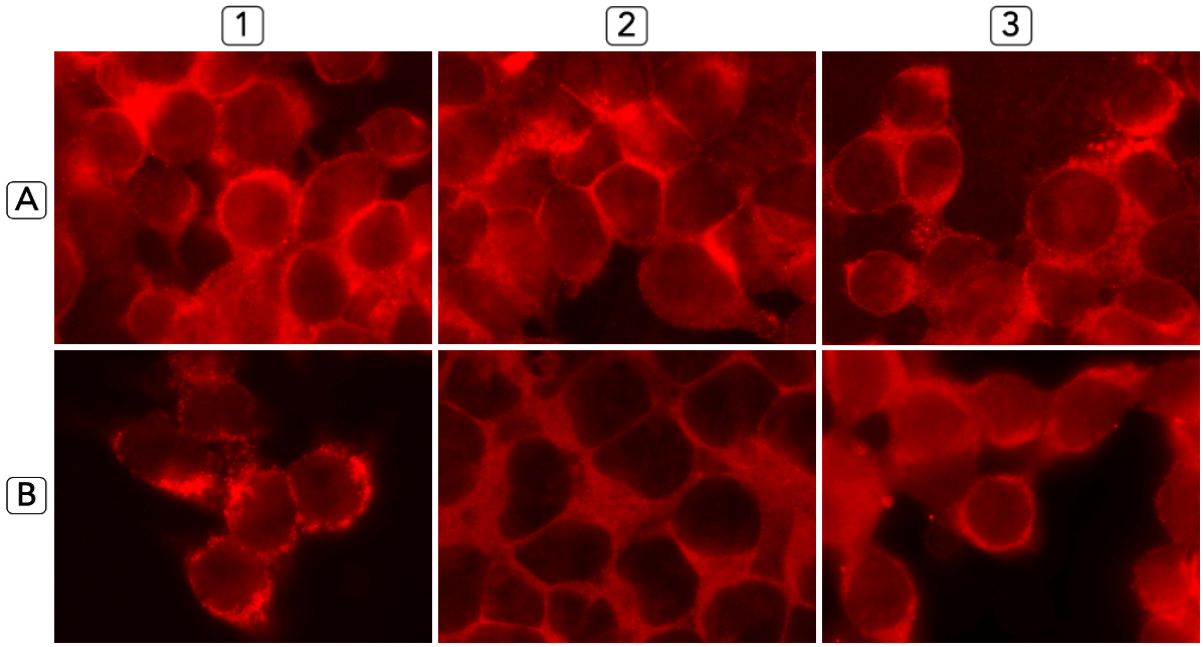


Figure 44: Non-specific membrane staining on the GAD65 antibody CBA
Fluorescence microscopy images (magnification x100, oil immersion). Serum samples (1:100) tested on GAD65 antibody CBA. Donkey anti-human IgG, Fc-gamma fragment-specific secondary antibody signal shown only. GAD65 antibody-negative patient samples produced non-specific membrane staining, which could potentially be mistaken for GAD65 antibody-specific positive signal at a lower magnification power. **(A1-3):** DRE patient samples. **(B1-2):** NOFE patient samples. **(B3):** TEA patient sample. *CBA*, cell-based assay; *DRE*, drug-resistant epilepsy; *GAD65*, glutamic acid decarboxylase 65; *IgG*, immunoglobulin G; *NOFE*, new-onset focal epilepsy; *and TEA*, transient epileptic amnesia.

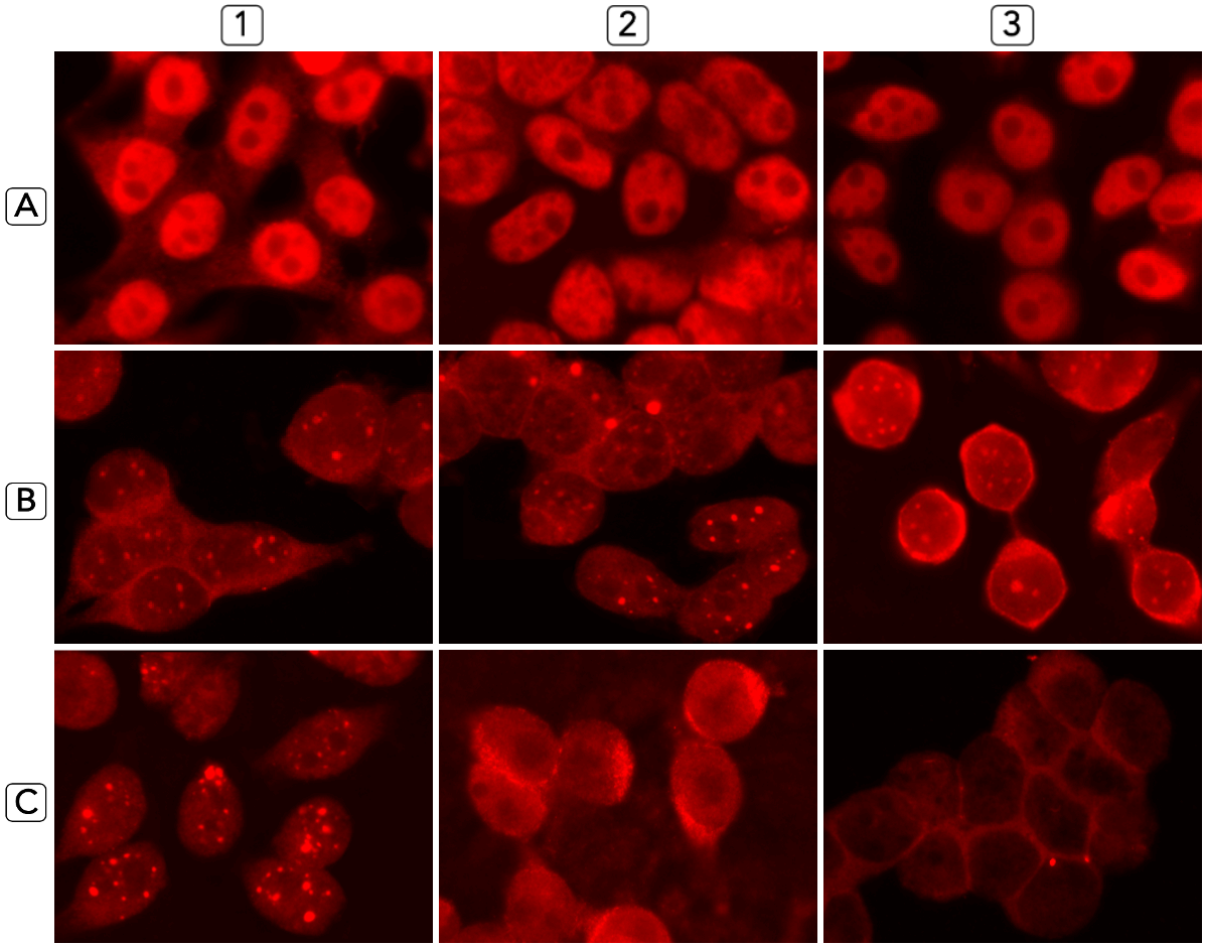


Figure 45: ANA and ANA-related antibody staining on the GAD65 antibody CBA
Fluorescence microscopy images (magnification x100, oil immersion). Serum samples (1:100) tested on GAD65 antibody CBA. Donkey anti-human IgG, Fc-gamma fragment-specific secondary antibody signal shown only. **(A1-3):** punctate, nucleolar ANA-like pattern. **(A1):** AQP4 Ab+ NMOSD patient sample. **(A2):** Healthy control sample. **(A3):** GAD65 Ab+ NOFE patient sample. **(B1):** Fine speckled ANA-like pattern (GAD65 Ab- DRE patient sample). **(B2):** Mixed fine speckled and punctate nucleolar ANA-like pattern (GAD65 Ab- NOFE patient sample). **(B3):** Fine speckled ANA-like pattern with GAD65 Ab+ signal peripherally (SPSD patient sample). **(C1):** Mixed coarse speckled and punctate nucleolar ANA-like pattern (GAD65 Ab- DRE patient sample). **(C2):** Punctate nucleolar ANA-like pattern (LGI1 Ab+, GAD65 Ab- patient sample). **(C3):** Faint punctate nucleolar ANA-like pattern with non-specific membrane staining (GAD65 Ab- DRE patient sample). *Ab-*, antibody-negative; *Ab+*, antibody-positive; *ANA*, antinuclear antigen; *AQP4*, aquaporin-4; *CBA*, cell-based assay; *DRE*, drug-resistant epilepsy; *GAD65*, glutamic acid decarboxylase 65; *IgG*, immunoglobulin G; *LGI1*, leucine-rich glioma inactivated-1; *NMOSD*, neuromyelitis optica spectrum disorder; *NOFE*, new-onset focal epilepsy; and *SPSD*, stiff person spectrum disorder.

4.14 Further development of the GAD65 CBA

To aid a higher throughput rate of sample screening, I sought to make the assay more straightforward to interpret by reducing the level of background and non-specific signal, and by tagging the GAD65 antigen with eGFP to allow confirmation of colocalisation.

Through modification of the transfection vector and the GAD65-encoding DNA insert, I planned to express eGFP-tagged GAD65 protein on the surface of live HEK-293T cells. This would obviate the need for cell permeabilisation (which allows binding of secondary antibody to non-target intracellular antigens) and cell fixation prior to primary antibody binding (which can alter antigens and interfere with antigen-antibody binding). The low expression of native HEK-293T cell surface proteins would also serve assay specificity. Figure 46 outlines the key differences between fixed permeabilised CBA for intracellularly located antigens and live CBA for cell surface-expressed antigens, and summarises how a live CBA is performed.

This work was performed in conjunction with Dr Patrick Waters and Dr Hannah Fox from the Oxford Autoimmune Neurology Group (OANG).

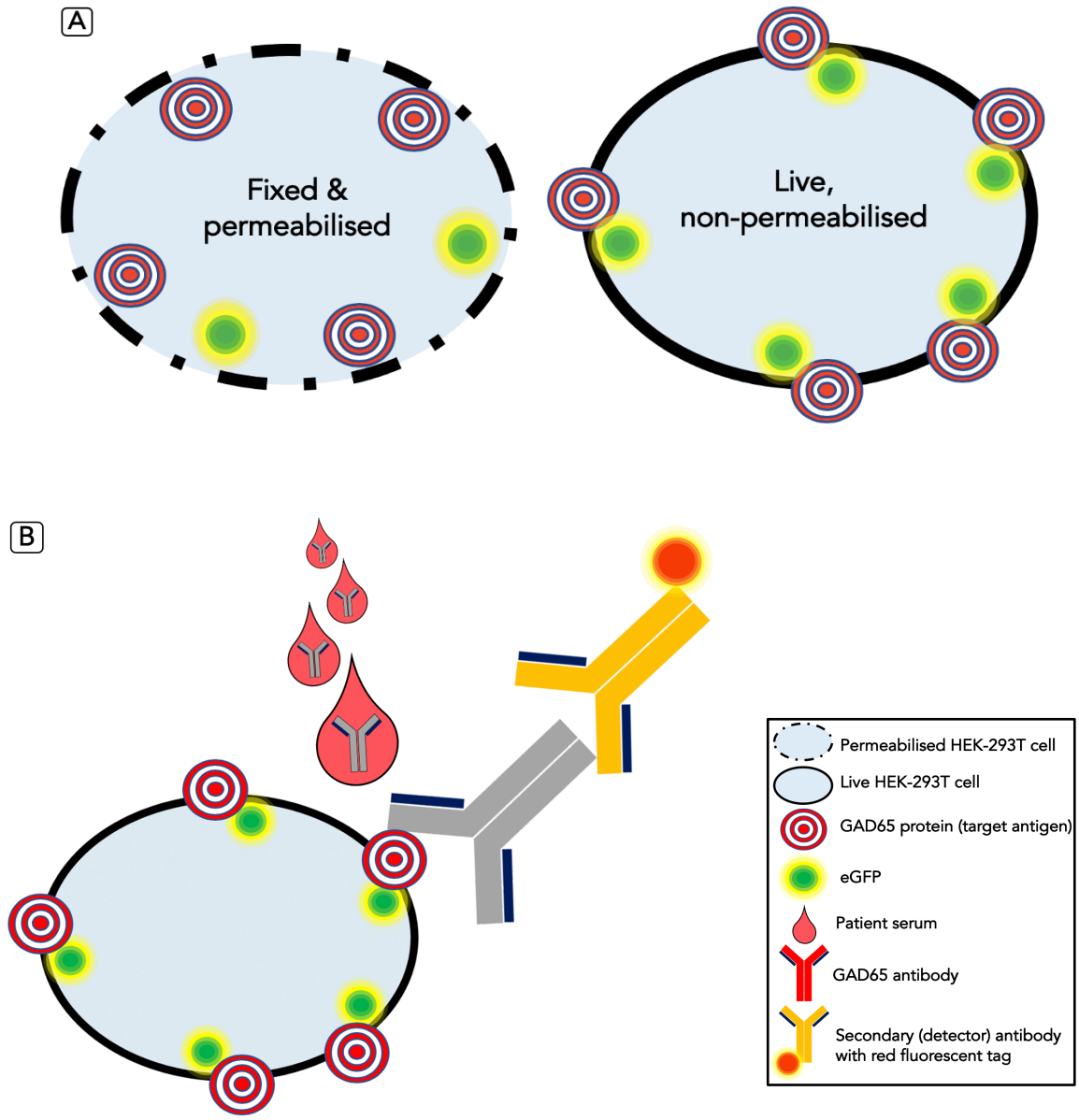


Figure 46: Comparison of fixed/permeabilised and live CBAs

(A): The permeabilised GAD65 CBA relies on intracellular, untagged target antigen. When primary and secondary antibodies enter cells, they can bind non-target antigen, creating non-specific signal, which makes the assay more challenging to interpret. By contrast, in a live CBA, primary antibody is incubated with an intact cell membrane, which has relatively few native antigens (not shown), producing less non-specific signal. An eGFP tag on the target antigen allows quicker and more reliable CBA interpretation (due to colocalisation) than separately transfected eGFP and antigen. **(B):** In a live CBA, patient serum is incubated with live HEK-293T cells. Antibodies present in the serum can bind with target antigen on the cell surface. The fluorescent tag conjugated to the secondary antibody colocalises with eGFP on fluorescence microscopy, helping to identify positive cells. CBA, cell-based assay; *eGFP*, enhanced green fluorescent protein; *GAD65*, glutamic acid decarboxylase 65; *HEK-293T cell*, human embryonic kidney 293T cell.

4.15 Modification of an existing LGI1 transfection vector

For the GAD65 protein to be expressed on the cell surface, the native N-terminal/5-prime-end GAD65 signal peptide needed to be replaced with a signal peptide which is known to mediate cell membrane expression. Coding sequences were required for adding an eGFP tag and a transmembrane domain to maintain the protein at the cell surface. The live LGI1 antibody CBA previously developed by the OANG[85] is based on a transfection vector called 'LCE' which contains a CASPR2 tail sequence (to anchor soluble LGI1 protein to the cell surface) and an eGFP tag within the multiple cloning site. Hence, I chose to adapt the existing LCE vector. An overview of the cloning strategy is outlined in **Figure 47**.

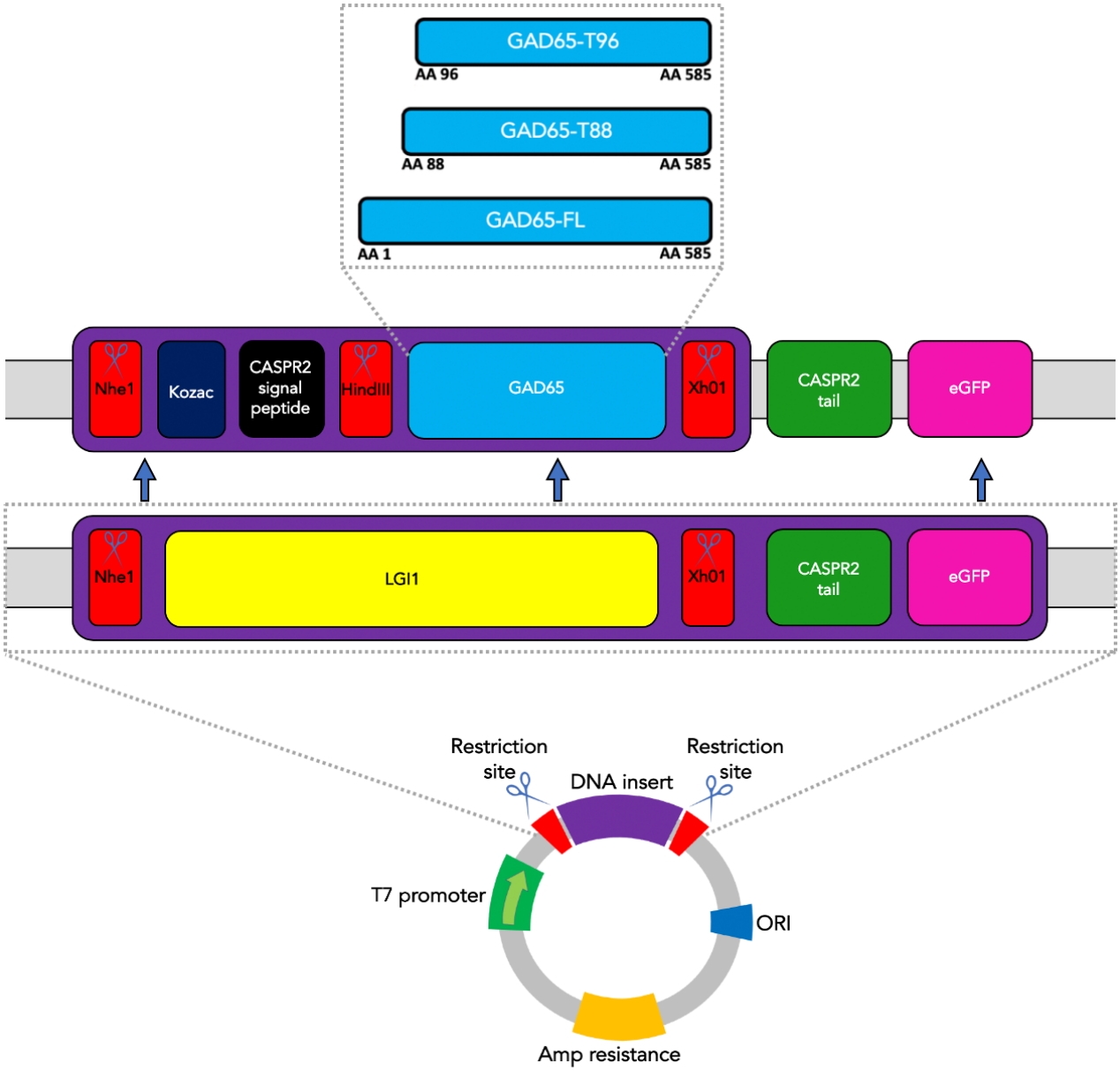


Figure 47: Plasmid vector and inserts

The pcDNA3.1(+) plasmid (depicted as a grey ring) is a mammalian expression vector with a T7 promoter for regulation of insert expression, an ampicillin resistance gene as a selectable marker and a bacterial origin of replication to enable replication within a bacterial cell. This vector was previously used by the OANG to create an LGI1 expression construct called the LCE plasmid, which includes a CASPR2 tail sequence (to anchor LGI1 to the cell membrane) and an eGFP tag within the multiple cloning site region. Molecular cloning plans were to: (1) swap the LGI1 insert for one of three different GAD65 gene fragments (FL, T88 and T96), using the restriction endonucleases NHE1-high fidelity and XH01; (2) add a CASPR2 signal sequence for surface expression of GAD65; and (3) make use of the CASPR2 tail (as a membrane anchor) and eGFP sequences already within the LCE plasmid. The Kozac sequence was added to enhance translation and the HindIII restriction site was added to facilitate future plasmid modification with other antigens. The GAD65 gene fragments utilise the start codons within the CASPR2 signal peptide and lack stop codons so that DNA polymerase continues through to the CASPR2 tail and eGFP. *AA*, amino acid; *Amp*, ampicillin; *CASPR2*, contactin-associated protein-2; *eGFP*, enhanced green fluorescent protein; *FL*, full length; *GAD65*, glutamic acid decarboxylase 65; *LGI1*,l leucine-rich glioma inactivated-1; *ORI*, origin of replication; *T88*, truncation at amino acid 88; and *T96*, truncation at amino acid 96.

4.16 GAD65 inserts for expression construct

To enable later work relating to possible distinct GAD65 epitopes, three different versions of a synthetic GAD65 gene fragment (i.e., double stranded DNA) were designed: full length GAD65 (FL), GAD65 truncated at amino acid 96 (T96), and GAD65 truncated at amino acid 88 (T88). An additional restriction site (to offer the flexibility of using the construct with other antigens in future) and a Kozak sequence (to enhance translation from the correct initiation codon) were included in the gene fragments (**Figure 48**). Appropriate primers were designed (**Table 36**). Gene fragments and primers were manufactured by a commercial supplier and received in lyophilised form.

Table 36: Custom primer nucleotide sequences
One pair of primers (forward and reverse) were designed for use with the full length insert, and another pair for both of the truncated versions, T96 and T88. *FL*, full length; *GAD65*, glutamic acid decarboxylase 65; and *trunc*, truncated version.

Primer	*Nucleotide sequence (5' to 3')*
GAD65-FL-FORWARD	GGA GAT TCT TAT GCA CTG TCA AAC
GAD65-FL-REVERSE	CCA TCA TCT TAT GTG GGT TCC
GAD65-TRUNC-FORWARD	CCT GAA GAA GAT GAG AGA GAT C
GAD65-TRUNC-REVERSE	GGT TCC ATG TCA CGC TGT TGG

5′-CGACTCACTATAGGGAGACCCAAGCTGGCTAGCCCACCATGCAGGCGGCTCCGCGCGCC
GGCTGCGGGGCAGCGCTCCTGCTGTGGATTGTCAGCAGCTGCCTCTGCAGAGCCTGGACG
GCTAAGCTTATGGCGTCACCCGGTAGTGGGTTTTGGAGTTTCGGGAGTGAAGATGGGAGTG
GTGATTCAGAGAATCCAGGGACGGCACGCGCGTGGTGCCAAGTAGCGCAAAAATTCACCGG
AGGGATTGGGAACAAGCTCTGTGCGCTTTTGTATGGGGACGCTGAGAAGCCGGCTGAGAGC
GGCGGCTCCCAACCTCCTAGGGCTGCGGCCAGGAAAGCTGCTTGCGCCTGCGATCAAAAG
CCATGTAGTTGCAGTAAAGTCGACGTAAACTATGCTTTCCTGCACGCAACCGATCTGCTTCCC
GCATGCGATGGAGAGAGGCCAACCCTTGCCTTCCTTCAAGATGTGATGAACATATTGCTTCA
GTATGTCGTCAAGTCATTCGACCGCAGCACAAAAGTTATCGACTTTCACTATCCAAATGAACT
TCTGCAGGAGTACAACTGGGAACTCGCGGATCAGCCGCAAAATCTTGATACCTTGAAATACG
CGATTAAGACCGGCCACCCAAGATACTTTAACCAACTCTCCACCGGGCTCGATATGGTGGGC
CTGGCAGCCGATTGGTTGACATCTACGGCTAATACGAATATGTTCACTTACGAAATTGCCCCA
GTGTTTGTGCTTCTTGAGTATGTCACACTCAAGAAGATGCGAGAAATCATCGGGTGGCCTGG
GGGCTCCGGTGACGGTATATTTAGTCCGGGTGGGGCGATTAGTAATATGTATGCAATGATGA
TCGCAAGATTCAAGATGTTTCCTGAGGTGAAGGAAAAAGGCATGGCTGCTTTGCCCAGACTT
ATTGCTTTTACTTCTGAACATAGCCACTTCAGTCTGAAAAAGGGGGCCGCTGCGCTCGGAAT
CGGGACGGACTCAGTGATCCTTATTAAATGCGATGAGCGAGGTAAGATGATTCCGTCTGATC
TCGAGCGGCGGATACTGGAAGCTAAGCAAAAAGGGTTTGTCCCATTCCTGGTATCTGCAACG
GCAGGGACAACAGTTTATGGGGCCTTTGATCCGCTTCTTGCGGTTGCTGATATCTGTAAGAA
GTACAAAATCTGGATGCACGTGGATGCTGCATGGGGTGGGGGGCTCCTGATGAGCCGGAA
GCACAAATGGAAACTTTCAGGGGTGGAGAGAGCGAATTCCGTCACATGAGTGCCTCTTCAGT
GCAGCGCCTTGCTTGTCAGGGAGGAAGGACTCATGCAGAATTGTAATCAGATGCATGCATCC
TACCTCTTCCAACAGGATAAACATTACGACCTCAGTTATGACACGGGTGATAAAGCCCTGCA
GTGTGGGCGCCATGTTGATGTTTTCAAGCTGTGGCTGATGTGGCGAGCGAAAGGTACAACTG
GCTTCGAGGCGCATGTCGATAAATGTTTGGAATTGGCAGAGTACTTGTACAACATTATCAAGA
ATAGGGAAGGTTATGAAATGGTGTTTGATGGCAAACCTCAGCACACAAATGTTTGCTTTTGGT
ACATCCCTCCCTCTTTGCGGACCCTCGAAGACAACGAAGAAAGAATGAGCAGATTGTCTAAA
GTGGCCCCAGTAATCAAGGCCCGGATGATGGAATACGGAACCACGATGGTATCCTACCAAC
CCCTCGGTGACAAAGTAAACTTCTTTCGAATGGTTATTAGTAACCCCGCAGCCACCCATCAG
GATATAGACTTTCTTATCGAAGAGATAGAGCGACTCGGTCAAGATTTAGGACTCGAGGGACA
AGGCCAAGCTATAAGAAATGG-3′

Figure 48: Gene fragment design for full length GAD65 insert

The vector nucleotide sequence is shaded in grey and the GAD65-FL sequence is light blue. Within the GAD65-FL insert, restriction sites (Nhe1, HindIII and Xho1) are in red, the Kozac sequence is navy, and the CASPR2 signal peptide is black. The stop codon was replaced with glycine (yellow) to allow DNA polymerase to continue reading along the sequence to the CASPR2 tail and the eGFP tag, and to engender flexibility to the GAD molecule at the C-terminal when expressed at the cell surface.". Gene fragments for the T96 and T88 inserts are similar. *CASPR2*, contactin-associated protein-2; *eGFP*, enhanced green fluorescent protein; *FL*, full length; *GAD65*, glutamic acid decarboxylase 65; *T88*, truncation at amino acid 88; and *T96*, truncation at amino acid 96.

The workflow is briefly outlined in Table 37 and described in detail in Chapter 2. DNA fragment size and PCR cycling conditions are noted in Table 38 and Table 39, respectively. DNA sequencing confirmed successful cloning of the three GAD65 inserts into the vector, along with the CASPR2 signal and tail sequences, and the eGFP tag.

Table 37: Workflow for cloning GAD65 expression constructs

The LCE plasmid vector was developed by the OANG for use in the LGI1 antibody CBA and contained an LGI1 insert, a CASPR2 tail and an eGFP sequence. *AGE*, agarose gel electrophoresis; *CASPR2*, contactin-associated protein-2; *CBA*, cell-based assay; *E.coli*, Escherichia coli; *eGFP*, enhanced green fluorescent protein; *FL*, full length; *GAD65*, glutamic acid decarboxylase 65; *LGI1*, leucine-rich glioma inactivated 1; *MRC WIMM*, Medical Research Council Weatherall Institute of Molecular Medicine at the University of Oxford; *OANG*, Oxford Autoimmune Neurology Group; *PCR*, polymerase chain reaction; *RE*, restriction endonuclease; *T88*, truncation at amino acid 88; and *T96*, truncation at amino acid 96.

1. PCR amplification of FL, T96 and T88 GAD65 gene fragments to make sufficient DNA for the planned experiments.
2. Agarose gel electrophoresis (AGE) of PCR products for separation by net electrical charge and size (Figure 49).
3. DNA gel extraction and purification.
4. Restriction digestion (double digest) of LCE plasmid vector backbone (containing the LGI1 insert), LGI1 insert and GAD65 inserts: The LCE vector and the GAD65 gene fragments were cut by the restriction endonucleases (REs) NHE1-HF and XH01 to create DNA fragments with single-stranded DNA overhangs (sticky ends). The LCE plasmid was split into a linearised backbone with sticky ends and a separate LGI1 insert.
5. AGE for separation of cut plasmid vector backbone, LGI1 insert and GAD65 inserts from intact (uncut) LCE plasmid and GAD65 gene fragments (Figure 50).
6. DNA gel extraction and purification.
7. Ligation of GAD65 inserts and plasmid vector backbone by T4 DNA ligase to form intact circular plasmids containing a GAD65 insert.
8. Bacterial transformation via heat shock: GAD65-insert containing plasmid vector was introduced into DH5-alpha strain of competent *E. coli*. The plasmid carries a bacterial origin of replication and an ampicillin resistance gene (selection marker).

9. Bacterial outgrowth and miniprep extraction/purification of plasmid vectors containing GAD65 inserts.
10. Colony PCR and AGE of PCR products to indicate which bacterial colonies produced GAD65-containing plasmids (**Figure 51** and **Figure 52**).
11. Restriction digest and AGE for secondary confirmation of cloning following colony PCR to select constructs for DNA sequencing (**Figure 53**).
12. Nanodrop, dilution to 300mg/microL, and Sanger DNA sequencing by the MRC WIMM Sequencing Facility to confirm that inserts were cloned in the correct orientation (**Figure 54**).
13. Maxiprep to isolate and purify plasmids.

Table 38: DNA fragment sizes

The LGI1 signal sequence is encoded by amino acids 1-34. *The LCE plasmid vector is not at any point entirely translated into protein. *CASPR2*, contactin-associated protein-2; *eGFP*, enhanced green fluorescent protein; *FL*, full length; *GAD65*, glutamic acid decarboxylase 65; *LGI1*, leucine-rich glioma inactivated 1; *N/A*, not applicable; *PCR*, polymerase chain reaction; *RE*, restriction endonuclease; *T88*, truncation at amino acid 88; and *T96*, truncation at amino acid 96.

DNA sequence	*Number of amino acids*	*Number of base pairs*
GAD65-FL insert	585	1918
GAD65-T96 insert	491	1633
GAD65-T88 insert	498	1657
LGI1 insert	557	1671
LCE plasmid (excluding LGI1)	N/A*	6330

Table 39: PCR cycling conditions

Temperature and duration of PCR stages. *PCR*, polymerase chain reaction.

Stage		*Details*
35 cycles of	Denaturation	95°C for 45 seconds
	Primer annealing	60.7°C for 30 seconds
	Extension	72°C for 2 minutes
Then	Final extension	72°C for 5 minutes

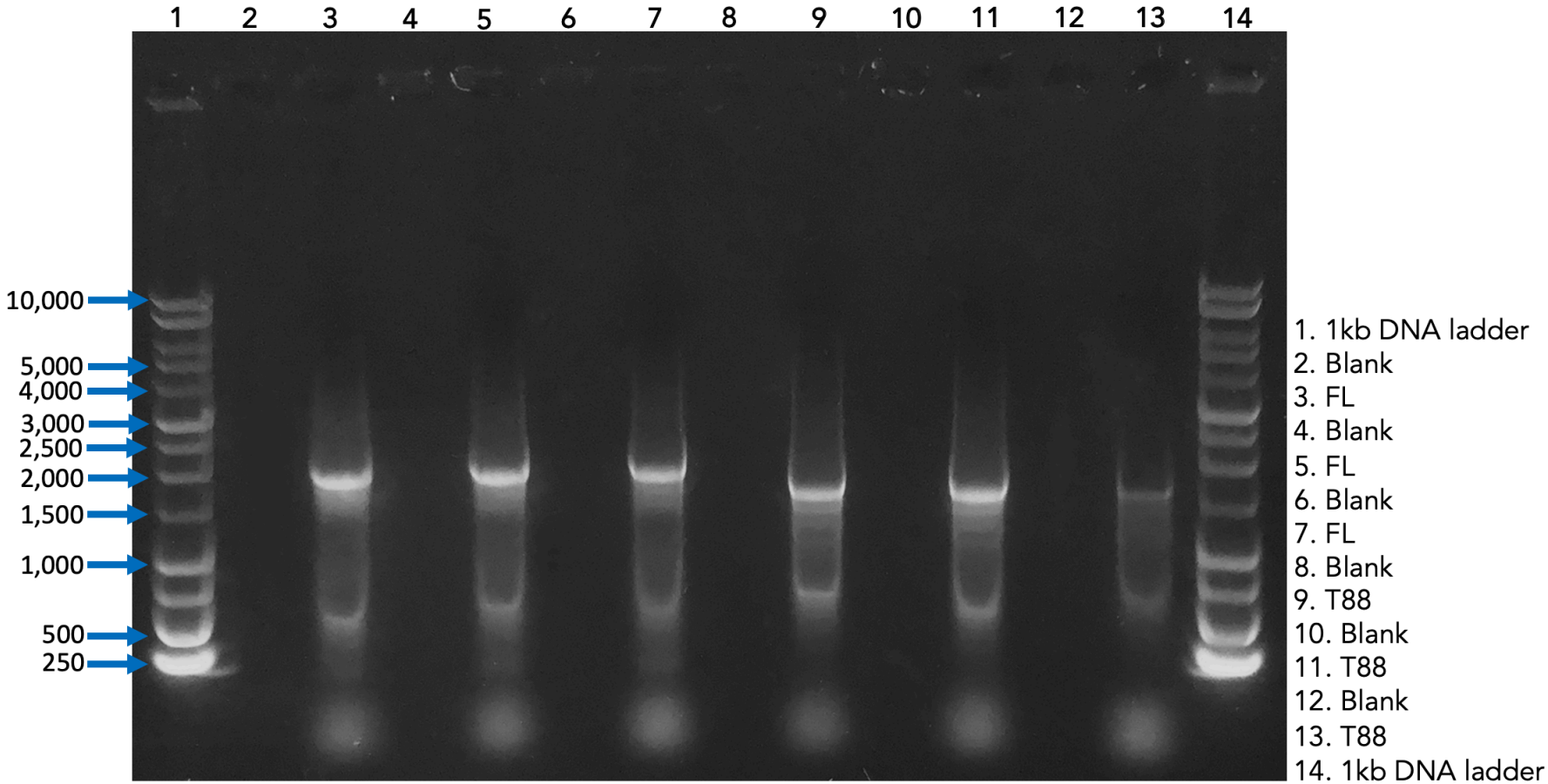


Figure 49: Gene fragment PCR amplification products

AGE photograph of PCR products showing modified FL gene fragment (**lanes 3, 5 and 7**) below the 2,000 bp marker (**lane 1**). The modified T88 gene fragment (**lanes 9, 11 and 13**) appeared below this, closer to the 1,500 bp marker. These results were in keeping with the anticipated product sizes. The modified T96 gene fragment is not shown. *AGE*, agarose gel electrophoresis; *FL*, full length; *PCR*, polymerase chain reaction; *T86*, truncation at amino acid 96; and *T96*, truncation at amino acid 96.

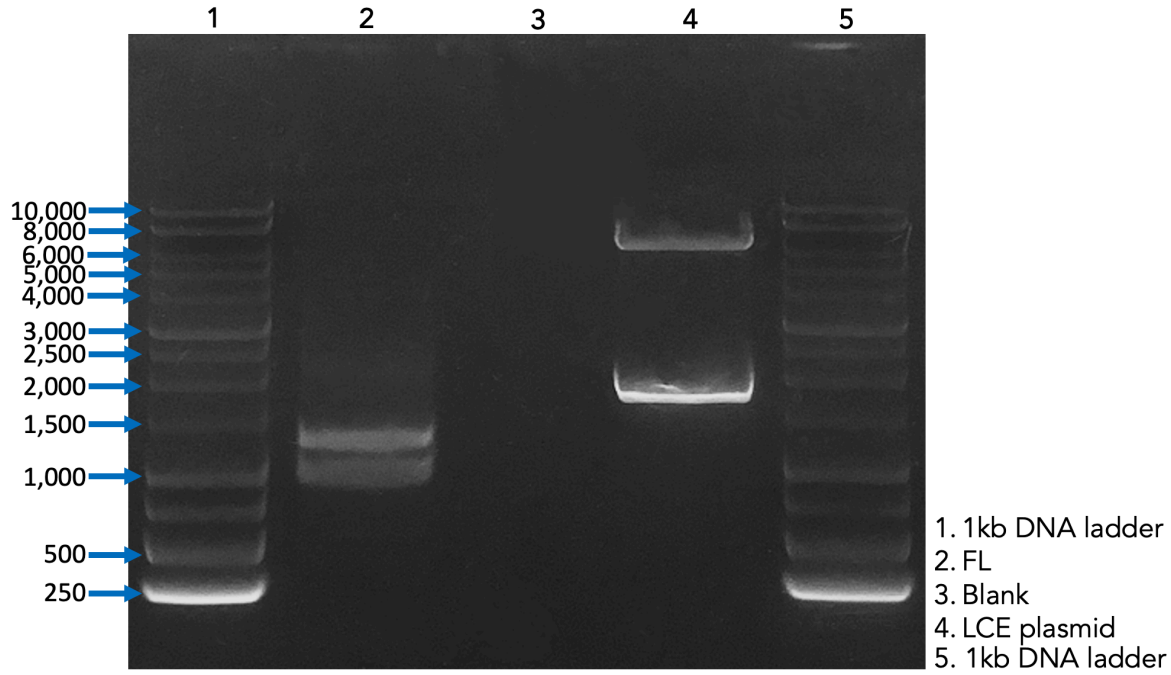


Figure 50: Restriction digest products for modified FL gene fragment and LCE plasmid
AGE photograph. The two bands for FL (**lane 2**) were unexpected and prompted review of the gene fragment sequence. This revealed an unintended extra restriction site for Xh01, which is responsible for producing the smaller product. Following redesign of the modified FL gene fragment, only one appropriately sized restriction digest product (gel not shown) was identified. The LCE plasmid (**lane 4**) product sizes were as expected, with the linearised, cut vector visible around 7,000 bp and the LGI1 insert just below the 2,000 bp marker. Restriction digest products for modified T96 and T88 are not shown. *AGE*, agarose gel electrophoresis; *FL*, full length; *LGI1*, leucine-rich glioma inactivated 1; *T86*, truncation at amino acid 96; and *T96*, truncation at amino acid 96.

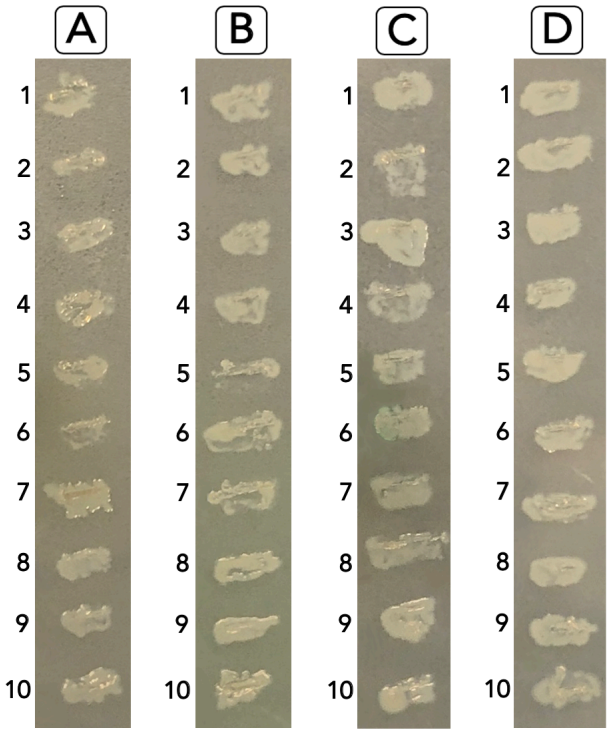


Figure 51: Bacterial colonies sampled for PCR
Photographs of bacterial colonies (post-transformation) on agar plates. Samples were taken for PCR screening for modified GAD65 constructs. **(A-B):** Modified T96 construct-expressing colonies. **(C-D):** Modified T88 construct-expressing colonies. *GAD65*, glutamic acid decarboxylase 65; and *PCR*, polymerase chain reaction.

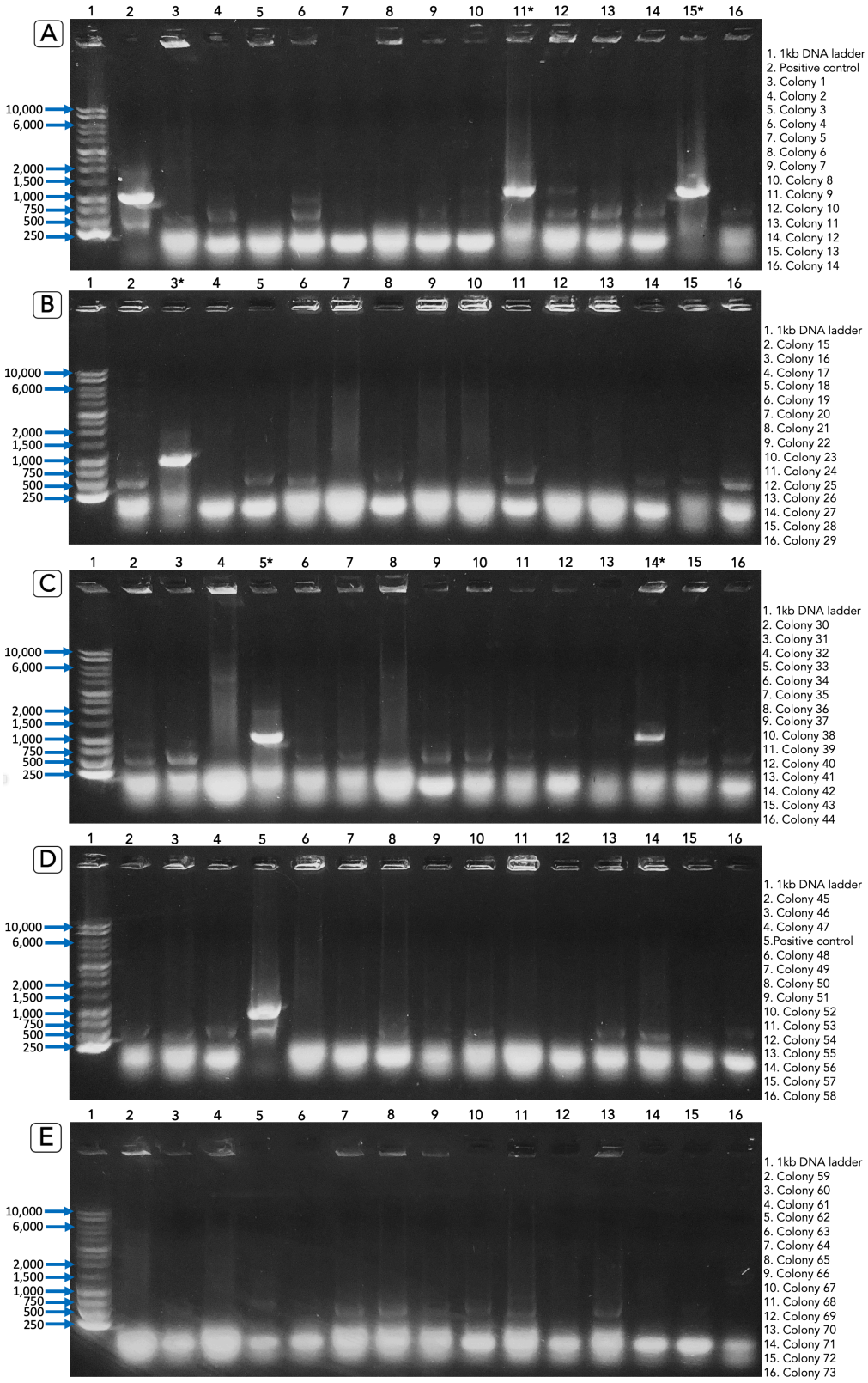


Figure 52: PCR products of modified T88 colony screen

AGE photographs from screening 73 different bacterial colonies for the modified T88 gene fragment-containing plasmid vectors. **Lanes A2 and D5**: Positive control modified T88-encoding plasmids prepared the previous day with suitably sized PCR products (approximately 1,000 bp). *****Colonies positive for the modified T88 plasmid (**lanes A11, A15, B3, C5, C14**) showed a modified T88 insert of the same size. Colony screens for modified FL and T96 are not shown. *AGE*, agarose gel electrophoresis; *FL*, full length; *PCR*, polymerase chain reaction; *T86*, truncation at amino acid 96; and *T96*, truncation at amino acid 96.

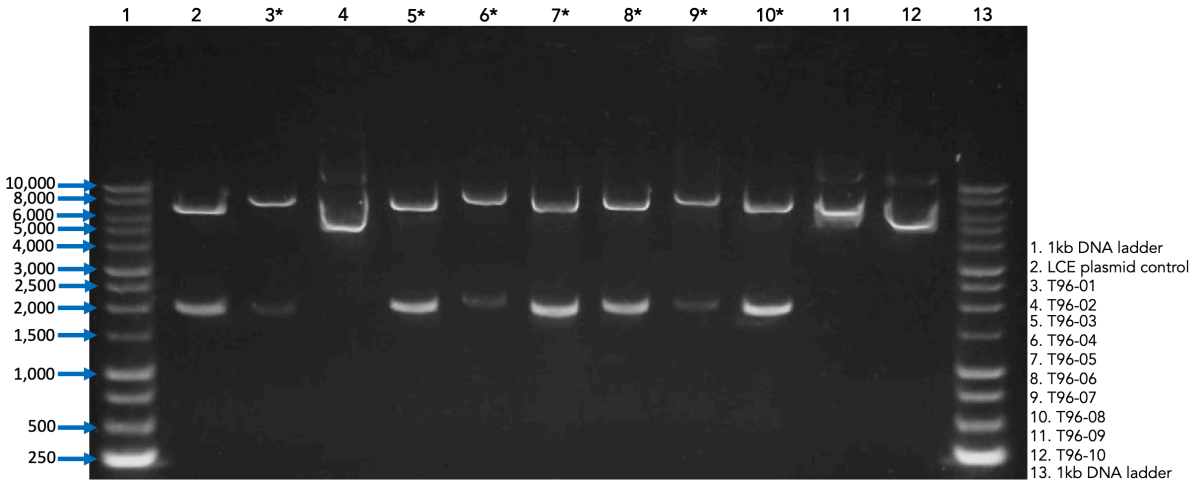


Figure 53: Restriction digest products for secondary confirmation of modified T96 cloning
AGE photographs. **Lane 2**: LCE plasmid control showed the plasmid backbone at approximately 6,000bp and the LGI1 insert at approximately 2,000 bp. ***Constructs positive for the T96 insert (**lanes 3, 5, 6, 7, 8, 9 and 10**). The T96 and LGI1 inserts were approximately the same sizes. *AGE*, agarose gel electrophoresis; *FL*, full length; *LGI1*, leucine-rich glioma inactivated 1; *T86*, truncation at amino acid 96; and *T96*, truncation at amino acid 96.

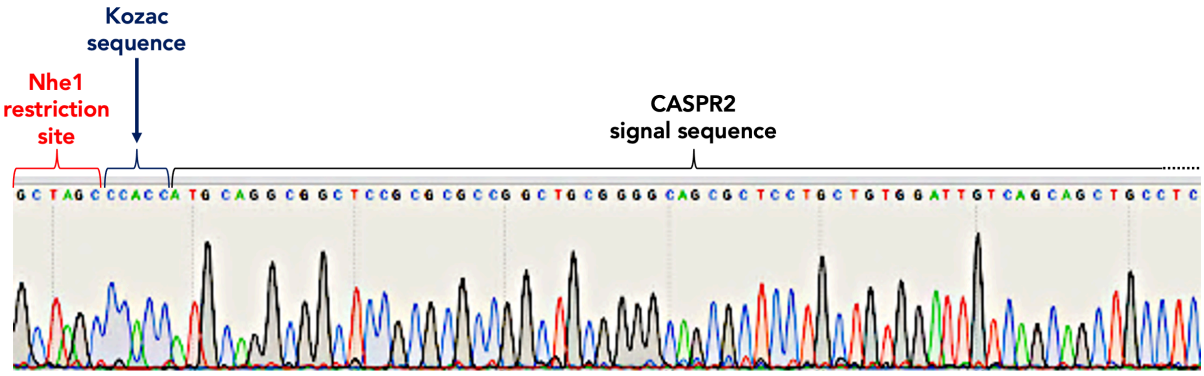


Figure 54: DNA sequencing chromatogram for the modified GAD65 T96 expression construct
Section of sequencing shows Nhe1 restriction site, Kozac sequence and part of the CASPR2 signal sequence. The nucleotide peaks (black, blue, red and green) were clear, with minimal noise (baseline). *CASPR2*, contactin-associated protein-2; *GAD65*, glutamic acid decarboxylase 65; *T96*, truncation at amino acid 96.

4.17 Live CBA testing of expression constructs

The three modified GAD65 expression constructs were expressed in a live CBA.

Intracellular eGFP aggregates were observed without cell surface expression of GAD65 (Figure 55).

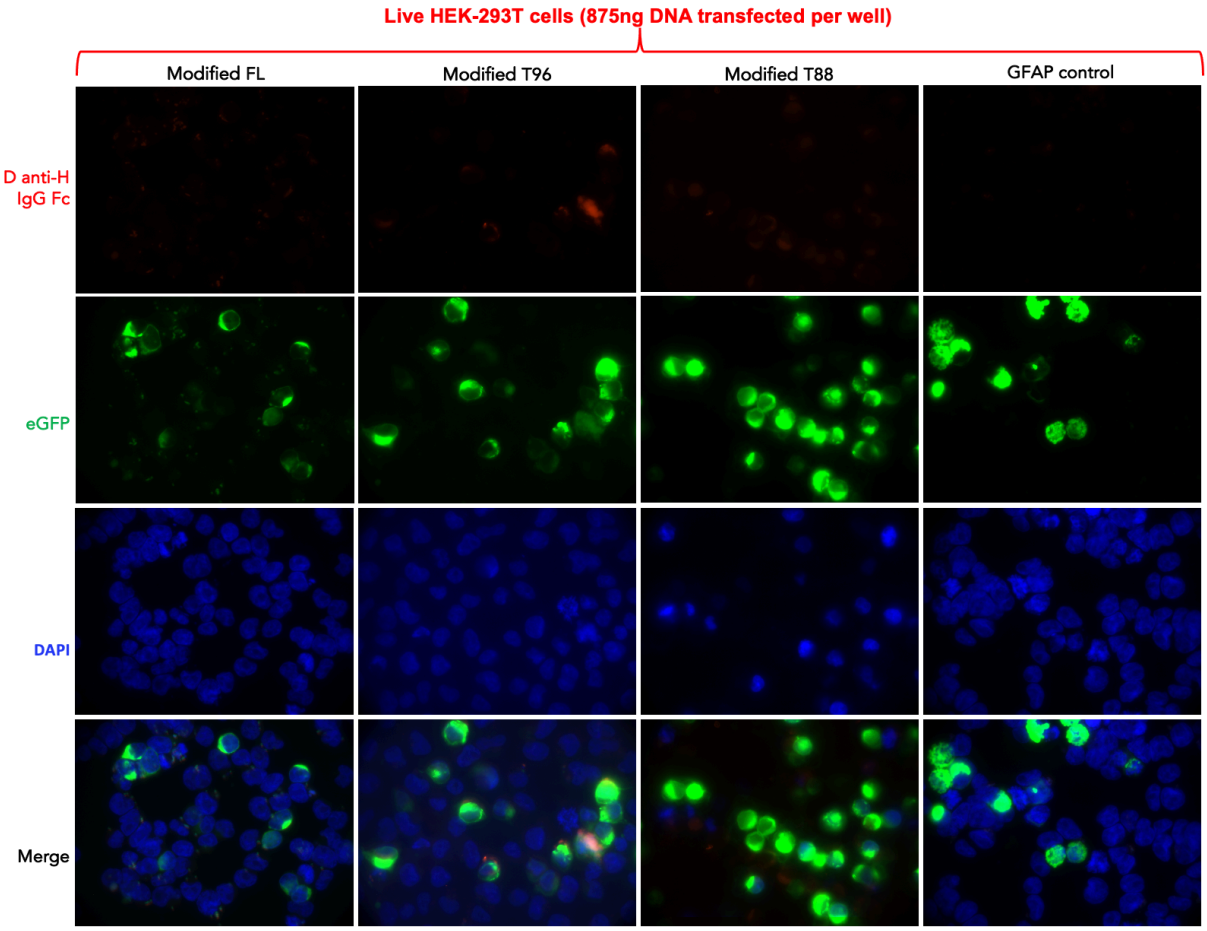


Figure 55: Live CBA test of modified GAD65 expression constructs
Fluorescence microscopy images (magnification x100, oil immersion). CBAs were performed on live HEK-293T cells transfected with FL, T96, T88 and GFAP (negative control) expression constructs. The amount of DNA transfected per well was 875ng, in keeping with the standard OANG laboratory protocol for CBAs. With AIN patient serum strongly positive for GAD65 antibodies (shown) and commercial rabbit polyclonal GAD65 antibody (not shown) at 1:100, no surface expression of GAD65 was apparent. Intracellular aggregates of eGFP suggested protein misfolding. *AIN*, autoimmune neurology; *CBA*, cell-based assay; *D anti-H IgG, Fc-gamma,* donkey anti-human IgG, Fc-gamma fragment-specific; *DAPI*, 4′,6-diamidino-2-phenylindole; *eGFP*, enhanced green fluorescent protein; *FL*, full length; *GAD65*, glutamic acid decarboxylase 65; *GFAP*, glial fibrillary acidic protein; *HEK-293T cells*, human embryonic kidney 293T cells; *OANG*, Oxford Autoimmune Neurology Group; *T86*, truncation at amino acid 96; and *T96*, truncation at amino acid 96.

To confirm that the GAD65 antigen was expressed intracellularly but not appropriately translocated to the HEK-293T cell surface, I tested the modified constructs on permeabilised CBA. This produced intensely staining intracellular aggregates of both GAD65 antigen and eGFP, without detectable GAD65 surface expression (**Figure 56**). Some weak, intracellular GAD65 antibody-positive signal was visible.

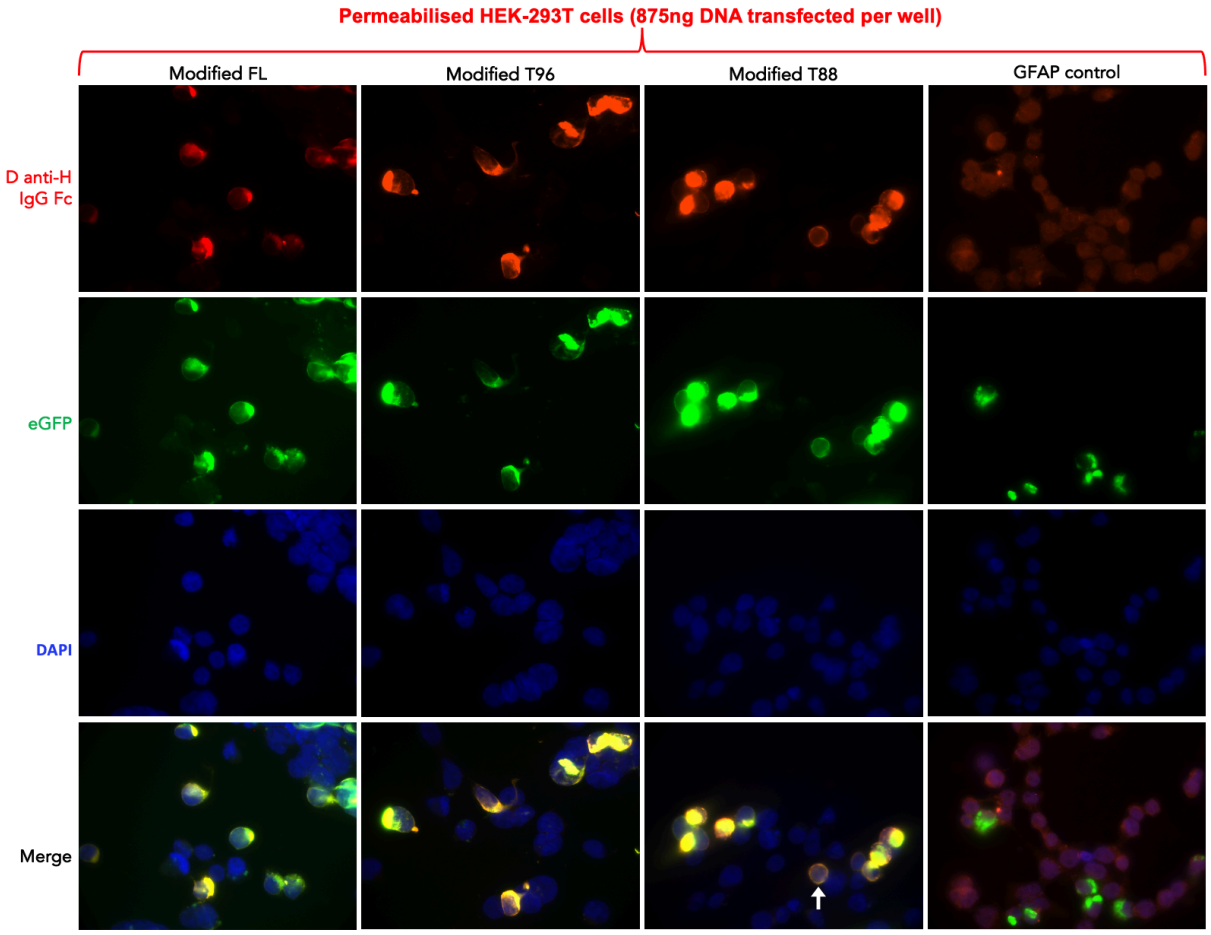


Figure 56: Permeabilised CBA test of modified GAD65 expression constructs
Fluorescence microscopy images (magnification x100, oil immersion). CBAs were performed on fixed and permeabilised HEK-293T cells transfected with FL, T96, T88 and GFAP (negative control) expression constructs using AIN patient serum strongly positive for GAD65 autoantibody (shown) and commercial rabbit polyclonal GAD65 antibody (not shown) at 1:100. The amount of DNA transfected per well was 875ng, in keeping with the standard OANG laboratory CBA protocol. Intensely staining intracellular aggregates of GAD65 and eGFP were observed, as well as weaker positive GAD65-specific intracellular, annular, pericytoplasmic staining in eGFP-positive cells (white arrow). Increased non-specific intracellular background signal due to cell permeabilisation was apparent on the GFAP-transfected negative control (compared to the live CBA in **Figure 55**). *CBA*, cell-based assay; *D anti-H IgG, Fc-gamma*, donkey anti-human IgG, Fc-gamma fragment-specific; *DAPI*, 4′,6-diamidino-2-phenylindole; *eGFP*, enhanced green fluorescent protein; *FL*, full length; *GAD65*, glutamic acid decarboxylase 65; *GFAP*, glial fibrillary acidic protein; *HEK-293T cells*, human embryonic kidney 293T cells; *OANG*, Oxford Autoimmune Neurology Group; *T86*, truncation at amino acid 96; and *T96*, truncation at amino acid 96.

Next, I explored whether the intracellular aggregates might be reduced by halving the amount of modified plasmid DNA transfected (as per the optimised permeabilised CBA protocol discussed earlier in this chapter). The lower DNA concentration produced fewer and smaller intracellular aggregates but the resultant GAD65 antibody-specific signal was also weaker than that generated by the unmodified T96 construct (**Figure 57**).

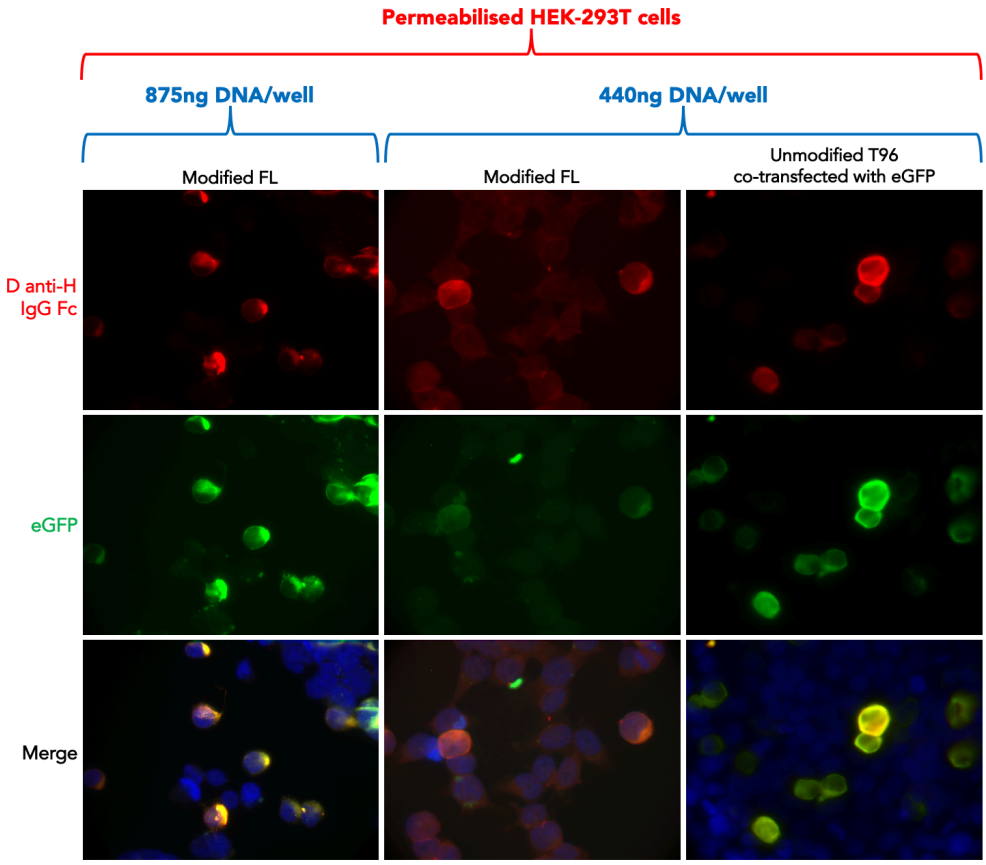


Figure 57: Permeabilised CBA test of modified GAD65 expression constructs with reduced DNA at transfection
Fluorescence microscopy images (magnification x100, oil immersion). CBAs were performed with a commercial rabbit polyclonal GAD65 antibody (1:100) on fixed and permeabilised HEK-293T cells transfected with the modified expression constructs at 875ng DNA/well (standard CBA protocol) and at 440ng DNA/well. Results were compared to the original unmodified T96 construct transfected at 440ng DNA/well. For the modified constructs (FL shown), the lower DNA concentration reduced intracellular aggregation of GAD65 and eGFP, and improved specific GAD65 antibody signal. However, GAD65 antibody-specific signal remained stronger with the unmodified T96 construct. *CBA*, cell-based assay; D anti-H IgG, Fc-gamma, donkey anti-human IgG, Fc-gamma fragment-specific; *DAPI*, 4′,6-diamidino-2-phenylindole; *eGFP*, enhanced green fluorescent protein; *FL*, full length; *GAD65*, glutamic acid decarboxylase 65; *GFAP*, glial fibrillary acidic protein; *HEK-293T* cells, human embryonic kidney 293T cells; *OANG*, Oxford Autoimmune Neurology Group; *T86*, truncation at amino acid 96; and *T96*, truncation at amino acid 96.

4.18 Summary

I developed and optimised a novel permeabilised CBA to detect GAD65 IgG autoantibodies using an expression construct encoding an untagged GAD65 protein with a truncation at amino acid 96 ('T96'). This CBA demonstrated inter-rater agreement and performed well compared to commercial GAD65 antibody RIPA and ELISA. Pilot serum screening for GAD65 IgM autoantibodies in a small group of GAD65 IgG-positive subjects was negative.

I applied molecular cloning techniques, aiming to produce a live CBA with surface-expressed antigen that could be interpreted more readily on microscopy. Three different GAD65 expression constructs (encoding full length GAD65 and two truncated versions) were designed with modifications intended for HEK293T cell surface translocation and anchoring, alongside the addition of an eGFP tag for colocalisation. GAD65 failed to express on the cell membrane with these modified constructs, rendering the live CBA ineffective. When tested on fixed and permeabilised CBA, the modified GAD65 expression constructs seemed to produce an intracellularly located eGFP-tagged GAD65 protein, suggesting that membrane targeting of the antigen with a CASPR2 signal peptide had been unsuccessful. Despite large intracellular eGFP and GAD65 aggregates, detection of GAD65 autoantibodies was still possible using the modified constructs in a permeabilised CBA. However, the positive signal was less intense when compared to the original unmodified and untagged T96 GAD65 construct.

These results are contextualised and discussed in Chapter 6.

Chapter 5 Cytokines and leukocyte phenotypes

5.1 Introduction

Improved understanding of the processes causing epilepsy could improve outcomes for people with drug-resistant epilepsy (DRE). At present, there is a lack of definitive evidence that epilepsy without concomitant autoimmune encephalitis (AIE) can be driven by autoantibodies. Accordingly, immunotherapy is generally not administered for seizure control in those without AIE.[311]

Epilepsy associated with GAD65 autoantibodies can be particularly resistant to conventional anti-seizure medications.[250] The role in epilepsy of autoantibodies against GAD65, an intracellular enzyme, is not known. These antibodies could be pathogenic[253] – if so, how antibody-antigen interaction occurs in vivo and which B cell subsets are responsible for antibody production in the long-term are questions to address. Alternatively, GAD65 autoantibodies could be bystanders – yet useful biomarkers – of a, to date, under-recognised disease process.[312]

Cytokines are soluble extracellular proteins or glycoproteins that modulate inflammation and cell signalling. Cytokines can have pro- or anti-inflammatory effects and their concentrations may fluctuate throughout a disease course. Distinct patterns of cytokines may implicate certain cell subsets in the pathology of an illness and pinpoint potential therapeutic targets. In plaque psoriasis, for example, recognition of elevated plasma interleukin-23 (IL23), along with expansion of Th17 cell populations and raised IL17 – all

components of the same pathogenic proinflammatory pathway[313] – gave rise to therapeutic use of the IL23-targetting monoclonal antibody, guselkumab.[314] Similarly, TNF antagonists, such as infliximab and adalimumab, are used in the treatment of inflammatory bowel disease, and the human IL1 receptor antagonist anakinra is used to treat rheumatoid arthritis.[315] Current clinical studies of epilepsy and cytokines do not report consistent findings and data pertaining to DRE are limited.[220,316]

Also, the immunocellular phenotype of autoimmune epilepsy is unexplored. If a detectable phenotypic signature of peripheral blood mononuclear cells (PBMCs) could distinguish between true autoimmune and non-autoimmune epilepsy, this could aid diagnosis and decision-making regarding immunotherapy, potentially improving clinical outcomes.

In this exploratory work, I aimed to:

- establish whether patients with GAD65 autoantibody-associated DRE have a particular cytokine profile, and use this to:
    - inform analysis of subsequent mass cytometry experiments,
    - determine whether the findings support a T cell-mediated pathogenic role for GAD65 autoantibodies,
    - select cytokine conditions for future work with PBMC cultures from GAD65 autoantibody-positive patients;
- characterise the immunocellular phenotype of GAD65 autoantibody-associated DRE, with a focus on:
    - exploring which B cell subsets are dominant in these patients,

- discerning evidence of T cell-mediated pathogenicity.

A collaboration with industry partners permitted the application of two innovative laboratory techniques – a flow cytometry multiplex bead-based immunoassay and mass cytometry.

5.2 Measurement of plasma cytokines

I opted to use a newly available and customised commercial bead-based immunoassay capable of simultaneously quantifying 13 human cytokines in a single plasma sample (Figure 58). I selected the panel of cytokines based on published literature and the availability of suitable antibodies from the manufacturer (Table 40).

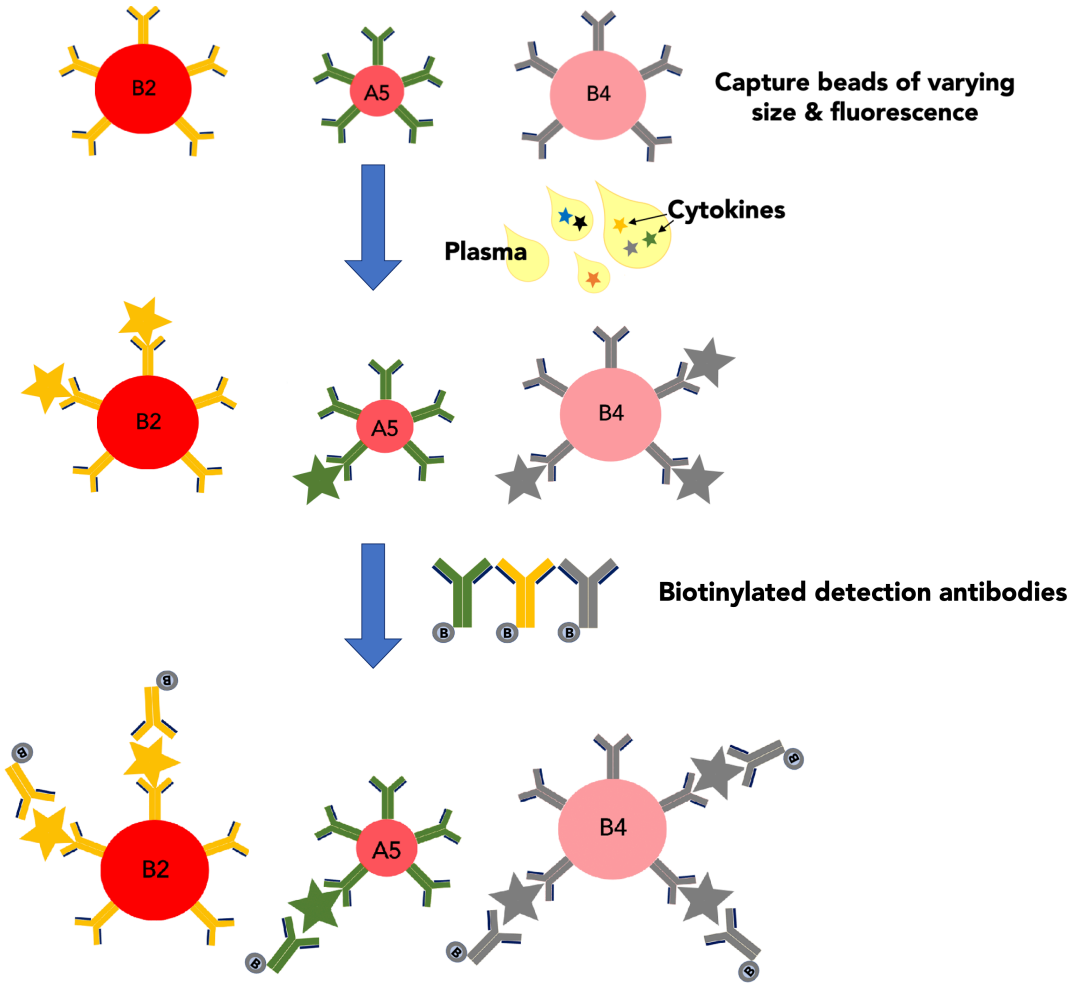


Figure 58: Overview of cytokine multiplex immunoassay
Beads can be distinguished by size (A and B) and varying levels of allophycocyanin (APC) fluorescence. Each bead is conjugated to a specific capture antibody for a particular cytokine. When a panel of capture beads are mixed together and incubated with an unknown plasma sample containing target cytokines, each cytokine binds to its specific capture bead. Biotinylated detection antibodies are added and each detection antibody then binds to its specific cytokine, forming a capture bead-analyte-detection antibody sandwich. Addition of streptavidin-phycoerythrin (SA-PE) (not depicted), which binds to the biotinylated detection antibodies, provides fluorescent signal with intensity proportional to the amount of bound cytokine. The PE and APC signal fluorescence intensities are then quantified by flow cytometry. Concentrations of cytokines are determined from a standard curve using LegendPlex analysis software. *APC*, allophycocyanin; *PE*, phycoerythrin; and *SA*, streptavidin.

Table 40: Rationale for cytokines included in testing panel

I established a custom panel of 13 cytokines based on relevant literature. *Chemokine. *AIE*, autoimmune encephalitis; *CA*, cerebellar ataxia; *CNS*, central nervous system; *DRE*, drug-resistant epilepsy; *HS*, hippocampal sclerosis; *LE*, limbic encephalitis; *mTLE*, mesial temporal lobe epilepsy; *PBMC*, peripheral blood mononuclear cell; *SE*, status epilepticus; *SPSD*, stiff person spectrum disorder; and *TLE*, temporal lobe epilepsy.

Cytokine	*Reported justification for inclusion in panel*
IL1b	• Genetic predisposition towards increased production in TLE with HS[317]. • Increased production in a cariaria lactone-induced epilepsy model using human microglial cells[318] • Up-regulation of mRNA in rat brain following amygdala kindling[319] • Increased serum levels in a rat model of SE[320] • Reduced hippocampal mRNA levels in mycophenolate mofetil-treated rat model of epilepsy[321] • Increased serum levels in the post-ictal period [322]
IL2	• Brain tissue levels elevated in DRE with mTLE [323] • Reduced hippocampal mRNA levels in mycophenolate mofetil-treated rat model of epilepsy[321] • Increased serum levels in the post-ictal period[322] • Stimulation of cultured PBMCs to produce GAD65 antibodies (SPSD, CA and LE only)[324]
IL4	• mTLE patients showed reduced frequency of CD8+ T lymphocytes expressing IL-4[325] • Brain tissue levels elevated in DRE with mTLE[323] • Increased serum levels in the post-ictal period [322]
IL6	• Increased production in a cariaria lactone-induced epilepsy model using human microglial cells [318] • Increased serum and CSF levels in people with severe epilepsy[316] • Increased frequency of CD4+ T lymphocytes expressing IL-6[325] in mTLE • Serum levels higher in refractory epilepsy patients[326] • Increased plasma and CSF levels in post-ictal period[327] • Increased inter- and post-ictal plasma levels in epilepsy patients[328] • Serum levels increased in epilepsy [329] • Post-ictal CSF and serum levels increased[330] • Increased plasma levels in new-onset epilepsy[331] • Post-ictal plasma level increased in TLE[332] • Increased serum levels in a rat model of SE[320]
IL10	• Increased production in a cariaria lactone-induced epilepsy model using human microglial cells [318] • Increased in sclerotic regions of resected brain tissue from patients with mTLE-HS[333] • Serum levels lower in epilepsy patients[334]
IL15	• Role in B cell activation[335]
IL17A	• Increased serum and CSF levels in people with severe epilepsy[316] • Reduced frequency of CD8+ T lymphocytes expressing IL-17[325] in mTLE • Increased inter- and post-ictal plasma levels in epilepsy patients[328] • Elevated brain tissue levels in DRE with mTLE[323] • Raised serum and CSF levels in epilepsy[336] • Expansion of IL17-producing CD4+ T cell subsets in DRE and AIE[337]
IL23	• Over-expressed in a rat model of neonatal SE[338] • Key role in a mouse model of CNS inflammation[339]
TNFa	• Increased production in a cariaria lactone-induced epilepsy model using human microglial cells [318] • Reduced frequency of CD8+ T lymphocytes expressing TNFa[325] in mTLE • Up-regulation of TNF-alpha mRNAs in rat brain following amygdala kindling[319] • Increased serum levels in a rat model of SE[320] • Increased serum levels in the post-ictal period[322]

Cytokine	*Reported justification for inclusion in panel*
IFNg	• Increased serum and CSF levels in people with severe epilepsy[316] • Increased inter- and post-ictal plasma levels in epilepsy patients[328] • Reduced frequency of CD8+ T lymphocytes expressing IFNg[325] in mTLE • Increased serum levels in the post-ictal period[322]
CXCL10 (IP10)*	• Role in neuroinflammatory CNS disorders[340] • Biomarker of trafficking of activated leukocytes into the subarachnoid and perivascular space in neuroinflammation[341]
sCD25	• Role in mouse model of T cell-driven brain inflammation[342] • Single nucleotide polymorphisms in or near the encoding gene are associated with increased risk of autoimmune disorders of the CNS[343]
sCD40L	• Successful B cell activation in vitro[344,345]

I tested previously unthawed plasma samples from GAD65 autoantibody-positive patients with epilepsy or another neurological condition and compared them to different control groups, including patients with autoimmune encephalitis (Table 41). None had received B cell-depleting therapies prior to plasma sampling.

The point at which certain samples became available for cytokine testing was beyond my control because extensive antibody screening was still ongoing in parallel and there were extensive delays in specimen transfer from external storage facilities. The COVID-19-related lockdown subsequently caused patient recruitment to cease and laboratory facilities to become inaccessible, precluding the testing of an additional assay plate, with a further 40 plasma samples.

Ideally, the numbers of plasma samples from each group would have been better balanced with more control groups. Autoantibody-positive DRE patients could be compared to age- and sex-matched autoantibody-negative DRE, autoantibody-positive SFE and GAD65 autoantibody-positive DRE, as well as to autoantibody-negative DRE patients with known structural brain lesions, such as hippocampal sclerosis or malformations of cortical

development (e.g., grey matter heterotopia, focal cortical dysplasia, polymicrogyria or pachygyria), cryptogenic focal epilepsy, autoantibody-negative patients in status epilepticus and patients with autoimmune neurological conditions, such as neuromyelitis optica spectrum disorders (i.e. autoantibody-driven) and multiple sclerosis (non-autoantibody-mediated). More healthy control samples were planned.

To explore whether antibody-positive DRE and antibody-positive autoimmune encephalitis reflect different ends of the same disease spectrum, LGI1 autoantibody-positive DRE patients without a history of encephalitis could be compared to LGI autoantibody-positive encephalitis.

Table 41: Plasma samples for cytokine testing

GAD65 autoantibody-positive patients included the eight patients with GAD65 autoantibody-positive DRE (including the patient with low GAD65 autoantibody EPT) and nine GAD65 autoantibody-positive autoimmune neurology clinic patients with conditions other than epilepsy. Plasma samples from 16 autoimmune encephalitis patients with LGI1 antibodies and 13 autoimmune encephalitis patients with NMDA receptor antibodies were included. DRE patients with positivity for other antibodies included eight with surface reactivity to cultured astrocytes or neurons, and eight who were positive for specific neuronal surface antibodies – contactin-2 (n=3), GABA-A receptor (n=2), GABA-B receptor and glycine receptor (n=1), NMDA receptor (n=1), and 1 DPPX (n=1). No patients had received B cell-depleting therapies. *CASPR2*, contactin-associated protein-2; *DPPX*, dipeptidyl-peptidase-like protein 6; *DRE*, drug-resistant epilepsy; *GABA-A*, gamma-aminobutyric acid receptor type A; *GABA-B*, gamma-aminobutyric acid receptor type B; *GAD65*, glutamic acid decarboxylase 65; *GAD65*, glutamic acid decarboxylase 65; *LGI1*, leucine-rich glioma inactivated-1; *NMDA*, N-methyl-D-aspartate receptor; and *SFE*, seizure-free epilepsy.

Patient group	*Number of subjects*	
GAD65 autoantibody-positive	17	13
Autoimmune encephalitis	29	1
DRE autoantibody-negative	32	
SFE autoantibody-negative	19	11
DRE autoantibody-positive	16	14
Healthy controls	2	

5.3 Analysis of cytokine multiplex immunoassay

Examples of flow cytometry gating are in **Figure 59**. Comparison of plasma concentrations showed statistically significant differences between patient groups for five markers – IL1b, IL4, IL10, IL15 and TNFa (**Figure 60**).

I used principal component analysis (PCA) as an exploratory data analysis tool, with the Prcomp script in RStudio and the visualisation packages Factoextra and Corrplot. PCA is a robust linear dimensionality reduction method that aids visualisation and interpretation of multivariate data while retaining variability. PCA involves constructing new variables (known as principal components or dimensions) as linear combinations of the original variables to maximise the variance. The first principal component describes the maximum amount of variation; the second component holds the next most, and so forth.

Eigenvalues showed that the first two principal components accounted for nearly 70% of the overall variation of the dataset (**Figure 61**). IL4 contributed most to the overall variance followed by IL6, IL23, IL1b, IL15 and TNFa (**Figure 62** and **Figure 63**).

Soluble CD40 ligand was the individual marker with the highest correlation coefficient (dimension 3), followed by IL17a (dimension 6, **Figure 64**). The GAD65 autoantibody-positive patients showed some separation from the other groups (**Figure 65**).

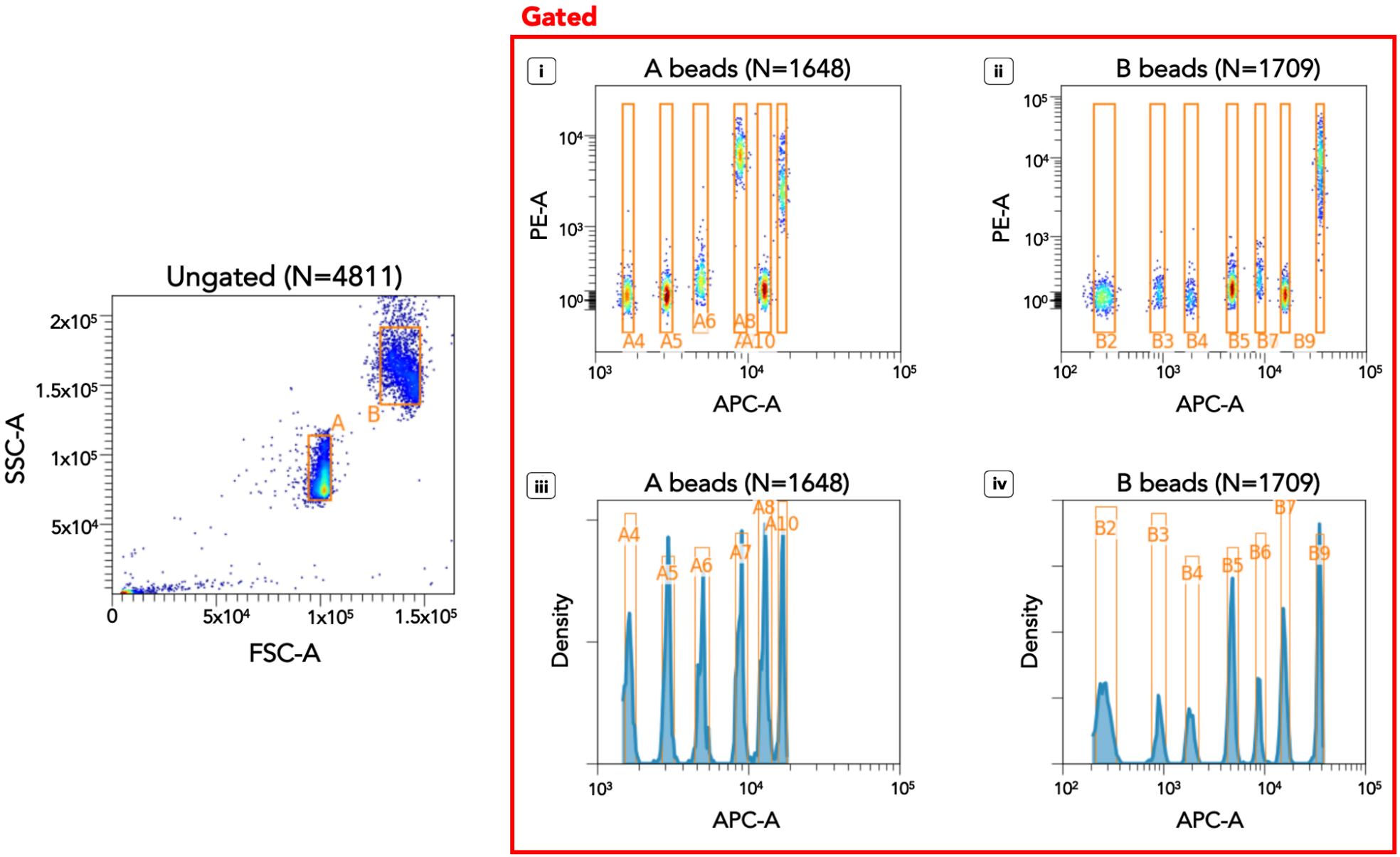


Figure 59: Flow cytometry gating

Ungated events: A and B bead populations were separated by size (proportional to forward scatter) and internal complexity (indicated by side scatter). Gated events: Dot plots (i & ii) and histograms (iii & iv). Gating by APC and PE fluorochromes subsequently identified 13 separate bead populations (A4-8, A10, B2-7 and B9), each corresponding to one of the 13 cytokines detected by the immunoassay. *APC-A*, allophycocyanin (area); *FCS-A*, forward scatter (area); *PE-A*, phycoerythrin (area); and *SSC-A*, side scatter (area).

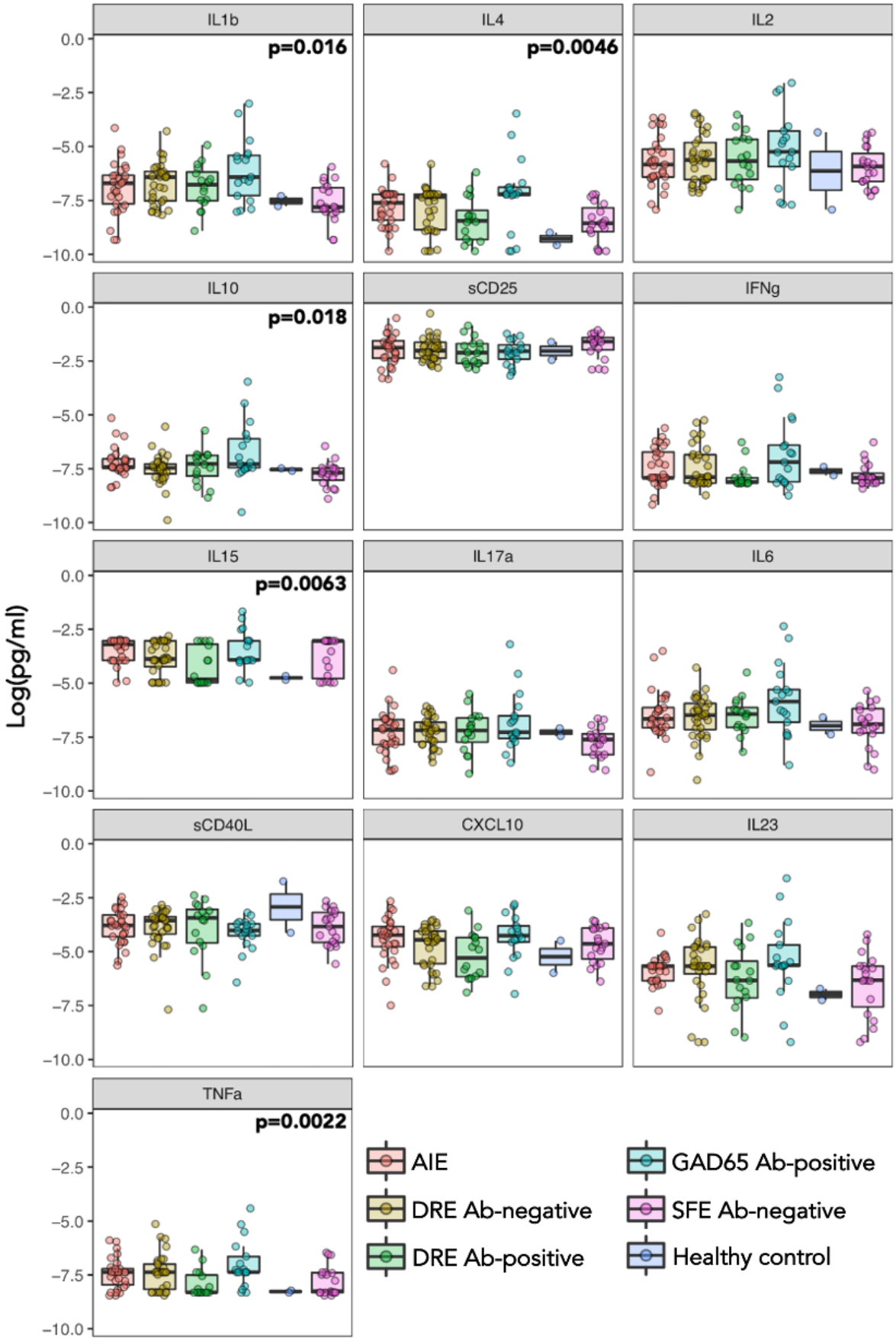


Figure 60: Boxplots of quantitative cytokine assay results across six patient groups

Boxplots show median values and quantiles. Significant differences were detected between the patient groups for five cytokines (IL1b, IL4, IL10, IL15 and TNFa) using the Kruskal-Wallis rank-based non-parametric test, $p<0.05$. Calibrators of known concentrations were included on each plate to permit inter-plate normalisation. Each sample was tested twice, and the mean value was used in the analysis. Values measured below the threshold for each marker were assigned the minimum detectable value if the threshold was >0. *Ab*, antibody; *AIE*, autoimmune encephalitis; *DRE*, drug-resistant epilepsy; *GAD65*, glutamic acid decarboxylase 65; and *SFE*, seizure-free epilepsy.

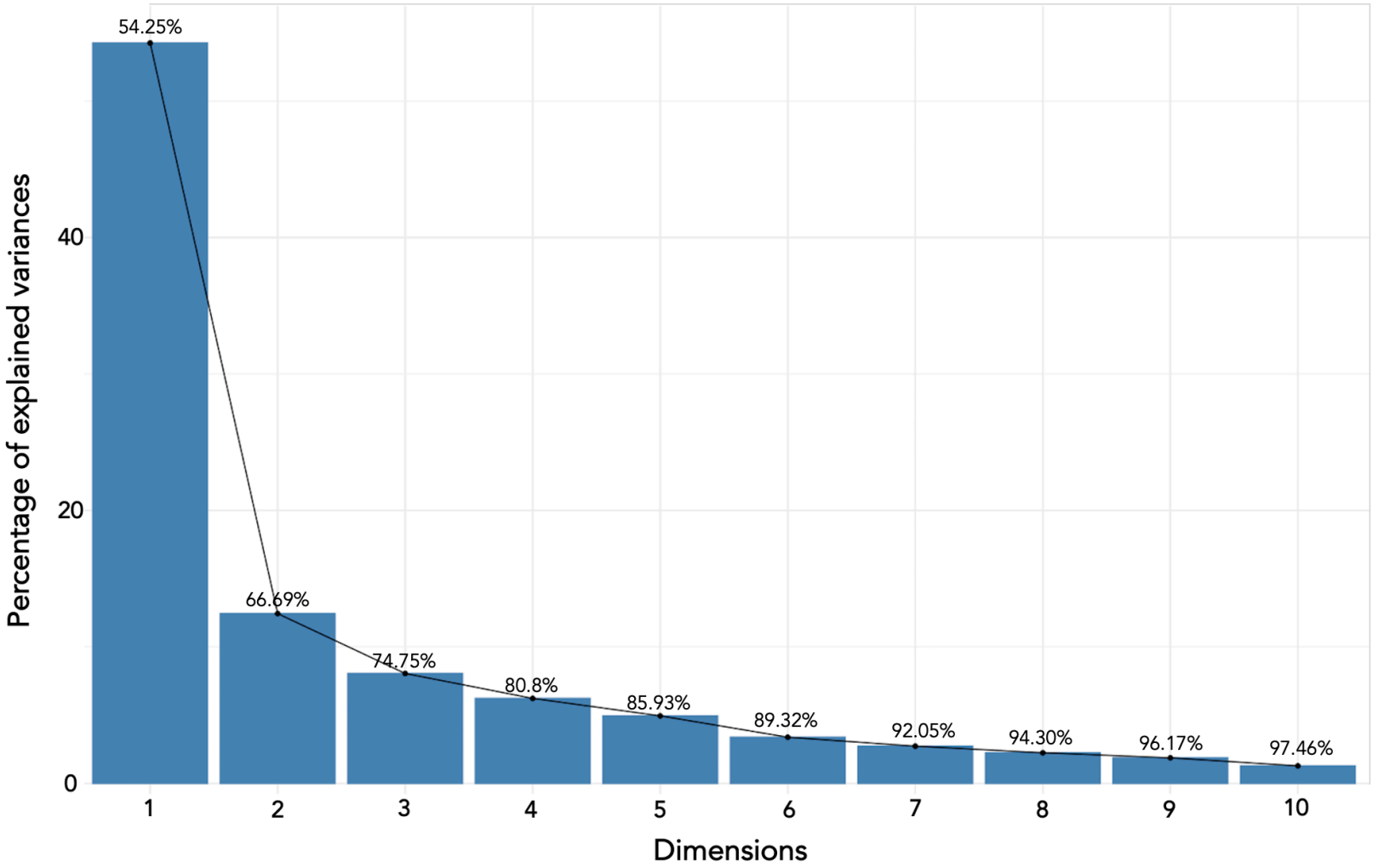


Figure 61: Scree plot

Eigenvalues – which indicate the amount of variation in a data set retained by each principal component (PC) – were expressed as a percentage of the total variance and plotted in decreasing order. The first two PCs accounted for nearly 70% of the variance. Beyond the fifth PC, the remaining Eigenvalues were relatively small and of comparable size. *PC*, principal component.

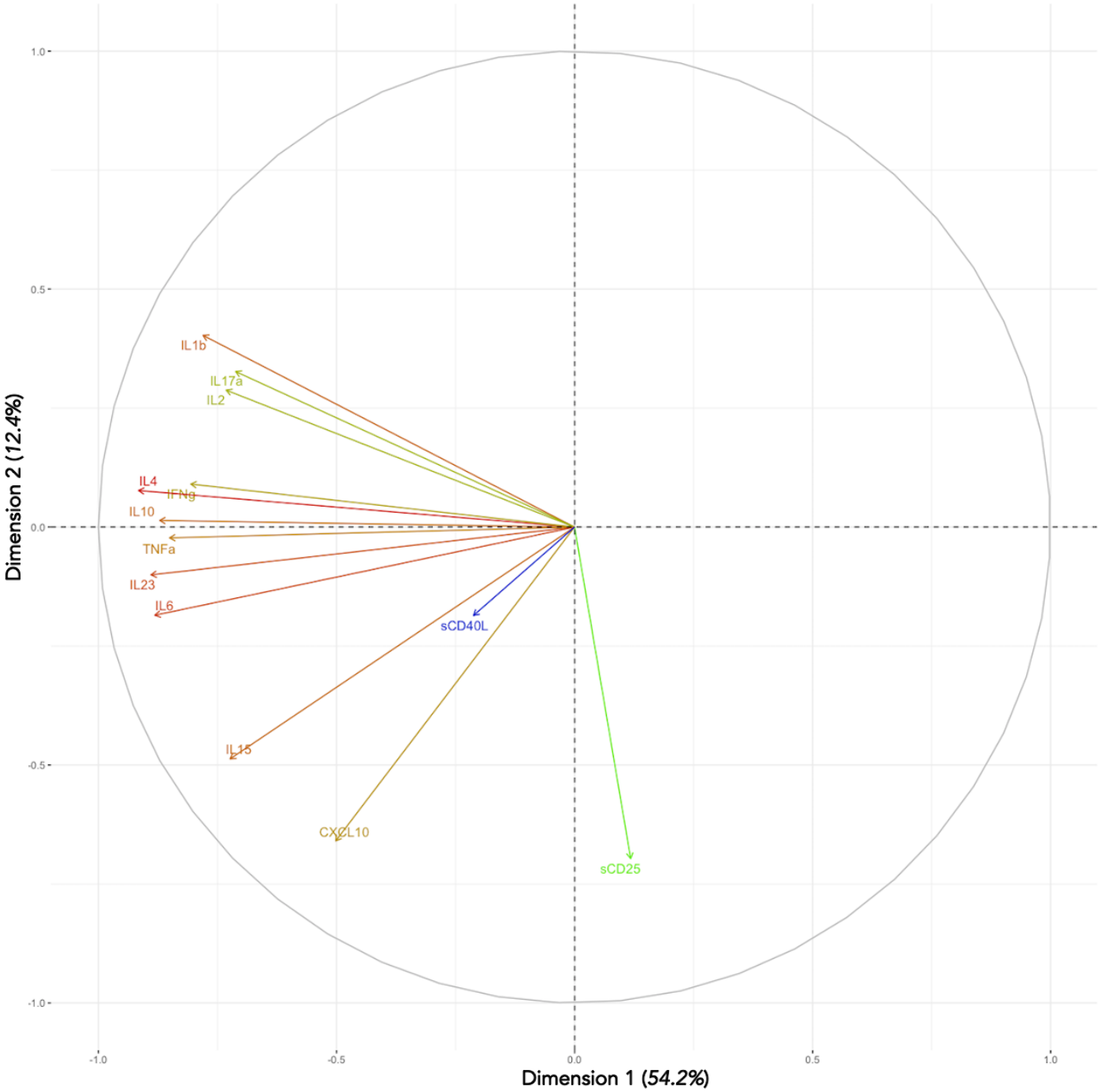


Figure 62: Variable correlation plot for PCA dimensions 1 and 2

The plot shows the relationships between the 13 cytokines, coloured by their contribution to the overall variance (with red representing the largest contribution and blue the smallest). Positively correlated variables are grouped together (e.g., IL23 and IL6), whereas negatively correlated variables are positioned on opposite quadrants (e.g., sCD25 and IL2). Variables that are further away from the origin are better represented on the factor map (e.g., IL4). In contrast, variables that are poorly represented by the principal components are plotted closer to the centre (e.g., sCD40L). *PCA*, principal component analysis.

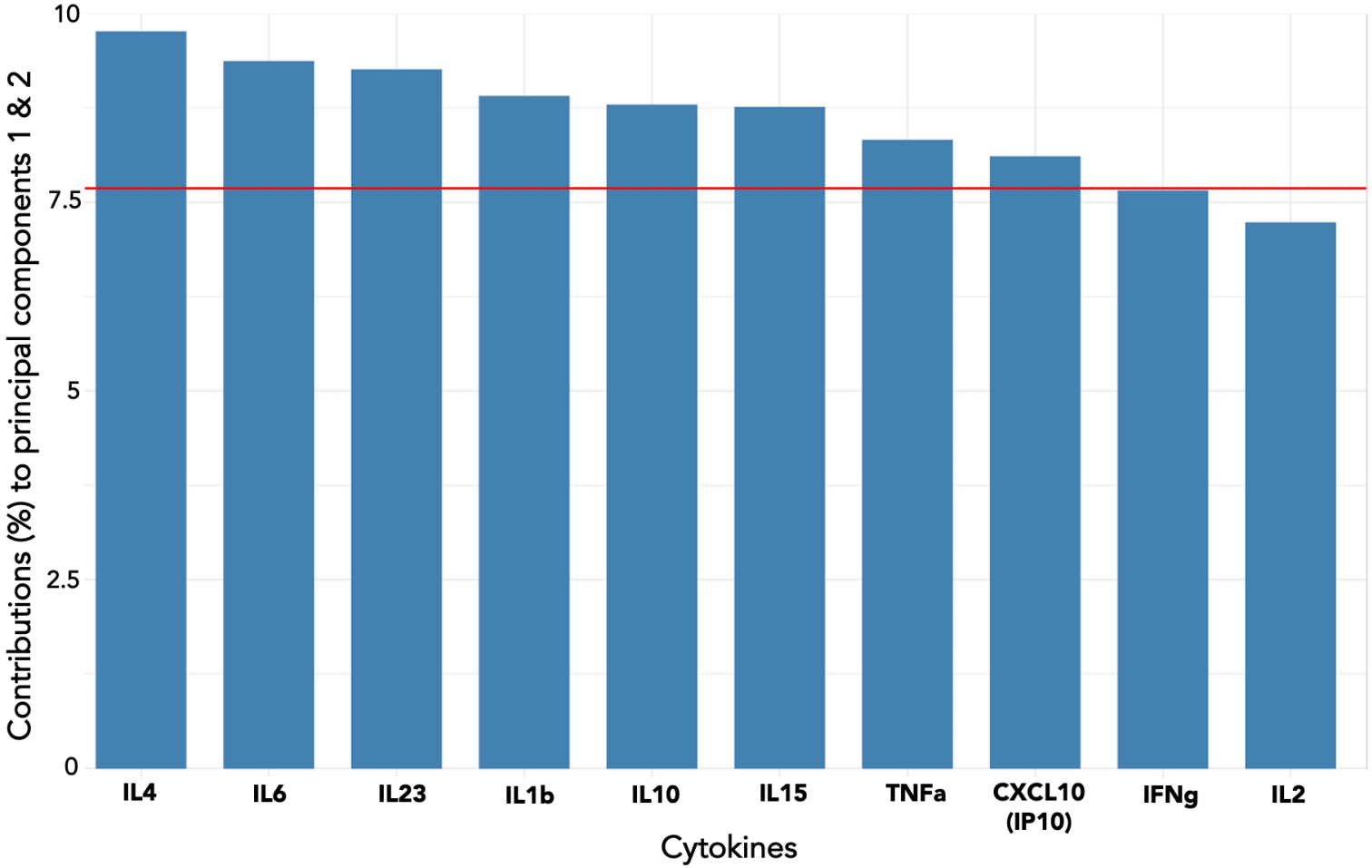


Figure 63: Contributions of variables to principal components 1 and 2

Dimensions 1 and 2 are the most important in explaining the variability in a data set. Only the ten highest contributing cytokines are shown. The red line indicates the expected average contribution of variables had all 13 cytokines contributed equally to the total variance.

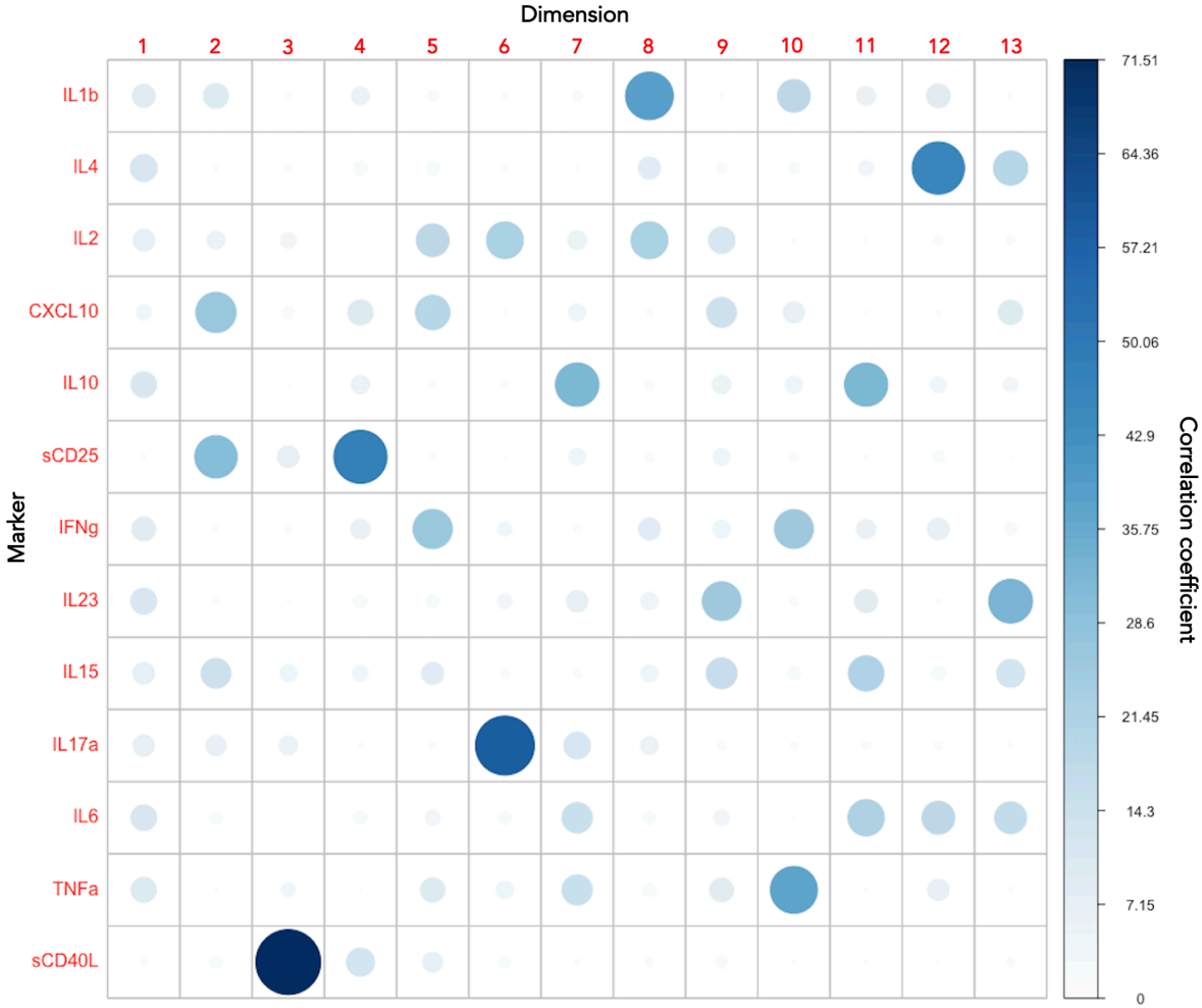


Figure 64: Correlation plot

The plot shows the contributions of all variables to each of 13 dimensions. The colour intensity and circle diameter are proportional to the correlation coefficient values.

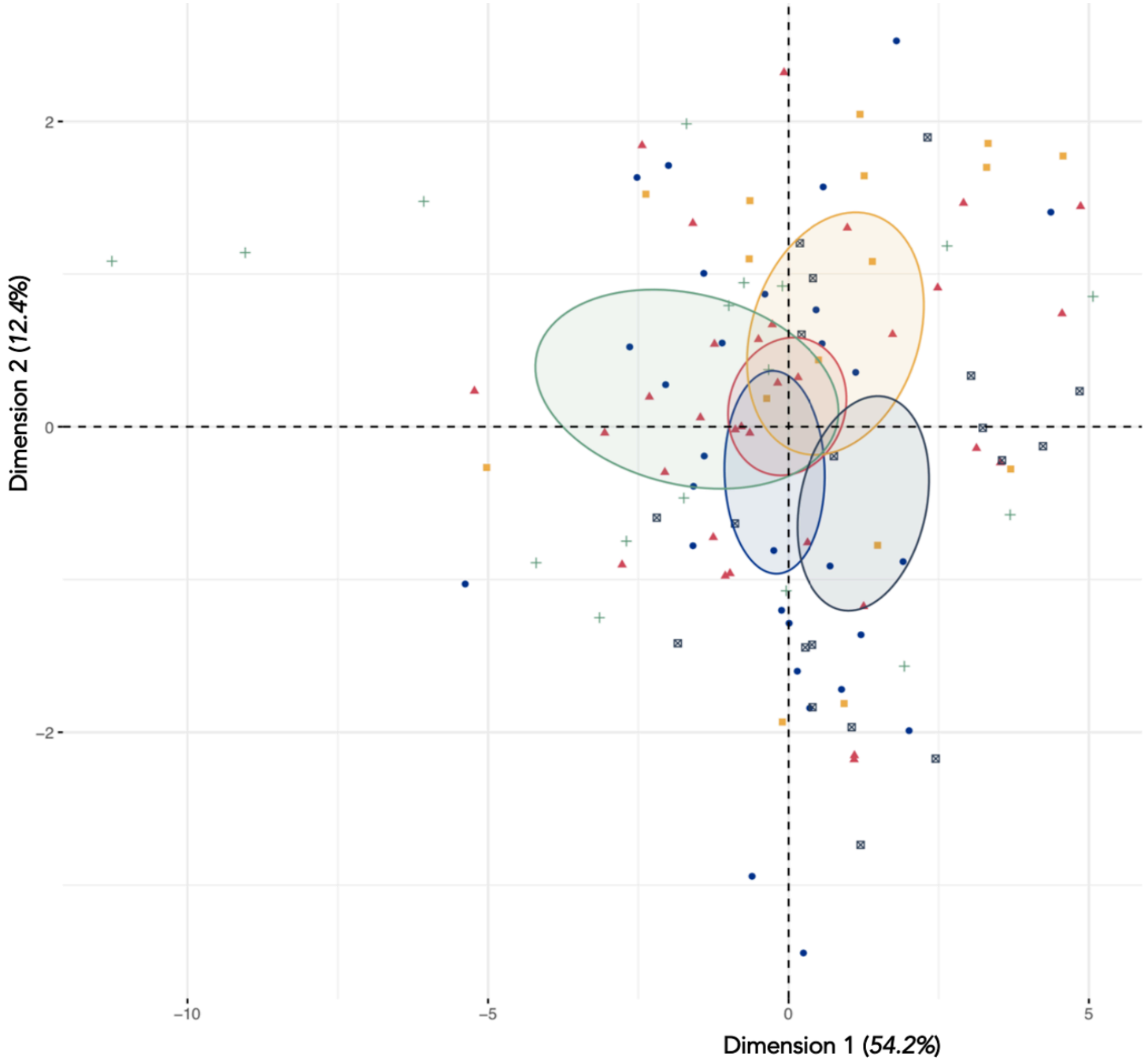


Figure 65: Biaxial plot of individual plasma samples in PCA

A plot of individual samples coloured by patient group, with 95% confidence ellipses. GAD65 autoantibody-positive patients (green ellipse) separate from the other groups. The two healthy control samples are not shown here. *Ab*, antibody; *AIE*, autoimmune encephalitis; *DRE*, drug-resistant epilepsy; *GAD65*, glutamic acid decarboxylase 65; *PCA*, principal component analysis; and *SFE*, seizure-free epilepsy

5.4 PBMC sample acquisition by mass cytometry

Mass cytometry – also known as cytometry by time-of-flight (CyTOF) or inductively-coupled plasma mass spectrometry by time-of-flight (ICP-MS-TOF) – is a technique that offers uniquely high dimensional measurement of single cell parameters using antibodies tagged with stable isotopes of rare earth heavy metals (**Figure 66**). The high number of parameters that can be simultaneously detected (>60 at present and expected to increase) compared to techniques such as flow cytometry (**Figure 67**) renders mass cytometry suitable for the exploratory analysis of mixed cell populations. **Table 42** summarises the workflow and **Figure 68** provides an overview of the technique.

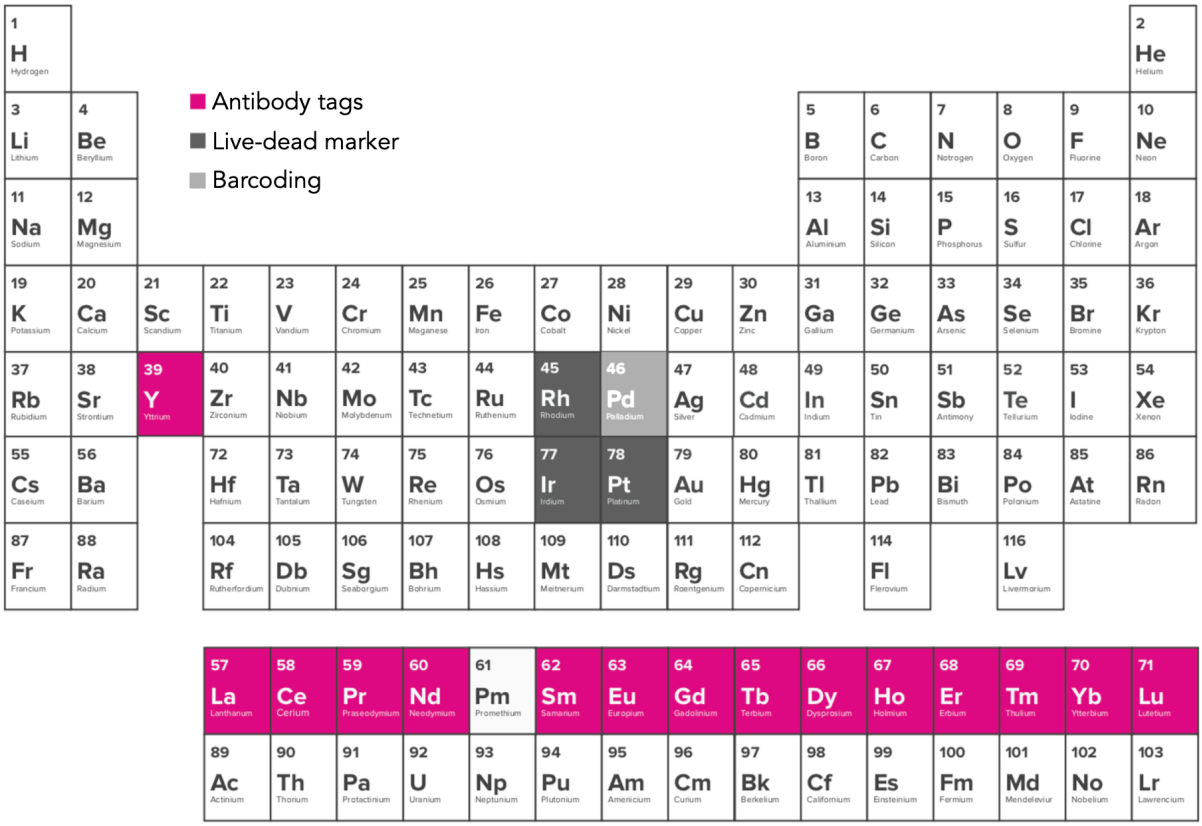


Figure 66: Elements used in mass cytometry
Cells are labelled with enriched, stable isotopes of heavy metal-conjugated antibodies in solution. These metals, typically from the lanthanide series, are naturally absent from biological tissues. DNA intercalators are used as live-dead markers to identify cells without antibody binding. Specific combinations of palladium isotopes can be used for sample barcoding. Adapted from the Fluidigm website.[346]

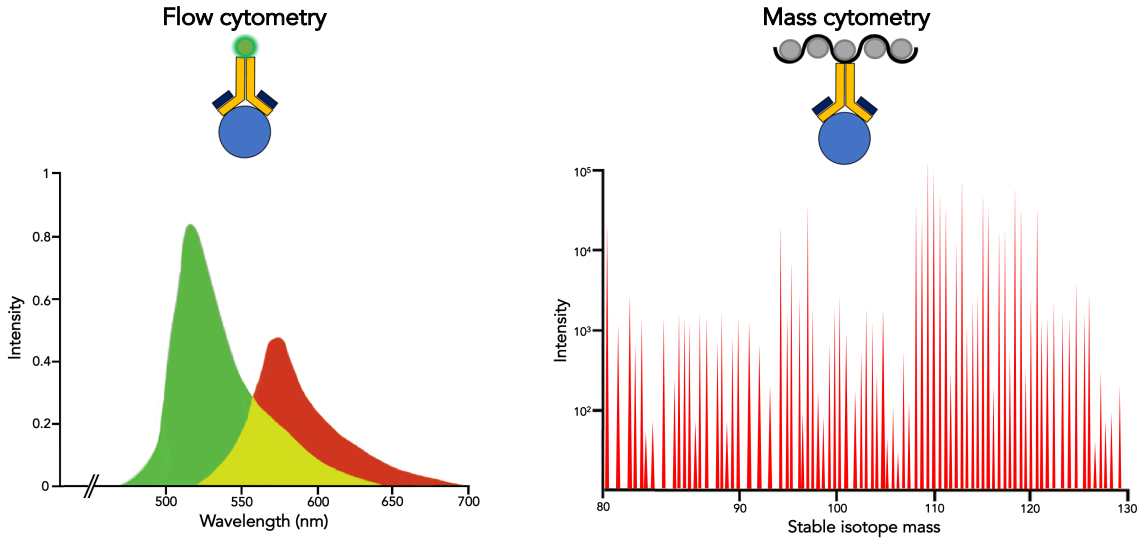


Figure 67: Comparison of flow cytometry and mass cytometry
Flow cytometry is a common laboratory technique for detecting cell markers based on antibodies conjugated to fluorochromes. As illustrated on the left, the emission spectra of fluorochromes can overlap (yellow). The resultant spill-over of signal into other detector channels limits the number of fluorochromes that can be used simultaneously. By contrast, in mass cytometry antibodies are conjugated to metal isotopes which produce discrete signals, with almost no spill-over, allowing the concurrent use of many more markers. Adapted from Maecker et al.[347]

Table 42: Mass cytometry workflow summary
Detailed methodology is contained in chapter 2.

Barcoding and antibody staining
• PBMC thawing • Cisplatin staining (cell viability marker) • Cell fixation • Barcoding of each sample • Pooling of barcoded samples • Fc receptor blocking • Antibody cocktail staining • Cell fixation • PBMC resuspension in freezing media and storage at -80°C
Sample acquisition
• PBMC thawing • Iridium staining (DNA intercalator) • Resuspension in EQ four element beads and cell acquisition solution • Acquisition at rate of 250-500 events per second
Data pre-processing and analysis
• Normalisation to EQ beads • File concatenation • Debarcoding • ArcSinh transformation • Removal of debris and doublets • Gating for live single cells • Iterative analysis with dimensionality reduction and clustering

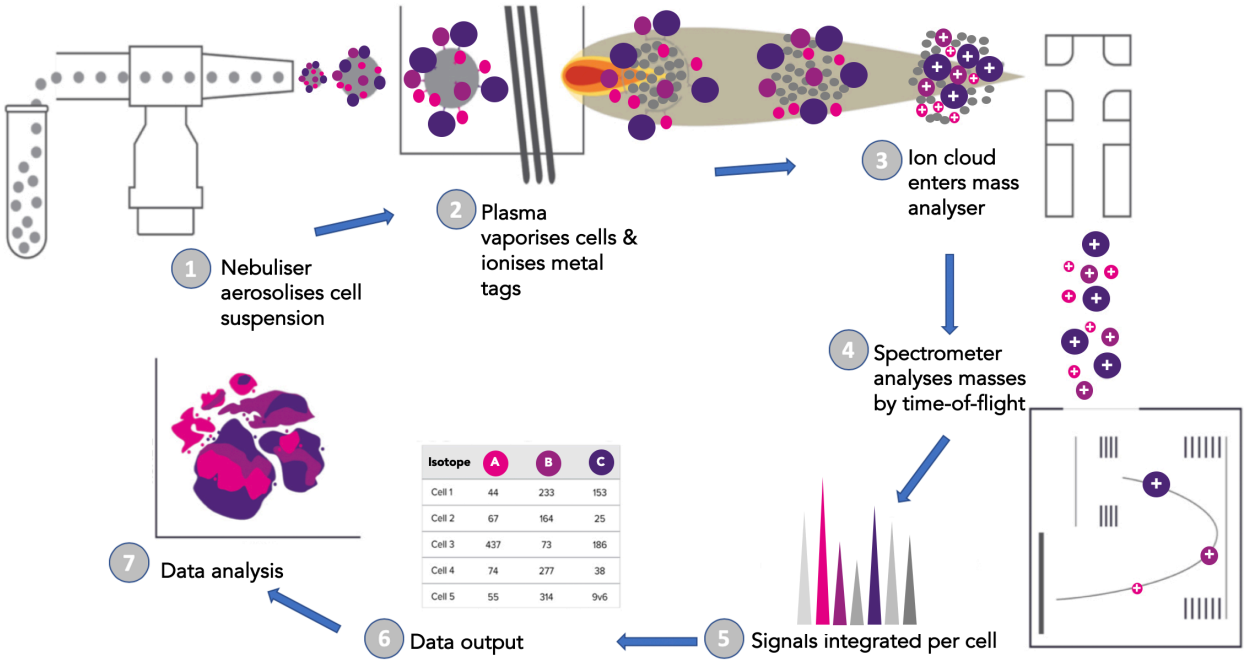


Figure 68: Mass cytometry overview
Cells, labelled with heavy metal-tagged antibodies targeting proteins of interest, are injected into the nebuliser and aerosolised to produce single cell-containing droplets. Droplets pass to the inductively-coupled argon plasma torch and are ionised. A radiofrequency quadrupole removes low atomic mass ions and guides the heavy metal ion cloud to the time-of-flight chamber. 13-microsecond slices of the ion stream ("pushes") enter the chamber at a time. Ions within a push are separated by mass and accelerated towards the detector, which quantifies metal isotopes for each cell. An event occurs when the ion signal intensity is above the threshold for ten pushes or more. Data is digitised, and events within the range of 10-150 pushes are exported in FCS format. Adapted from the Fluidigm website.[346]

Intending to produce a large, robust dataset for longer-term analysis, I studied a total of 100 PBMC samples on mass cytometry. I selected frozen PBMCs from patients with DRE, autoimmune encephalitis and appropriate controls; with and without autoantibodies (**Table 43**). None of the patients had received B cell-depleting therapies.

I selected samples using available antibody screening results at the time of instrument availability. The COVID-19-related lockdown forced patient recruitment to end and prevented a planned sixth batch of 20 PBMC samples from being tested, which would have ensured better balancing of the numbers of patients in each group and the inclusion of more healthy controls.

Table 43: PBMCs for acquisition by mass cytometry

PBMCs from 14 autoimmune encephalitis patients with LGI1 antibodies and 14 autoimmune encephalitis patients with NMDA receptor antibodies (three of whom had ovarian teratomas) were included. DRE autoantibody-positive patients included seven with surface reactivity to cultured astrocytes or neurons, and eight who were positive for specific neuronal surface antibodies – contactin-2 (n=3), GABA-A receptor (n=2), GABA-B receptor and glycine receptor (n=1), NMDA receptor (n=1), and DPPX (n=1). *Three unique healthy control samples but seven healthy control samples were tested in total, as one healthy control doubled as a technical control, with their sample divided into aliquots prior to freezing, and one aliquot included in each of five acquisition batches. No patients received B cell-depleting therapies. The COVID-19 lockdown prevented a planned further 20 samples from being tested, which included additional unique healthy controls. CASPR2, contactin-associated protein-2; DPPX, dipeptidyl-peptidase-like protein 6; DRE, drug-resistant epilepsy; GABA-A, gamma-aminobutyric acid receptor type A; GABA-B, gamma-aminobutyric acid receptor type B; GAD65, glutamic acid decarboxylase 65; GAD65, glutamic acid decarboxylase 65; LGI1, leucine-rich glioma inactivated-1; NMDA, N-methyl-D-aspartate receptor; *PBMC*, peripheral blood mononuclear cell; and SFE, seizure-free epilepsy.

Patient group	*Number of subjects*
Autoimmune encephalitis	28
DRE autoantibody-negative	29
DRE autoantibody-positive	15
DRE with high endpoint titre GAD65 autoantibodies	5
SFE autoantibody positive	2
SFE autoantibody-negative	14
Healthy controls	3*

For the purposes of this exploratory chapter, I selected five GAD65 autoantibody-positive DRE patients, five age- and sex-matched autoantibody-negative SFE patients, and three unique healthy controls for analysis. A sample size of 13 is relatively large for a mass cytometry project with human PMBCs (e.g., a rheumatoid arthritis study reported in Nature by Rao et al. analysed cells from three patients[348]). Iterative analysis of mass cytometry data is typically completed over 6-12 months.

As conjugation of a single antibody to a metal tag can take several months of optimisation work, I opted to use a commercial panel of pre-conjugated and optimised antibodies covering a range of immune markers (**Figure 69**).

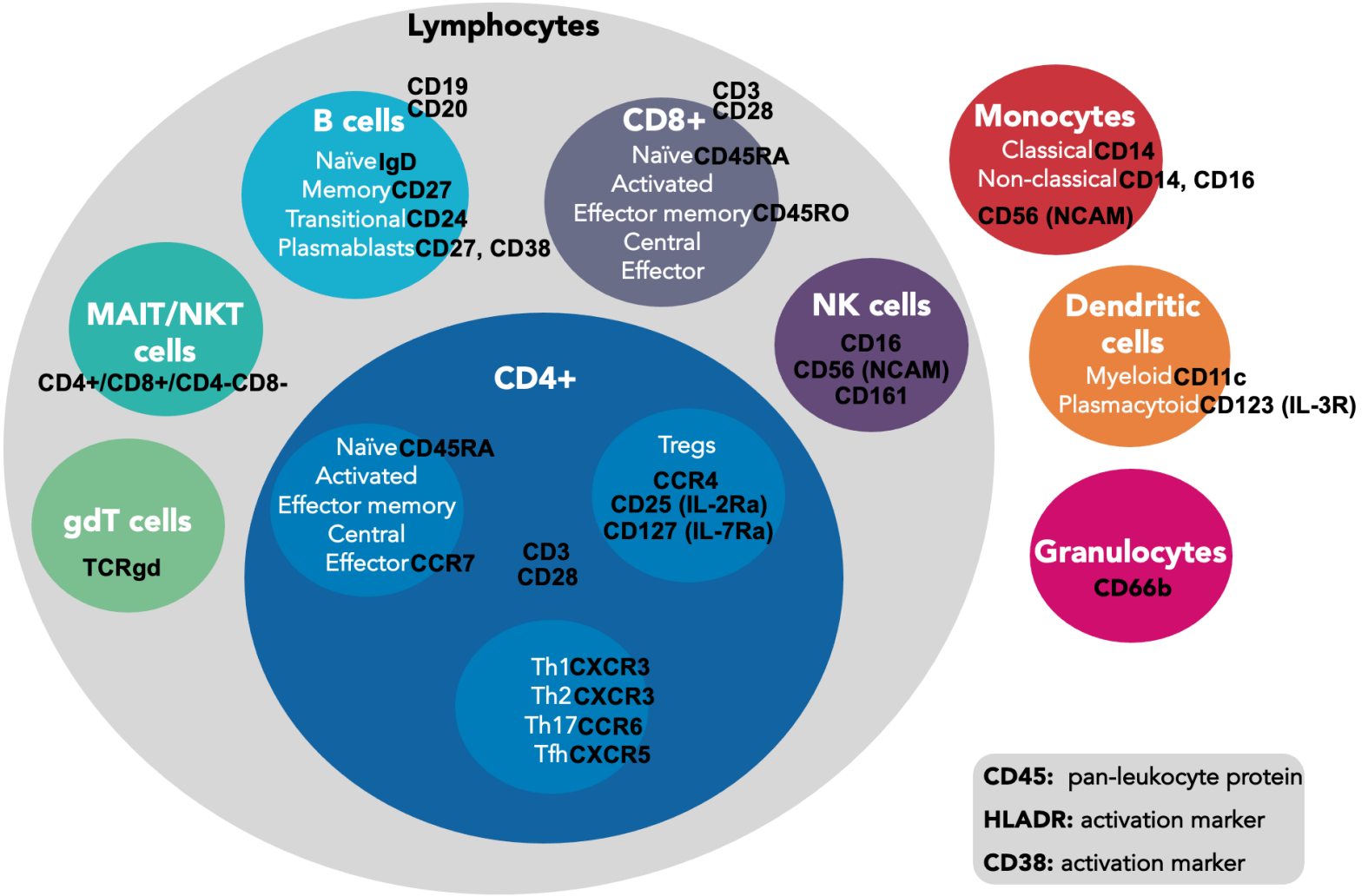


Figure 69: Antibody panel targeting key leukocyte subpopulations

Approximately 1.5-3 million PBMCs per patient were stained with 29 antibodies against a range of immune cell markers. Chemokine markers (CCR4, CCR6, CCR7, CXCR3 and CXCR5) do not survive the fixation for barcoding. T cells are generally defined as positive for CD4 or CD8; additional types include invariant natural killer T cells (NKT), and mucosal-associated invariant T cells (MAIT). B cells emerge into the periphery from bone marrow as new emigrant B cells (*CD10+ CD19+ CD20+ IgM+ IgD+ CD27-*). Once mature naïve B cells (*CD10- CD19+ CD20+ IgM+ IgD+ CD27-*) have encountered antigen, they can enter germinal centres, interact with T cells and become activated mature naïve B cells (*CD30+ CD69+ CD80+ CD86+*). Germinal centres are also the site of T cell-dependent immunoglobulin class switch recombination and somatic hypermutation. Switched memory B cells (*CD30+ CD69+ IgM- IgD-*) and unswitched memory B cells (*CD19+ CD20+ CD27+ IgM+ IgD+*) exit germinal centres and give rise to antibody-secreting cells – plasmablasts (*CD19+ CD20+/- CD27++ CD38++ CD138+/-*), short-lived plasma cells (*CD19+ CD20- CD27++ CD38++ CD138+/-*) and long-lived plasma cells (*CD19+/- CD20- CD27++ CD38++ CD138++*).[232] Figure adapted from the Fluidigm website.[349] *gdT*, gamma-delta T; *MAIT*, mucosal-associated invariant T cell; *NK*, natural killer cell; *NKT*, natural killer T cell; *Tfh*, follicular helper T cell; *Th*, helper T cell; and *Treg*, regulatory T cell.

To reduce intraassay variation, I elected to use barcoding. Samples were divided into equally sized batches, each comprising a mix of patient groups. Within a batch, samples were allocated unique barcodes of palladium isotopes and then pooled before antibody staining and acquisition (**Figure 70**).

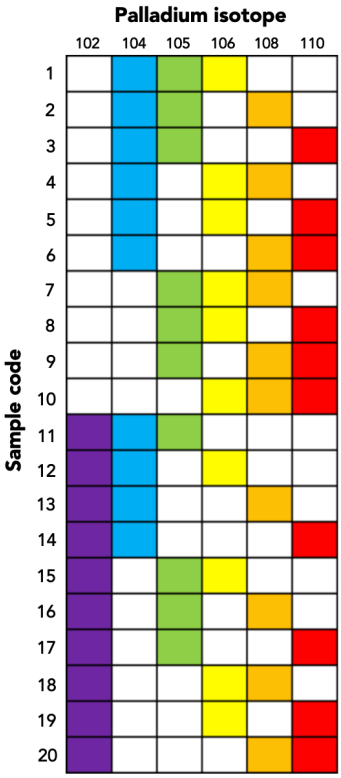


Figure 70: Barcoding for sample multiplexing. Combinations of six different palladium isotopes form 20 unique 3-digit barcodes. Therefore, 20 different patient samples can be barcoded, combined, antibody-stained and acquired as one multiplexed sample before debarcoding with software. Multiplexing samples improves data quality by eliminating variations in sample-specific staining and acquisition. Adapted from Fluidigm website.[350]

To facilitate assessment of interassay variation (and to permit subsequent batch normalisation measures, if necessary), I included the same healthy control sample in each batch. I also opted to use a human Fc receptor blocker to reduce non-specific background signal, as Fc receptors for IgG are present on many types of immune cells, with high expression on monocytes, granulocytes, and B cells.

5.5 Acquisition and pre-analysis processing of mass cytometry data

To maximise the chances of capturing rare cell types, I ran all samples to completion rather than setting a pre-defined event limit. Screenshots of live data acquisition are shown in Figure 71 and Figure 72.

Following sample acquisition, I normalised the data to a calibration bead-based passport specific to the manufactured bead lot. Data files were concatenated and debarcoded with Fluidigm CyTOF software (Figure 73). I could then extract the files required for the current analysis. Data was transformed and gated to live single cells using a density-driven automated gating script in RStudio (Figure 74), and down-sampled to 20,000 cells per sample to reduce the computation time associated with extensive data sets.

Dimensionality reduction with t-distributed stochastic neighbour embedding (tSNE) and unsupervised cell clustering with PhenoGraph was implemented using the Cytofkit package in RStudio. PhenoGraph divided the cells into 21 clusters. A set of tSNE maps for individual samples did not show any apparent differences between DRE GAD65 autoantibody-positive patients, SFE patients or healthy controls (Figure 75).

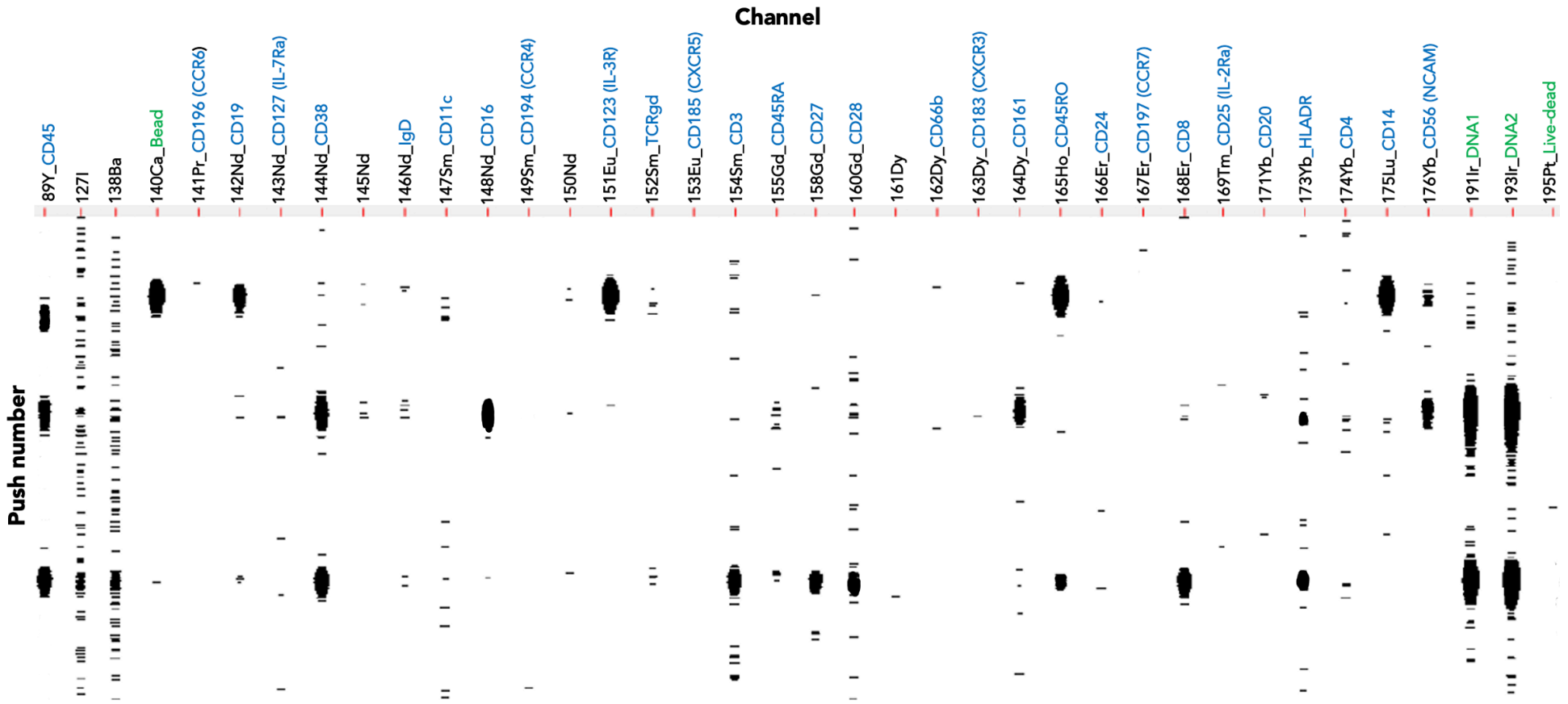


Figure 71: Rain plot of live detector signal

Raw data acquisition (healthy control PBMCs) provided a crude indication of cell phenotype. Speckling in channels denoted individual soluble ions striking the detector, whereas darker clouds were produced by cells or nanoparticles. The first event (top row of signals) represented a normalisation bead which lacks DNA signal. The second event (middle row) was characterised by signal for CD45, CD38, CD16, CD161, CD56 and DNA, representing a natural killer cell. The third event (bottom row) was positive for CD45, CD38, CD3, CD27, CD28, CD45RO, CD8, HLADR and DNA, indicating a CD8+ T cell. Traces from environmental iodine and barium were observed in the second and third channels from the left.

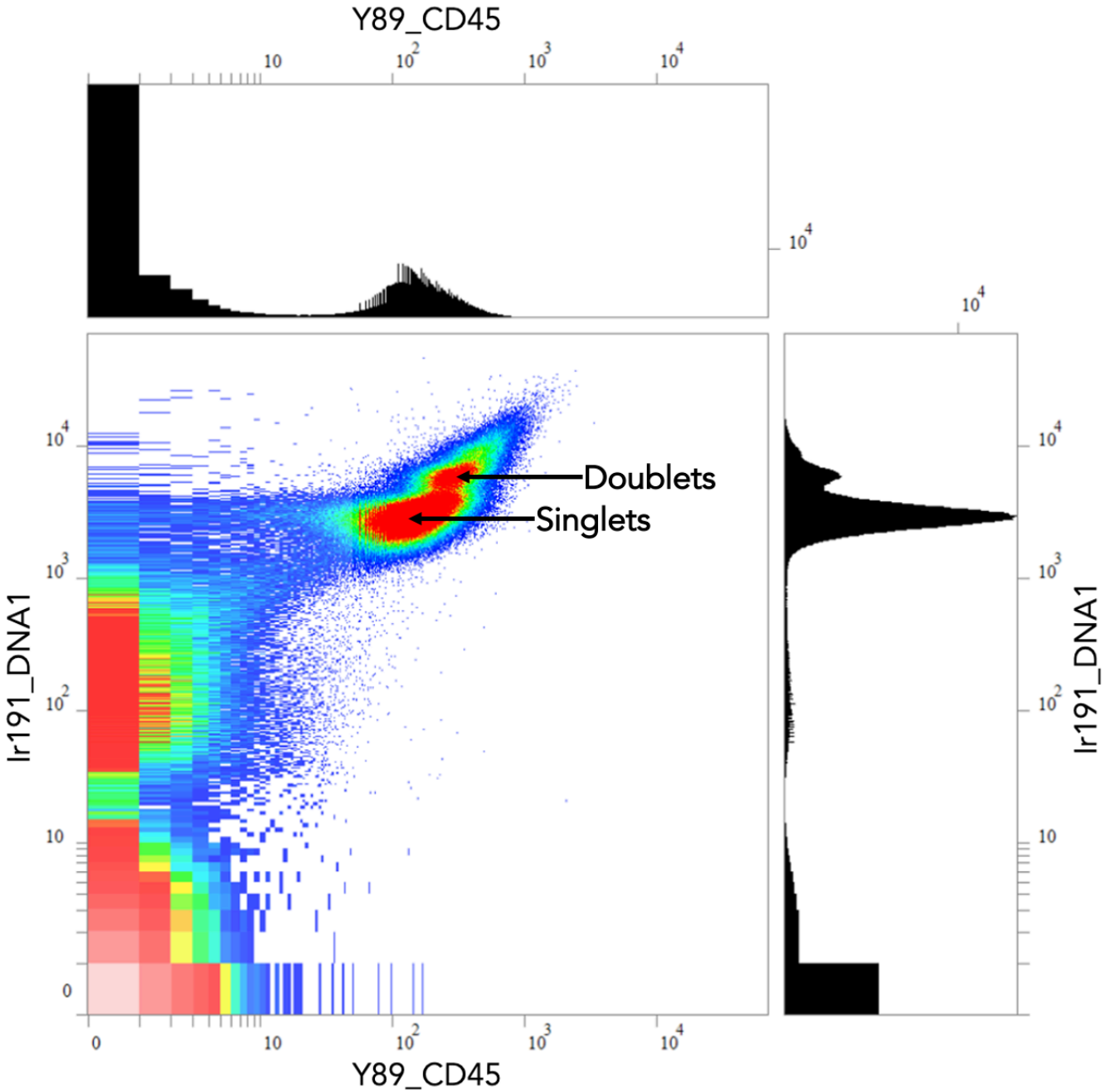


Figure 72: Live plot of captured events
A live plot with gating for CD45 and DNA allowed monitoring of acquisition. CD45+ DNA+ events were immune cells of interest. The two DNA peaks within this population were due to singlets and doublets.

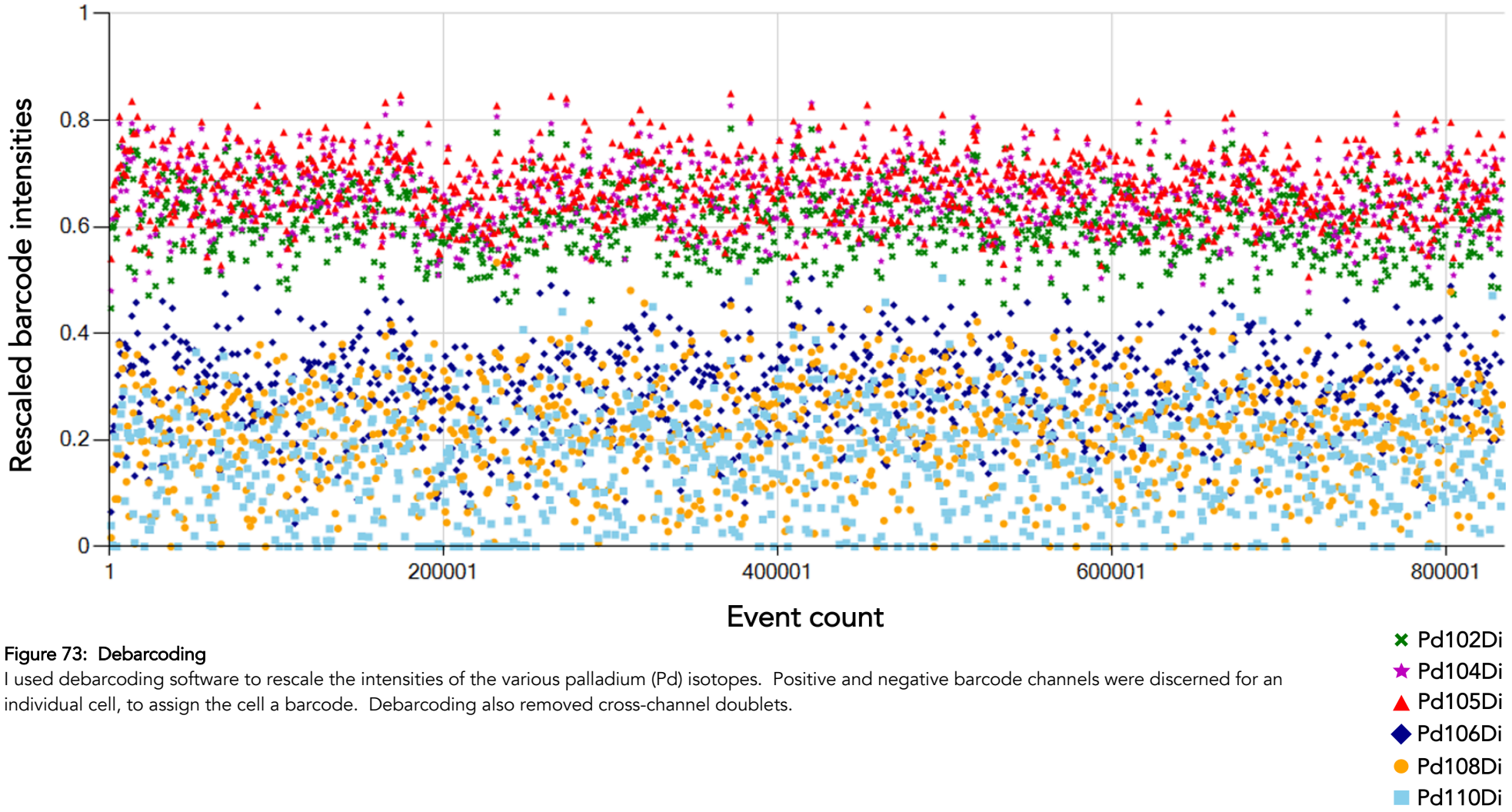


Figure 73: Debarcoding

I used debarcoding software to rescale the intensities of the various palladium (Pd) isotopes. Positive and negative barcode channels were discerned for an individual cell, to assign the cell a barcode. Debarcoding also removed cross-channel doublets.

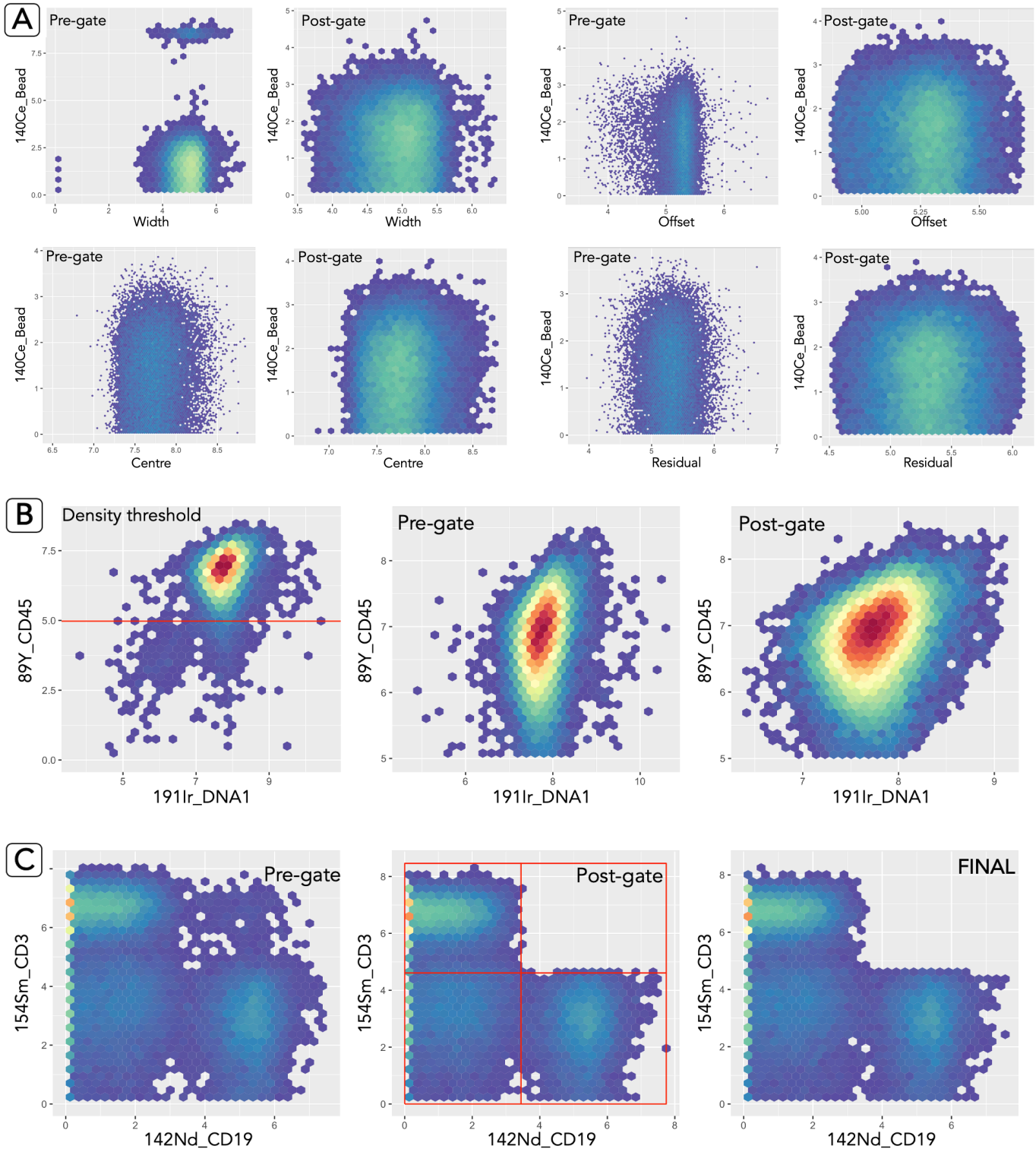


Figure 74: Gating strategy for singlets

Data ArcSinh-transformed. Normalisation beads, debris and doublets were gated out based on the distribution of events across an axis. Gates were automatically assigned to select regions of highest density corresponding to the main cell population. **(A):** Clean-up with Gaussian parameters (width, offset, centre and residual). **(B):** DNA and CD45 gate for immune cells (red line = density cut-off). **(C):** CD3 and CD19 gate for singlets. CD19-positive CD3-negative cells (B cells), CD19-negative CD3-positive cells (T cells), and CD19-negative CD3-negative cells (other immune cells) were taken forward for analysis.

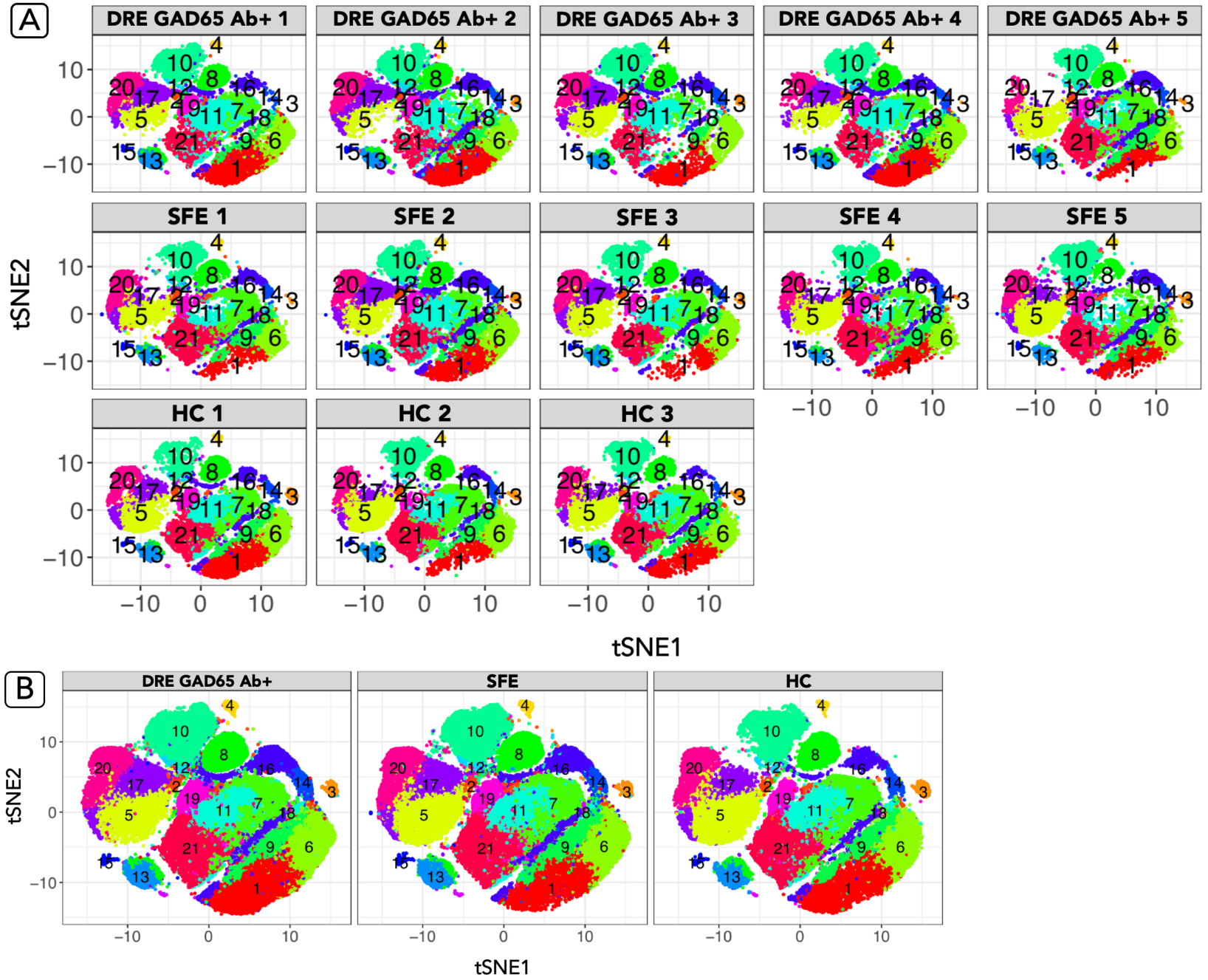


Figure 75: tSNE maps for individuals and patient groups
Two-dimensional visual representation of single-cell data generated by tSNE for basic qualitative assessment only. The x and y axes correspond to tSNE1 and tSNE2 dimensions, respectively. Each cell is plotted as a dot and coloured by 21 PhenoGraph-derived cell clusters. Although cells close to each other are more similar, nothing can be reliably inferred from the distances across white space. Subtle differences in cell populations may not be apparent in this visualisation.
(A): individual patients.
(B): patient groups: DRE GAD65 autoantibody-positive (n=5); age- and sex-matched autoantibody-negative SFE (n=5); and autoantibody-negative healthy controls (n=3). No marked differences in cell clusters were consistently observed between patients within a group or between groups. *Ab-*, antibody-negative; *Ab+*, antibody-positive; *DRE*, drug-resistant epilepsy; *GAD56*, glutamic acid decarboxylase 65; *HC*, healthy control; *SFE*, seizure-free epilepsy; and *tSNE*, t-distributed stochastic neighbour embedding.

I used patterns of median marker expression to identify the likely predominant cell type within most clusters (**Figure 76**). A tSNE map for aggregated data showed good separation of cell populations (**Figure 77**).

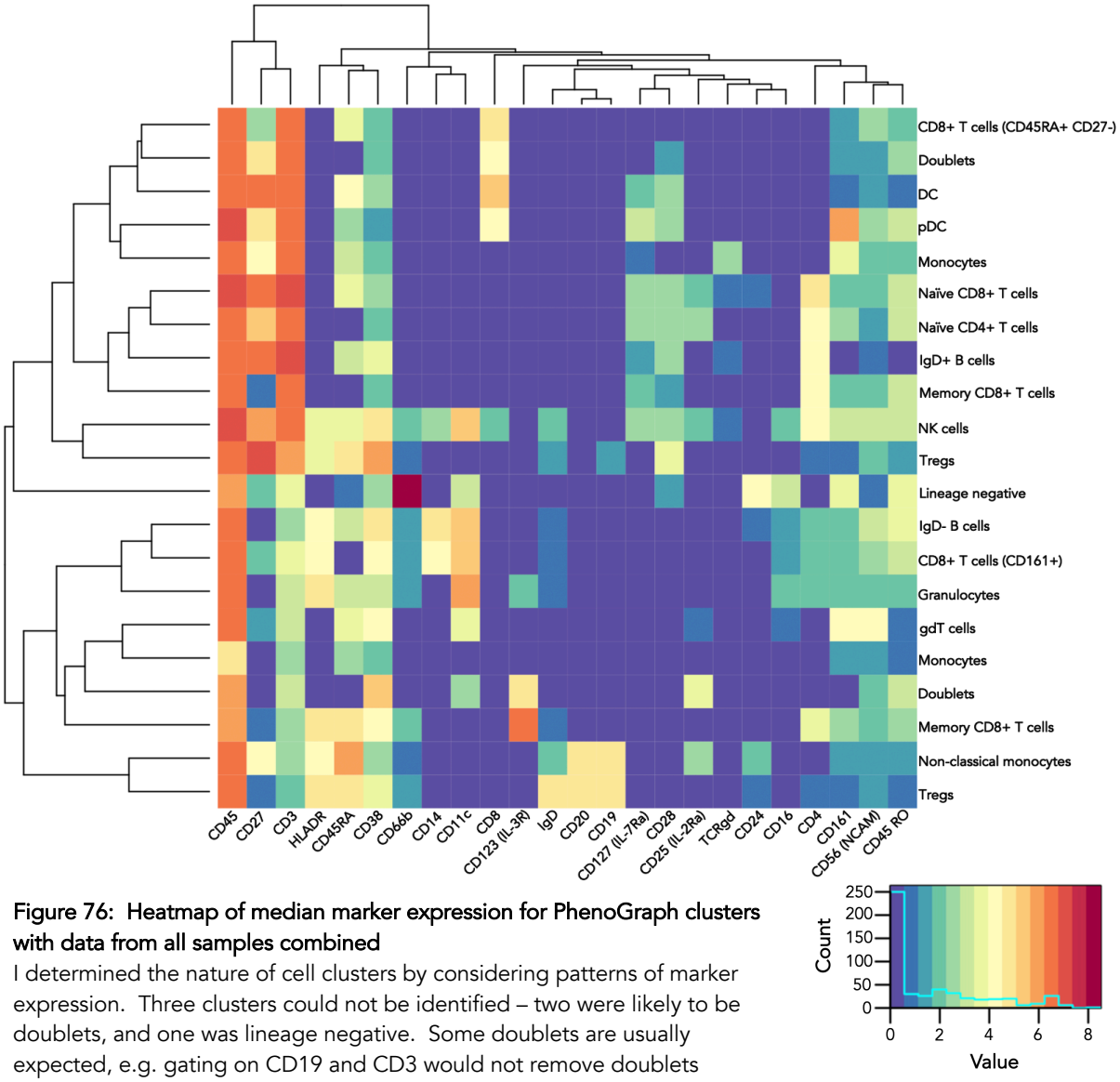


Figure 76: Heatmap of median marker expression for PhenoGraph clusters with data from all samples combined

I determined the nature of cell clusters by considering patterns of marker expression. Three clusters could not be identified – two were likely to be doublets, and one was lineage negative. Some doublets are usually expected, e.g. gating on CD19 and CD3 would not remove doublets comprising monocytes and T cells. Lineage negative cells could have lost markers during the experiment or may have been mixed cell populations incorrectly grouped as a result of suboptimal clustering. The nature of the lineage negative cells could still be resolved by further clustering iterations with PhenoGraph or alternative algorithms. *DC*, dendritic cells; *gdT* cells, gamma-delta T cells; *IgD*, immunoglobulin D; *NK* cells, natural killer cells; *pDC*, plasmacytoid dendritic cells; and *Tregs*, regulatory T cells.

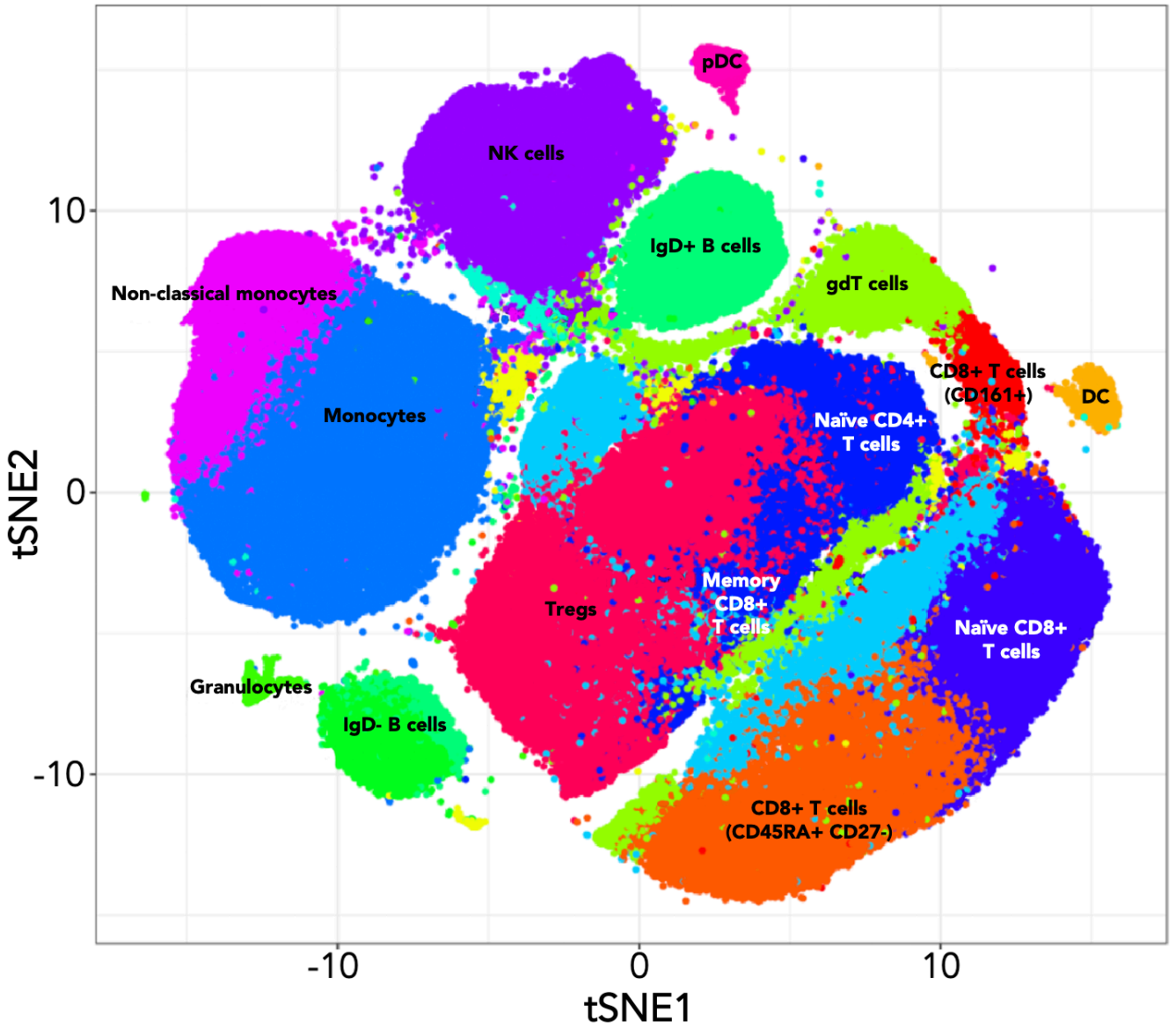


Figure 77: tSNE map with data from all samples combined

Coloured by PhenoGraph clusters and re-labelled with identified cell types. The cell clusters generated by PhenoGraph were well separated by tSNE in this case, making it more likely that clustering algorithms may accurately identify at least some of these subpopulations. *DC*, dendritic cells; *gdT* cells, gamma-delta T cells; *IgD*, immunoglobulin D; *NK* cells, natural killer cells; *pDC*, plasmacytoid dendritic cells; *Tregs*, regulatory T cells; and *tSNE*, t-distributed stochastic neighbour embedding.

Further tSNE maps overlaid with expression profiles for T cells (**Figure 78**), B cells (**Figure 79**), and dendritic cells, monocytes and natural killer cells (**Figure 80**) showed good separation of cell types.

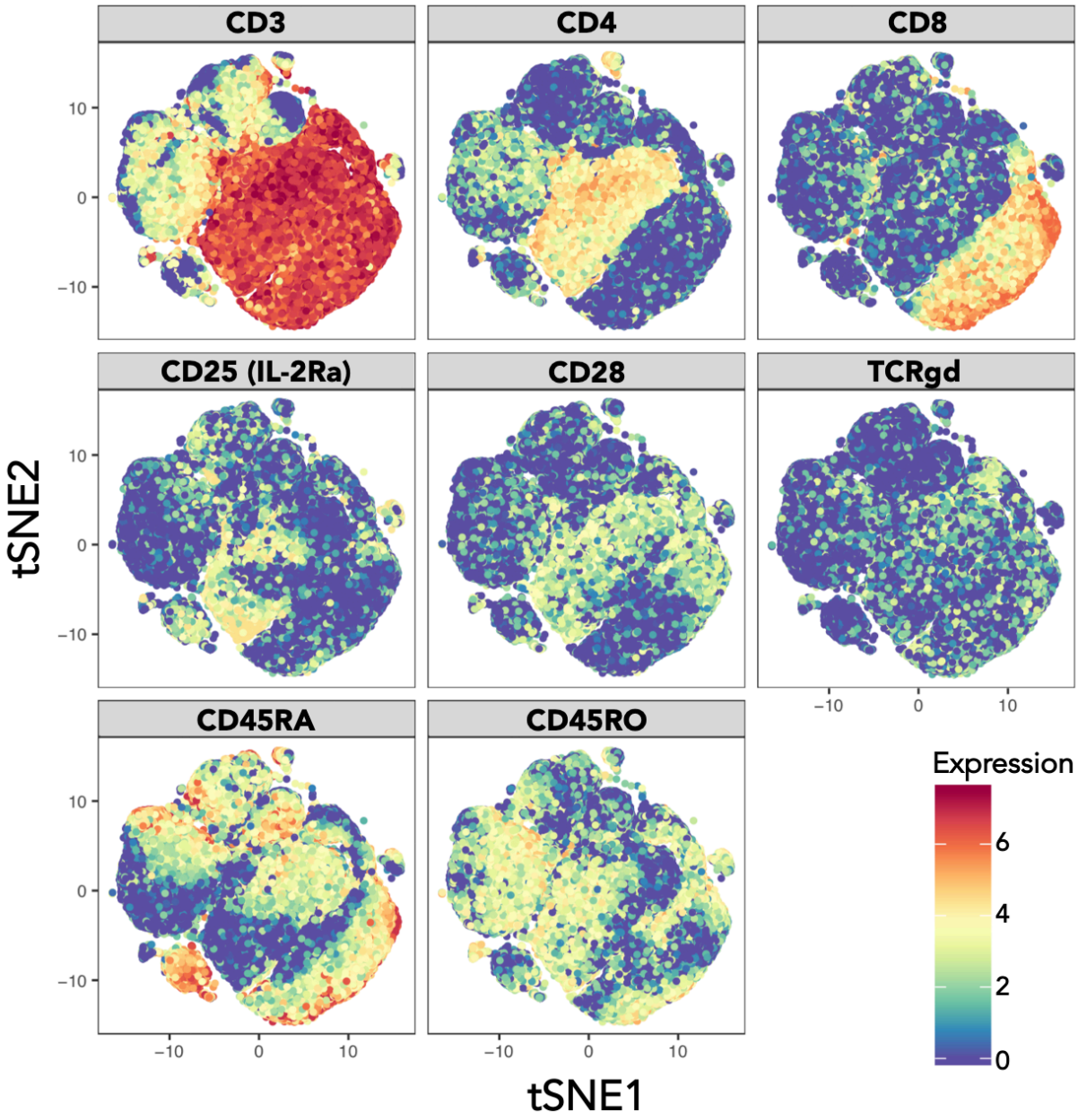


Figure 78: T cell marker expression profiles overlayed on tSNE plot with data from all samples combined
The T cell markers separated well by tSNE, suggesting that differences in cell populations may be genuine. *tSNE*, t-distributed stochastic neighbour embedding.

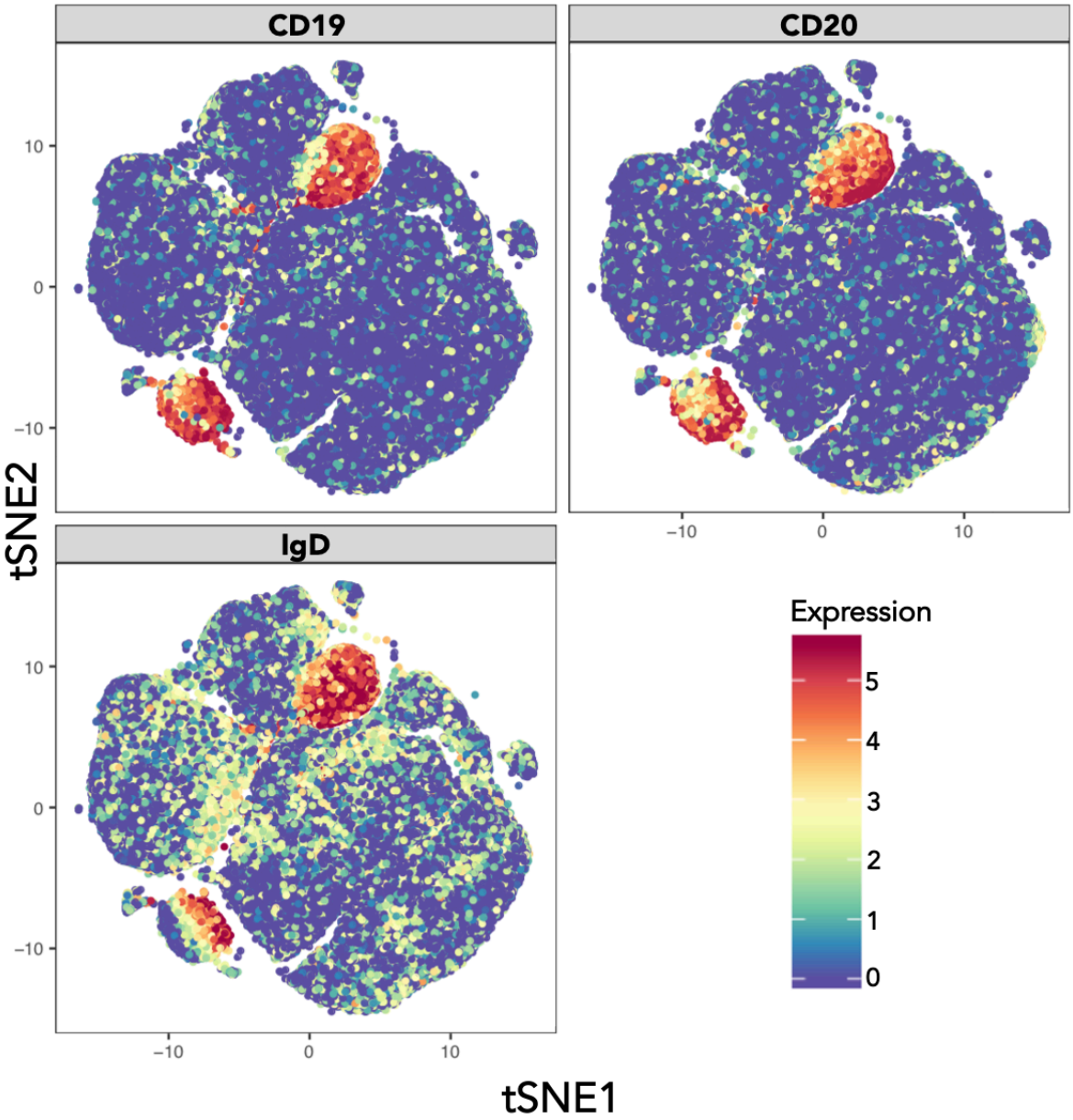


Figure 79: B cell marker expression profiles overlayed on tSNE plot with data from all samples combined
Cell populations expressing CD19, CD20 and IgD (B cell markers) form discrete islands. *tSNE*, t-distributed stochastic neighbour embedding.

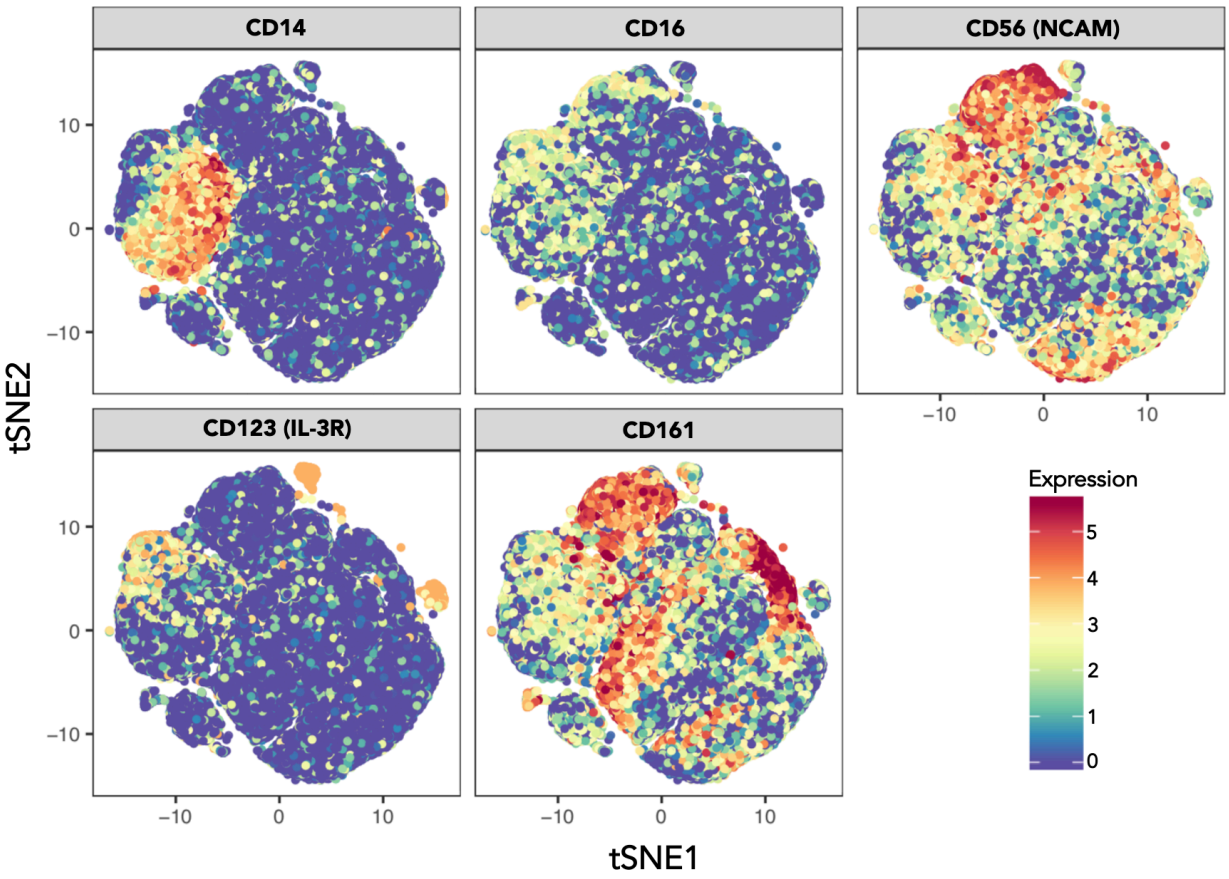
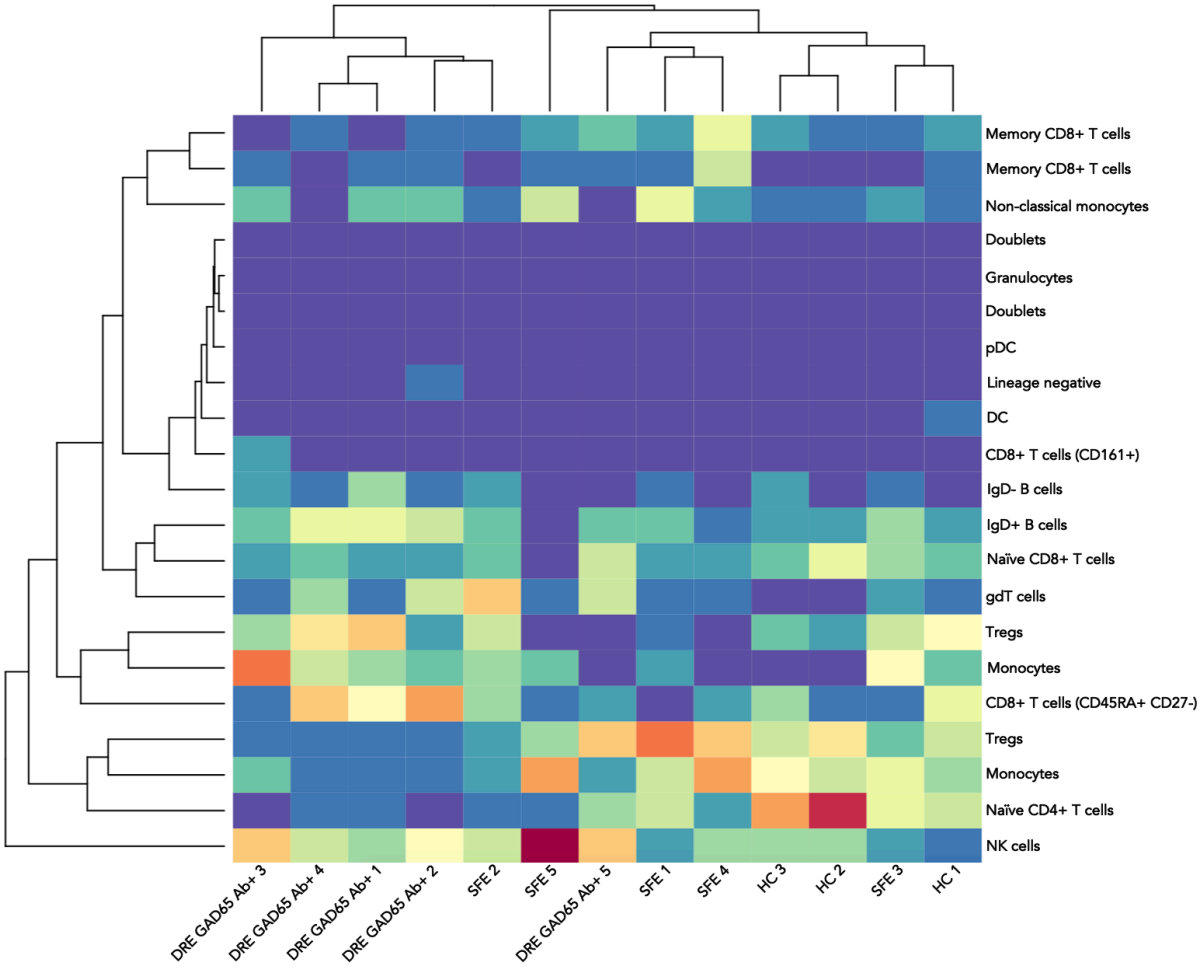


Figure 80: Dendritic cell, monocytes and natural killer cell expression profiles overlayed on tSNE plot with data from all samples combined
Cells expressing these markers also form well defined islands. *tSNE*, t-distributed stochastic neighbour embedding.

The abundance of cell subtypes within PhenoGraph clusters according to individual patients did not reveal any apparent trends (**Figure 81**). Hierarchical clustering did not distinguish between all DRE GAD65 Ab+, SFE and HC patients at a global level but the four DRE GAD56 Ab+ patients with the highest endpoint titres appeared to group together, more locally.

When analysed by patient groups, NK cells and IgD+ B cells (unswitched memory B cells) appeared more abundant in DRE GAD65 Ab+ patients compared to controls (**Figure 82**).



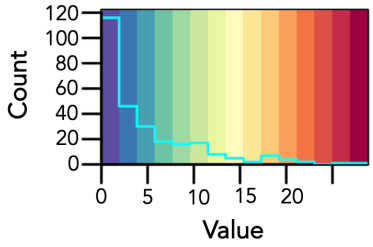
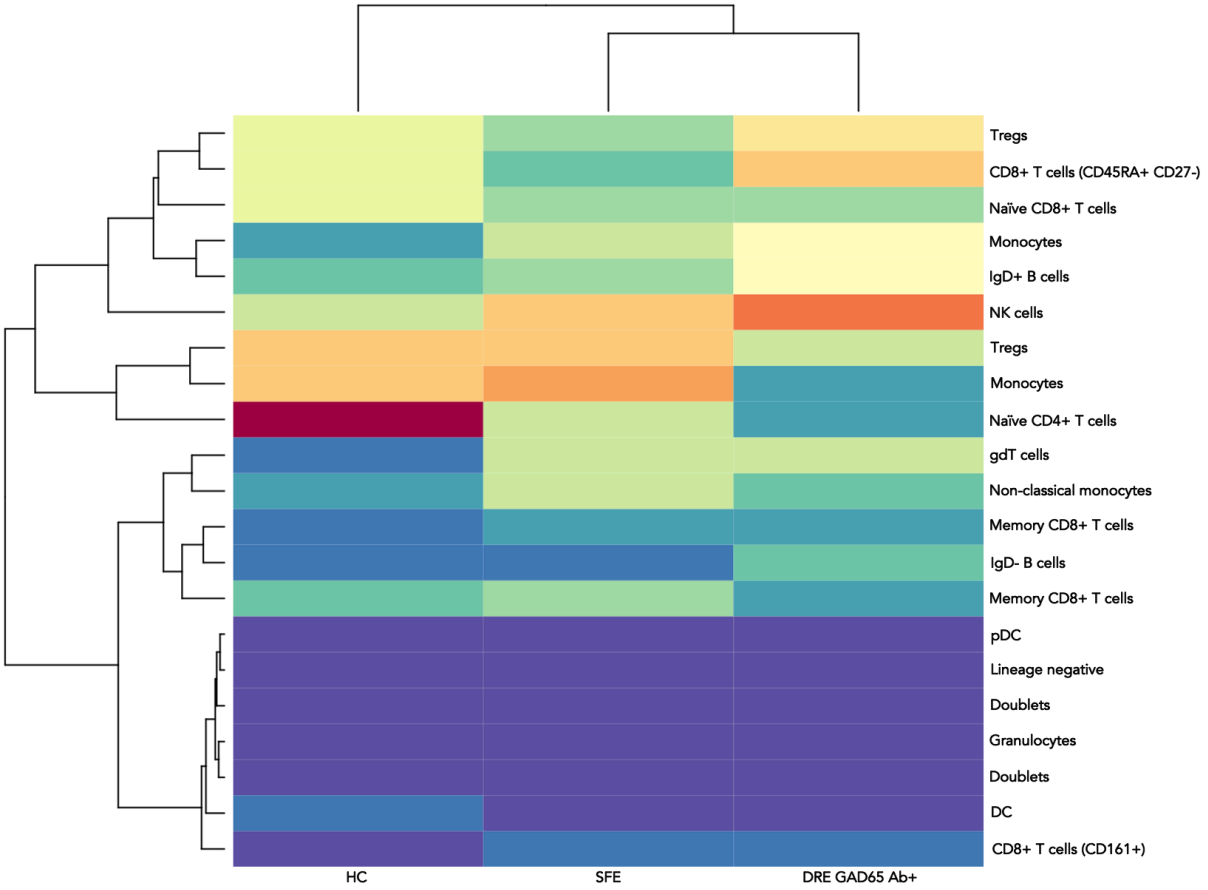


Figure 81: Heatmap showing the abundance of cell subtypes within each PhenoGraph cluster according to 13 individual samples
No distinct trends were observed between patient groups. Hierarchical clustering (dendrogram) did not distinguish between all DRE GAD65 Ab+, SFE and HC patients at a global level. However, the four DRE GAD65 Ab+ patients with the highest endpoint titres grouped together locally. Endpoint titres (expressed as dilution factors): DRE GAD65 Ab+ patient 1 (409,600), patients 2-4 (25,600) and patient 5 (6,400). *Ab+*, antibody-positive; *DC*, dendritic cells; *DRE*, drug-resistant epilepsy; *GAD56*, glutamic acid decarboxylase 65; *gdT* cells, gamma-delta T cells; *HC*, healthy control; *IgD*, immunoglobulin D; *NK* cells, natural killer cells; *pDC*, plasmacytoid dendritic cells; *SFE*, seizure-free epilepsy; and *Tregs*, regulatory T cells.



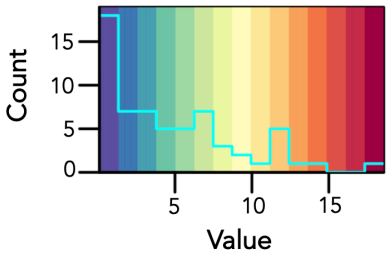


Figure 82: Heatmap showing the abundance of cell subtypes within each PhenoGraph cluster according to three patient groups
The heatmap suggested a difference in the abundance of cells in specific clusters for DRE GAD65 Ab+ patients compared to SFE and HCs. For example, NK cells and IgD+ B cells (unswitched memory B cells) appeared more abundant in DRE GAD65 Ab+ samples. *Ab+*, antibody-positive; *DC*, dendritic cells; *DRE*, drug-resistant epilepsy; *GAD56*, glutamic acid decarboxylase 65; *gdT* cells, gamma-delta T cells; *HC*, healthy control; *IgD*, immunoglobulin D; *NK* cells, natural killer cells; *pDC*, plasmacytoid dendritic cells; *SFE*, seizure-free epilepsy; and *Tregs*, regulatory T cells.

Marker expression histograms for the three patient groups were broadly similar across all samples within each group (**Figure 83**, **Figure 84** and **Figure 85**).

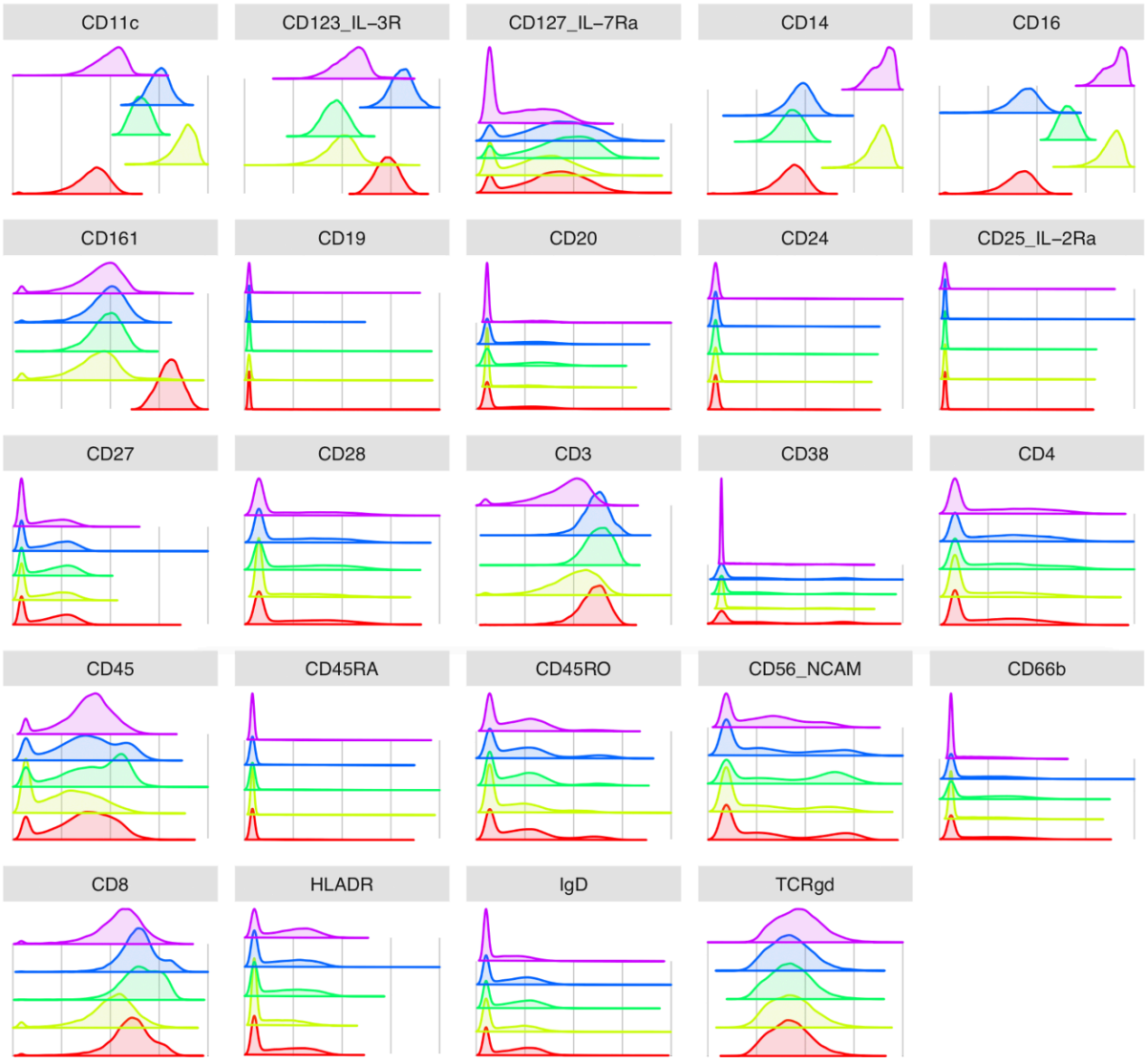


Figure 83: Marker expression histogram for five GAD65 Ab-positive patients

Each histogram shows a measure of signal intensity on the x-axis for a different marker and events at the far left have an intensity of zero. The height of the curve on the y-axis corresponds to the fraction of the cell population at the given intensity. The expression profiles were broadly similar across the five DRE GAD65 Ab+ samples, and no differences seemed to correspond to antibody endpoint titres (shown in the key in grey). *Ab+*, antibody-positive; *DRE*, drug-resistant epilepsy; *EPT*, endpoint titre; and *GAD56*, glutamic acid decarboxylase 65.

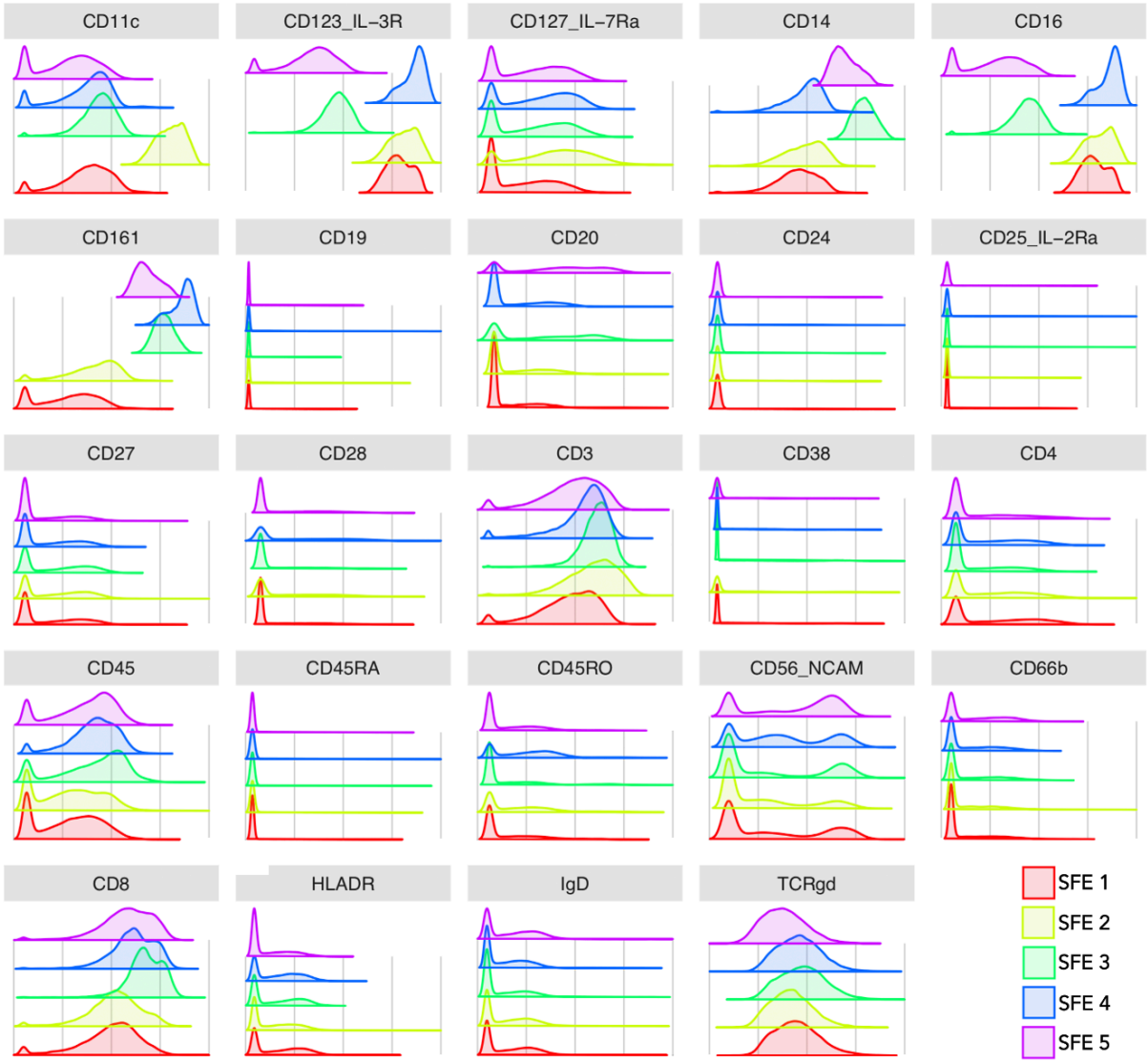


Figure 84: Marker expression histogram for five SFE patients

The expression profiles appeared broadly similar across the five SFE samples. *SFE*, seizure-free epilepsy.

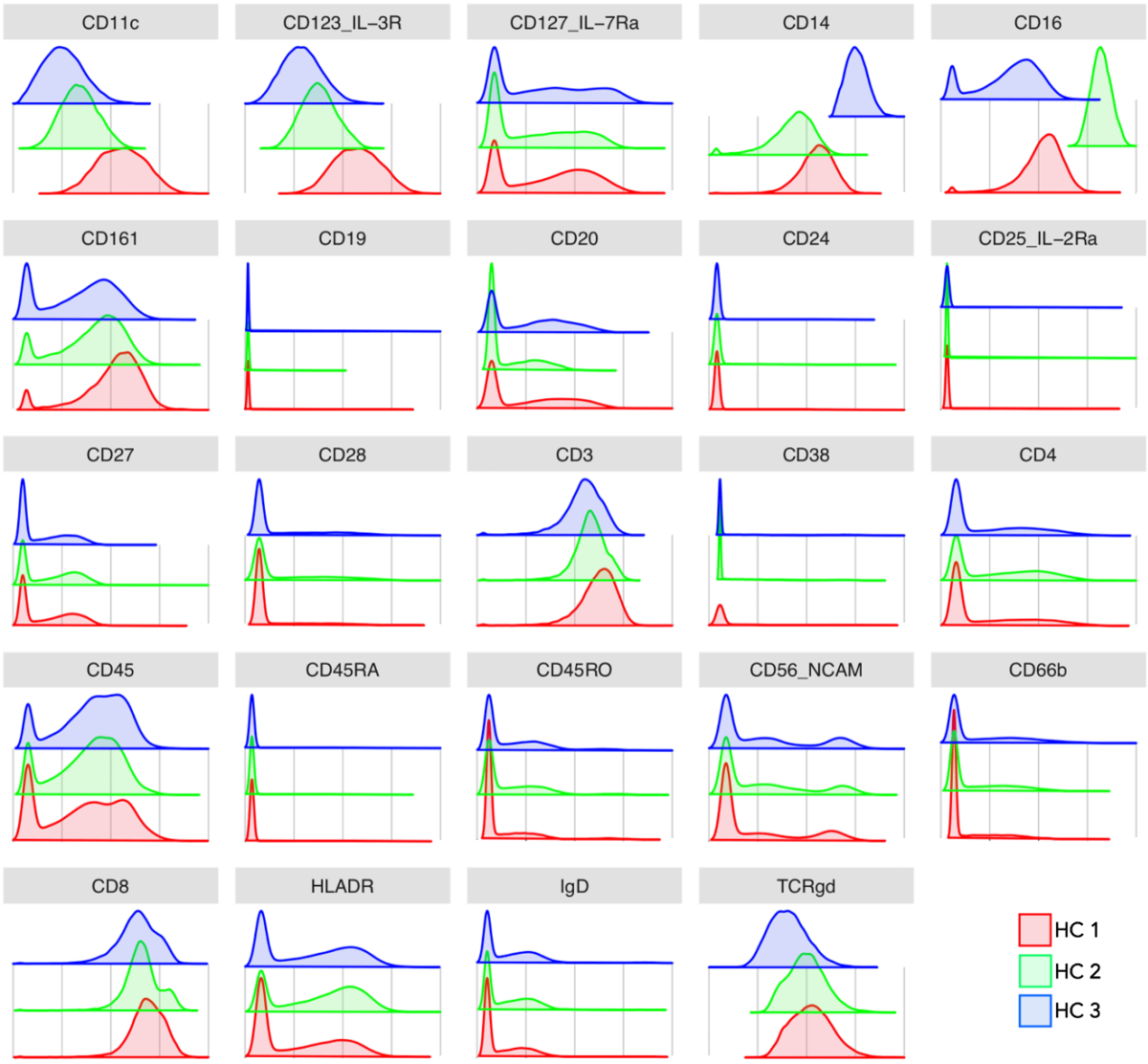


Figure 85: Marker expression histogram for three healthy controls

The expression profiles were broadly similar across the three samples. *HC*, healthy control.

5.6 Batch controls

I assessed the technical control sample included in each batch, a key control which is rarely undertaken in CyTOF experiments.[351] Comparison of tSNE maps for the individual batch controls did not show any noticeable differences (**Figure 86**). However, I identified small variations that could represent batch effects – batch 1 on heatmaps of cell abundance (**Figure 87**) and batch 3 on marker expression histograms (**Figure 88**). In addition, a tSNE map coloured by batch suggested predominance by batch control 3 (**Figure 89**). However, data from all batch controls fell in common tSNE regions, meaning that, overall, batch effects were probably minimal.

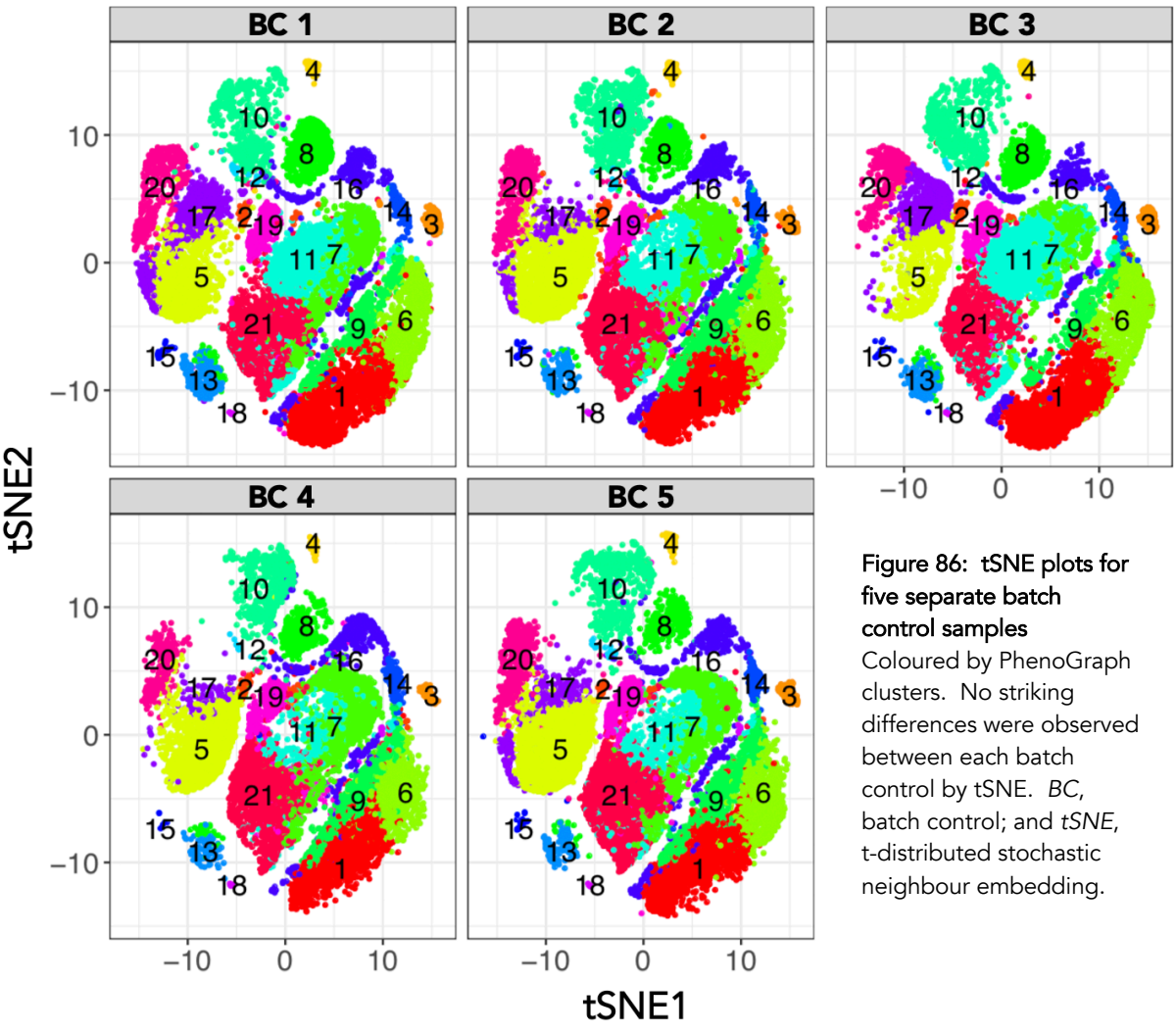


Figure 86: tSNE plots for five separate batch control samples
Coloured by PhenoGraph clusters. No striking differences were observed between each batch control by tSNE. *BC*, batch control; and *tSNE*, t-distributed stochastic neighbour embedding.

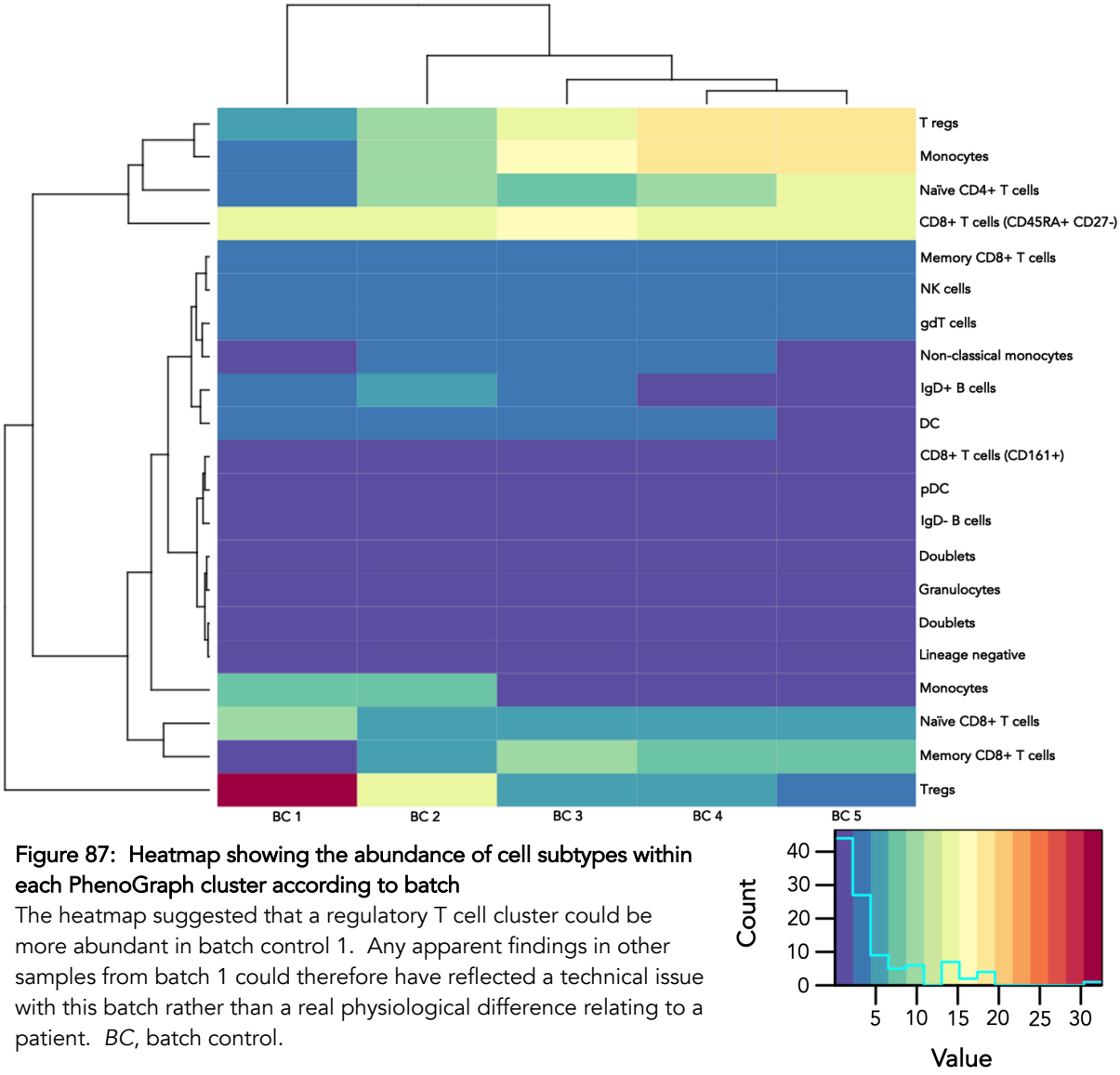


Figure 87: Heatmap showing the abundance of cell subtypes within each PhenoGraph cluster according to batch

The heatmap suggested that a regulatory T cell cluster could be more abundant in batch control 1. Any apparent findings in other samples from batch 1 could therefore have reflected a technical issue with this batch rather than a real physiological difference relating to a patient. *BC*, batch control.

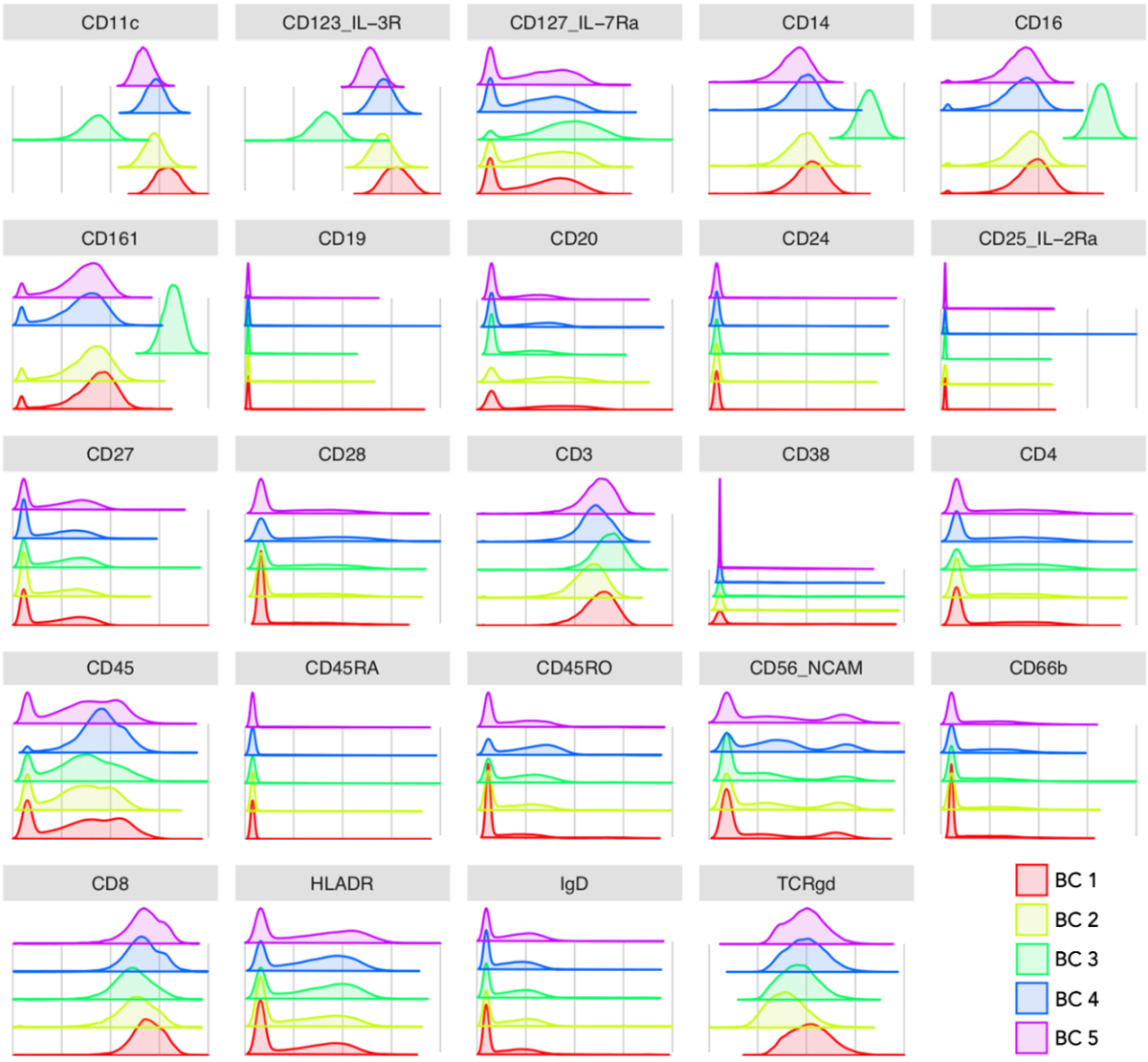


Figure 88: Marker expression histograms for five inter-batch controls

Batch control 3 showed different expression profiles for CD11c, CD123, CD14, CD16 and CD161. The cause of this was not known. Any apparent findings in other samples from batch 3 could therefore have indicated a technical problem with this batch rather than a valid biological variation. *BC*, batch control.

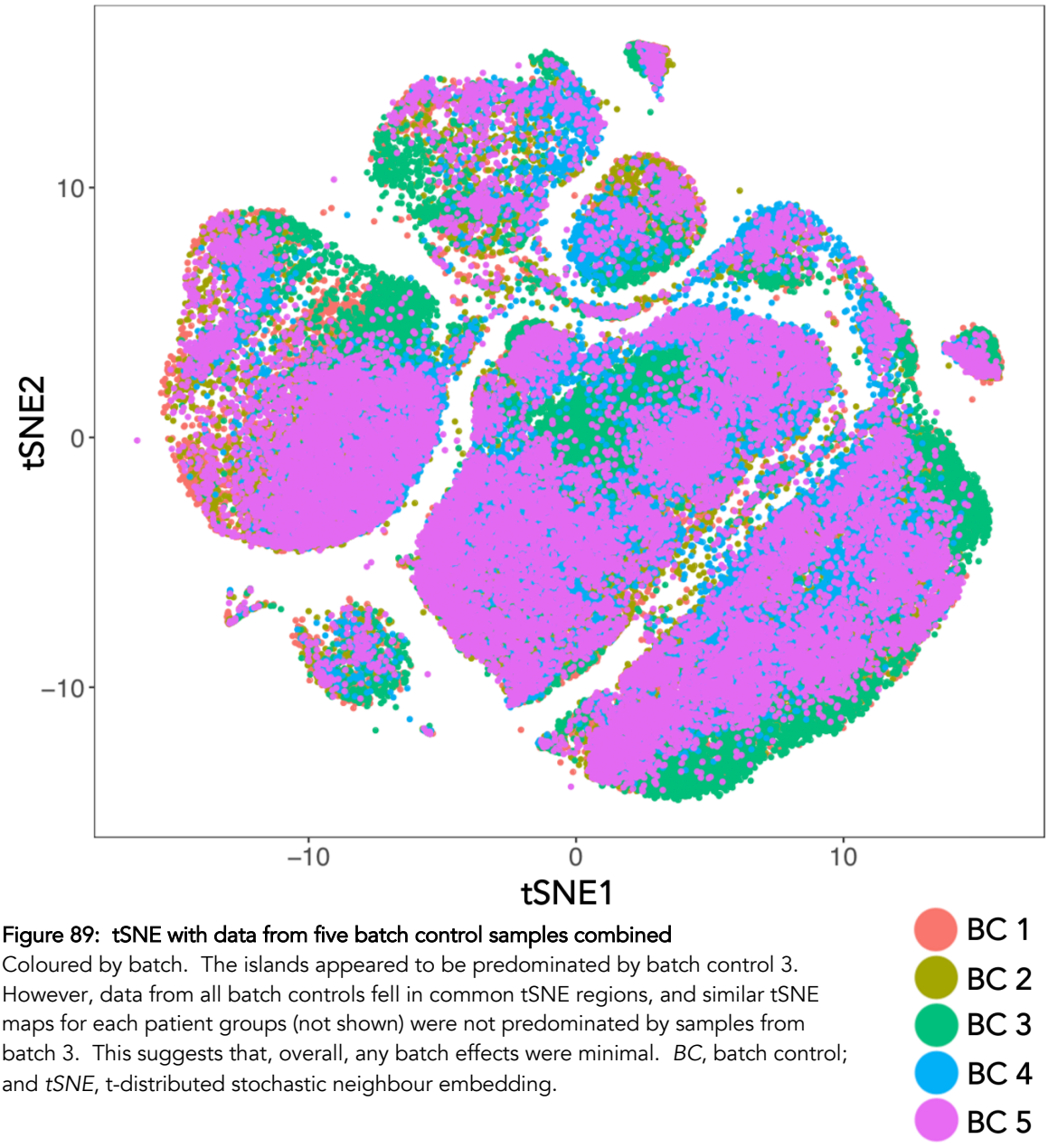


Figure 89: tSNE with data from five batch control samples combined
Coloured by batch. The islands appeared to be predominated by batch control 3. However, data from all batch controls fell in common tSNE regions, and similar tSNE maps for each patient groups (not shown) were not predominated by samples from batch 3. This suggests that, overall, any batch effects were minimal. *BC*, batch control; and *tSNE*, t-distributed stochastic neighbour embedding.

5.7 Summary

Principal component analysis of plasma cytokine measurements suggested that the GAD65 autoantibody-positive patient group were enriched for five cytokines (IL1b, IL4, IL10, IL15 and TNFa) compared to patients with autoimmune encephalitis, autoantibody-negative DRE, neuronal surface antibody-positive DRE and SFE.

I demonstrated an effective mass cytometry workflow, from antibody staining to data clean-up. In the first round of analysis, tSNE maps produced good separation of cell islands, which correlated well with PhenoGraph generated cell clusters. This suggests that the analysis pipeline is capable of accurately detecting cell populations. Patterns of marker expression allowed identification of the cellular phenotype for 18/21 cell clusters. Hierarchical clustering on cell type abundance did not distinguish between all 13 patients, but the four DRE GAD65 autoantibody-positive patients with the highest endpoint titres grouped together locally. NK cells, CD8+ T cells (CD45RA+ and CD27-), IgD+ B cells, and one regulatory T cell subset were more abundant among the GAD65 antibody-positive DRE patients compared to SFE patients and healthy controls. The latter three populations have not been fully characterised. Further iterations of clustering may reallocate these cells to other populations or they could represent candidate novel populations.

These results are contextualised and discussed in Chapter 6.

Chapter 6 Discussion

6.1 Summary of key findings

6.1.1 Autoantibody prevalence in epilepsy

The overall prevalence of specific serum autoantibodies in epilepsy patients was 42/479 (8.8%). High endpoint titre (EPT) glutamic acid decarboxylase-65 (GAD65) autoantibodies were present only in a small number of individuals with drug-resistant epilepsy (DRE). Five new-onset focal epilepsy (NOFE) patients and 23 DRE patients demonstrated surface reactivity against cultured neurons and astrocytes, potentially indicative of novel autoantibodies.

6.1.2 Autoantibodies in epilepsy over time

Autoantibody status did not predict clinical outcome or correlate with a range of clinical features for 13 NOFE patients who enrolled in our second study, approximately three years later. None became seropositive for GAD65 autoantibodies.

Seven DRE patients with high EPT GAD65 autoantibodies remained seropositive during serial follow-up over 1-2 years. EPTs for individuals generally persisted at the same order of magnitude throughout this period.

Our DRE study was intended to longitudinally examine autoantibody status for the whole patient cohort. Unfortunately, the COVID-19 pandemic halted patient recruitment and lab

work and, consequently, only samples from the first of six visits for each patient have been tested for the full battery of autoantibodies.

6.1.3 Clinical features predictive of autoantibody status in new-onset focal epilepsy

Our multivariate regression model identified ictal piloerection, low mood and MRI limbic system changes – but not cognitive impairment or movement disorders – as predictive clinical factors of positive neuronal surface-directed antibody (NSA) status in NOFE. This model was more sensitive and specific for predicting NSA-seropositivity in patients with isolated epilepsy (i.e., without autoimmune encephalitis) than the published Antibody Prevalence in Epilepsy and Encephalopathy (APE2) score.[283] Of those with NSAs and isolated epilepsy, almost all were treated solely with anti-seizure medications (ASMs) and 11/16 (68.8%) were asymptomatic at 3-year follow-up.

6.1.4 Clinical phenotype of GAD65 autoantibody-associated epilepsy

Of seven high EPT GAD65 autoantibody-positive patients, all had DRE and were female, with a median age at epilepsy onset of 20 years. Five had temporal lobe epilepsy, three had type I diabetes mellitus (TIDM) with adult-onset epilepsy and two had bilateral hippocampal sclerosis. Three reported pain as a seizure trigger. None received immunotherapy. Compared to autoantibody-negative DRE patients, they had similar duration of epilepsy but less frequent seizures, fewer lifetime generalised tonic-clonic seizures and trialled fewer ASMs.

6.1.5 Development of a novel GAD65 antibody cell-based assay

I developed a novel permeabilised cell-based assay (CBA) for the detection of GAD65 IgG autoantibodies which demonstrated good inter-rater performance and performed well compared to commercial GAD65 antibody radioimmunoprecipitation assay (RIPA) and enzyme-linked immunosorbent assay (ELISA). Pilot serum screening for GAD65 IgM autoantibodies in a small group of GAD65 IgG-positive subjects was negative.

6.1.6 Plasma cytokines in epilepsy

Analysis of concentrations of 13 plasma cytokines suggested GAD65 autoantibody-positive patients show enrichment for IL1b, IL4, IL10, IL15 and TNFa relative to patients with autoimmune encephalitis (AIE), autoantibody-negative DRE, NSA-positive DRE and seizure-free epilepsy (SFE).

6.1.7 Immunocellular phenotype of GAD65 autoantibody-positive DRE

Mass cytometry of peripheral blood mononuclear cells (PBMCs) was undertaken. Hierarchical clustering showed local grouping of DRE GAD65 Ab-positive patients with the highest EPTs, in whom natural killer cells, CD8-positive T cells (CD45RA+ and CD27-), IgD-positive B cells, and a regulatory T cell subset were more abundant compared to SFE patients and healthy controls.

6.2 Interpretation and context

6.2.1 Autoantibody prevalence in epilepsy

A literature review of adult epilepsy studies screening for multiple autoantibodies identified 17 papers, with a median autoantibody prevalence of 20.8% (range 3–76.5%, **Table 44**). So that our findings would be relevant to the general population of people with epilepsy, we recruited consecutive outpatients from epilepsy clinics. As the majority of people attending epilepsy clinics respond at least partially to conventional ASMs and do not have a history of AIE, it was improbable that we would find an autoantibody frequency at the higher end of the published range. Our relatively low observed frequency of 8.8% is likely explained by different methodological approaches. For example, the recruitment of hospital inpatients, as illustrated by Dubey et al., 2017[61], can enrich a cohort for acute symptomatic seizures, paraneoplastic conditions, refractory status epilepticus (including new onset refractory status epilepticus (NORSE) and acute psychiatric illnesses. Such presentations are more commonly autoantibody-mediated than isolated seizures. Studies which recruit from clinical or research registries (e.g. Ansari et al., 2019[352] and Bien et al., 2007[353]) can demonstrate considerable ascertainment bias if potential participants have already been filtered by clinical suspicion of autoimmunity. Retrospective patient enrolment (e.g. Dubey et al., 2015[63] and Majoie et al., 2006[117]) is more likely to introduce sources of bias. Compared to MRI and EEG, autoantibody testing does not constitute routine practice in most epilepsy clinics and so autoantibody-mediated isolated epilepsy may go unrecognised, with patients characterised as having epilepsy of unknown cause. It follows, therefore, that excluding patients with apparently established epilepsy aetiologies could augment the ratio of

antibody positive-to-negative findings, (for example, Bozzetti et al., 2020;[112] and Tecellioglu et al., 2018[354]).

The field of autoimmune neurology has advanced rapidly in recent years and – compared to more long-established neurology research fields including stroke, multiple sclerosis or Parkinson's disease – there is perhaps more variation in how studies are conducted. The number of antibodies included in a screening panel, their likely clinical relevance in epilepsy, the specificity/sensitivity of the assays used for testing, and the cut-offs applied to results are variables worth considering when evaluating autoantibody prevalence rates from different epilepsy studies. VGKCc antibodies, for instance, are now known to be clinically immaterial when not accompanied by antibodies against a specific antigen such as CASPR2 or LGI1, and can be present in healthy individuals.[65,143] We therefore did not test for VGKC antibodies in our study, but others have conveyed so-called 'double-negative' VGKC antibodies as positive findings, (e.g., Tecellioglu et al., 2018;[354] Gozubatik-Celik et al., 2017;[125] and Dubey et al., 2017[61]). The inclusion of anti-thyroid peroxidase, anti-nuclear antigens, anti-phospholipid, anti-cardiolipin and DNA antibodies – not usually germane to epilepsy but commonly detected at low levels in the healthy population[355–359] – can similarly inflate reported autoantibody prevalence figures, as can the inclusion of paraneoplastic antibodies. We did not include testing for these antibodies in our study. We may have encountered a lower rate of false positive results for NSAs due to the use of live CBAs, which have greater sensitivity and specificity than many of the detection methods in more widespread use.[202,203]

The significance of autoantibodies in isolated epilepsy is not clear. Notwithstanding the phenomenon of 'phenotype spread' – where an erstwhile well-defined clinical syndrome associated with a particular autoantibody broadens over time – the detection of DPPX autoantibodies in one of the DRE patients who lacks the core gastrointestinal and cognitive features usually coupled with these antibodies, is surprising.

We did not discover high-titre GAD65 autoantibodies in any new-onset epilepsy patients. This is in keeping with the findings of Von Podewils et al., 2017,[111] where 0/66 new-onset cases were GAD65 autoantibody-positive. Although there are some reports of GAD65 autoantibodies in new-onset epilepsy, these are difficult to interpret. For example, Zelano et al., 2019,[360] detected GAD65 antibody positivity in 1/21 epilepsy patients but did not publish an antibody titre or a description of the result as high or low; Brenner et al., 2013,[281] found "elevated" GAD65 autoantibodies in 3/181 subjects measuring >100 units/ml by RIPA; and Dubey et al., 2017,[61] recorded 4/13 patients with GAD65 autoantibodies >20 nmol/L (some of whom probably had acute AIE). Malter et al., 2010,[174] described 9/53 adults with new-onset epilepsy and high-titre GAD65 autoantibodies in the range of 1,798–12,030 unit/ml by RIPA but all, in fact, had GAD65 antibody limbic encephalitis. If high-titre GAD65 autoantibodies are genuinely absent in new-onset epilepsy, a possible interpretation is that they are a biomarker of chronic seizure-related neuronal damage rather than directly pathogenic.

Our observed prevalence of high-titre GAD65 autoantibodies in DRE was 7/479 (1.5%). This was significant compared to the NOFE group (0/219; p=0.006, Fisher's exact test). A

review of screening studies reporting "high-titre" GAD65 autoantibodies in adults with epilepsy found a mean prevalence of 8.8% (median 3.2%, range 0–41.7%, Table 45). It is not possible to make direct comparisons to these studies due to varying antibody detection methods and thresholds, with six studies omitting all details of assay cut-offs. Nevertheless, high-titre GAD65 autoantibodies do not seem to be common in isolated epilepsy and our observed frequency is within the published range.

We identified patient serum with surface reactivity to cultured neurons and astrocytes that lacked specific NSAs. Although potentially consistent with autoantibodies other than those tested for within our panel, including novel antibodies, the high number of these results suggests that at least some may be false positives due to non-specific background signal. It may be that neuron- and astrocyte-based assays are more appropriately employed for testing patients with certain clinical phenotypes instead of large cohort screening. No screening studies of large epilepsy cohorts were identified which reported potential novel antibodies using these assays. In isolation, non-specific surface reactivity with neurones would not provide sufficient grounds to justify the risks of trialling immunotherapy in people with epilepsy.

Table 44: Studies screening for multiple autoantibodies in adult epilepsy patients

Studies listed chronologically. There is marked variation in patient inclusion criteria and in the constitution of antibody testing panels. "Specific NSA (OANG)" refers to the panel of NSAs tested in our epilepsy studies (see Chapter 3). *Retrospective enrolment of study participants. *Ab*, antibody; *ACL*, anticardiolipin; *AI*, autoimmune; *ANA*, antinuclear antibodies; *APL*, antiphospholipid; *DRE*, drug-resistant epilepsy; *dsDNA*, double-stranded DNA; *ED*, emergency department; *GAD65*, glutamic acid decarboxylase 65; *GFAP*, glial fibrillary acidic protein; *HS*, hippocampal sclerosis; *IMF*, immunofluorescence; *LE*, limbic encephalitis; *mGluR5*, metabotropic glutamate receptor 5; *MOG*, Myelin Oligodendrocyte Glycoprotein; *MTLE*, mesial temporal lobe epilepsy; *MTS*, mesial temporal sclerosis; *NR*, not reported; *NSA*, neuronal surface-directed antibody; *OANG*, Oxford autoimmune neurology group; *PN*, paraneoplastic; *PNES*, psychogenic non-epileptic seizures; *ssDNA*, single-stranded DNA; *TPO*, thyroid peroxidase; *VGCC*, voltage-gated calcium channels; and *VGKCc*, voltage-gated potassium channel complex.

Study	*Patient cohort*	*Serum Ab tests performed*				*Ab prevalence*
		Specific PN	*Specific NSA (OANG)*	*GAD65*	*Other*	
Bozzetti 2020[12]	Epilepsy of unknown aetiology (n=92)	13	9	Yes	MOG, GFAP	29 (31.5%)
Falip 2020[90]	Seizures or epilepsy with suggestive clinical features of AI aetiology (n=109)	8	6	Yes	N/A	27 (24.8%)
Zelano 2019[360]	First seizure clinic attendees aged >25 "Recruitment was not systematic, and no screening log was kept" (n=44; at one-year follow-up, new-onset epilepsy confirmed in 21)	11	6	Yes	N/A	2 (4.5%) (both confirmed as new-onset epilepsy)
*Ansari 2019**[352]	TLE, aged 15-50 Excluded structural brain lesions; MTS included (n=33)	10	6	Yes	dsDNA, ANA, APL	16 (48.5%)
Elisak 2018[116]	EEG-confirmed TLE of duration >1 year Excluded acute encephalopathy, primary neuroglial tumour and brain metastases (n=163)	10	5	Yes	N/A	8 (4.9%)
Nóbrega Jr 2018[62]	MTLE-HS (n=100)	NR	5	Yes	NR	3 (3%)
Tecellioglu 2018[354]	DRE of unknown cause Excluded structural brain lesions, metabolic abnormalities, proven or suspected genetic syndromes, and malignancy (n=77)	2	N/A	Yes	VGKCc, TPO, ANA, APL ACL	17 (22.1%)

Study	*Patient cohort*	*Serum Ab tests performed*				*Ab prevalence*
		Specific PN	*Specific NSA (OANG)*	*GAD65*	*Other*	
Von Podewils 2017[111]	ED presentation of single seizure or new-onset epilepsy within previous 6 months; aged >55 Excluded history of neoplasia, epileptogenic lesions. Included LE (n=66)	NR	7	Yes	mGluR5, VGKCc	2 (3%)
Gozubatik-Celik 2017[125]	Focal epilepsy of unknown cause (n=94)	NR	5	Yes	VGKCc, VGCC	13 (13.8%)
Dubey 2017[61]	Inpatients & outpatients with new-onset epilepsy & long-standing epilepsy of unknown cause Excluded metabolic abnormality, structural brain lesions; genetic/metabolic syndromes with developmental delay and seizures Included idiopathic MTS (n=112)	11	4	Yes	VGKCc, TPO, muscle AChR, ganglionic AChR	39 (34.8%)
Vanli-Yavuz 2016[110]	MTLE-HS (n=111)	NR	6	Yes	VGKCc	25 (22.5%)
Dubey 2015[*63]	Inpatients with suspected autoimmune epilepsy (n=34)	2	2	Yes	VGKCc, ganglionic AChR	26 (76.5%)
Brenner 2013[281]	Established & new-onset epilepsy Excluded history of alcohol/substance misuse, suspected PNES or progressive neurological disorders (n=416)	NR	5	Yes	VGKCc, VGCC, AChR	46 (11.1%)
Malter 2010[74]	New-onset TLE of unclear aetiology (n=138)	NR	NR	Yes	VGKCc	19 (13.8%)
Bien 2007[*353]	TLE-HS patients with epilepsy onset at >20 years of age (n=38)	4	NR	NR	VGKCc	• VGKCc 4/15 (26.7%) • onconeuronal 2/19 (10.5%)
Majoie 2006[*117]	Female epilepsy patients (n=106)	NR	NR	Yes	VGKCc, VGCC	7 (6.6%)
McKnight 2005[*361]	Epilepsy & seizure-related diseases (n=139)	NR	NR	Yes	VGKCc, VGCC, ganglioside GM1, GluR3, ACL, ssDNA, dsDNA, ANA	20 (14.4%)

Table 45: Studies reporting high-titre GAD65 autoantibodies in adult epilepsy patients

Studies listed chronologically. While the proportion of participants that meet criteria for DRE are not always stated, studies are largely carried out in specialist clinic cohorts and would be expected to be predominantly DRE. *Ab+*, antibody-positive; *AD*, Alzheimer's disease; *AI*, autoimmune; *CBA*, cell-based assay; *CD*, cortical dysplasia; *CG*, cortical gliosis; *DD*, demyelinating disease; *DR*, drug-resistant; *DRE*, drug-resistant epilepsy; *ELISA*, enzyme-linked immunosorbent assay; *F:M*, female:male; *GAD65*, glutamic acid decarboxylase 65; *GGE*, genetic generalised epilepsy; *HC*, healthy control; *HS*, hippocampal sclerosis; *HT*, hypothyroidism; *JME*, juvenile myoclonic epilepsy; *JRA*, juvenile rheumatoid arthritis; *LE*, limbic encephalitis; *MS*, multiple sclerosis; *MTLE*, mesial temporal lobe epilepsy; *MTS*, mesial temporal sclerosis; *NR*, not reported; *PA*, pernicious anaemia; *PC*, prospective cohort; *RA*, rheumatoid arthritis; *RBA*, radiobinding assay; *RC*, retrospective cohort; *SD*, standard deviation; *SPSD*, stiff person spectrum disorder; and *T1DM*, type 1 diabetes mellitus.

Study	*Design*	*Number of sample time points*	*Patient cohort*	*Number of high-titre GAD65 Ab+ patients*	*Controls*	*Assay type (result range)*	*GAD65 Ab positivity cut-off*	*Threshold for high GAD65 Ab titre*	*F:M*	*Age range (years) at epilepsy onset*	*DRE*	*AI disease*
Tizazu 2020[205]	RC	1	Biobank: epilepsy	2/270 (0.7%)	23 biobank samples matched by age, gender & ethnicity; no T1DM or epilepsy	CBA (1:12,800–1:204,800); rat brain IHC	NR	NR	1:1	NR	NR	NR
Aguiar 2019[206]	RC	1	T1DM registry screened for epilepsy of unknown aetiology	5/12 (41.7%)	24 T1DM matched by age, gender & T1DM duration; no epilepsy	NR (134.1–312.1 IU/ml)	>=1 IU/ml	>=100 IU/ml	6:4	6–22	2/5 (40%)	NR
Falip 2019[207]	RC	1	Focal epilepsy patients (with or without preceding limbic encephalitis) with epilepsy duration >5 years and high titre GAD65 antibody serum titres	13 (number screened NR)	9 unilateral MTS with at least 1 year of post-epilepsy surgery seizure-freedom & 8 bilateral MTS of known, non-autoimmune origin	ELISA (NR)	NR	>2,000 IU/ml	7:6	11–72	7/13 (54%)	11 (details NR)

Study	*Design*	*Number of sample time points*	*Patient cohort*	*Number of high-titre GAD65 Ab+ patients*	*Controls*	*Assay type (result range)*	*GAD65 Ab positivity cut-off*	*Threshold for high GAD65 Ab titre*	*F:M*	*Age range (years) at epilepsy onset*	*DRE*	*AI disease*
Nóbrega Jr 2018[62]	PC	1	MTLE-HS	2/100 (2%)	50 age- & gender-matched controls; no neuro, psychiatric or AI disease	ELISA (NR)	>10 IU/ml	>1,000 IU/ml	2:0	NR	NR	NR
Ceyhan Dirican 2016[208]	RC	1	Inpatients with DR-MTLE-HS & JME Excluded other neurological symptoms	0/54 (0%)	26 age-matched HC	RIPA (NR)	1 U/ml	NR	NR	NR	NR	NR
Moloney 2016[209]	PC	1	Outpatients with epilepsy & T1DM	7/25 (28%)	36 T1DM	RIPA (9,550–59,200 U/ml)	>10 U/ml	>1,000 U/ml	NR	NR	5/7 (71%)	NR
Lilleker 2014[189]	RC	1	Unexplained adult-onset epilepsy Excluded antecedent cerebral insults, epileptogenic lesions or inflammation on MRI, GGE, symptomatic epilepsies, LE	6/112 (5.4%)	NR	RIPA or ELISA (NR)	RIPA >=1 U/ml or ELISA >=5 U/ml	RIPA >1,000 U/ml or ELISA >50,000 U/ml	6:0	18–40	6/6 (100%)	4 (RA & HT; T1DM & coeliac; HT; coeliac & PA)
Falip 2012[210]	PC	1	Epilepsy onset >30 years-old with semiological, MRI and EEG features of TLE	2/42 (4.8%)	NR	RIPA (1,207–87,510 IU/ml)	NR	>1,000 IU/ml	2:0	NR	NR	5 (T1DM; psoriatic arthritis & HT; T1DM; T1DM, coeliac & HT; T1DM)

Study	*Design*	*Number of sample time points*	*Patient cohort*	*Number of high-titre GAD65 Ab+ patients*	*Controls*	*Assay type (result range)*	*GAD65 Ab positivity cut-off*	*Threshold for high GAD65 Ab titre*	*F:M*	*Age range (years) at epilepsy onset*	*DRE*	*AI disease*
Malter 2010[74]	PC	1	New-onset TLE of unclear aetiology	9/53 (17%)	NR	RIPA (1,798 – 12,030 U/ml)	>=1 U/ml	NR	NR	NR	9/9 (100%)	NR
Liimatainen 2010[86]	PC	1	Outpatients with epilepsy & recurrent seizures	7/253 (2.8%)	200 epilepsy-free controls	RIPA (1,680–207,770 RU/ml)	5.36 RU/ml	>=1,000 RU/ml	5:2	NR	NR	5 (coeliac; thyroiditis & psoriasis; asthma; coeliac, IgA deficiency & JRA; T1DM & DD)
Errichiello 2009[88]	PC	1	Epilepsy outpatients Excluded additional neurological signs	6/233 (2.6%)	250 T1DM	RIPA (1.93–78.79 U/ml)	0.9 U/ml	NR	NR	8–49	4/6 (67%)	2 (T1DM)
Sokol 2004[211]	PC	1	Consecutive outpatients undergoing epilepsy surgery evaluation	1/31 (3.2%)	4 high-titre anti-GAD65 Ab+ SPSD & 50 GAD65 Ab-negative controls with other neuro diseases	ELISA (NR)	NR	Control mean + 2 SD	0:1	NR	1/1 (100%)	0
Kwan 2000[212]	PC	1	Outpatients with JME or focal epilepsy due to MTS, CD or CG	4/105 (3.8%)	NR	RIPA (6.3–170.4 U/ml)	NR	NR	4:0	NR	4/4 100%	0
Peltola 2000[84]	PC	1	Outpatients with focal DRE & GGE	2/100 (2%)	48 HC, 18 MS, 20 AD, 124 T1DM; no epilepsy	RBA (53,000–107,000 RU)	HC mean + 3 SD	NR	1:1	16 & 16	2/2 100%	1 (HT)

6.2.2 Autoantibodies in epilepsy over time

The half-life of human IgG is approximately 21 days,[362] so the finding that high EPT GAD65 autoantibodies persisted over the observed 1-2 years suggests continuous and long-term antibody production. It is not known which B cell subsets are the major contributors to circulating GAD65 autoantibodies or whether ongoing antigen exposure is required.

One NOFE patient remained GABA-R receptor autoantibody-positive at 35 months, despite becoming seizure-free. Another NOFE patient, initially seronegative, tested positive for GABA-A-R autoantibodies after 32 months, by which time they had developed DRE. This could reflect a mechanistic role for autoantibodies in some patients but not in others.

None of the NOFE subjects were GAD65 antibody-positive and none of the 13 'study cross-over' patients (i.e., participants in both the NOFE study and the later DRE study) became positive for GAD65 autoantibodies over time, inferring that GAD65 autoantibodies may be specific to DRE and not simply a 'by-product' of chronic seizures.

No epilepsy studies with sequential autoantibody testing are available for comparison but sustained NMDA-R and aquaporin-4 antibody production has been demonstrated beyond three years into the disease course in autoimmune encephalitis and neuromyelitis optica spectrum disorders (NMOSD), respectively.[306,363]

6.2.3 Clinical features predictive of autoantibody status in new-onset focal epilepsy

Seizure semiology and mood phenotypes, in conjunction with inflammatory investigation findings, can identify NSAs among unselected adults with NOFE. With a sensitivity of 66.7% and a specificity of 84.9%, our multivariate regression model for predicting NSA status performed better than the APE2 score (sensitivity 43.5% and specificity 79.1%). Furthermore, the APE2 score did not perform as well as previously reported (**Table 46**). This is most probably due to the considerable ascertainment bias for AIE in other APE2 validation studies and because AIE is favoured by the APE2 parameters, in that many of the APE2 criteria are in fact typical features of AIE (e.g., acute changes in cognition with neuropsychiatric features, new-onset seizures, ASM-refractoriness, CSF inflammation and abnormal signal within the temporal lobes on brain MRI).[284] The seemingly favourable immunotherapy-independent outcomes of NSA-positive patients with isolated epilepsy suggest immunotherapy administration should be guided by clinical features of encephalitis, rather than autoantibody positivity in itself.

Our findings appear to blur the distinction between autoimmune encephalitis and autoimmune epilepsy. Previous studies of NSAs and immunotherapy in epilepsy do not provide the disaggregated data necessary to assess outcomes for their NSA-positive patients with isolated epilepsy who did not receive immunotherapy.[59,91,94,107,108,113] A randomised controlled trial of immunotherapy in NSA-positive patients with isolated DRE could provide useful evidence to inform clinical practice. Validation of our autoantibody prediction model in a prospective study is necessary.

Table 46: APE2 score performance in three cohorts.
The NOFE cohort is the first independent, prospective study of epilepsy patients used to validate the APE2 score. *APE2*, antibody prevalence in epilepsy and encephalopathy score; and *CSF*, cerebrospinal fluid.

Study	*Patient cohort*	*Sensitivity*	*Specificity*
Dubey et al., 2019[365]	• APE2 score applied to a cohort previously reported by the same group (Dubey et al., 2017).[97] • Retrospective interrogation of lab registry to identify all patients already tested for neural autoantibodies due to a clinical suspicion of autoimmune encephalopathy, autoimmune epilepsy or autoimmune dementia. • Subsequent selection of children & adults meeting diagnostic criteria for epilepsy.	98%	85%
Bozzetti et al., 2020[12]	• Retrospective interrogation of lab registry to identify all patients already tested for anti-neural antibodies. • Subsequent selection of children & adults with new-onset epilepsy, status epilepticus or chronic epilepsy of unknown aetiology. • Excluded those without paired serum & CSF samples, and without a full clinical dataset. • Excluded those with a defined epilepsy aetiology, acute symptomatic seizures or neurodegenerative processes.	90%	33%
NOFE study	• Adults with new-onset focal epilepsy within prior 12 months.	43.5%	79.1%

6.2.4 Clinical phenotype of GAD65 autoantibody-associated epilepsy

Few studies relating to GAD65 autoantibodies distinguish between epilepsy and autoimmune encephalitis. Even then, it is unusual for studies to provide details on a patient-by-patient basis. Joubert et al., 2020[366] reported long-term outcomes for a small group of patients with very similar characteristics to the seven high EPT GAD65 autoantibody patients identified in our DRE study. From 35 patients with GAD65 autoantibody-associated syndromes, the authors describe four patients with isolated epilepsy who had no history of acute autoimmune encephalitis or other GAD65 autoantibody-associated neurological conditions. All were female, with a median age at onset of 32 years (range 23-38) and serum GAD65 autoantibodies measured by ELISA were >250 IU/ml. They each presented with seizures and were diagnosed with drug-resistant

temporal lobe epilepsy refractory to at least two immunotherapies. Two individuals had MRI brain changes consistent with bilateral hippocampal sclerosis. Memory difficulties developed in each case. At follow-up approximately ten years after seizure-onset, only one patient was still able to continue working full-time. No information was provided regarding ASMs, T1DM or seizure triggers.

It is quite striking that 3/7 of our high EPT GAD65 autoantibody DRE patients recognised pain as a seizure trigger. This is uncommon in epileptology and could be consistent with a reflex seizure mechanism, for which there is precedent in the GAD65 autoantibody-associated epilepsy literature.[91,367]

6.2.5 Development of a novel fixed and permeabilised GAD65 IgG antibody CBA

As indicated by its detection of GAD65 antibodies in PBMC culture supernatant, as well as in the serum of patients with known high-titre antibodies, the novel GAD65 antibody CBA has a wide dynamic range. Gresa-Arribas et al., 2015,[248] developed a similar CBA but validation experiments failed to detect antibodies in low-titre T1DM patients who were positive by RIPA. A microscopy photograph of another in-house GAD65 antibody CBA published by Tizazu et al., 2020, does not appear to generate much positive signal intensity, even with a high-titre antibody sample (**Figure 90**).

Given that a large number of healthy control samples tested negative on the CBA, low EPT GAD65 autoantibodies may be relevant, possibly representing early-stage disease.

Discrepancies between measurements by the GAD65 antibody ELISA kits and the CBA could reflect the fact that ELISAs are more susceptible to manual pipetting errors and that they make use of short, linear sequence-derived peptides which cannot always effectively bind antibodies. The antibody EPTs measured in the DRE patients can be orders of magnitude greater that the levels in T1DM. It's possible that different epitopes are relevant in each condition and that the ELISA preferentially binds T1DM-associated epitopes.

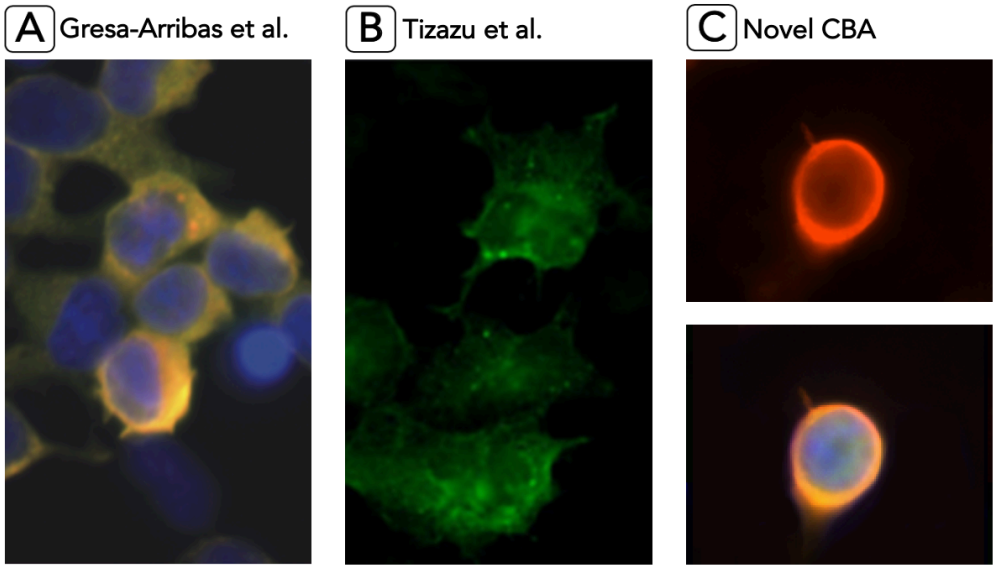


Figure 90: Comparison of two previously published CBAs to the novel CBA
All three fixed and permeabilised CBAs show a positive GAD65 antibody result for serum (samples from three different patients). **(A):** From Gresa-Arribas et al., 2015.[248] HEK293T cells transfected with full length GAD65 expressing an N-terminal myc tag (green) and a commercial antibody against myc tag (red); cell nuclei stained with DAPI (blue); merged reactivity (yellow). (doi.org/10.1371/journal.pone.0121364 (*Creative Commons Attribution Licence, CC BY*). **(B):** From Tizazu et al., 2020.[205] AD293 cells transfected with GAD65 (no methodological details provided by authors). Patient sera incubated with cells and secondary fluorescent antibody (green). (*Copyright Clearance Center Licence Number 4915770181128*). **(C):** Novel GAD65 antibody CBA developed as part of the work in this thesis. HEK293T cells co-transfected with GAD65 truncated at amino acid 96 and eGFP (green, not shown). Secondary antibody (red). Cell nuclei stained with DAPI (blue). Merge (yellow). In contrast to the peri-membrane staining observed in the novel CBA (C), the staining patterns produced in the other two assays (A and B) appear more cytoplasmic, with possible staining of inclusion bodies. *AD293*, adenovirus-transformed HEK cells; *CBA*, cell-based assay; *DAPI*, 4′,6-diamidino-2-phenylindole; *eGFP*, enhanced green fluorescent protein; *GAD65*, glutamic acid decarboxylase 65; and *HEK-293T*, human embryonic kidney 293T cells.

6.2.6 Pilot of GAD65 IgM autoantibody detection

It is not possible to determine whether GAD65 IgM autoantibodies were genuinely absent from patient sera, or these were false negative results. The CBA may have failed to detect IgM antibodies if the more abundant IgG autoantibodies interfered with IgM binding to the secondary detection antibody or if the assay's sensitivity was insufficient for IgM at serum dilutions of 1:100.

6.2.7 Expression construct modification for GAD65 IgG antibody live CBA

It is unclear why the live CBA using modified expression constructs did not work. Dysfunctional membrane trafficking may underlie the apparent lack of GAD65 surface expression when tested with a polyclonal commercial GAD65 antibody. Even if GAD65 were present on the surface but abnormally folded, some commercial antibody binding would have been expected, hence absence of the protein at the target site is perhaps more likely.

If the problem were that an unrecognised trafficking signal had been removed from the truncated constructs, the full-length construct should have surface-expressed, but this was not the case. Perhaps an unidentified endoplasmic reticulum retention signal is responsible, or cofactors within neurally-derived HEK cells are capable of interacting with GAD65 and preventing it from trafficking to the surface. The use of the permeabilisation agent Triton may have affected the nuclear membrane and disrupted intracellular trafficking. In vivo, GAD65 forms a functional dimer. Whether dimerisation must occur

intracellularly (from the expression construct-produced monomers) in order for surface expression to occur is not known.

6.2.8 Plasma cytokines in epilepsy

The complex interaction between cytokines is not fully understood.[340] The effects of a given cytokine can differ depending on its source, timing of production, concentration and consumption.[368] Cytokine synthesis from one cell population can alter the same molecule's output by other cell types. The interpretation of cytokine profiles is further complicated by the phenomena of pleiotropy (the ability of a cytokine to exert many types of responses), redundancy (when multiple cytokines are capable of exerting similar responses) and synergy (when several cytokines interact to produce a greater effect than would be expected by addition of the effects of the same cytokines individually).[369,370]

Overall, the findings of elevated IL1b, IL4, IL10, IL15 and TNFa in GAD65 autoantibody-positive epilepsy are consistent with a pro-inflammatory state, B cell activation and T cell proliferation and differentiation. TNFa induces IL1b release, a potent pro-inflammatory molecule that promotes proliferation and differentiation of activated B cells into plasma cells.[371,372] IL4 and IL15 have been linked with autoantibody-mediated autoimmune disease and promote B cell growth, differentiation and immunoglobulin secretion.[373,374] IL4 induces T cell proliferation and differentiation into Th2 cells.[375] IL4 is also produced by Th2 cells, and supports B cell survival, proliferation and immunoglobulin class switching, as well as B cell expression of class II major histocompatibility complex (MHC).[372,373] IL15 also stimulates activated B cell proliferation and immunoglobulin synthesis.[376] IL10 is a broadly expressed

cytokine with anti-inflammatory properties[372,377] and may be raised in response to the IL1b and TNFa levels.

Of studies exploring interictal cytokine concentrations among adult epilepsy patients (**Table 47**), the cytokine panels, range of assay methods, sample types and inclusion criteria are not broadly comparable. However, in keeping with our findings, IL1b was previously described as being increased in epilepsy.[378,379] In contrast to the literature, we did not observe interictal elevation of IL6 – this may in part be due to other studies' use of serum testing instead of plasma,[220,326,329,336] and broader focus on epilepsy rather than GAD65-autoantibody-positive epilepsy.

Each of the five markers in the putative cytokine profile for GAD65 autoantibody-positive epilepsy presents a potential therapeutic target. For example, anakinra is a recombinant IL1 receptor antagonist which reduces IL-1b activity;[380] the recombinant IL4 receptor altrakincept acts as an antagonist to IL4;[381] pascolizumab is a monoclonal antibody against IL4;[381] and soluble TNFa is neutralised by infliximab, adalimumab, golimumab, certolizumab pegol and etanercept.[382] Animal models have demonstrated that mithramycin suppresses IL10 production[383] and an IL15 isoform lacking exon-6 is a natural IL15 antagonist.[384]

Table 47: Studies of interictal cytokine concentrations in adult epilepsy patients

Considerable variation in inclusion/exclusion criteria exists between studies (listed chronologically). *ASM*, anti-seizure medication; *CBZ*, carbamazepine; *CNS*, central nervous system; *DRE*, drug-resistant epilepsy; *ELISA*, enzyme-linked immunosorbent assay; *GGE*, genetic generalised epilepsy; *HC*, healthy control; *HS*, hippocampal sclerosis; *LEV*, levetiracetam; *LTG*, lamotrigine; *N/A*, not applicable; *PBMC*, peripheral blood mononuclear cell; *RIA*, radioimmunoassay; *T1DM*, type 1 diabetes mellitus; *TLE*, temporal lobe epilepsy; *WCC*, white cell count;

Study	*Patient cohort*	*Number of cytokines tested*	*Findings*	*Assay type*	*Sample*	*Control group*
Mochol et al., 2020[385]	Epilepsy patients on CBZ/LTG/LEV monotherapy >6 months. Excluded autoimmune disorders, mental retardation, anti-inflammatory medications, oral contraceptives, any other ASM within prior year. (n=119)	2	IL18 & IL18BP increased in epilepsy	ELISA	Plasma	HC (n=80)
Basnyat et al., 2020[386]	TLE with HS, TLE without HS, extra-temporal epilepsy, multifocal epilepsy, focal epilepsy of unknown lobe of onset & GGE. (n=270)	1	IL10 lower in TLE with HS than in TLE without HS	ELISA	Plasma	N/A
Ethemoglu et al., 2018[826]	DRE & controlled epilepsy. Excluded if seizure within last 24 hours, any medications other than ASMs, chronic systemic disease. (n=59)	1	IL6 higher in DRE than in controlled epilepsy & HC	ELISA	Serum	HC (n=29)
Gao et al., 2017[828]	Active focal epilepsy with >1 seizure/2 months & >18 years-old. Excluded infectious or systemic inflammatory disease, severe psychiatric or neurological disease, immunomodulatory treatment within last 6 months, malignancy, surgery or trauma within last 2 weeks, hepatic or renal insufficiency or pregnancy. (n=48)	6	IL6 & L17A increased in epilepsy	ELISA	Plasma	Age- & sex-matched HC (n=30)
Mao et al., 2013[879]	Probable symptomatic epilepsy, >7 days after last seizure. Excluded if autoimmune disease, allergic response, immunodeficiency, T1DM, psychiatric illness, malignancy, severe cognitive impairment, systemic or CNS infection in prior 2 weeks. (n=70)	6	IL6, IL17a, IFNg, IL1b increased in epilepsy	ELISA	Plasma	Age- & sex-matched HC (n=68)

Study	*Patient cohort*	*Number of cytokines tested*	*Findings*	*Assay type*	*Sample*	*Control group*
Nowak et al., 2011[887]	Active epilepsy. Excluded if seizure within prior 3 days, malignancy inflammatory disease, neurological disease, immunosuppressant treatment in last six months, surgery or trauma within two weeks, hepatic or renal insufficiency, severe psychiatric disease or pregnancy. (n=101)	3	IL6 increased in epilepsy	ELISA	Serum	HC (n=36)
Liimatainen et al., 2009[329]	Focal epilepsy. (n=91)	2	IL6 increased in epilepsy	ELISA	Serum	HC (n=63)
Hulkkonen et al., 2004[888]	DRE >48hours from previous seizure. (n=10)	3	IL1a lower in epilepsy	ELISA & flow cytometry	Supernatants of cultured PBMCs (spontaneously and after mitogen stimulation)	HC (n=400)
Pacifici et al., 1995[878]	Seizure-free epilepsy for prior 6 months, ASM monotherapy and ASM plasma concentration within therapeutic range. Excluded if WCC >10,000 /microL or if known illness affecting immunocompetence. (n=76)	4	IL1a & IL1b increased in epilepsy	RIA	Supernatants of cultured PBMCs (after mitogen stimulation)	HC (n=32)

6.2.9 Immunocellular phenotype of GAD65 autoantibody-positive DRE

To our knowledge, this is the first application of mass cytometry to autoantibodies in epilepsy. Our data suggest that high titre GAD65 autoantibody-positive DRE patients may have a unique profile of PBMCs. The incomplete resolution of three PhenoGraph clusters at this stage of the analysis limits what can be inferred. It is intriguing that two of the distinctive subsets are T cells, as cytosolic antibodies such as GAD65 antibodies may exert their effect via T cell-mediated paths. Regulatory T cells, one of the more abundant subsets in the GAD65 autoantibody-positive patients, have a key role in the maintenance of immune tolerance. As with all mass cytometry data, determining whether these subsets are of clinical significance will require longer-term iterative analysis.

There may be some parallels with paraneoplastic neurological syndromes, in which antibodies targeting intracellular antigens are proposed to mediate their effects via CD8-positive cytotoxic T cells.[389,390] For example, among patients with Hu autoantibody-positive paraneoplastic encephalomyelopathy, PBMCs exhibit expansion of activated CD4-positive T cells[391] and T cell receptor analysis of frozen tissue suggests an antigen-driven CD8-positive cytotoxic T cell response.[392]

Given that the patients provided blood samples as outpatients and did not have any clinical features to suggest an acute pro-inflammatory state, it is surprising to see a detectable difference in the lymphocyte populations. Vieira et al., 2016,[393] used multi-colour flow cytometry to investigate peripheral leukocytes in 20 people with temporal lobe epilepsy (TLE) and hippocampal sclerosis and in 19 healthy controls They showed that TLE patients

had an activation picture, predominantly in effector T cells, consistent with low-grade inflammation (e.g. higher expression of HLADR, CD69, CTLA4 and CD25 in CD4-positive lymphocytes).

The large number of PBMC samples already acquired on mass cytometry will allow the comparison of different groups, (e.g. DRE vs SFE, autoantibody-associated encephalitis versus autoantibody-associated isolated epilepsy) and analysis according to patient characteristics (e.g. degree of drug refractoriness, seizure frequency, co-existing autoimmune disease).

6.3 Strengths and limitations

6.3.1 Autoantibody prevalence in epilepsy

Excluding patients with known non-immune-mediated causes of epilepsy (e.g., malformations of cortical development) may have potentially decreased the signal-to-noise ratio in relation to genuine underlying immune dysregulation. However, the recruitment of consecutive clinic patients much more closely represents and informs real-world clinical practice than studies with highly selected cohorts and is a key strength of this study.

The set of specific autoantibodies tested for in these studies (i.e., ten NSAs plus GAD65 antibodies) is not exhaustive and there is no consensus in the literature on which autoantibodies to test for in epilepsy. Yet our autoantibody screening panel is broader and more clinically relevant when compared to most published epilepsy studies, and it is unlikely that a recognised, common, clinically relevant autoantibody has been excluded.

Additionally, the use of cultured neurons and astrocytes was intended to detect any NSAs not specifically screened for by CBA.

The validity of live CBA results without additional verification by separate assay methods might be questioned by some researchers who advocate confirmatory tests, such as indirect tissue immunofluorescence and immunohistochemistry. Yet the live CBAs used by the Oxford Autoimmune Neurology Group have been shown to provide antigen-specific results in rigorous testing against a range of antigen-transfected cells, and arguably have greater sensitivity and specificity than these confirmatory tests.[202,203]

Paired serum-CSF samples for each patient would be more informative regarding antibodies with putative roles in CNS pathology. A subset of autoantibody-positive and -negative patients was selected for CSF testing but sampling was cancelled due to the SARS-CoV-2 pandemic and has, to date, not been able to resume.

The large number of positive NBA and ABA results without detection of concomitant NSAs prompts consideration of low-affinity or low-titre, and disease-irrelevant autoantibodies. However, the distribution frequency of these results across groups (i.e., DRE>NOFE>HC) and their specificity – given their typical selectivity for a single cell surface-expressed autoantigen – offers some reassurance. It may be that NBAs and ABAs are most apposite for testing patients presenting with precise clinical phenotypes. Calibrating NBAs and ABAs to accommodate a high degree of background signal when testing a large group of

patients may lead to the masking of true low-positive results. This may call into question the suitability of these assays for blind cohort screening.

The reliance on patient-reported seizure counts is a common methodological weakness in epilepsy studies. Data reliability might be feasibly improved by combining daily seizure diaries with non-EEG-based seizure detection systems contingent on peri-ictal changes in cardiac rhythm, respiration, body movements, muscle activity, sweating, urination, vocalisations, blood oxygen saturation or blood pressure.[394–397]

Although study visits were halted because of COVID-19, the comprehensive phenotyping database, with prepopulated responses intended to facilitate consistency in data collection and coding, is a particular strength of the DRE study. The large patient cohort and uniquely rich longitudinal follow-up data should produce robust findings and may offer some compelling insights into the potential role of autoantibodies in epilepsy.

6.3.2 Autoantibodies in epilepsy over time and the clinical phenotype of high EPT GAD65 autoantibody-associated epilepsy

The NOFE patients who later developed DRE and enrolled in our second study, and the high EPT GAD65 autoantibody-positive DRE patients were few in number. There is low generalisability, statistical power and reproducibility inherent in such samples, and so no firm conclusions have been drawn. Future collaboration with other epilepsy centres to identify additional patients with high EPT GAD65 autoantibodies could help to address this. Clinical documentation tended to capture whether seizure control was the same, better or

worse, rather than specific seizure counts. It was therefore not possible to fully complete the seizure frequency data fields in the phenotyping database in each case and the correlation between number of seizures over time and GAD65 antibody EPT could not be explored in more detail. Serum samples from most of the DRE study visits remain untested and in frozen storage as a consequence of COVID-19 restrictions but future screening of these samples could provide useful serial data for a large cohort of clinically phenotyped people with epilepsy.

6.3.3 Clinical features predictive of autoantibody status in new-onset focal epilepsy

The limited CSF autoantibody measurements for the NOFE patients probably reflects the relatively conservative use of lumbar puncture in the UK. Although a diagnosis of NMDA-R antibody encephalitis is possible without this parameter, two of our four patients with serum NMDA-R antibodies did not have any features consistent with encephalitis, and intrathecal titres of autoantibodies could have aided interpretation of the serum findings.

Among the NOFE cohort, 9/219 (4.1%) had clinically diagnosed autoimmune encephalitis. This small proportion may nevertheless be considered substantial, given the largely outpatient-based recruitment. The high 23/219 (10.5%) seroprevalence rate of NSAs may reflect a referral bias, given Oxford's interest in autoimmune encephalitis, but is well-aligned with other available estimates. The Oxford University Hospitals NHS Foundation Trust serves a population of around 2.5 million people – it is a tertiary referral centre with its own catchment as a District General Hospital. As such, the whole spectrum of epilepsy is captured, although there is an increase in people with DRE.

We did not examine long-term seizure status in the 5/16 patients (31%) who had NSAs, no diagnosis of autoimmune encephalitis and 3-year mRS>0. In these patients, it remains possible that immunotherapy would have been beneficial. However, this finding could be considered consistent with the predicted one-third of all epilepsy patients who become ASM-resistant. This provides a testable hypothesis for a future randomised controlled trial.

The NOFE database had some missing clinical phenotyping data. We addressed this by imputing a relatively conservative proportion of information using the missForest R package. This did not materially affect our analysis, as the same constituent terms appeared in the final multivariate stepwise regression model. I developed the DRE phenotyping database in response, recognising that the free-text fields in the NOFE database were inconsistently completed and required a lot of data cleaning, or were left blank.

6.3.4 Development of a novel GAD65 IgG antibody cell-based assay

CBA output can be considered semi-quantitative but CBA scores (0-4) and endpoint titres are subjective, and transient protein expression can cause inter-assay variability. Notwithstanding the difficulties of comparing results from different patient sera, the novel CBA appears to perform at least as well as two published assays (**Figure 90**). For logistical reasons, the CBA optimisation work was not exhaustive, and it is possible that untested protocol adjustments may have further improved the assay. The cell transfection rate, for example, still seems poor compared to the LGI1 antibody CBA, even after a series of

experiments to address this specific issue. Confocal microscopy might have provided a more reliable method of visualising the CBA than fluorescence microscopy but the considerable increase in expense and time would not have been appropriate for screening such a large number of samples. Use of a 96-well plate format, with only positive or uncertain results repeated on 24-well plates with glass cover slips, would have increased sample throughput but would have required considerable additional optimisation time. Developing a stably transfected cell line expressing GAD65 antigen would minimise inter-assay variability but would require using HEK293 cells without the SV40 large T antigen – this would likely decrease GAD65 antigen expression and assay sensitivity.

The fact that the GAD65 CBA appears to detect antinuclear antibodies may alter the typical GAD65 antibody binding patterns, which could make the assay more difficult to interpret or could even alter antibody binding and give unreliable results. I found that practised reading makes the GAD65 and ANA patterns more easily distinguishable. Further exploration, by systematically testing samples for ANA as well as GAD65 could resolve this issue.

Permeabilised CBAs are associated with more non-specific background signal than live CBAs, due to the large number of intracellular non-GAD65 antigens accessible to the secondary antibody relative to the cell surface. The fixation process may alter epitopes and produce binding that would not occur physiologically. Apparent GAD65 antibody-positive signal may be produced by non-GAD65 antibody binding of secondary antibody (e.g., molecular mimicry), non-specific antibody interactions (e.g., based on electrical charge) or

by the detection of other IgG unidentified antibodies present in sera capable of producing a similar binding pattern (e.g., antinuclear antibodies can produce a peripheral staining pattern). This observation prompted me to try to produce an assay with non-fixed, non-permeabilised live cells, expressing the GAD65 antigen on the surface by way of a CASPR2 signal sequence and tail.

6.3.5 Pilot of GAD65 IgM autoantibody detection

The COVID-19 lockdown prevented attempts to improve the validity of the GAD65 IgM autoantibody CBA through IgG depletion (e.g., achieved by sample incubation with protein G Sepharose beads) and to optimise the assay's sensitivity for IgM by varying the dilution of test sera.

6.3.6 Expression construct modification for GAD65 IgG antibody live CBA

The HEK cell media contained the activated form of PLP (the co-factor for GAD65) but it could be the case that this became depleted and further supplementation was necessary for GAD65 to dimerise and successfully surface-express. Triton was chosen as the permeabilisation agent because of its successful use in other permeabilised CBAs in our laboratory and its immediate availability. It may have been that an alternative permeabilisation agent, such as Tween or saponin, may have caused less disruption to the nuclear membrane and better facilitated cell surface expression but this would have required additional optimisation work and laboratories were closed due to COVID-19 restrictions, preventing me from doing this. Further attempts to surface-express and eGFP-

tag the target antigen should be made, as this may yield objective output measurements by flow cytometry with a broader dynamic range compared to a CBA score or CBA EPT.

A more robust comparison of CBA to RIPA and ELISA would have required a larger set of serum samples tested on all three assays. However, many of the GAD65 autoantibody-positive patients had not been recruited before the radiotracer in the last available RIPA kits decayed and the number of samples screened by commercial ELISA was limited by cost.

Clinical GAD65 autoantibody results from testing by the hospital immunology laboratory were intended to provide a benchmark for the other assays. Ultimately, only a small minority of patients in the DRE study had been tested on a clinical basis and this testing was by the same commercial ELISA kit which I used, except that the hospital laboratory protocol diverged from that provided by the kit manufacturer. This meant that the comparison work was undertaken with a lack of true positive and true negative results. An analysis could therefore not produce robust positive and negative predictive values for each assay but I chose a pragmatic approach and generated estimates of CBA sensitivity and specificity.

The very good inter-rater concordance of the GAD65 antibody CBA does not reflect the level of difficulty involved in reading this assay. By the point of the inter-rater assessment, I had accumulated over one year's practice in reading the assay (with which there was a clear learning curve), while the second rater was a postdoctoral scientist experienced in interpretating clinical diagnostic tests.

6.3.7 Plasma cytokines in epilepsy and the immunocellular phenotyping of GAD65 autoantibody-positive DRE

Some cytokines can degrade in plasma if there is even a short delay between sampling, processing and storage. I did not have oversight of these logistical areas but I avoided repeat freeze-thaw cycle degradation by ensuring that I only used previously unthawed plasma samples.

Freezing PBMCs and storing them over a prolonged period can affect the surviving cell population frequency and can alter cell surface markers.[398,399] The use of fresh PBMCs would be preferable for this project but not logistically feasible. During optimisation, I compared the antibody panel on fresh and frozen healthy control PBMC samples, and there were no clear differences.

For disease control PBMC and plasma samples collected prior to the DRE study, relatively limited clinical information was available. It was therefore not possible to control for some factors which may have altered inflammatory markers, such as seizure activity, anti-seizure medications or coexisting autoimmune diseases. For mass cytometry, I was able to ensure that the GAD65 autoantibody-positive DRE patients were age- and sex- matched to SFE controls, and I selected patients who had never received B cell depleting agents.

Data from PBMCs and plasma cytokines may not be representative of immune activity within the central nervous system. I initially planned to confirm any potentially significant findings on CSF samples but COVID-19 restrictions prevented CSF collection.

Cytokine profiles can be difficult to interpret. The apparent involvement of particular signalling pathways would require confirmation. For example, mass cytometry measurement of phosphorylated signalling proteins, such as NF-kB, could identify the activation status of inflammation signalling pathways.

Some markers were not possible to include on the cytokine panel, as kit-compatible antibodies were not manufactured. B cell activating factor (BAFF), CXCL13 (a plasma biomarker of germinal centre activity)[400], IL8 (a proinflammatory cytokine) and HMGB1 (an initiator of neuroinflammation implicated in epilepsy)[401] could prove valuable to include in future.

Five chemokine markers on the mass cytometry antibody panel could not be used due to the fixation required for the barcoding process. This restricted information about B cell maturation and T helper cell subsets but barcoding minimised variability in antibody staining and instrument sensitivity between samples.

Although the clean-up gating of mass cytometry data was based on assumptions regarding cell populations that may have missed rare cell subsets, the gating strategy I applied is well established and considered robust.[402] Down-sampling of data incorporated only a proportion of cells for analysis and, again, rare populations might have been overlooked. Iterative analysis with increasing cell sample size may help to overcome this and I selected an unsupervised clustering algorithm to reduce the risk of bias in the analysis.

Differences in cell clusters may have been more striking if PBMC stimulation had been undertaken prior to antibody staining. I did not stimulate cells to avoid inducing biological activity that might not occur in vivo.

Sample acquisition in batches risks conflating batch effects with physiological changes. I took extensive steps to minimise other technical sources of variation, such as sample barcoding, calibration beads for sample normalisation, daily instrument tuning and calibration, and 4-hourly quality control checks during acquisition. The inclusion of batch controls will permit the use of emerging batch normalisation algorithms.[403]

6.4 Impact of COVID-19

The COVID-19 lockdown prevented:

- DRE patient follow-up (all face-to-face outpatient and research clinics were halted)
- antibody panel screening for samples obtained from any study follow-up visits completed prior to lockdown;
- completion of the mental health and cognition screening questionnaires for DRE patients at study visit six;
- CSF sampling from high EPT GAD65 autoantibody-positive patients (all scheduled appointments were cancelled);
- ELISA and CBA testing of an additional 160 samples for comparison to previously determined RIPA GAD65 antibody titres;
- cytokine screening of an additional 40 plasma samples, including healthy controls;

- mass cytometry of an additional 20 PBMC samples, including healthy controls;
- further optimisation of the novel fixed and permeabilised CBA for detecting GAD65 antibodies;
- further attempts at development of a novel live CBA for detecting GAD65 antibodies;
- ABA screening of sera from 219 NOFE subjects and 55 healthy controls already tested on NBA;
- serum autoantibody screening (nine NSAs, ABA and NBA) of an additional 55 healthy controls.

6.5 Future directions

6.5.1 Hypothesis: DRE patients with positive NBA or ABA results, but lacking specific autoantibodies (to ten established antigens by CBA), may harbour novel NSAs

Antigen discovery by immunoprecipitation and tandem mass spectrometry[364,404] may permit screening of patients for these autoantibodies to determine if an associated clinical phenotype exists.

6.5.2 Hypothesis: GAD65 autoantibody-positive DRE represents a distinct clinical subgroup

Increasing the size of this cohort by working with collaborators at other epilepsy centres and performing a review of the literature to systematically extract clinical details from published cases could help to clarify this.

6.5.3 Hypothesis: High titre GAD65 autoantibodies have a pathogenic role in DRE

Iterative analysis of mass cytometry PBMC data may establish whether these patients have a distinct set of PBMC surface markers and offer insight into the production of GAD65 autoantibodies. Detection of an expanded subset of naïve B cells, for instance, could indicate failure of an immune checkpoint and release of autoreactive cells, potentially explaining autoantibody production in the absence of antigen.

Identification of CNS-specific immune cell subsets might be possible through simultaneous sampling of multiple immune compartments for analysis by mass cytometry and flow cytometry. For example, on the day of epilepsy surgery it might be feasible in a small number of patients to obtain resected brain tissue, CSF, bone marrow aspirates, and PBMCs. Alternatively, CSF, bone marrow and PBMC collection could be scheduled for a larger proportion of patients in a single outpatient visit. Mass cytometry could also be deployed to investigate possible differences in cell signalling function and immune-checkpoint molecule expression on T cells in response to treatment.

Culturing patient PBMCs with the cytokine conditions identified in chapter 5 would test whether these promote GAD65 antibody secretion. In combination with mass cytometry analysis, flow cytometry of cultured immune cells could identify the antibody-secreting B cell populations. Addition of immunotherapy agents to the PBMC cultures could explore strategies to prevent antibody production.

A GAD67-encoding gene block could be substituted for the GAD65 insert in the current

CBA expression vector and used to screen the DRE cohort. GAD isoform autoantibody cross-reactivity might be restricted to subgroups (e.g., cerebellar ataxia versus epilepsy), which would suggest that clinical phenotypes may be partly explained by difference epitopes.

Isolation of monoclonal GAD65 autoantibodies from patients would enable epitope mapping with targeted mutations introduced through PCR. Comparison between patients with T1DM, GAD65 autoantibody-positive epilepsy and other GAD65 autoantibody-associated neurological syndromes could aid development of more specific assays with possible implications for diagnosis, prognostication and monitoring treatment response.

Evidence of antibody pathogenicity could be obtained from animal studies. Mice could be used for passive transfer of CSF GAD65 autoantibodies from patients with isolated DRE and for active immunisation with GAD65 antigen followed by adoptive transfer of GAD65-specific T cells. In parallel, these experiments could be performed in GAD65-knockout mice to demonstrate that any putative GAD65 antibody-induced changes do not occur in the absence of target antigen.

6.5.4 Hypothesis: autoantibody-positive epilepsy and autoantibody-positive autoimmune encephalitis are part of the same disease spectrum

Analysis of the large mass cytometry dataset from PMBCs of autoantibody-positive patients with isolated epilepsy and AIE may permit exploration of whether these clinical phenotypes reflect manifestations of a common pathogenic process.

HLA typing of epilepsy patients with LGI1 and CASPR2 autoantibodies may help to address this same issue. If isolated epilepsy patients were to show an overrepresentation of the same HLA alleles as those with LGI1 and CASPR2 autoantibody-positive AIE, (e.g., HLA-DRB1*07:01 and HLA-DRB1*11:01, respectivey[405]), this would provide compelling evidence of a shared disease aetiology. Distinct allelic associations between T1DM, GAD65 autoantibody-positive epilepsy and other GAD65 autoantibody-positive autoimmune neurology conditions could help to clinically stratify these groups.

6.5.5 Hypothesis: Non-antibody-mediated autoimmune mechanisms contribute to epilepsy

A number of studies point towards a disease-relevant role for the complement pathway. Xiong et al. showed in a rat model that membrane attack complex formation within the hippocampus was associated with seizure-onset.[228] A study by Kopczynska et al. found higher plasma concentrations of factor H and terminal complement complex in people with epilepsy compared to controls.[406] Screening the DRE study cohort for complement dysfunction may contribute to the discovery of epilepsy biomarkers or drug targets.

There is evidence from pilot clinical studies that vagal nerve stimulation (VNS) can modulate inflammatory responses and may inhibit cytokine release.[407,408] The precise therapeutic mechanisms of VNS in epilepsy are not understood and it is not currently possible to predict which patients will benefit. As a result, half of those who undergo device implantation experience treatment failure.[409] PBMC phenotyping and plasma cytokine

profiling before VNS implantation, followed by serial long-term sampling may identify particular patterns of inflammatory pathway activation that differentiate between VNS responders and non-responders.

6.6 Conclusions

This work provides valuable insights into clinical and immunological aspects of epilepsy. The estimated autoantibody prevalence rate of 9% is more generalisable to the outpatient population of people with epilepsy in the UK than previously reported figures. A model was derived which accurately predicted the serum autoantibody status of epilepsy patients from clinical features. NSA-positive patients with isolated epilepsy had good long-term outcome without immunotherapy. A novel CBA was developed to detect GAD65 autoantibodies. This assay was applied to identify DRE patients with high titre GAD65 autoantibodies, which clinical and experimental data suggest may represent a distinct subgroup. Patients with isolated DRE should be screened for GAD65 autoantibodies and monitored for the development of autoimmune diseases, particularly T1DM. To aid interpretation of future research, AIE with acute symptomatic seizures should be differentiated from epilepsy, and GAD65 autoantibody assay details should be routinely disclosed, including criteria for positive and high positive values, and how these were determined from controls.

Appendices

Appendix A: Clinical features which predict neuronal surface autoantibodies in new-onset focal epilepsy – implications for immunotherapies

McGinty RN, Handel A, Moloney T, et al. Journal of Neurology, Neurosurgery and Psychiatry, November 2020. doi:10.1136/jnnp-2020-325011[282]

Published paper based on data from chapter 2

OPEN ACCESS

Short report

Clinical features which predict neuronal surface autoantibodies in new-onset focal epilepsy: implications for immunotherapies

Ronan N McGinty [1,2] Adam Handel [1,2] Teresa Moloney,[1] Archana Ramesh,[1,2] Andrew Fower,[1,2] Emma Torzillo,[1,2] Holger Kramer,[3] Stephen Howell,[4] Patrick Waters [1] Jane Adcock,[1,2] Arjune Sen,[1,2] Bethan Lang,[1] Sarosh R Irani [1,2]

[1]Oxford Autoimmune Neurology Group, Nuffield Department of Clinical Neurosciences, University of Oxford, Oxford, UK
[2]Department of Neurology, John Radcliffe Hospital, Oxford University Hospitals, Oxford, UK
[3]MRC London Institute of Medical Sciences, Imperial College, London, UK
[4]Department of Neurology, Sheffield Teaching Hospitals NHS Foundation Trust, The University of Sheffield, Sheffield, UK

Correspondence to
Dr Sarosh R Irani, Oxford Autoimmune Neurology Group, Nuffield Dept of Clinical Neurosciences, John Radcliffe Hospital, Oxford OX3 9DU, UK; sarosh.irani@ndcn.ox.ac.uk

RNM, AH and TM are joint first authors.
BL and SRI are joint senior authors.

Received 31 August 2020
Revised 28 September 2020
Accepted 8 October 2020

Check for updates

© Author(s) (or their employer(s)) 2020. Re-use permitted under CC BY. Published by BMJ.

To cite: McGinty RN, Handel A, Moloney T, *et al*. *J Neurol Neurosurg Psychiatry* Epub ahead of print: [*please include* Day Month Year]. doi:10.1136/jnnp-2020-325011

ABSTRACT

Objective To generate a score which clinically identifies surface-directed autoantibodies in adults with new-onset focal epilepsy, and evaluate the value of immunotherapy in this clinical setting.

Methods Prospective clinical and autoantibody evaluations in a cohort of 219 consecutive patients with new-onset focal epilepsy.

Results 10.5% (23/219) of people with new-onset focal epilepsy had detectable serum autoantibodies to known or novel cell surface antigenic targets. 9/23 with autoantibodies were diagnosed with encephalitis, by contrast to 0/196 without autoantibodies ($p<0.0001$). Multivariate analysis identified six features which predicted autoantibody positivity (area under the curve=0.83): age ≥54 years, ictal piloerection, lowered self-reported mood, reduced attention, MRI limbic system changes and the absence of conventional epilepsy risk factors. 11/14 (79%) patients with detectable autoantibodies, but without encephalitis, showed excellent long-term outcomes (modified Rankin Score=0) despite no immunotherapy. These outcomes were superior to those of immunotherapy-treated patients with confirmed autoantibody-mediated encephalitis ($p<0.05$).

Conclusions Seizure semiology, cognitive and mood phenotypes, alongside inflammatory investigation findings, aid the identification of surface autoantibodies among unselected people with new-onset focal epilepsy. The excellent immunotherapy-independent outcomes of autoantibody-positive patients without encephalitis suggests immunotherapy administration should be guided by clinical features of encephalitis, rather than autoantibody positivity. Our findings suggest that, in this cohort, immunotherapy-responsive seizure syndromes with autoantibodies largely fall under the umbrella of autoimmune encephalitis.

INTRODUCTION

Neuronal surface-directed antibodies (NSAbs) are considered pathogenic in patients with autoimmune encephalitis (AE). AE commonly presents with prominent seizures and neuropsychiatric features and shows a preferential response to immunotherapies versus anti-seizure medications (ASMs).[1–4] This has prompted the introduction of 'epilepsy of immune aetiology' within the International League Against Epilepsy (ILAE) 2017 classification.[5] The same NSAbs, as well as high levels of antibodies to intraneuronal glutamic acid decarboxylase-65 (GAD65), are also described in the serum of people with more isolated forms of epilepsy, without core features of encephalitis.[6–8] In this context, their clinical, aetiological and therapeutic relevance is unclear, but of major potential importance to all neurologists who manage new-onset epilepsy. In our large, prospective, real-world study of new-onset focal epilepsy, we predicted that *formes frustes* of AE would help identify clinical features suggesting the presence of NSAbs and asked whether detection of these NSAbs should alter patient management.

MATERIALS AND METHODS

Between 9 December 2011 and 4 November 2015, consecutive adult patients (≥18 years) with a diagnosis of new-onset focal epilepsy and their first seizure within the previous 12 months were prospectively recruited from the routine practice of two epileptologists at the Oxford University Hospitals NHS Foundation Trust. Written informed consent and sera were obtained (Ethical approvals: Oxfordshire RECA 07/Q160X/28 and REC16/YH/0013). Clinical data gathered at onset (online supplemental table 1) included detailed phenotype and investigation results, Quality of Life in Epilepsy-31, Hospital Anxiety and Depression Score, Addenbrooke's Cognitive Examination (ACE) and modified Rankin Score (mRS); as well as information to inform the Antibody Prevalence in Epilepsy and Encephalopathy (APE2) score (online supplemental table 2)[9 10] and diagnostic criteria for possible or definite AE.[11] Subsequently, 1-year and 3-year mRS were ascertained from patients with NSAbs.

For NSAbs, sera were tested against autoantigen-expressing live HEK293 cells (live cell-based assay; online supplemental table 3), and for reactivity with the surface of live cultured hippocampal neurons, using sensitive protocols.[12 13] Autoantibodies to GAD65 were determined using a commercial radioimmunoprecipitation assay.

Statistical analysis was conducted in R (V.3.6.1). Dimensionality reduction was performed using Multiple Factor Analysis in 'FactoMineR' with up to 10% missing data imputed using missForest. Stepwise Bayesian general linear modelling analysis was

Table 1 Clinical and laboratory features of patients with epilepsy and positive neuronal surface autoantibodies

Age	Sex	Autoantibody	Live hippocampal neuron binding	APE2 score	Criteria AE	Clinical AE	Pilo	Epil RF	Lowered Mood	ACE Att	MRI Δlimbic	Number of ASMs	mRS 1 year	mRS 3 years	Immunotherapy
79	M	CASPR2	+	3	Definite	Yes	No	None	No	14	Yes	2	3	2	IVMP, Pred, IVIg, PLEX
55	F	CASPR2		6	Definite	Yes	No	None	Yes	18	Yes	3	2	2	IVMP, Pred, IVIg, PLEX
55	F	$GABA_BR$	+	9	Definite	Yes	No	None	No	NA	Yes	6	6	NA	IVMP, Pred, PLEX
18	F	NMDAR	+	8	Definite	Yes	No	None	Yes	15	Yes	3	2	2	IVMP, Pred, PLEX, Aza, MMF
60	F	NMDAR		4	Definite	Yes	No	None	Yes	13	No	3	0	0	Pred
77	F	$GABA_AR$, $GABA_BR$	+	8	Possible	Yes	No	None	Yes	18	Yes	4	1	0	Pred
54	M	LGI1	+	6	Possible	Yes	Yes	None	Yes	18	Yes	2	0	0	None
59	F	LGI1	+	4	No	Yes	No	None	Yes	18	No	1	1	0	None
69	M	Unknown	+	4	No	Yes	No	None	No	13	No	1	1	2	Pred, Aza
63	M	AMPAR	+	2	No	No	No	None	No	NA	No	1	0	0	None
28	M	CASPR2		2	No	No	No	FHx	Yes	17	No	1	0	0	None
41	F	CASPR2		2	No	No	No	None	Yes	18	No	0	0	0	None
75	F	Contactin-2		1	No	No	No	None	No	NA	No	1	0	0	None
37	F	$GABA_AR$		2	No	No	No	None	Yes	18	No	2	0	0	None
36	F	$GABA_BR$		2	No	No	No	None	No	18	No	1	1	0	None
69	F	GlyR		4	No	No	No	None	Yes	15	No	4	1	1	None
61	M	LGI1	+	2	No	No	Yes	None	Yes	18	No	1	0	0	None
36	F	NMDAR		2	No	No	No	None	Yes	18	No	1	2	2	None
68	F	NMDAR, $GABA_AR$		1	No	No	No	None	No	18	No	1	0	0	None
77	F	Unknown	+	2	No	No	No	None	Yes	NA	No	0	0	NA	None
55	F	Unknown	+	4	No	No	No	None	Yes	18	No	5	2	2	None
91	M	Unknown	+	1	No	No	No	None	No	9	No	1	6	NA	None
37	M	Unknown	+	2	No	No	No	None	Yes	18	No	2	0	0	None

APE2 score of 4 or more is considered positive. Diagnosis of encephalitis based on clinical impression ('Clinical AE'; corresponding rows shaded in grey) or published criteria ('Criteria AE'), as per Graus *et al*.[11]
'Unknown' autoantibody specificities reflect IgG binding to the surface of live hippocampal neurons, without a known antigenic target.
ACE Att, Addenbrooke's Cognitive Examination attention domain score; AE, autoimmune encephalitis; APE2, Antibody Prevalence in Epilepsy and Encephalopathy Score; ASM, anti-seizure medication; Aza, azathioprine; Epil RF, epilepsy risk factors (neonatal, perinatal, focal neurological insults, family history of epilepsy or Alzheimer's disease); FHx, family history; IVIg, intravenous immunoglobulin; IVMP, intravenous methylprednisolone; mRS, modified Rankin Score; Myco, mycophenolate; NA, not available; PLEX, plasma exchange; Pred, prednisolone.

undertaken using 'arm'. Wilson 95% CIs with continuity correction were calculated using 'DescTools'.

RESULTS

NSAb findings

Of 241 recruited patients, 22 were excluded (online supplemental table 4). Of the remaining 219, median age was 49 years (range 16–91) and 109 (49.8%) were female. In 23/219 (10.5%) patients, serum NSAbs were detected across candidate and novel autoantigens (table 1) including roughly equal frequencies against leucine-rich glioma inactivated-1 (LGI1), contactin-associated protein-like 2 (CASPR2), plus the *N*-methyl-D-aspartate receptor (NMDAR) and γ-aminobutyric acid $_{A/B}$ receptors ($GABA_AR$ and $GABA_BR$). An additional five patients had antibodies to the surface of live neurons, without an established autoantigen. Autoantibodies to contactin-2, the glycine receptor and the α-amino-3-hydroxy-5-methyl-4-isoxazole propionic acid receptor (AMPAR) were each found in one patient. No dipeptidyl-peptidase-like protein 6 (DPPX) or high-titre GAD65 antibodies were detected. Overall, from the 23 people with NSAbs, 9 had a clinical diagnosis of AE (7/9 fulfilling published criteria).[11] By contrast, none of the 196 without NSAbs had a clinical diagnosis of AE ($p<0.0001$; Fisher's exact test).

Factors associated with the presence of NSAbs and AE

Dimensionality reduction with multiple factor analysis showed that patients were highly heterogeneous and the modest clustering of those with NSAbs was largely driven by a clinical diagnosis of AE (figure 1A,B). Univariate analysis identified 11 clinical parameters that differed significantly between patients with and without NSAbs: age ($p=0.04$), ictal piloerection ($p=0.02$), lesional MRI ($p=0.04$), self-reported mood disturbance ($p=0.007$), ACE attention domain ($p=0.01$), ACE total score ($p=0.04$), QOLIE-31 score ($p=0.02$), self-reported neuropsychiatric features ($p=0.03$), epilepsy risk factors ($p=0.05$), inflammatory cerebrospinal fluid (CSF; $p=0.004$) and limbic system lesions on MRI ($p=0.0002$). A multivariate stepwise regression model allocated weighted scores to six of these: age ≥54 years=+1, self-reported mood disturbance=+1, limbic system lesions on MRI=+2, ictal piloerection=+2.5, ACE attention score ≥16=−1.5 and epilepsy risk factors=−1.5 (figure 1C). The probability of NSAb positivity increased with higher scores (Spearman's $\rho=0.99$, $p<0.0001$; figure 1C) and receiver operating characteristic (ROC) analysis confirmed these features strongly predicted NSAb status (area under the curve (AUC)=0.83; total score ≥0; sensitivity=66.7%, specificity=84.9%; figure 1D). By contrast, the APE2 score performed less well in predicting NSAb status (sensitivity 43.5%, specificity 79.1%, AUC=0.68) and more accurately predicted criteria-defined AE, particularly if associated with NSAbs (sensitivity 85.7%, specificity 78.8%, AUC=0.94; figure 1E).

Comparisons of those with and without AE

From 23 patients with NSAbs (table 1), a comparison of those with (n=9) and without (n=14) a clinical diagnosis of AE revealed several differences in the AE cohort: more ASMs

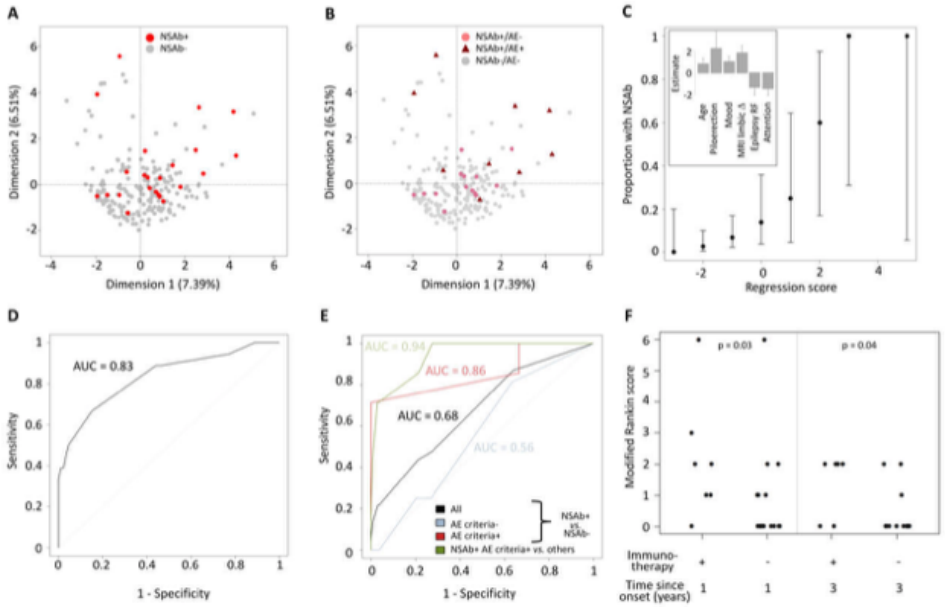


Figure 1 Clinical phenotypes associated with NSAb status in new-onset focal epilepsy. The first two dimensions are shown, highlighting: (A) NSAb-positive (red) or NSAb-negative (grey) status and (B) NSAb-positive (pale red) or NSAb-negative (grey) without encephalitis (dots), or NSAb-positive (dark red) with clinically diagnosed autoimmune encephalitis (triangles). (C) The proportion of patients by total model score. Error bars show 95% CIs. The inset shows the weighting and SE of each factor within the regression model. (D) Receiver operator characteristic (ROC) curve of the total model score for predicting NSAb status across all patients. (E) ROC curve of the APE2 score for predicting NSAb status across all patients (black), patients not meeting the criteria for autoimmune encephalitis (blue), patients meeting the criteria for autoimmune encephalitis (red) and predicting NSAb-positive criteria-confirmed autoimmune encephalitis across all patients. (F) Scatter plot of modified Rankin score in NSAb-positive patients by immunotherapy status over time (Mann-Whitney U test p values<0.05). AE, autoimmune encephalitis; APE2, Antibody Prevalence in Epilepsy and Encephalopathy; epilepsy RF, epilepsy risk factors; MRI limbic Δ, changes within the limbic system on MRI.

(median of 3 vs 1; p=0.0073), more frequent immunotherapies (7/9 vs 0/14, p=0.0001), higher APE2 scores (median of 6 vs 2; p<0.0001), more frequent MRI limbic inflammation (6/9 vs 0/14; p=0.0008) and a trend towards greater positivity of serum IgGs targeting the surface of live neurons (7/9 vs 5/14, p=0.09). Compared with the seven patients administered immunotherapy, those with NSAbs who were not administered immunotherapy showed lower disability after 1 and 3 years (both p<0.05), and 11/16 (68.8%) were asymptomatic at 3-year follow-up (mRS=0 ; figure 1F). Hence, despite no immunotherapy, patients with NSAbs, but without AE, generally showed good outcomes.

DISCUSSION

In this prospective study of 219 consecutive adults with new-onset focal epilepsy, NSAb status was best predicted by a combination of clinical parameters which closely resemble features observed in AE. Almost half of our patients with NSAbs were diagnosed with AE, and ~30% fulfilled stringent criteria for AE.[11] Of those with NSAbs and more isolated forms of epilepsy, without individual features of AE, almost all were treated with ASMs alone and typically remained asymptomatic at long-term follow-up. Overall, these findings suggest that detection of NSAbs in patients with new-onset seizures, but without features of AE, should not alter current clinical management. Our observations should help guide the frequent clinical dilemma of which patients with new-onset seizures to test for autoantibodies and subsequently treat with immunotherapy. Taken together, our data suggest the clinical phenotype is paramount in guiding the relevance of autoantibody results, and provide data to address an outstanding question from a recent ILAE consensus statement.[7]

This ILAE statement also highlighted controversy over the term 'autoimmune epilepsy'.[7] In routine clinical practice, this nomenclature acts as a valuable signpost and aide memoire when seeing patients with seizures.[2 14] However, 'epilepsy' carries several social stigmata and is defined by an enduring tendency to seizures. In AE, this lifelong risk is refuted by a recent study,[4] despite several forms of AE commonly leading to hippocampal atrophy.[2–4 7 10] The alternative concept of acute symptomatic seizures may more accurately capture the nature of seizures in patients with AE. Data-driven modifications to nomenclature will benefit from longer-term follow-up studies.

Ictal piloerection, low mood and attention and MRI limbic system changes are recognised features of late-onset AE, particularly in association with LGI1 antibodies.[2 4 14 15] The absence of movement disorders or more diffuse cognitive impairment as predictive factors in our model suggests the overall syndrome may reflect a *formes frustes* of AE. This contrasts with APE2 score parameters,[9] which appear to largely reflect more florid features seen in classical AE.

Our observational study has several limitations. These include limited CSF autoantibody measurements, which reflected UK practice particularly at the start of the study period. Yet,without this valuable parameter, a diagnosis of NMDAR-antibody encephalitis is still possible.[11] Yet, two of our four patients with serum NMDAR antibodies did not have features consistent with encephalitis, likely suggesting detection of clinically unrelated

serum antibodies in these cases. In addition, our series in total only identified nine AE cases, although this may be considered substantial given the largely outpatient-based recruitment. This, and the high (~10%) seroprevalence rate, may reflect a referral bias given Oxford's interest in AE, but is well aligned with other available estimates.[6 9 10] Our serological data identified some samples with NSAbs proven by live cell-based assays, but without concomitant cell surface neuronal reactivities. This was especially evident in the cohort without a clinical diagnosis of AE, and perhaps these antibodies reflect low-affinity or low-titre autoantibodies which are not disease relevant. Their specificity, however, remains reassuring given their typical selectivity for just one of eight surface-expressed autoantigens.

In the future, our prediction model will benefit from validation in independent, larger studies which may compare the risk of enduring seizures in the NSAb-positive versus NSAb-negative populations, with and without AE, something which we did not survey at follow-up. Hence, we cannot comment on long-term seizure status in the 5/16 patients (31%) who had NSAbs, no diagnosis of AE and 3-year mRS >0. In these patients, it remains possible that immunotherapy would have led to a greater benefit. However, in our view, this finding is more likely to be consistent with the predicted ~30% of all people with epilepsy who are known to become ASM resistant: this provides a testable hypothesis for a future randomised controlled trial.

Overall, our observations support the concept that, in patients who present with new-onset focal seizures, clinical features which are consistent with a 'mild encephalitis' helps identify those with NSAbs which should alter patient management. This clinico-serological syndrome appeared characteristic and its recognition will improve detection and treatment of these patients. These findings should discourage widespread screening strategies to identify patients with autoantibodies among unselected seizure cohorts.

Correction notice This article has been corrected since it appeared Online First. Author initial and ORCID have been added for Ronan N McGinty.

Twitter Sarosh R Irani @ANG_Oxford

Contributors Conception and design: BL, JA, AS, SRI. Acquisition of data: all authors. Analysis or interpretation of data: RMcG, AH, AR, SRI. Drafting of the manuscript: RMcG, AH, SRI. Critical revision of the manuscript for important intellectual content: all authors. Statistical analysis: AH, AR, RMcG.

Funding NIHR Clinical Lectureship to AH. SRI is supported by Epilepsy Research UK (P1201), the Wellcome Trust (104079/Z/14/Z), the UCB–Oxford Alliance, BMA Research Grants—Vera Down grant (2013) and Margaret Temple (2017), the Fulbright UK–US commission (MS-Society Research Award) and by the NIHR Oxford Biomedical Research Centre.

Disclaimer The views expressed are those of the authors and not necessarily those of the NHS, the NIHR or the Department of Health. The funders had no role in the design and conduct of the study; collection, management, analysis and interpretation of the data; preparation, review or approval of the manuscript; and decision to submit the manuscript for publication.

Competing interests SRI and PW are coapplicants and receive royalties on patent application WO/210/046716 (UK patent no. PCT/GB2009/051441) entitled 'Neurological Autoimmune Disorders'. The patent has been licensed for the development of assays for LGI1 and other VGKC-complex antibodies.

Patient consent for publication Not required.

Provenance and peer review Not commissioned; externally peer reviewed.

Supplemental material This content has been supplied by the author(s). It has not been vetted by BMJ Publishing Group Limited (BMJ) and may not have been peer-reviewed. Any opinions or recommendations discussed are solely those of the author(s) and are not endorsed by BMJ. BMJ disclaims all liability and responsibility arising from any reliance placed on the content. Where the content includes any translated material, BMJ does not warrant the accuracy and reliability of the translations (including but not limited to local regulations, clinical guidelines, terminology, drug names and drug dosages), and is not responsible for any error and/or omissions arising from translation and adaptation or otherwise.

Open access This is an open access article distributed in accordance with the Creative Commons Attribution 4.0 Unported (CC BY 4.0) license, which permits others to copy, redistribute, remix, transform and build upon this work for any purpose, provided the original work is properly cited, a link to the licence is given, and indication of whether changes were made. See: https://creativecommons.org/licenses/by/4.0/.

ORCID iDs
Ronan N McGinty http://orcid.org/0000-0002-4606-7783
Adam Handel http://orcid.org/0000-0001-8385-6346
Patrick Waters http://orcid.org/0000-0003-4142-2667
Sarosh R Irani http://orcid.org/0000-0002-7667-9748

REFERENCES

1 Irani SR, Michell AW, Lang B, *et al*. Faciobrachial dystonic seizures precede Lgi1 antibody limbic encephalitis. *Ann Neurol* 2011;69:892–900.
2 Thompson J, Bi M, Murchison AG, *et al*. The importance of early immunotherapy in patients with faciobrachial dystonic seizures. *Brain* 2018;141:348–56.
3 Geis C, Planagumà J, Carreño M, *et al*. Autoimmune seizures and epilepsy. *J Clin Invest* 2019;129:926–40.
4 de Bruijn MAAM, van Sonderen A, van Coevorden-Hameete MH, *et al*. Evaluation of seizure treatment in anti-LGI1, anti-NMDAR, and anti-GABABR encephalitis. *Neurology* 2019;92:e2185–96.
5 Scheffer IE, Berkovic S, Capovilla G, *et al*. ILAE classification of the epilepsies: position paper of the ILAE Commission for Classification and Terminology. *Epilepsia* 2017;58:512–21.
6 Brenner T, Sills GJ, Hart Y, *et al*. Prevalence of neurologic autoantibodies in cohorts of patients with new and established epilepsy. *Epilepsia* 2013;54:1028–35.
7 Steriade C, Britton J, Dale RC, *et al*. Acute symptomatic seizures secondary to autoimmune encephalitis and autoimmune-associated epilepsy: conceptual definitions. *Epilepsia* 2020;61:1341–51.
8 von Podewils F, Suesse M, Geithner J, *et al*. Prevalence and outcome of late-onset seizures due to autoimmune etiology: a prospective observational population-based cohort study. *Epilepsia* 2017;58:1542–50.
9 Dubey D, Alqallaf A, Hays R, *et al*. Neurological autoantibody prevalence in epilepsy of unknown etiology. *JAMA Neurol* 2017;74:397–402.
10 Dubey D, Kothapalli N, McKeon A, *et al*. Predictors of neural-specific autoantibodies and immunotherapy response in patients with cognitive dysfunction. *J Neuroimmunol* 2018;323:62–72.
11 Graus F, Titulaer MJ, Balu R, *et al*. A clinical approach to diagnosis of autoimmune encephalitis. *Lancet Neurol* 2016;15:391–404.
12 Makuch M, Wilson R, Al-Diwani A, *et al*. N-Methyl-D-aspartate receptor antibody production from germinal center reactions: therapeutic implications. *Ann Neurol* 2018;83:553–61.
13 Ramberger M, Berretta A, Tan JMM, *et al*. Distinctive binding properties of human monoclonal LGI1 autoantibodies determine pathogenic mechanisms. *Brain* 2020;143:1731–45.
14 Quek AML, Britton JW, McKeon A, *et al*. Autoimmune epilepsy: clinical characteristics and response to immunotherapy. *Arch Neurol* 2012;69:582–93.
15 Rocamora R, Becerra JL, Fossas P, *et al*. Pilomotor seizures: an autonomic semiology of limbic encephalitis? *Seizure* 2014;23:670–3.

Supplementary Table 1. Information captured by clinical phenotyping database

Clinical features
Sex
Antibody status
Date of birth
Date of study recruitment
Date of first seizure
Epilepsy risk factors (neonatal, perinatal, focal neurological insults, family history of epilepsy or Alzheimer's disease)
Formal psychiatric disorder prior to epilepsy diagnosis
Personal or family history of autoimmunity
Personal history of malignancy
History of status epilepticus
Self-reported neuropsychiatric changes (memory/psychosis/mood/anxiety) Number of seizures in 2/6/12/24/36/48 months from onset
Total number, type and duration of anti-seizure medications (ASMs) trialled
Non-ASM medications including immunotherapy trials for seizure-control (date/type/route/course length/dose)
Number of seizures in first 3/6/12/24/36/48 months after ASM commenced
Seizure-cessation reached (Yes/No)
Time to seizure-cessation from starting ASM (months)
Adverse effect from ASM
Investigations
Serum sodium
MRI result
EEG result
Clinical assessments/scores
Hospital Anxiety and Depression Score (HADS)
Addenbrooke's Cognitive Examination-Revised (ACE-R) score
Quality of Life in Epilepsy-31 (QOLIE-31) score
Antibody Prevalence in Epilepsy and Encephalopathy (APE2) score
Autoimmune encephalitis (clinical diagnosis and as defined by Graus et al[11])

Supplementary Table 2. Antibody Prevalence in Epilepsy and Encephalopathy Score (APE2) criteria. The maximum score is 18 points, and a total score of 4 or more has been considered suggestive for underlying autoantibodies.[10]

Criteria	Points
New-onset, rapidly progressive mental status changes or new-onset seizure activity	**+1**
Neuropsychiatric changes	**+1**
Autonomic dysfunction	**+1**
Viral prodrome	**+2**
Faciobrachial dystonic movements	**+3**
Facial dyskinesias without faciobrachial dystonic movements	**+2**
Seizures refractory to at least two anti-seizure medicines	**+2**
CSF inflammation	**+2**
Brain MRI consistent with encephalitis	**+2**
Systemic malignancy within five years of neurological symptom onset	**+2**

Supplementary Table 3. Autoantibody detection. Live cell-based assays (CBA) were used to detect NSAbs to leucine-rich glioma inactivated-1 (LGI1), contactin-associated protein-like 2 (CASPR2), contactin-2, dipeptidyl-peptidase-like protein 6 (DPPX), N-methyl-D-aspartate receptor (NMDA-R), α-amino-3-hydroxy-5-methyl-4-isoxazole propionic acid receptor (AMPA-R), γ-aminobutyric acid A receptor ($GABA_AR$), γ-aminobutyric acid B receptor ($GABA_BR$) and the glycine receptor. A radioimmunoprecipitation assay (RIPA) was used to detect antibodies to glutamic acid decarboxylase-65 (GAD65). Live neuronal-based assays (NBA) tested for antibody binding to neuronal surface antigens.

Target antigen	Assay method
GAD65	RIPA
LGI1	Live CBA
CASPR2	Live CBA
Contactin-2	Live CBA
AMPA-R	Live CBA
$GABA_AR$	Live CBA
$GABA_BR$	Live CBA
Glycine receptor	Live CBA
NMDA-R	Live CBA
Hippocampal neuron surface binding without the above reactivities	Live NBA

Supplementary Table 4. Patients excluded from study

Reason for exclusion	Number of patients
<18 years	1
Duplicate registration	1
Generalised epilepsy	3
Epilepsy diagnosis >12months	5
Focal epilepsy diagnosis unconfirmed	9
Clinical information unavailable	1
No serum samples received	2

Appendix B: Diagnostic criteria for autoimmune encephalitis

Adapted from Graus F, Titulaer MJ, Balu R, et al. Position Paper: A clinical approach to diagnosis of autoimmune encephalitis. Lancet Neurol. 2016;15(April):391-404. doi:10.1016/S1474-4422(15)00401-9[284]

Possible autoimmune encephalitis (AIE) (all three criteria)

1. <3 months of (one of:)
    - memory deficits
    - mental state changes (one of:)
        - decreased **or** altered level of consciousness
        - lethargy
        - personality change
    - psychiatric symptoms
2. >One of:
    - new focal central nervous system (CNS) findings
    - new onset seizures
    - CSF white cell count (WCC) >5
    - MRI suggestive of encephalitis
        - hyperintense FLAIR signal to one **or** both medial temporal lobe(s)
        - multifocal grey matter **or** white matter **or** both, compatible with demyelination **or** inflammation
3. Reasonable exclusion of alternative causes

Definite autoimmune limbic encephalitis (AI LE) (all four criteria)

1. <3 months of (one of:)
    - memory deficits
    - seizures
    - psychiatric symptoms suggesting limbic system involvement
2. Bilateral brain abnormalities on FLAIR restricted to medial temporal lobes
3. > One of:
    - CSF WCC >5
    - EEG (one of:)
        - Epileptic activity involving temporal lobes
        - Slow wave activity involving temporal lobes
4. Reasonable exclusion of alternative causes

Definite acute disseminated encephalomyelitis (ADEM) (all five criteria)

1. First multifocal, clinical CNS event of presumed inflammatory demyelinating cause
2. Encephalopathy unexplained by fever
3. Abnormal brain MRI (one of:)
    - diffuse poorly demarcated large (>1-2cm) lesions predominantly involving cerebral white matter
    - T1 hypointense lesions in white matter (rare)
    - deep grey matter abnormalities (e.g. thalamus **or** basal ganglia)
4. No new clinical **or** MRI findings after 3 months of symptom onset
5. Reasonable exclusion of alternative causes

Probable anti-NMDA-R encephalitis (first three criteria +/- forth)

1. <3months of (>four of):
    - abnormal (psychiatric) behaviour **or** cognitive dysfunction
    - speech dysfunction (pressured speech **or** verbal reduction **or** mutism)
    - seizures
    - movement disorder **or** dyskinesias **or** rigidity/abnormal postures
    - decreased level of consciousness
    - autonomic dysfunction **or** central hypoventilation
2. >One of:
    - Abnormal EEG (one of:)
        - focal slow activity
        - diffuse slow activity
        - disorganised activity
        - epileptic activity
        - extreme delta brush)
    - CSF with pleocytosis **or** oligoclonal bands
3. Reasonable exclusion of other disorders
4. Teratoma: Yes / No

Definite anti-NMDA-R encephalitis (all three criteria)

1. >1 of:
    - abnormal (psychiatric) behaviour **or** cognitive dysfunction
    - speech dysfunction (pressured speech **or** verbal reduction **or** mutism)
    - seizures
    - movement disorder **or** dyskinesias **or** rigidity/abnormal postures
    - decreased level of consciousness
    - autonomic dysfunction **or** central hypoventilation
2. IgG anti-GluN1 antibodies
3. Reasonable exclusion of alternative causes

Autoantibody negative but probable autoimmune encephalitis (all four criteria)

1. <3 months of (one of:)
    - memory deficits
    - mental state changes (one of:)
    - decreased **or** altered level of consciousness
    - lethargy
    - personality change
    - psychiatric symptoms
2. Exclusion of well-defined syndromes of AIE (e.g. typical LE, Bickerstaff's brainstem encephalitis, ADEM)
3. Absence of well characterised autoantibodies in serum and CSF
   PLUS >2 of:
    - MRI abnormalities suggestive of AIE;
    - CSF pleocytosis, CSF-specific oligoclonal bands or elevated CSF IgG index or both
    - brain biopsy showing inflammatory infiltrates and excluding other disorders (e.g. tumour)
4. Reasonable exclusion of alternative causes

Appendix C: Clinical phenotyping database for the drug-resistant epilepsy study

Ronan McGinty

Selected categories and pre-populated responses from database

Ethic background
1|African-British Black
2|African-North African
3|African-Sub Saharan African
4|American-African-American
5|American-Black Caribbean
6|American-Latin American
7|American-White American
8|Asian-Bangladeshi
9|Asian-Chinese Han
10|Asian-Chinese Other
11|Asian-Filipino
12|Asian-Indian
13|Asian-Japanese
14|Asian-Korean
15|Asian-Other
16|Asian-Pakistani
17|Middle Eastern
18|Pacific Islander
19|Not known
20|Other mixed background
21|White and Asian
22|White and Black African
23|White and Black Caribbean
24|White
25|White-Irish
26|White-Other
27|White-Northern European
28|White-Southern European

Living circumstances
1|Alone
2|Not known
3|With friend(s)
4|With kids
5|With parents
6|With partner
7|With partner & kids
8|With partner, parents & kids
9|With partner & parents
10|Away at university

Relationship status
1|Long-term partner, never married/civil partnered
2|Long-term partner, previously divorced
3|Married/civil partnered, never married/civil partnered
4|Married/civil partnered, previously divorced
5|Not known
6|Single, never married/civil partnered
7|Single, previously divorced
8|Widow/widower

Employment status
1|Full time paid work
2|Full time student
3|Full time voluntary work
4|Not known
5|Part time paid work
6|Part time student
7|Part time student with part time paid work
8|Part time student with part time voluntary work
9|Part time voluntary work
10|Retired at expected age
11|Retired early (unrelated to epilepsy)
12|Retired early due to epilepsy
13|Unemployed (unrelated to epilepsy)
14|Unemployed due to epilepsy

Highest level of education (including ongoing studies)
1|Below GCSE level or equivalent
2|GCSEs or equivalent
3|A-levels or equivalent
4|Sub-degree higher level education
5|Degree higher level education
6|Post-graduate level higher education
7|Special School
8|Not known

Alcohol Intake
1|less than 5 units/week
2|5 – 10 units/week
3|11 – 15 units/week

4|16 – 20 units/week
5|21 – 25 units/week
6|26 – 30 units/week
7|31 – 35 units/week
8|36 – 40 units/week
9|41 – 45 units/week
10| 46 – 50 units/week
11| > 50 units/week
12| None
13|Not known

Smoking status
1|Current smoker
2|Ex-smoker
3|Lifelong non-smoker
4|Not known

Illicit drug use
1|Never in life
2|Not known
3|Cannabis (< 5 times per year at present)
4|Cannabis (< 5 times per year in past)
5|Cannabis (daily at present)
6|Cannabis (daily in past)
7|Cannabis (not daily but most weeks at present)
8|Cannabis (not daily but most weeks in past)
9|Cannabis (not weekly but most months at present)
10|Cannabis (not weekly but most months in past)
11|Cocaine (<5 times per year at present)
12|Cocaine (<5 times per year in past)
13|Cocaine (daily at present)
14|Cocaine (daily in past)
15|Cocaine (not daily but most weeks at present)
16|Cocaine (not daily but most weeks in past)
17|Cocaine (not weekly but most months at present)
18|Cocaine (not weekly but most months in past)
19|Ecstasy (< 5 times per year at present)
20|Ecstasy (< 5 times per year in past)
21|Ecstasy (daily at present)
22|Ecstasy (daily in past)
23|Ecstasy (not daily but most weeks at present)
24|Ecstasy (not daily but most weeks in past)
25|Ecstasy (not weekly but most months at present)
26|Ecstasy (not weekly but most months in past)
27|Heroin (< 5 times per year at present)
28|Heroin (< 5 times per year in past)
29|Heroin (daily at present)
30|Heroin (daily in past)
31|Heroin (not daily but most weeks at present)
32|Heroin (not daily but most weeks in past)
33|Heroin (not weekly but most months at present)
34|Heroin (not weekly but most months in past)
35|LSD (< 5 times per year at present)
36|LSD (< 5 times per year in past)
37|LSD (daily at present)
38|LSD (daily in past)
39|LSD (not daily but most weeks at present)
40|LSD (not daily but most weeks in past)
41|LSD (not weekly but most months at present)
42|LSD (not weekly but most months in past)
43|Magic mushrooms (< 5 times per year at present)
44|Magic mushrooms (< 5 times per year in past)
45|Magic mushrooms (daily at present)
46|Magic mushrooms (daily in past)
47|Magic mushrooms (not daily but most weeks at present)
48|Magic mushrooms (not daily but most weeks in past)
49|Magic mushrooms (not weekly but most months at present)
50|Magic mushrooms (not weekly but most months in past)
51|Spice (< 5 times per year at present)

52|Spice (< 5 times per year in past)
53|Spice (daily at present)
54|Spice (daily in past)
55|Spice (not daily but most weeks at present)
56|Spice (not daily but most weeks in past)
57|Spice (not weekly but most months at present)
58|Spice (not weekly but most months in past)

Driving status
1|Legally driving
2|Licence but doesn't drive
3|Licence withdrawn by DVLA due to epilepsy
4|Licence withdrawn by DVLA (non-epilepsy related)
5|Never had licence (non-epilepsy related)
6|Never had licence due to epilepsy
7|Not known

Chronic autoimmune disease
1|None
2|Alopecia
3|Atopy (asthma, allergic rhinitis, eczema)
4|Autoimmune hepatitis
5|Coeliac disease
6|Crohn's disease
7|Diabetes mellitus type I
8|Hyperthyroidism
9|Hypothyroidism (autoimmune)
10|Hypothyroidism (post-autoimmune hyperthyroidism treatment)
11|Multiple sclerosis
12|Myasthenia Gravis
13|Neuromyelitis optica spectrum disorders
14|Psoriasis
15|Psoriatic arthritis
16|Rheumatoid arthritis
17|Sjögren's
18|Systemic lupus erythematosus (SLE)
19|Ulcerative colitis
20|Vitiligo
21|Interstitial pneumonitis
22|Chronic idiopathic urticaria
23|Lichen Planus
24|Chronic anterior uveitis
25|Juvenile Onset Rheumatoid Arthritis
26|Anti-phospholipid syndrome
27|Reactive Arthritis
28|Polymyalgia rheumatica

Formal psychiatric diagnosis
1|Anxiety
2|Anxiety and depression
3|Bipolar disorder
4|Depression
5|Eating disorder
6|None
7|Not Known
8|Obsessive compulsive disorder
9|Organic Personality Disorder
10|Personality disorder
11|Psychosis
12|Schizophrenia
13|Substance misuse/dependence (incl. alcohol)
14|Apathy
15|Functional neurological disorder
16|Prolonged grief reaction
17|Post traumatic stress disorder
18|ADHD

Detention under Mental Health Act
1|No
2|Not known
3|Yes (>1)
4|Yes (once only)

History of peri-ictal psychosis
1|No
2|Not known
3|Yes (once only)
4|Yes (>1)

Non-Epilepsy Related Medication
1|None
2|Alendronic acid
3|Amiloride
4|Amitriptyline

5|Amlodipine
6|Apixiban
7|Aspirin
8|Atenolol
9|Atorvastatin
10|Bendroflumethiazide
11|Bisoprolol
12|Bumetanide
13|Calcium
14|Candesartan
15|Citalopram
16|Clopidogrel
17|Co-codamol
18|Codeine
19|Colecalciferol
20|Cyclizine
21|Diclofenac
22|Diltiazem
23|Doxazosin
24|Esomeprazole
25|Ferrous sulphate
26|Fluoxetine
27|Folic acid
28|Furosemide
29|Gliclazide
30|Haliperidol
31|Ibuprofen
32|Indapamide
33|Insulin
34|Ipratroprium
35|Lactulose
36|Lansoprazole
37|Levothyroxine
38|Lisinopril
39|Losartan
40|Metformin
41|Metoclopramide
42|Mirtazapine
43|Movicol
44|Multivitamins
45|Naproxen
46|Nifedipine
47|Olanzapine
48|Omeprazole
49|Paracetamol
50|Pravastatin
51|Quinine
52|Ramipril
53|Ranitidine
54|Rivaroxaban
55|Salbutamol
56|Senna
57|Sertraline
58|Simvastatin
59|Sipronolactone
60|Sodium docusate
61|Tamsulosin
62|Theophylline
63|Thiamine
64|Tiotropium
65|Tramadol
66|Venlafaxine
67|Warfarin
68|Zopiclone

Handedness
1|Ambidextrous
2|Left-handed but previously right-handed
3|Left-handed lifelong
4|Not known
5|Right-handed but previously left-handed
6|Right-handed lifelong

Seizure onset localisation
1|Not known
2|EEG confirmed: Bilateral hemispheric involvement at onset
3|EEG confirmed: Frontal – bilateral
4|EEG confirmed: Frontal – left
5|EEG confirmed: Frontal – right
6|EEG confirmed: Left hemispheric lateralisation at onset
7|EEG confirmed: Occipital – bilateral
8|EEG confirmed: Occipital – left
9|EEG confirmed: Occipital – right
10|EEG confirmed: Parietal – bilateral
11|EEG confirmed: Parietal – left
12|EEG confirmed: Parietal – right

13|EEG confirmed: Right hemispheric lateralisation at onset
14|EEG confirmed: Temporal – bilateral
15|EEG confirmed: Temporal – left
16|EEG confirmed: Temporal – right
17|Presumed extratemporal – unknown lateralisation
18|Presumed frontal – left
19|Presumed frontal – right
20|Presumed frontal – unknown lateralisation
21|Presumed occipital – left
22|Presumed occipital – right
23|Presumed occipital – unknown lateralisation
24|Presumed parietal – left
25|Presumed parietal – right
26|Presumed parietal – unknown lateralisation
27|Presumed temporal – left
28|Presumed temporal – right
29|Presumed temporal – unknown lateralisation
30|Scalp EEG non-localising, presumed focal
31|Scalp EEG non-localising, presumed generalised
32|Multifocal
33|Presumed left hemisphere onset
34|Presumed right hemisphere onset
35|Scalp EEG non-localising, presumed generalised and focal

Presumed epilepsy aetiology

1|Amyloid angiopathy
2|Arteriovenous malformation
3|Autoimmune encephalitis (antibody detected)
4|Autoimmune encephalitis (no antibody detected)
5|Bacterial meningitis/meningoencephalitis
6|Brain tumour – primary
7|Cerebral angioma/Cavernoma
8|Cerebral malaria
9|Cerebral toxoplasmosis
10|Cerebrovascular disease (no stroke)
11|Cerebrovascular disease (stroke)
12|Chromosomal abnormality
13|Cryptogenic (no cause identified)
14|Dysembryoplastic neuroepithelial tumour (DNET)
15|Encephalitis (no cause identified)
16|Focal cortical dysplasia (FCD)
17|FCD & DNET
18|FCD & ganglioglioma
19|Ganglioglioma
20|Genetic (previously 'idiopathic')
21|Genetic syndrome (known gene)
22|Genetic syndrome (no gene identified)
23|Grey matter heterotopia
24|Hemimegalencephaly
25|Hippocampal sclerosis
26|Human immunodeficiency virus (HIV)
27|Hydrocephalus
28|Hypothalamic hamartoma
29|Hypoxic ischaemic injury
30|Immune
31|Lissencephaly
32|Metabolic
33|Mitochondrial disease
34|Neurocysticercosis
35|Neurofibromatosis
36|Perinatal insult/stroke
37|Polymicrogyria
38|Porencephalic cyst
39|Rassmussan's encephalitis
40|Recreational drugs/ETOH
41|Schizencephaly
42|Storage disorder
43|Stroke – ischaemic/haemorrhagic
44|Sturge Weber syndrome
45|Subcortical band heterotopia
46|Traumatic brain injury
47|Tuberculosis
48|Tuberous sclerosis
49|Viral encephalitis
50|Not known
51|Meningioma

Specific epilepsy syndrome

1|Aicardi syndrome

2|Angelman syndrome
3|Autosomal dominant epilepsy with auditory features
4|Autosomal dominant nocturnal frontal lobe epilepsy
5|Benign myoclonic epilepsy in infancy
6|Benign neonatal convulsions
7|Benign partial epilepsy in infancy
8|Benign rolandic epilepsy
9|Childhood absence epilepsy (CAE)
10|Dravet syndrome
11|Early myoclonic encephalopathy
12|Electrical status epilepticus during slow-wave sleep (ESESS)
13|Epilepsy with GTCS alone
14|Epilepsy of infancy with migrating focal seizures
15|Epilepsy with myoclonic absences
16|Eyelid myoclonia with absences (EMA)
17|Familial focal epilepsy with variable foci
18|Focal epilepsy – not specified
19|Focal and generalised epilepsy
20|Frontal lobe epilepsy
21|GLUT1 deficiency syndrome
22|Gelastic Epilepsy
23|Generalised epilepsy – not specified
24|Generalised epilepsy with febrile seizure plus (GEFS+)
25|Juvenile absence epilepsy
26|Juvenile myoclonic epilepsy
27|Lafora disease
28|Landau-Kleffner syndrome
29|Late-onset myoclonic epilepsy in Down's syndrome
30|Lennox-Gastaut syndrome or phenotype
31|Mitochondrial disorders
32|Myoclonic astatic epilepsy (Doose syndrome)
33|Mitochondrial encephalomyopathy, lactic acidosis, and stroke-like episodes (MELAS)
34|Myoclonic epilepsy with ragged red fibres (MERRF)
35|Occipital lobe epilepsy
36|Ohtahara syndrome
37|Panayiotopoulos syndrome
38|Photosensitive occipital lobe epilepsy
39|POLG1
40|Progressive myoclonus epilepsy
41|Rasmussen's encephalitis/Rasmussen syndrome
42|Reflex epilepsy
43|Rett syndrome
44|Ring chromosome 20
45|Self-limiting late onset occipital epilepsy
46|Sturge-Weber syndrome
47|Temporal lobe epilepsy (lateral/neocortical)
48|Temporal lobe epilepsy (mesial)
49|Temporal lobe epilepsy (unspecified)
50|Unverricht-Lundborg disease
51|West syndrome
52|No specific syndrome identified

Epilepsy Risk Factor
1|Alzheimer's disease
2|Austistic spectrum disorder
3|Brain tumour
4|Cerebal abscess
5|Childhood developmental delay
6|Down's syndrome
7|Encephalitis (autoimmune)
8|Encephalitis (infectious)
9|Encephalitis (Unknown aetiology)
10|Family history of epilepsy (1st degree relative)
11|Family history of epilepsy (non-1st degree relative)
12|Family history of neurological disorder
13|Febrile convulsion (not specified)
14|Febrile convulsion-complex (focal, recurrence within 24hrs, 15-30mins)
15|Febrile convulsion-simple (generalised, once in 24hrs, <15mins)
16|Febrile status epilepticus (>30mins)
17|Head injury requiring neurosurgical intervention
18|Learning disability not otherwise stated
19|Meningitis (bacterial)
20|Meningitis (viral)

21|Meningitis (cause not known)
22|Neonatal complication (during first 4 weeks of life)
23|Neurocutaneous syndrome (incontinentia pigmenti, neurofibromatosis type 1, Sturge Weber Syndrome, tuberous sclerosis complex)
24|Perinatal complication (before or immediately after birth)
25|Post-vaccine seizure
26|Small vessel ischaemic disease
27|Stroke
28|None
29|Not known
30|Head injury – nil neurosurgical intervention required

Total number of GTCS in lifetime
1|0
2|1 – 10
3|11 – 50
4|51 – 100
5|>100

Longest-ever period of seizure-freedom
1|<24 hours
2|>24 hours and <1 week
3|1-2 weeks
4|3-4 weeks
5|4-8 weeks
6|3-6 months
7|6-12 months
8|1-2 years
9|>2 years
10|Not known

Cause of Epilepsy in 1st Degree Relative
1|Acquired(i.e. secondary to prenatal complications, traumatic brain injury, stroke, tumour, cerebrovascular disease etc)
2|Non-acquired (i.e. genetic)
3|Not known

Known genetic mutations pre-enrolment
1|never been tested
2|tested
3|tested but no mutations identified
4|tested but result not known

MRI Key Findings
1|Acute inflammatory change
3|Amygdala dysplasia
4|Arteriovenous malformation
5|Brain metastases
6|Brain tumour – extra-axial
7|Brain tumour – intra-axial
8|Cerebral angioma/Cavernoma
9|Cerebellar atrophy
10|Cerebral atrophy – focal
11|Cerebral atrophy – generalized
12|Cerebral infection
13|Cortical dysplasia – focal
14|Cortical dysplasia – multifocal
15|Cortical Tubers/Hamartomas
16|Dysembryoplastic neuroepithelial tumour (DNET)
17|Encephalocele
18|Encephalomalacia/gliosis
19|Encephalitis
20|Ganglioglioma
21|Glioma – anaplastic astrocytoma, WHO III
22|Glioma – glioblastoma multiforme, WHO IV
23|Glioma – low-grade, WHO I – II
24|Grey matter heterotopia – periventricular nodular heterotopia, bilateral
25|Grey matter heterotopia – periventricular nodular heterotopia, unilateral,
26|Grey matter heterotopia – subcortical band heterotopia/Double cortex
27|Hemimegalencephaly – right
28|Hemimegalencephaly – left
29|Hemimegalencephaly – bilateral
30|Hippocampal atrophy – bilateral
31|Hippocampal atrophy – unilateral, left
32|Hippocampal atrophy – unilateral, right
33|Hydrocephalus
34|Hypothalamic Hamartoma
35|Hypoxic ischaemic injury

36|Increased T2 signal hippocampus – bilateral
37|Increased T2 signal hippocampus – unilateral, left
38|Increased T2 signal hippocampus – unilateral, right
39|Lissencephaly/lissencephaly-agyria-pachygyria complex
40|Meningioma
41|Meningitis/Meningoencephalitis
42|Mitochondrial disease changes
43|MVNT – Multiloculated and vacuolating neuronal tumour
44|Normal
45|Not known
46|Perinatal insult
47|Polymicrogyria – bilateral and diffuse
48|Polymicrogyria – focal or multifocal
49|Porencephalic cyst
50|Schizencephaly
51|Small Vessel Disease
52|Stroke – haemorrhagic or ischaemic
53|Sturge-Weber syndrome changes
54|Superficial siderosis
55|Traumatic gliosis
56|Ventriculomegaly
57|Malrotation or inversion abnormalities of the hippocampi
58|Developmental venous anomalies
59|Arachnoid cyst
60|Ulegyria
61|Hippoplasia of the hippocampi +/-other structures
62|Skull or other bony abnormalities
63|Meningioangiomatosis
64|Rosette forming glioneuronal tumour
65|Aneurysm

PET Key Finding
1|Focal hypometabolism – frontal lobe, left
2|Focal hypometabolism – frontal lobe, right
3|Focal hypometabolism – frontal lobes, bilateral
4|Focal hypometabolism – not specified
5|Focal hypometabolism – occipital lobe, left
6|Focal hypometabolism – occipital lobe, right
7|Focal hypometabolism – occipital lobes, bilateral
8|Focal hypometabolism – parietal lobe, left
9|Focal hypometabolism – parietal lobe, right
10|Focal hypometabolism – parietal lobes, bilateral
11|Focal hypometabolism – temporal lobe, left
12|Focal hypometabolism – temporal lobe, right
13|Focal hypometabolism – temporal lobes, bilateral
14|Normal
15|Not performed

EEG Key Findings
1|Definite focal epileptiform abnormalities
2|Definite generalised epileptiform abnormalities
3|Focal slowing
4|Focal fast activity
5|Generalised slowing
7|Normal
8|Photosensitivity
9|Slow spike and wave
10|Suspected focal epileptiform abnormalities
11|Suspected generalised epileptiform abnormalities
12|Non-specific abnormalities
13|No EEG performed

Seizure facilitating triggers
1|None recognised
2|Alcohol intake
3|Exercise
4|Menstruation
5|Missed meals
6|Non-Compliance with Medication
7|Pain
8|Psychological stress
9|Sleep
10|Sleep-deprivation

11|Not known
12|Ambient heat
13|Hunger
14|Relaxation or 'let down'
15|Strong emotions
16|Other

Seizure-related injuries
1|Burns requiring skin graft – multiple times
2|Burns requiring skin graft – once only
3|Burns without complication – multiple times
4|Burns without complication – once only
5|Dental injuries – multiple times
6|Dental injuries – once only
7|Head injury (mild/moderate severity) – multiple times
8|Head injury (mild/moderate severity) – once only
9|Head injury requiring neurosurgical intervention – multiple times
10|Head injury requiring neurosurgical intervention – once only
11|Joint dislocation requiring orthopaedic surgery – multiple times
12|Joint dislocation requiring orthopaedic surgery – once only
13|Joint dislocation treated with closed reduction – multiple times
14|Joint dislocation treated with closed reduction – once only
15|Limb fracture(s) – multiple times
16|Limb fracture(s) – once only
17|None
18|Road traffic accident (driver) – multiple times
19|Road traffic accident (driver) – once only
20|Road traffic accident (pedestrian) – multiple times
21|Road traffic accident (pedestrian) – once only
22|Spinal fracture(s) – multiple times
23|Spinal fracture(s) – once only
24|Superficial soft tissue injuries
25|Tongue biting
26|Not known
27|Eye injury
28|Vascular injury
29|Near drowning/drowning
30|Other

Localisation suggested by EEG
1|Focal
2|Generalised
3|None / unclear
4|Focal and generalised

Syndrome suggested by EEG
1|Landau-Klefner syndrome
2|Progressive myoclonic epilepsy
3|Genetic generalised epilepsy
4|Temporal lobe epilepsy
5|Frontal lobe epilepsy
6|Occipital lobe epilepsy
7|Parietal lobe epilepsy
8|Epileptic encephalopathy
9|Lennox-Gastaut syndrome
10|None / unclear

Reflex epilepsy traits
1|Audiogenic
2|Eye closure sensitivity
3|Fixation-off
4|Gustatory
5|Hot water
6|Kinaesthetic
7|Musicogenic
8|None
9|Not known
10|Olfactory
11|Pattern sensitivity
12|Photosensitivity
13|Praxis
14|Primary reading epilepsy
15|Somatosensory
16|Startle
17|Thinking
18|Vestibulogenic

Seizure type (most frequent first)
1|Focal onset (impaired awareness)
2|Focal onset (aware)
3|Focal onset (impaired awareness) to bilateral tonic-clonic
4|Focal onset (aware) to bilateral tonic-clonic
5|Generalised onset
6|Unknown onset

Motor or non-motor onset
1|Motor
2|Non-motor
3|Not known

Very first feature(s) at seizure onset (aura)
1|Atonia (loss of muscle tone)
2|Atypical absence (slow onset/offset, marked change in tone, EEG spike-waves <3Hz)
3|Behaviour arrest (prominent feature of entire Sz)
4|Blinking
5|Burping
6|Cardiac palpitations
7|Clonus – unilateral
8|Clonus – bilateral
9|Cognitive (impaired language/other cog domains; positive features, eg déjà vu, hallucinations, perceptual distortions)
10|Complex motor/hypermotor activity
11|Crying
12|Cyanosis
13|Déjà vu
14|Diaphoresis
15|Drop attack
16|Dystonic posturing – unilateral
17|Dystonic posturing – bilateral asymmetric
18|Emotional features (anxiety, fear, joy etc)
19|Epileptic spasms (1-2 secs, cluster)
20|Eyelid myoclonia
21|Flushing
22|Forced speech
23|Gastrointestinal symptoms
24|Hyperkinetic (including leg pedalling)
25|Hypersalivation
26|Indescribable aura
27|Incontinence
28|Jamais vu
29|Laughter
30|Manual automatisms (complex movement without conscious awareness or purposeful intent)
31|Mydriasis/miosis
32|Myoclonic absence
33|Myoclonic-atonic movements
34|Myoclonic-tonic-clonic movements
35|Myoclonus (regular non-sustained jerking for milliseconds)
36|Nausea
37|No recalled aura
38|Olfactory aura
39|Orofacial automatisms (complex movement without conscious awareness or purposeful intent)
40|Pilo erection
41|Respiratory change
42|Rising epigastric sensation
43|Sensory symptoms
44|Speech disturbance
45|Staring/loss of facial expression
46|Tonic movements (muscle stiffening)
47|Tonic-clonic movements
48|Transient epileptic amnesia
49|Typical absence
50|Vertigo/dizziness
51|Versive head turn
52|Visual aura
53|Visual aura - unilateral
54|Vomiting
55|Not known
56|Auditory Aura
57|Gustatory aura
58|Cephalic Aura
59|Pallor
60|Autonomic symptoms
61|Palpitations
62|Choking sensation

Early observed clinical signs
1|Atonia (loss of muscle tone)
2|Atypical absence (slow onset/offset, marked change in tone, EEG spike-waves <3Hz)
3|Behaviour arrest (prominent feature of entire Sz)
4|Blinking
5|Burping
6|Cardiac palpitations
7|Clonus – unilateral
8|Clonus – bilateral
9|Cognitive (impaired language/other cog domains; positive features, e.g. déjà vu, hallucinations, perceptual distortions)
10|Complex motor/hypermotor activity
11|Crying
12|Cyanosis
13|Déjà vu
14|Diaphoresis
15|Drop attack
16|Dystonic posturing - unilateral
17|Dystonic posturing - bilateral asymmetric
18|Emotional features (anxiety, fear, joy etc)
19|Epileptic spasms (1-2 secs, cluster)
20|Eyelid myoclonia
21|Flushing
22|Forced speech
23|Gastrointestinal symptoms
24|Hyperkinetic (including leg pedalling)
25|Hypersalivation
26|Indescribable aura
27|Incontinence
28|Jamais vu
29|Laughter
30|Manual automatisms (complex movement without conscious awareness or purposeful intent)
31|Mydriasis/miosis
32|Myoclonic absence
33|Myoclonic-atonic movements
34|Myoclonic-tonic-clonic movements
35|Myoclonus (regular non-sustained jerking for milliseconds)
36|Nausea
37|No recalled aura
38|Olfactory aura
39|Orofacial automatisms (complex movement without conscious awareness or purposeful intent)
40|Pilo erection
41|Respiratory change
42|Rising epigastric sensation
43|Sensory symptoms
44|Speech disturbance
45|Staring/loss of facial expression
46|Tonic movements (muscle stiffening)
47|Tonic-clonic movements
48|Transient epileptic amnesia
49|Typical absence
50|Vertigo/dizziness
51|Versive head turn
52|Visual aura
53|Visual aura - unilateral
54|Vomiting
55|Not known
56|Auditory Aura
57|Gustatory aura
58|Cephalic Aura
59|Pallor
60|Autonomic symptoms
61|Palpitations
62|Choking sensation

Seizure frequency
Free-text number
Per:
1|Day
2|Week
3|Fortnight
4|Month
5|Year

Number of clusters
Free-text number
Per:
1|Day
2|Week
3|Fortnight

4|Month
5|Year

Anti-seizure medications
1|Brivaracetam (BRI)
2|Carbamazepine (CBZ)
3|Clobazam (CLB)
4|Clonazepam (CLN)
5|Diazepam (DZP)
6|Eslicarbazepine (ESL)
7|Ethosuximide (ESM)
8|Felbamate (FMB)
9|Gabapentin (GBP)
10|Lacosamide (LCM)
11|Levetiracetam (LEV)
12|Lamotrigine (LTG)
13|Lorazepam (LZP)
14|Nitrazepam (NTZ)
15|Oxcarbazepine (OXC)
16|Phenobarbital (PB)
17|Perampanel (PER)
18|Pregabalin (PGB)
19|Phenytoin (PHT)
20|Primidone (PRM)
21|Rufinamide (RTG)
22|Retigabine (RTG)
23|Sodium Valproate (VPA)
24|Tiagabine (TGB)
25|Topiramate (TPM)
26|Vigabatrin (VGB)
27|Zonisamide (ZNS)
28|None
29|Acetazolamide (AZT)

Rescue medication
1|Clobazam (CLB) PO
2|Diazepam (DZP) PR
3|Midazolam (MDZ) BUCCAL
4|None
5|Not used for >1 year

Adverse Effects
1|Angioedema
2|Antiepileptic hypersensitivity syndrome
3|Appetite change
4|Ataxia
5|Behavioural change
6|Blood disorder
7|Cardiac disorders
8|Confusion
9|Dermatitis
10|Dizziness
11|Drowsiness, fatigue, lethargy or somnolence
12|Drug rash with eosinophilia and systemic symptoms (DRESS) syndrome
13|Erythema multiforme
14|Gastrointestinal disturbance
15|Gingival hypertrophy
16|Gynaecomastia
17|Hair loss
18|Headache
19|Hepatic dysfunction
20|Hirsutism
21|Hyperammonaemia
22|Hyponatraemia
23|Impaired concentration or memory
24|Insomnia
25|Mood disturbance
26|Nystagmus
27|Polyarteritis nodosa
28|Renal dysfunction
29|Renal or urinary calculi
30|Seizure exacerbation
31|Skin rash-not specified
32|Stevens-Johnson syndrome
33|Systemic lupus erythematosus
34|Toxic epidermal necrolysis
35|Tremor
36|Urticaria
37|Visual disturbance
38|Visual field defect
39|Weight change
40|Not known
41|None
42|Drug interaction
43|Nephrolithiasis
44|Osteopenia/Osteoporosis

45|Other adverse drug reaction
46|Patient decision
47|Pregnancy planning
48|Seizure improvement

Likely reasons for change in seizure frequency
1|No change in Sz frequency
2|No reason identified
3|Medication change
4|Lifestyle change
5|New epilepsy surgery
6|New VNS implant
7|Depleted VNS battery replaced
8|Immunotherapy

Immunotherapy
1|N/A
2|Azathiaprine
3|Dexametasone
4|Intravenous immunoglobulin (IVIg)
5|Intravenous methylprednisolone (IVMP)
6|Mycophenolate
7|Plasma exchange/PLEX
8|Prednisolone
9|Rituximab
10|Not known

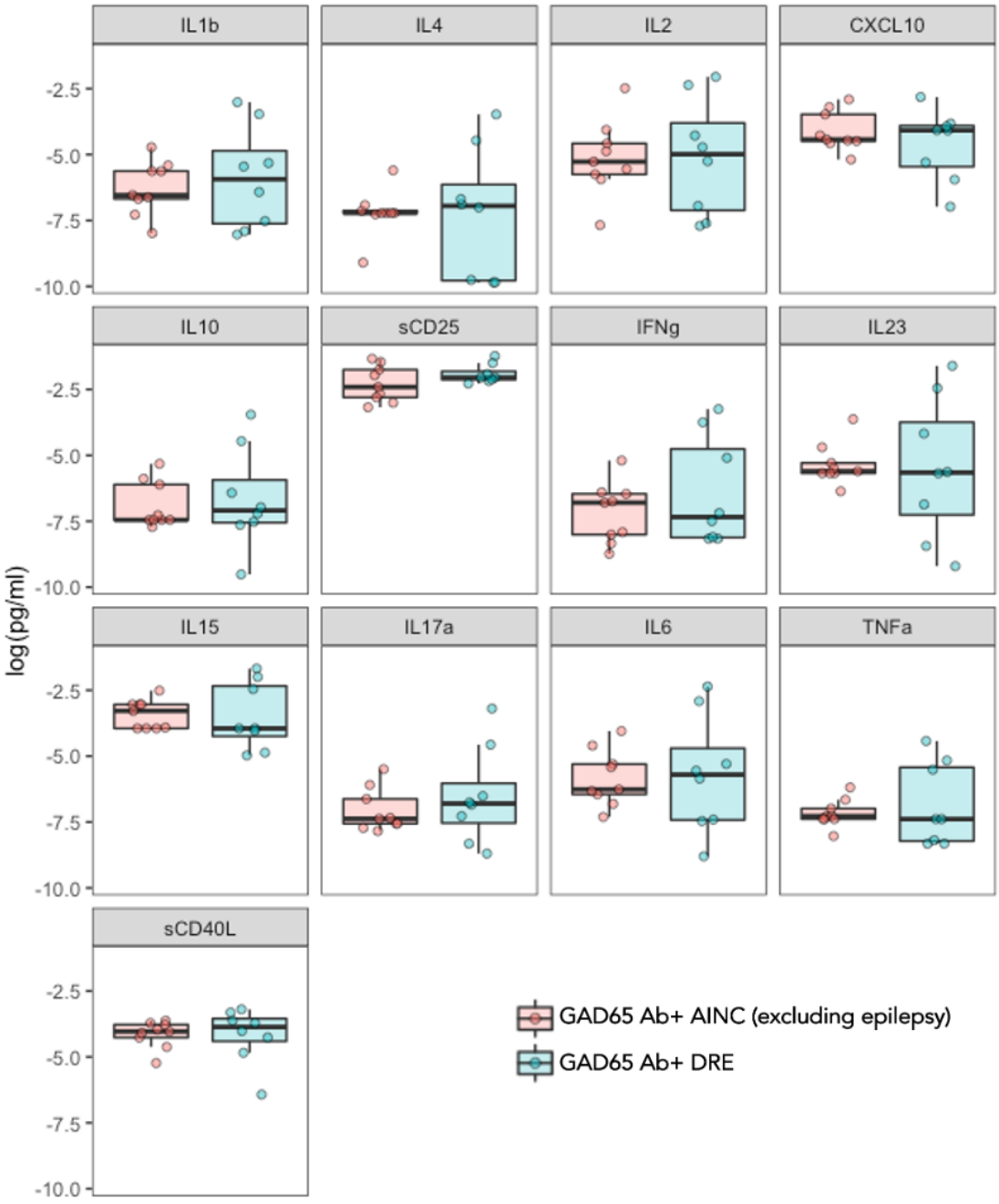
IT course description
1|N/A
2|Single course
3|Multiple courses
4|Long-term
5|Not known

Clinical response to IT
1|N/A
2|No clear response
3|<50% reduction in seizure frequency without complete control
4|>50% reduction in seizure frequency without complete control
5|Complete seizure control

Autoantibodies detected
None
AMPA-R
CASPR2
Contactin-2
DPPX
GABA-A-R
GABA-B-R
GAD65
Glycine-alpha1-R
LGI1
NMDA-R
Neurones
Astrocyte

Appendix D: Comparison of GAD65 antibody-positive DRE and autoimmune neurological conditions (excluding epilepsy)

Boxplots show median values and quantiles for each marker. No significant differences were detected between patient groups for any cytokine (Kruskal-Wallis test).



References

1. Fisher RS, Boas W van E, Blume W, et al. Epileptic Seizures and Epilepsy: Definitions Proposed by the International League Against Epilepsy (ILAE) and the International Bureau for Epilepsy (IBE). *Epilepsia*. 2005;46(4):470-472. doi:10.1111/j.0013-9580.2005.66104.x

2. Forsgren L, Beghi E, Oun A, Sillanpää M. The epidemiology of epilepsy in Europe - a systematic review. *Eur J Neurol*. 2005;12(4):245-253. doi:10.1111/j.1468-1331.2004.00992.x

3. World Health Organization. *Epilepsy: A Public Health Imperative.*; 2019. https://www.who.int/mental_health/neurology/epilepsy/report_2019/en/.

4. Scheffer IE, Berkovic S, Capovilla G, et al. ILAE classification of the epilepsies: Position paper of the ILAE Commission for Classification and Terminology. *Epilepsia*. 2017;58(4):512-521. doi:10.1111/epi.13709

5. Banerjee PN, Filippi D, Allen Hauser W. The descriptive epidemiology of epilepsy-A review. *Epilepsy Res*. 2009;85(1):31-45. doi:10.1016/j.eplepsyres.2009.03.003

6. Bell GS, Sander JW. CPD - Education and self-assessment. The epidemiology of epilepsy: The size of the problem. *Seizure*. 2001;10(4):306-316. doi:10.1053/seiz.2001.0584

7. Severino M, Geraldo AF, Utz N, et al. Definitions and classification of malformations of cortical development: practical guidelines. *Brain*. August 2020. doi:10.1093/brain/awaa174

8. Health NI of. Genetics Home Reference. https://medlineplus.gov/genetics/gene/. Accessed October 3, 2020.

9. Smith D. The management of epilepsy. *J Neurol Neurosurg Psychiatry*. 2001;70(90002):15ii - 21. doi:10.1136/jnnp.70.suppl_2.ii15

10. Schmidt D, Schachter SC. Drug treatment of epilepsy in adults. *BMJ*. 2014;348:g254. doi:10.1136/bmj.g254

11. Abou-Khalil BW. Update on Antiepileptic Drugs 2019. *Continuum (Minneap Minn)*. 2019;25(2):508-536. doi:10.1212/CON.0000000000000715

12. Vajda FJE, Eadie MJ. The clinical pharmacology of traditional antiepileptic drugs. *Epileptic Disord*. 2014;16(4):395-408. doi:10.1684/epd.2014.0704

13. Kwan P, Arzimanoglou A, Berg AT, et al. Definition of drug resistant epilepsy: Consensus proposal by the ad hoc Task Force of the ILAE Commission on Therapeutic Strategies. *Epilepsia*. 2010;51(6):1069-1077. doi:10.1111/j.1528-1167.2009.02397.x

14. Chen Z, Brodie MJ, Liew D, Kwan P. Treatment outcomes in patients with newly diagnosed epilepsy treated with established and new antiepileptic drugs a 30-year longitudinal cohort study. *JAMA Neurol*. 2018;75(3):279-286. doi:10.1001/jamaneurol.2017.3949

15. Kwan P, Brodie MJ. Early Identification of Refractory Epilepsy. *N Engl J Med*. 2000;342(5):314-319. doi:10.1056/NEJM200002033420503

16. Engel J. What can we do for people with drug-resistant epilepsy? *Neurology*. 2016;87(23):2483-2489. doi:10.1212/WNL.0000000000003407

17. Harden C, Tomson T, Gloss D, et al. Practice guideline summary: Sudden unexpected death in epilepsy incidence rates and risk factors: Report of the Guideline Development, Dissemination, and Implementation Subcommittee of the American Academy of Neurology and the American Epilepsy Society. *Neurology*. 2017;88(17):1674-1680. doi:10.1212/WNL.0000000000003685

18. Laxer KD, Trinka E, Hirsch LJ, et al. The consequences of refractory epilepsy and its treatment. *Epilepsy Behav*. 2014;37:59-70. doi:10.1016/j.yebeh.2014.05.031

19. Watila MM, Balarabe SA, Ojo O, Keezer MR, Sander JW. Overall and cause-specific premature mortality in epilepsy: A systematic review. *Epilepsy Behav*. 2018;87:213-225. doi:10.1016/j.yebeh.2018.07.017

20. Mahler B, Carlsson S, Andersson T, Tomson T. Risk for injuries and accidents in epilepsy. *Neurology*. 2018;90(9):e779-e789. doi:10.1212/WNL.0000000000005035

21. Beghi E. Addressing the burden of epilepsy: Many unmet needs. *Pharmacol Res*. 2016;107:79-84. doi:10.1016/j.phrs.2016.03.003

22. Luoni C, Bisulli F, Canevini MP, et al. Determinants of health-related quality of life in pharmacoresistant epilepsy: Results from a large multicenter study of consecutively enrolled patients using validated quantitative assessments. *Epilepsia*. 2011;52(12):2181-2191. doi:10.1111/j.1528-1167.2011.03325.x

23. Deleo F, Quintas R, Pastori C, et al. Quality of life, psychiatric symptoms, and stigma perception in three groups of persons with epilepsy. *Epilepsy Behav*. 2020;110:107170. doi:10.1016/j.yebeh.2020.107170

24. Nogueira MH, Yasuda CL, Coan AC, Kanner AM, Cendes F. Concurrent mood and anxiety disorders are associated with pharmacoresistant seizures in patients with MTLE. *Epilepsia*. 2017;58(7):1268-1276. doi:10.1111/epi.13781

25. Ridsdale L, Wojewodka G, Robinson E, et al. Characteristics associated with quality of life among people with drug-resistant epilepsy. *J Neurol*. 2017;264(6):1174-1184. doi:10.1007/s00415-017-8512-1

26. Margolis SA, Gonzalez JS, Faria C, Kenney L, Grant AC, Nakhutina L. Anxiety disorders in predominantly African American and Caribbean American adults with intractable epilepsy: The role of perceived epilepsy stigma. *Epilepsy Behav*.

2019;99:106450. doi:10.1016/j.yebeh.2019.106450

27. Boylan LS, Flint LA, Labovitz DL, Jackson SC, Starner K, Devinsky O. Depression but not seizure frequency predicts quality of life in treatment-resistant epilepsy. *Neurology*. 2004;62(2):258-261. doi:10.1212/01.WNL.0000103282.62353.85

28. Begley CE, Durgin TL. The direct cost of epilepsy in the United States: A systematic review of estimates. *Epilepsia*. 2015;56(9):1376-1387. doi:10.1111/epi.13084

29. Löscher W, Klitgaard H, Twyman RE, Schmidt D. New avenues for anti-epileptic drug discovery and development. *Nat Rev Drug Discov*. 2013;12(10):757-776. doi:10.1038/nrd4126

30. Gray RA, Whalley BJ. The proposed mechanisms of action of CBD in epilepsy. *Epileptic Disord*. 2020;22(S1):10-15. doi:10.1684/epd.2020.1135

31. Krauss GL, Klein P, Brandt C, et al. Safety and efficacy of adjunctive cenobamate (YKP3089) in patients with uncontrolled focal seizures: a multicentre, double-blind, randomised, placebo-controlled, dose-response trial. *Lancet Neurol*. 2020;19(1):38-48. doi:10.1016/S1474-4422(19)30399-0

32. Devinsky O, Schein A, Najjar S. Epilepsy associated with systemic autoimmune disorders. *Epilepsy Curr*. 2013;13(2):62-68. doi:10.5698/1535-7597-13.2.62

33. Ong MS, Kohane IS, Cai T, Gorman MP, Mandl KD. Population-level evidence for an autoimmune etiology of epilepsy. *JAMA Neurol*. 2014;71(5):569-574. doi:10.1001/jamaneurol.2014.188

34. Lin Z, Si Q, Xiaoyi Z. Association between epilepsy and systemic autoimmune diseases: A meta-analysis. *Seizure*. 2016;41:160-166. doi:10.1016/j.seizure.2016.08.003

35. Wie Børsheim A, Engeland A, Gilhus NE. Epilepsy and autoimmune diseases: Comorbidity in a national patient cohort. *Seizure*. 2020;75:89-95. doi:10.1016/j.seizure.2019.12.015

36. Dafoulas GE, Toulis KA, Mccorry D, et al. Type 1 diabetes mellitus and risk of incident epilepsy: a population-based, open-cohort study. *Diabetologia*. 2017;60(2):258-261. doi:10.1007/s00125-016-4142-x

37. Keezer MR, Novy J, Sander JW. Type 1 diabetes mellitus in people with pharmacoresistant epilepsy: Prevalence and clinical characteristics. *Epilepsy Res*. 2015;115:55-57. doi:10.1016/j.eplepsyres.2015.05.008

38. Varadkar S. Continuous spike-wave during sleep: treating an epilepsy without seizures. *Dev Med Child Neurol*. 2018;60(3):220-220. doi:10.1111/dmcn.13650

39. Nariai H, Duberstein S, Shinnar S. Treatment of Epileptic Encephalopathies: Current State of the Art. *J Child Neurol*. 2018;33(1):41-54. doi:10.1177/0883073817690290

40. Illum N, Taudorf K, Heilmann C, et al. Intravenous Immunoglobulin: A Single-Blind

Trial in Children with Lennox-Gastaut Syndrome. *Neuropediatrics*. 1990;21(02):87-90. doi:10.1055/s-2008-1071468

41. Pardo CA, Vining EPG, Guo L, Skolasky RL, Carson BS, Freeman JM. The Pathology of Rasmussen Syndrome: Stages of Cortical Involvement and Neuropathological Studies in 45 Hemispherectomies. *Epilepsia*. 2004;45(5):516-526. doi:10.1111/j.0013-9580.2004.33103.x

42. Toledano M, Pittock S. Autoimmune Epilepsy. *Semin Neurol*. 2015;35(03):245-258. doi:10.1055/s-0035-1552625

43. Jobst BC. The epidemic of autoantibody-mediated epilepsies-insights into pathophysiology and yet another syndrome. *Epilepsy Curr*. 2014;14(5):266-269. doi:10.5698/1535-7597-14.5.266

44. Davis R, Dalmau J. Autoimmunity, seizures, and status epilepticus. *Epilepsia*. 2013;54(SUPPL. 6):46-49. doi:10.1111/epi.12276

45. Iizuka T, Kanazawa N, Kaneko J, et al. Cryptogenic NORSE. *Neurol - Neuroimmunol Neuroinflammation*. 2017;4(6):e396. doi:10.1212/NXI.0000000000000396

46. Li J, Saldivar C, Maganti RK. Plasma exchange in cryptogenic new onset refractory status epilepticus. *Seizure*. 2013;22(1):70-73. doi:10.1016/j.seizure.2012.09.011

47. Dickstein LP, Liow J-S, Austermuehle A, et al. Neuroinflammation in neocortical epilepsy measured by PET imaging of translocator protein. *Epilepsia*. 2019;60(6):1248-1254. doi:10.1111/epi.15967

48. Gershen LD, Zanotti-Fregonara P, Dustin IH, et al. Neuroinflammation in Temporal Lobe Epilepsy Measured Using Positron Emission Tomographic Imaging of Translocator Protein. *JAMA Neurol*. 2015;72(8):882-888. doi:10.1001/jamaneurol.2015.094

49. Graus F, Elkon KB, Lloberes P, et al. Neuronal antinuclear antibody (anti-Hu) in paraneoplastic encephalomyelitis simulating acute polyneuritis. *Acta Neurol Scand*. 1987;75(4):249-252. doi:10.1111/j.1600-0404.1987.tb07928.x

50. Dalmau J, Graus F, Rosenblum MK, Posner JB. Anti-Hu--associated paraneoplastic encephalomyelitis/sensory neuronopathy. A clinical study of 71 patients. *Medicine (Baltimore)*. 1992;71(2):59-72. doi:10.1097/00005792-199203000-00001

51. Steriade C, Britton J, Dale RC, et al. Acute symptomatic seizures secondary to autoimmune encephalitis and autoimmune-associated epilepsy: Conceptual definitions. *Epilepsia*. June 2020:epi.16571. doi:10.1111/epi.16571

52. Irani SR, Buckley C, Vincent A, et al. Immunotherapy-responsive seizure-like episodes with potassium channel antibodies. *Neurology*. 2008;71(20):1647-1648. doi:10.1212/01.wnl.0000326572.93762.51

53. Irani SR, Michell AW, Lang B, et al. Faciobrachial dystonic seizures precede Lgi1

antibody limbic encephalitis. *Ann Neurol*. 2011;69(5):892-900. doi:10.1002/ana.22307

54. Toledano M, Britton JW, McKeon A, et al. Utility of an immunotherapy trial in evaluating patients with presumed autoimmune epilepsy. *Neurology*. 2014;82(18):1578-1586. doi:10.1212/WNL.0000000000000383

55. Spatola M, Dalmau J. Seizures and risk of epilepsy in autoimmune and other inflammatory encephalitis. *Curr Opin Neurol*. 2017;30(3):345-353. doi:10.1097/WCO.0000000000000449

56. Sculier C, Gaspard N. New onset refractory status epilepticus (NORSE). *Seizure*. 2019;68:72-78. doi:10.1016/j.seizure.2018.09.018

57. Neligan A, Kerin B, Walker MC, Rajakulendran S. New-Onset Refractory Status Epilepticus (NORSE): The Queen Square Neuro-ICU experience. *Epilepsy Behav*. 2021;125:108387. doi:10.1016/j.yebeh.2021.108387

58. Lattanzi S, Leitinger M, Rocchi C, et al. Unraveling the enigma of new-onset refractory status epilepticus: a systematic review of aetiologies. *Eur J Neurol*. November 2021. doi:10.1111/ene.15149

59. Fisher RS, Acevedo C, Arzimanoglou A, et al. ILAE Official Report: A practical clinical definition of epilepsy. *Epilepsia*. 2014;55(4):475-482. doi:10.1111/epi.12550

60. Ganor Y, Goldberg-Stern H, Lerman-Sagie T, Teichberg VI, Levite M. Autoimmune epilepsy: Distinct subpopulations of epilepsy patients harbor serum autoantibodies to either glutamate/AMPA receptor GluR3, glutamate/NMDA receptor subunit NR2A or double-stranded DNA. *Epilepsy Res*. 2005;65(1-2):11-22. doi:10.1016/j.eplepsyres.2005.03.011

61. Dubey D, Alqallaf A, Hays R, et al. Neurological autoantibody prevalence in epilepsy of unknown etiology. *JAMA Neurol*. 2017;74(4):397-402. doi:10.1001/jamaneurol.2016.5429

62. Nóbrega-Jr AW, Gregory CP, Schlindwein-Zanini R, et al. Mesial temporal lobe epilepsy with hippocampal sclerosis is infrequently associated with neuronal autoantibodies. *Epilepsia*. 2018;59(9):e152-e156. doi:10.1111/epi.14534

63. Dubey D, Samudra N, Gupta P, et al. Retrospective case series of the clinical features , management and outcomes of patients with autoimmune epilepsy. *Seizure Eur J Epilepsy*. 2015;29:143-147. doi:10.1016/j.seizure.2015.04.007

64. Kohno Y, Yamaguchi F, Saito K, Niimi H, Nishikawa T, Hosoya T. Anti-thyroid peroxidase antibodies in sera from healthy subjects and from patients with chronic thyroiditis: differences in the ability to inhibit thyroid peroxidase activities. *Clin Exp Immunol*. 2008;85(3):459-463. doi:10.1111/j.1365-2249.1991.tb05749.x

65. Michael S, Waters P, Irani SR. Stop testing for autoantibodies to the VGKC-complex: only request LGI1 and CASPR2. *Pract Neurol*. 2020;20(5):377-384.

doi:10.1136/practneurol-2019-002494

66. Sørgjerd EP, Thorsby PM, Torjesen PA, Skorpen F, Kvaløy K, Grill V. Presence of anti-GAD in a non-diabetic population of adults; time dynamics and clinical influence: results from the HUNT study. *BMJ Open Diabetes Res Care*. 2015;3(1):e000076. doi:10.1136/bmjdrc-2014-000076

67. Brenner T, Sills GJ, Hart Y, et al. Prevalence of neurologic autoantibodies in cohorts of patients with new and established epilepsy. *Epilepsia*. 2013;54(6):1028-1035. doi:10.1111/epi.12127

68. Beghi E. The Epidemiology of Epilepsy. *Neuroepidemiology*. 2020;54(Suppl. 2):185-191. doi:10.1159/000503831

69. López-Chiriboga AS, Klein C, Zekeridou A, et al. LGI1 and CASPR2 neurological autoimmunity in children. *Ann Neurol*. 2018;84(3):473-480. doi:10.1002/ana.25310

70. Favier M, Joubert B, Picard G, et al. Initial clinical presentation of young children with N-methyl- d -aspartate receptor encephalitis. *Eur J Paediatr Neurol*. 2018;22(3):404-411. doi:10.1016/j.ejpn.2017.12.014

71. Milos R-I, Szimacsek M, Leutmezer F, et al. Clinical and magnetic resonance imaging features of children, adolescents, and adults with a clinically isolated syndrome. *Eur J Paediatr Neurol*. 2018;22(6):1087-1094. doi:10.1016/j.ejpn.2018.08.003

72. Dubey D, Farzal Z, Hays R, Brown LS, Vernino S. Evaluation of positive and negative predictors of seizure outcomes among patients with immune-mediated epilepsy: A meta-analysis. *Ther Adv Neurol Disord*. 2016;9(5):369-377. doi:10.1177/1756285616656295

73. Chang BS, Krishnan V, Dulla CG, et al. Epilepsy Benchmarks Area I: Understanding the Causes of the Epilepsies and Epilepsy-Related Neurologic, Psychiatric, and Somatic Conditions. *Epilepsy Curr*. 2020;20(1_suppl):5S-13S. doi:10.1177/1535759719895280

74. Binder DK, Boison D, Eid T, et al. Epilepsy Benchmarks Area II: Prevent Epilepsy and Its Progression. *Epilepsy Curr*. 2020;20(1_suppl):14S-22S. doi:10.1177/1535759719895274

75. Jones JE, Asato MR, Brown M-G, et al. Epilepsy Benchmarks Area IV: Limit or Prevent Adverse Consequence of Seizures and Their Treatment Across the Life Span. *Epilepsy Curr*. 2020;20(1_suppl):31S-39S. doi:10.1177/1535759719895277

76. Jarius S, Paul F, Aktas O, et al. MOG encephalomyelitis: international recommendations on diagnosis and antibody testing. *J Neuroinflammation*. 2018;15(1):134. doi:10.1186/s12974-018-1144-2

77. Fang B, McKeon A, Hinson SR, et al. Autoimmune glial fibrillary acidic protein astrocytopathy: A novel meningoencephalomyelitis. *JAMA Neurol*. 2016;73(11):1297-1307. doi:10.1001/jamaneurol.2016.2549

78. Pitsch J, Kamalizade D, Braun A, et al. Drebrin Autoantibodies in Patients with Seizures and Suspected Encephalitis. *Ann Neurol*. 2020;87(6):869-884. doi:10.1002/ana.25720

79. Spatola M, Sabater L, Planagumà J, et al. Encephalitis with mGluR5 antibodies. *Neurology*. 2018;90(22):e1964-e1972. doi:10.1212/WNL.0000000000005614

80. Gresa-Arribas N, Planagumà J, Petit-Pedrol M, et al. Human neurexin-3**α** antibodies associate with encephalitis and alter synapse development. *Neurology*. 2016;86(24):2235-2242. doi:10.1212/WNL.0000000000002775

81. Petit-Pedrol M, Armangue T, Peng X, et al. Encephalitis with refractory seizures, status epilepticus, and antibodies to the GABAA receptor: a case series, characterization of the antigen, and analysis of the effects of antibodies . *Lancet Neurol*. 2014;13(March):276-286.

82. Lancaster E, Lai M, Peng X, et al. Antibodies to the GABAB receptor in limbic encephalitis with seizures: case series and characterisation of the antigen. *Lancet Neurol*. 2010;9(1):67-76. doi:10.1016/S1474-4422(09)70324-2

83. Boronat A, Gelfand JM, Gresa-Arribas N, et al. Encephalitis and antibodies to dipeptidyl-peptidase-like protein-6, a subunit of Kv4.2 potassium channels. *Ann Neurol*. 2013;73(1):120-128. doi:10.1002/ana.23756

84. Mas N, Saiz A, Leite MI, et al. Antiglycine-receptor encephalomyelitis with rigidity. *J Neurol Neurosurg Psychiatry*. 2011;82(12):1399-1401. doi:10.1136/jnnp.2010.229104

85. Irani SR, Alexander S, Waters P, et al. Antibodies to Kv1 potassium channel-complex proteins leucine-rich, glioma inactivated 1 protein and contactin-associated protein-2 in limbic encephalitis, Morvan's syndrome and acquired neuromyotonia. *Brain*. 2010;133(9):2734-2748. doi:10.1093/brain/awq213

86. Lai M, Hughes EG, Peng X, et al. AMPA receptor antibodies in limbic encephalitis alter synaptic receptor location. *Ann Neurol*. 2009;65(4):424-434. doi:10.1002/ana.21589

87. Dalmau J, Tüzün E, Wu HY, et al. Paraneoplastic anti-N-methyl-D-aspartate receptor encephalitis associated with ovarian teratoma. *Ann Neurol*. 2007;61(1):25-36. doi:10.1002/ana.21050

88. Buckley C, Oger J, Clover L, et al. Potassium channel antibodies in two patients with reversible limbic encephalitis. *Ann Neurol*. 2001;50(1):73-78. doi:10.1002/ana.1097

89. Liu W, Wang M, Zhang C, Zhao CW, Xiao B, Zeng C. Application of the APE2-CHN and RITE2-CHN scores for autoimmune seizures and epilepsy in Chinese patients: A retrospective study. *Seizure*. 2020;81:63-70. doi:10.1016/j.seizure.2020.07.021

90. Falip M, Jaraba S, Rodríguez-Bel L, et al. Seizures and epilepsy of autoimmune origin: A long-term prospective study. *Seizure*. 2020;81:157-165. doi:10.1016/j.seizure.2020.07.019

91. Jesus-Ribeiro J, Bozorgi A, Alkhaldi M, Shaqfeh M, Fernandez-Baca Vaca G, Katirji B. Autoimmune musicogenic epilepsy associated with anti-glutamic acid decarboxylase antibodies and Stiff-person syndrome. *Clin Case Reports*. 2020;8(1):61-64. doi:10.1002/ccr3.2538

92. Feyissa AM, Lamb C, Pittock SJ, et al. Antiepileptic drug therapy in autoimmune epilepsy associated with antibodies targeting the leucine-rich glioma-inactivated protein 1. *Epilepsia Open*. 2018;3(3):348-356. doi:10.1002/epi4.12226

93. Makhija P, Gopinath S, Kannoth S, Radhakrishnan K. A case of post-leptospirosis autoimmune epilepsy presenting with sleep-related hypermotor seizures. *Epileptic Disord*. 2017;19(4):456-460. doi:10.1684/epd.2017.0941

94. Varrasi C, Vecchio D, Magistrelli L, Strigaro G, Tassi L, Cantello R. Auditory seizures in autoimmune epilepsy: a case with anti-thyroid antibodies. *Epileptic Disord*. 2017;19(1):99-103. doi:10.1684/epd.2017.0904

95. Steriade C, Tang-Wai DF, Krings T, Wennberg R. Claustrum hyperintensities: A potential clue to autoimmune epilepsy. *Epilepsia Open*. 2017;2(4):476-480. doi:10.1002/epi4.12077

96. Feyissa AM, López Chiriboga AS, Britton JW. Antiepileptic drug therapy in patients with autoimmune epilepsy. *Neurol - Neuroimmunol Neuroinflammation*. 2017;4(4):e353. doi:10.1212/NXI.0000000000000353

97. Dubey D, Singh J, Britton JW, et al. Predictive models in the diagnosis and treatment of autoimmune epilepsy. *Epilepsia*. 2017;58(7):1181-1189. doi:10.1111/epi.13797

98. Malter MP, Widman G, Galldiks N, et al. Suspected new-onset autoimmune temporal lobe epilepsy with amygdala enlargement. *Epilepsia*. 2016;57(9):1485-1494. doi:10.1111/epi.13471

99. Baysal-Kirac L, Tuzun E, Altindag E, et al. Are There Any Specific EEG Findings in Autoimmune Epilepsies? *Clin EEG Neurosci*. 2016;47(3):224-234. doi:10.1177/1550059415595907

100. Murata Y, Watanabe O, Taniguchi G, et al. A case of autoimmune epilepsy associated with anti-leucine-rich glioma inactivated subunit 1 antibodies manifesting electrical shock-like sensations and transparent sadness. *Epilepsy Behav case reports*. 2015;4:91-93. doi:10.1016/j.ebcr.2015.08.004

101. Miró J, Fortuny R, Juncadella M, et al. Antithyroid antibodies as a potential marker of autoimmune-mediated late onset temporal lobe epilepsy. *Clin Neurol Neurosurg*. 2014;121:46-50. doi:10.1016/j.clineuro.2014.03.017

102. Dubey D, Konikkara J, Modur PN, et al. Effectiveness of multimodality treatment for autoimmune limbic epilepsy. *Epileptic Disord*. 2014;16(4):494-499. doi:10.1684/epd.2014.0703

103. Suleiman J, Brilot F, Lang B, Vincent A, Dale RC. Autoimmune epilepsy in children:

Case series and proposed guidelines for identification. *Epilepsia*. 2013;54(6):1036-1045. doi:10.1111/epi.12142

104. Quek AML, Britton JW, McKeon A, et al. Autoimmune epilepsy: clinical characteristics and response to immunotherapy. *Arch Neurol*. 2012;69(5):582-593. doi:10.1001/archneurol.2011.2985

105. van Sonderen A, Thijs RD, Coenders EC, et al. Anti-LGI1 encephalitis: Clinical syndrome and long-term follow-up. *Neurology*. 2016;87(14):1449-1456. doi:10.1212/WNL.0000000000003173

106. Irani SR, Pettingill P, Kleopa KA, et al. Morvan syndrome: Clinical and serological observations in 29 cases. *Ann Neurol*. 2012;72(2):241-255. doi:10.1002/ana.23577

107. Steriade C, Moosa ANV, Hantus S, Prayson RA, Alexopoulos A, Rae-Grant A. Electroclinical features of seizures associated with autoimmune encephalitis. *Seizure*. 2018;60(May):198-204. doi:10.1016/j.seizure.2018.06.021

108. Titulaer MJ, McCracken L, Gabilondo I, et al. Late-onset anti-NMDA receptor encephalitis. *Neurology*. 2013;81(12):1058-1063. doi:10.1212/WNL.0b013e3182a4a49c

109. Zuliani L, Graus F, Giometto B, Bien C, Vincent A. Central nervous system neuronal surface antibody associated syndromes: Review and guidelines for recognition. *J Neurol Neurosurg Psychiatry*. 2012;83(6):638-645. doi:10.1136/jnnp-2011-301237

110. Vanli-Yavuz EN, Erdag E, Tuzun E, et al. Neuronal autoantibodies in mesial temporal lobe epilepsy with hippocampal sclerosis. *J Neurol Neurosurg Psychiatry*. 2016;87(7):684-692. doi:10.1136/jnnp-2016-313146

111. von Podewils F, Suesse M, Geithner J, et al. Prevalence and outcome of late-onset seizures due to autoimmune etiology: A prospective observational population-based cohort study. *Epilepsia*. 2017;58(9):1542-1550. doi:10.1111/epi.13834

112. Bozzetti S, Rossini F, Ferrari S, et al. Epileptic seizures of suspected autoimmune origin: a multicentre retrospective study. *J Neurol Neurosurg Psychiatry*. August 2020:jnnp-2020-323841. doi:10.1136/jnnp-2020-323841

113. Baysal-Kirac L, Tuzun E, Erdag E, et al. Neuronal autoantibodies in epilepsy patients with peri-ictal autonomic findings. *J Neurol*. 2016;263(3):455-466. doi:10.1007/s00415-015-8002-2

114. Bien C, Elger C. Epilepsia partialis continua: Semiology and differential diagnoses. *Epileptic Disord*. 2008;10(1):3-7. doi:10.1684/epd.2008.0161

115. Aurangzeb S, Symmonds M, Knight RK, Kennett R, Wehner T, Irani SR. LGI1-antibody encephalitis is characterised by frequent, multifocal clinical and subclinical seizures. *Seizure*. 2017;50:14-17. doi:10.1016/j.seizure.2017.05.017

116. Elisak M, Krysl D, Hanzalova J, et al. The prevalence of neural antibodies in temporal

lobe epilepsy and the clinical characteristics of seropositive patients. *Seizure*. 2018;63:1-6. doi:10.1016/j.seizure.2018.09.009

117. Majoie HJM, de Baets M, Renier W, Lang B, Vincent A. Antibodies to voltage-gated potassium and calcium channels in epilepsy. *Epilepsy Res*. 2006;71(2-3):135-141. doi:10.1016/j.eplepsyres.2006.06.003

118. Dalmau J, Gleichman AJ, Hughes EG, et al. Anti-NMDA-receptor encephalitis: case series and analysis of the effects of antibodies. *Lancet Neurol*. 2008;7(12):1091-1098. doi:10.1016/S1474-4422(08)70224-2

119. Irani SR, Stagg CJ, Schott JM, et al. Faciobrachial dystonic seizures: The influence of immunotherapy on seizure control and prevention of cognitive impairment in a broadening phenotype. *Brain*. 2013;136(10):3151-3162. doi:10.1093/brain/awt212

120. Tan KM, Lennon VA, Klein CJ, Boeve BF, Pittock SJ. Clinical spectrum of voltage-gated potassium channel autoimmunity. *Neurology*. 2008;70(20):1883-1890. doi:10.1212/01.wnl.0000312275.04260.a0

121. Finke C, Prüss H, Heine J, et al. Evaluation of cognitive deficits and structural hippocampal damage in encephalitis with leucine-rich, glioma-inactivated 1 antibodies. *JAMA Neurol*. 2017;74(1):50-59. doi:10.1001/jamaneurol.2016.4226

122. Thompson J, Bi M, Murchison AG, et al. The importance of early immunotherapy in patients with faciobrachial dystonic seizures. *Brain*. 2018;141(2):348-356. doi:10.1093/brain/awx323

123. Dalmau J. NMDA receptor encephalitis and other antibody-mediated disorders of the synapse. *Neurology*. 2016;87(23):2471-2482. doi:10.1212/WNL.0000000000003414

124. Dalmau J, Lancaster E, Martinez-Hernandez E, Rosenfeld MR, Balice-Gordon R. Clinical experience and laboratory investigations in patients with anti-NMDAR encephalitis. *Lancet Neurol*. 2011;10(1):63-74. doi:10.1016/S1474-4422(10)70253-2

125. Gozubatik-Celik G, Ozkara C, Ulusoy C, et al. Anti-Neuronal Autoantibodies in Both Drug Responsive and Resistant Focal Seizures with Unknown Cause. *Epilepsy Res*. 2017;135(May 2016):131-136. doi:10.1016/j.eplepsyres.2017.06.008

126. Beimer NJ, Selwa LM. Seizure semiology of anti-LGI1 antibody encephalitis. *Epileptic Disord*. 2017;19(4):461-464. doi:10.1684/epd.2017.0936

127. Gofshteyn JS, Yeshokumar AK, Jette N, et al. Clinical and electrographic features of persistent seizures and status epilepticus associated with anti-NMDA receptor encephalitis (anti-NMDARE). *Epileptic Disord*. 2020;22(6):739-751. doi:10.1684/epd.2020.1218

128. Schmitt SE, Pargeon K, Frechette ES, Hirsch LJ, Dalmau J, Friedman D. Extreme delta brush: A unique EEG pattern in adults with anti-NMDA receptor encephalitis. *Neurology*. 2012;79(11):1094-1100. doi:10.1212/WNL.0b013e3182698cd8

129. Sonderen A van, Arends S, Tavy DLJ, et al. Predictive value of electroencephalography in anti-NMDA receptor encephalitis. *J Neurol Neurosurg Psychiatry*. 2018;89(10):1101-1106. doi:10.1136/jnnp-2018-318376

130. Steriade C, Hantus S, Moosa ANV, Rae-Grant AD. Extreme delta – With or without brushes: A potential surrogate marker of disease activity in anti-NMDA-receptor encephalitis. *Clin Neurophysiol*. 2018;129(10):2197-2204. doi:10.1016/j.clinph.2018.02.130

131. Freund B, Ritzl EK. A review of EEG in anti-NMDA receptor encephalitis. *J Neuroimmunol*. 2019;332:64-68. doi:10.1016/j.jneuroim.2019.03.010

132. Theroux LM, Goodkin HP, Heinan KC, Quigg M, Brenton JN. Extreme delta brush and distinctive imaging in a pediatric patient with autoimmune GFAP astrocytopathy. *Mult Scler Relat Disord*. 2018;26:121-123. doi:10.1016/j.msard.2018.09.015

133. Xiping W, Guomin X, Haifeng W, Qi S, Liping Z. Etoposide and immunotherapy can improve the outcome of severe anti-GABAB R encephalitis presenting with delta brush. *Medicine (Baltimore)*. 2020;99(37):e22087. doi:10.1097/MD.0000000000022087

134. Chauhan V, Niepel G, Richardson A, Mohanraj R. PO008 Extreme delta brush on eeg – secondary to ketamine use? *J Neurol Neurosurg Psychiatry*. 2017;88(Suppl 1):A14.4-A15. doi:10.1136/jnnp-2017-ABN.45

135. Flanagan EP, Kotsenas AL, Britton JW, et al. Basal ganglia T1 hyperintensity in LGI1-autoantibody faciobrachial dystonic seizures. *Neurol - Neuroimmunol Neuroinflammation*. 2015;2(6):e161. doi:10.1212/NXI.0000000000000161

136. Holtmann O, Schlossmacher I, Moenig C, et al. Amygdala enlargement and emotional responses in (autoimmune) temporal lobe epilepsy. *Sci Rep*. 2018;8(1):9561. doi:10.1038/s41598-018-27914-z

137. Lv R-J, Sun Z-R, Cui T, Guan H-Z, Ren H-T, Shao X-Q. Temporal lobe epilepsy with amygdala enlargement: a subtype of temporal lobe epilepsy. *BMC Neurol*. 2014;14(1):194. doi:10.1186/s12883-014-0194-z

138. Cui J, Bu H, He J, et al. The gamma-aminobutyric acid-B receptor (GABAB) encephalitis: clinical manifestations and response to immunotherapy. *Int J Neurosci*. 2018;128(7):627-633. doi:10.1080/00207454.2017.1408618

139. Finke C, Prüss H, Heine J, et al. Evaluation of cognitive deficits and structural hippocampal damage in encephalitis with leucine-rich, glioma-inactivated 1 antibodies. *JAMA Neurol*. 2017;74(1):50-59. doi:10.1001/jamaneurol.2016.4226

140. Berkovic SF. Genetics of epilepsy in clinical practice. *Good data Exist to Provid empiric risks based epilepsy Syndr diagnosis*. 2015;15(4):192-196.

141. Ottman R, Winawer MR, Kalachikov S, et al. LGI1 mutations in autosomal dominant partial epilepsy with auditory features. *Neurology*. 2004;62(7):1120-1126.

doi:10.1212/01.WNL.0000120098.39231.6E

142. Falip M, Rodriguez-Bel L, Castañer S, et al. Musicogenic reflex seizures in epilepsy with glutamic acid decarbocylase antibodies. *Acta Neurol Scand*. 2018;137(2):272-276. doi:10.1111/ane.12799

143. van Sonderen A, Schreurs MWJ, de Bruijn MAAM, et al. The relevance of VGKC positivity in the absence of LGI1 and Caspr2 antibodies. *Neurology*. 2016;86(18):1692-1699. doi:10.1212/WNL.0000000000002637

144. Tényi D, Bóné B, Horváth R, Komoly S, Illés Z, Beier CP. Seizure : European Journal of Epilepsy Ictal piloerection is associated with high-grade glioma and autoimmune encephalitis — Results from a systematic review. 2018;(July):3-7.

145. Rocamora R, Becerra JL, Fossas P, et al. Pilomotor seizures: An autonomic semiology of limbic encephalitis? *Seizure*. 2014;23(8):670-673. doi:10.1016/j.seizure.2014.04.013

146. Stefan H, Pauli E, Kerling F, Schwarz A, Koebnick C. Autonomic Auras: Left Hemispheric Predominance of Epileptic Generators of Cold Shivers and Goose Bumps? *Epilepsia*. 2002;43(1):41-45. doi:10.1046/j.1528-1157.2002.21001.x

147. Dove GH, Buchhalter JR, Cascino GD. Acute repetitive pilomotor seizures (goose bumps)in a patient with right mesial temporal sclerosis. *Clin Neurophysiol*. 2004;115(11):2511-2513. doi:10.1016/j.clinph.2004.05.030

148. Roze E. Status-like recurrent pilomotor seizures: case report and review of the literature. *J Neurol Neurosurg Psychiatry*. 2000;68(5):647-649. doi:10.1136/jnnp.68.5.647

149. Andermann F, Gloor P. Pilomotor seizures. *Neurology*. 1984;34(12):1623-1623. doi:10.1212/WNL.34.12.1623

150. Green JB. Pilomotor seizures. *Neurology*. 1984;34(6):837-837. doi:10.1212/WNL.34.6.837

151. Gillinder L, Tjoa L, Mantzioris B, Blum S, Dionisio S. Refractory chronic epilepsy associated with neuronal auto-antibodies: could perisylvian semiology be a clue? *Epileptic Disord*. 2017;19(4):439-449. doi:10.1684/epd.2017.0946

152. Beimer NJ, Selwa LM. Seizure semiology of anti-LGI1 antibody encephalitis. *Epileptic Disord*. 2017;19(4):461-464. doi:10.1684/epd.2017.0936

153. Bakpa OD, Reuber M, Irani SR. Antibody-associated epilepsies: Clinical features, evidence for immunotherapies and future research questions. *Seizure*. 2016;41:26-41. doi:10.1016/j.seizure.2016.07.002

154. Tillakaratne NJK, Erlander MG, Collard MW, Greif KF, Tobin AJ. Glutamate Decarboxylases in Nonneural Cells of Rat Testis and Oviduct: Differential Expression of GAD 65 and GAD 67. *J Neurochem*. 1992;58(2):618-627. doi:10.1111/j.1471-

4159.1992.tb09763.x

155. Okada Y, Taniguchi H, Schimada C. High concentration of GABA and high glutamate decarboxylase activity in rat pancreatic islets and human insulinoma. *Science (80-)*. 1976;194(4265):620-622. doi:10.1126/science.185693

156. Erlander MG, Tillakaratne NJK, Feldblum S, Patel N, Tobin a J. Two genes encode distinct gluamate decarboxylases. *Neuron*. 1991;7:91-100.

157. Bu DF, Erlander MG, Hitz BC, et al. Two human glutamate decarboxylases, 65-kDa GAD and 67-kDa GAD, are each encoded by a single gene. *Proc Natl Acad Sci*. 1992;89(6):2115-2119. doi:10.1073/pnas.89.6.2115

158. Sheikh SN, Martin SB, Martin DL. Regional distribution and relative amounts of glutamate decarboxylase isoforms in rat and mouse brain. *Neurochem Int*. 1999;35(1):73-80. doi:S0197-0186(99)00063-7 [pii]

159. Reetz A, Solimena M, Matteoli M, Folli F, Takei K, De Camilli P. GABA and pancreatic beta-cells: colocalization of glutamic acid decarboxylase (GAD) and GABA with synaptic-like microvesicles suggests their role in GABA storage and secretion. *EMBO J*. 1991;10(5):1275-1284. doi:10.1016/0962-8924(91)90073-I

160. Kaufman DL, Houser CR, Tobin AJ. Two Forms of the gamma-Aminobutyric Acid Synthetic Enzyme Glutamate Decarboxylase Have Distinct Intraneuronal Distributions and Cofactor Interactions. *J Neurochem*. 1991;56(2):720-723. doi:10.1111/j.1471-4159.1991.tb08211.x

161. Roth FC, Draguhn A. GABA metabolism and transport: Effects on synaptic efficacy. *Neural Plast*. 2012;2012. doi:10.1155/2012/805830

162. Fenalti G, Buckle AM. Structural biology of the GAD autoantigen. *Autoimmun Rev*. 2010;9(3):148-152. doi:10.1016/j.autrev.2009.05.003

163. Christgau S, Aanstoot HJ, Schierbeck H, et al. Membrane anchoring of the autoantigen GAD65 to microvesicles in pancreatic beta-cells by palmitoylation in the NH2-terminal domain. *J Cell Biol*. 1992;118(2):309-320. doi:10.1083/jcb.118.2.309

164. Graus F, Saiz A, Dalmau J. GAD antibodies in neurological disorders — insights and challenges. *Nat Rev Neurol*. 2020;16(7):353-365. doi:10.1038/s41582-020-0359-x

165. Martin DL, Liu H, Martin SB, Wu SJ. Structural features and regulatory properties of the brain glutamate decarboxylases. *Neurochem Int*. 2000;37(2-3):111-119. doi:10.1016/S0197-0186(00)00014-0

166. Jayakrishnan B, Hoke DE, Langendorf CG, Buckle AM, Rowley MJ. An Analysis of the Cross-Reactivity of Autoantibodies to GAD65 and GAD67 in Diabetes. Sechi LA, ed. *PLoS One*. 2011;6(4):e18411. doi:10.1371/journal.pone.0018411

167. Seissler J, Amann J, Mauch L, et al. Prevalence of autoantibodies to the 65- and 67-kD isoforms of glutamate decarboxylase in insulin-dependent diabetes mellitus. *J*

Clin Invest. 1993;92(3):1394-1399. doi:10.1172/JCI116714

168. Guasp M, Solà-Valls N, Martínez-Hernández E, et al. Cerebellar ataxia and autoantibodies restricted to glutamic acid decarboxylase 67 (GAD67). *J Neuroimmunol*. 2016;300:15-17. doi:10.1016/j.jneuroim.2016.09.019

169. Tuomilehto J, Vidgren G, Toivanen L, et al. Antibodies to glutamic acid decarboxylase as predictors of insulin-dependent diabetes mellitus before clinical onset of disease. *Lancet*. 1994;343(8910):1383-1385. doi:10.1016/S0140-6736(94)92521-6

170. Luhder F, Schlosser M, Mauch L, et al. Autoantibodies Against Gad 65 Rather Than Gad 67 Precede the Onset of Type 1 Diabetes. *Autoimmunity*. 1994;19(2):71-80. doi:10.3109/08916939409009534

171. Dotta F, Falorni A, Tiberti C, et al. Autoantibodies to the GM2-1 Islet Ganglioside and to GAD-65 at Type 1 Diabetes Onset. *J Autoimmun*. 1997;10(6):585-588. doi:10.1006/jaut.1997.0166

172. Kaufman DL, Erlander MG, Clare-Salzler M, Atkinson MA, Maclaren NK, Tobin AJ. Autoimmunity to two forms of glutamate decarboxylase in insulin-dependent diabetes mellitus. *J Clin Invest*. 1992;89(1):283-292. doi:10.1172/JCI115573

173. Solimena M, Folli F, Denis-Donini S, et al. Autoantibodies to glutamic acid decarboxylase in a patient with stiff-man syndrome, epilepsy, and type I diabetes mellitus. *N Engl J Med*. 1988;318(16):1012-1020. doi:10.1056/NEJM198804213181602

174. Malter MP, Helmstaedter C, Urbach H, Vincent A, Bien CG. Antibodies to glutamic acid decarboxylase define a form of limbic encephalitis. *Ann Neurol*. 2010;67(4):470-478. doi:10.1002/ana.21917

175. Nakajima H, Nakamura Y, Inaba Y, et al. Neurologic disorders associated with anti-glutamic acid decarboxylase antibodies: A comparison of anti-GAD antibody titers and time-dependent changes between neurologic disease and type I diabetes mellitus. *J Neuroimmunol*. 2018;317(December 2017):84-89. doi:10.1016/j.jneuroim.2018.01.007

176. Baekkeskov S, Aanstoot H-J, Christgai S, et al. Identification of the 64K autoantigen in insulin-dependent diabetes as the GABA-synthesizing enzyme glutamic acid decarboxylase. *Nature*. 1990;347(6289):151-156. doi:10.1038/347151a0

177. Kim J, Namchuk M, Bugawan T, et al. Higher autoantibody levels and recognition of a linear NH2-terminal epitope in the autoantigen GAD65, distinguish stiff-man syndrome from insulin-dependent diabetes mellitus. *J Exp Med*. 1994;180(2):595-606. doi:10.1084/jem.180.2.595

178. Baizabal-Carvallo JF. The neurological syndromes associated with glutamic acid decarboxylase antibodies. *J Autoimmun*. 2019;101:35-47. doi:10.1016/j.jaut.2019.04.007

179. Damato V, Balint B, Kienzler A-K, Irani SR. The clinical features, underlying immunology, and treatment of autoantibody-mediated movement disorders. *Mov Disord*. 2018;33(9):1376-1389. doi:10.1002/mds.27446

180. Saiz A, Blanco Y, Sabater L, et al. Spectrum of neurological syndromes associated with glutamic acid decarboxylase antibodies: Diagnostic clues for this association. *Brain*. 2008;131(10):2553-2563. doi:10.1093/brain/awn183

181. McKeon A, Tracy JA. GAD65 neurological autoimmunity. *Muscle and Nerve*. 2017;56(1):15-27. doi:10.1002/mus.25565

182. Balint B, Vincent A, Meinck HM, Irani SR, Bhatia KP. Movement disorders with neuronal antibodies: Syndromic approach, genetic parallels and pathophysiology. *Brain*. 2018;141(1):13-36. doi:10.1093/brain/awx189

183. Dayalu P, Teener JW. Stiff Person syndrome and other anti-GAD-associated neurologic disorders. *Semin Neurol*. 2012;32(5):544-549. doi:10.1055/s-0033-1334477

184. Peltola J, Kulmala P, Isojärvi J, et al. Autoantibodies to glutamic acid decarboxylase in patients with therapy-resistant epilepsy. *Neurology*. 2000;55(1):46-50. http://www.ncbi.nlm.nih.gov/pubmed/10891904.

185. Walikonis JE, Lennon VA. Radioimmunoassay for glutamic acid decarboxylase (GAD65) autoantibodies as a diagnostic aid for stiff-man syndrome and a correlate of susceptibility to type 1 diabetes mellitus. *Mayo Clin Proc*. 1998;73(12):1161-1166. doi:10.4065/73.12.1161

186. Liimatainen S, Peltola M, Sabater L, et al. Clinical significance of glutamic acid decarboxylase antibodies in patients with epilepsy. *Epilepsia*. 2010;51(5):760-767. doi:10.1111/j.1528-1167.2009.02325.x

187. Malter MP, Frisch C, Zeitler H, et al. Treatment of immune-mediated temporal lobe epilepsy with GAD antibodies. *Seizure*. 2015;30:57-63. doi:10.1016/j.seizure.2015.05.017

188. Errichiello L, Perruolo G, Pascarella A, et al. Autoantibodies to glutamic acid decarboxylase (GAD) in focal and generalized epilepsy: A study on 233 patients. *J Neuroimmunol*. 2009;211(1-2):120-123. doi:10.1016/j.jneuroim.2009.04.010

189. Lilleker JB, Biswas V, Mohanraj R. Glutamic acid decarboxylase (GAD) antibodies in epilepsy: Diagnostic yield and therapeutic implications. *Seizure*. 2014;23(8):598-602. doi:10.1016/j.seizure.2014.04.009

190. Vianello M, Keir G, Giometto B, Betterle C, Tavolato B, Thompson EJ. Antigenic differences between neurological and diabetic patients with anti-glutamic acid decarboxylase antibodies. *Eur J Neurol*. 2005;12(4):294-299. doi:10.1111/j.1468-1331.2004.00933.x

191. Meinck H-M. Antibodies against glutamic acid decarboxylase: prevalence in

neurological diseases. *J Neurol Neurosurg Psychiatry*. 2001;71(1):100-103. doi:10.1136/jnnp.71.1.100

192. Niskanen LK, Tuomi T, Karjalainen J, Groop LC, Uusitupa MIJ. GAD Antibodies in NIDDM: Ten-year follow-up from the diagnosis. *Diabetes Care*. 1995;18(12):1557-1565. doi:10.2337/diacare.18.12.1557

193. Petersen JS, Hejnæs KR, Moody A, et al. Detection of GAD65 antibodies in diabetes and other autoimmune diseases using a simple radioligand assay. *Diabetes*. 1994;43(3):459-467. doi:10.2337/diabetes.43.3.459

194. Vianello M, Keir G, Giometto B, Betterle C, Tavolato B, Thompson EJ. Antigenic differences between neurological and diabetic patients with anti-glutamic acid decarboxylase antibodies. *Eur J Neurol*. 2005;12(4):294-299. doi:10.1111/j.1468-1331.2004.00933.x

195. Daif A, Lukas R V., Issa NP, et al. Antiglutamic acid decarboxylase 65 (GAD65) antibody-associated epilepsy. *Epilepsy Behav*. 2018;80:331-336. doi:10.1016/j.yebeh.2018.01.021

196. Oikawa Y, Tanaka H, Uchida J, et al. Slowly progressive insulin-dependent (type 1) diabetes positive for anti-GAD antibody ELISA test may be strongly associated with a future insulin-dependent state. *Endocr J*. 2017;64(2):163-170. doi:10.1507/endocrj.EJ16-0328

197. Kawasaki E, Okada A, Uchida A, et al. Discrepancy of glutamic acid decarboxylase 65 autoantibody results between RSR radioimmunoassay and enzyme-linked immunosorbent assay in patients with type 1 diabetes is related to autoantibody affinity. *J Diabetes Investig*. 2019;10(4):990-996. doi:10.1111/jdi.12996

198. Brooking H, Ananieva-Jordanova R, Arnold C, et al. A sensitive non-isotopic assay for GAD65autoantibodies. *Clin Chim Acta*. 2003;331(1-2):55-59. doi:10.1016/S0009-8981(03)00088-3

199. National Institute for Biological Standards and Control. WHO Reference Reagent, Islet Cell Antibodies, NIBSC code 97/550 (version 4). https://www.nibsc.org/documents/ifu/97-550.pdf. Published 2013. Accessed July 9, 2020.

200. Vincent A, Waters P, Leite MI, et al. Antibodies identified by cell-based assays in myasthenia gravis and associated diseases. *Ann N Y Acad Sci*. 2012;1274:92-98. doi:10.1111/j.1749-6632.2012.06789.x

201. Kim Y, Hyun J-W, Woodhall MR, et al. Refining cell-based assay to detect MOG-IgG in patients with central nervous system inflammatory diseases. *Mult Scler Relat Disord*. 2020;40:101939. doi:10.1016/j.msard.2020.101939

202. Waters P, Reindl M, Saiz A, et al. Multicentre comparison of a diagnostic assay: aquaporin-4 antibodies in neuromyelitis optica. *J Neurol Neurosurg Psychiatry*. 2016;87(9):1005-1015. doi:10.1136/jnnp-2015-312601

203. Waters P, Pettingill P, Lang B. Detection methods for neural autoantibodies. *Handb Clin Neurol*. 2016;133:147-163. doi:10.1016/B978-0-444-63432-0.00009-8

204. Bien CG, Scheffer IE. Autoantibodies and epilepsy. *Epilepsia*. 2011;52(SUPPL. 3):18-22. doi:10.1111/j.1528-1167.2011.03031.x

205. Tizazu E, Ellis CA, Reichert J, Lancaster E. Low rate of glutamic acid decarboxylase 65 (GAD-65) antibodies in chronic epilepsy. *Seizure*. 2020;80:38-41. doi:10.1016/j.seizure.2020.05.008

206. Aguiar TS, Dantas JR, Cabral DB, et al. Association between high titers of glutamic acid decarboxylase antibody and epilepsy in patients with type 1 diabetes mellitus: A cross-sectional study. *Seizure*. 2019;71:318-321. doi:10.1016/j.seizure.2019.09.003

207. Falip M, Rodriguez-Bel L, Castañer S, et al. Hippocampus and Insula Are Targets in Epileptic Patients With Glutamic Acid Decarboxylase Antibodies. *Front Neurol*. 2019;9. doi:10.3389/fneur.2018.01143

208. Ceyhan Dirican A, Elibirlik S, Koksal A, et al. Evaluation of Glutamic Acid Decarboxylase Antibody Levels in Patients with Juvenile Myoclonic Epilepsy and Mesial Temporal Lobe Epilepsy with Hippocampal Sclerosis. *Noro Psikiyatr Ars*. 2016;53(3):253-256. doi:10.5152/npa.2015.9948

209. Moloney TC, Idris I, Waters P, et al. Autoantibodies to glutamic acid decarboxylase in patients with epilepsy and their relationship with type 1 diabetes: a pilot study: Table 1. *J Neurol Neurosurg Psychiatry*. 2016;87(6):676-677. doi:10.1136/jnnp-2015-310512

210. Falip M, Carreño M, Miró J, et al. Prevalence and immunological spectrum of temporal lobe epilepsy with glutamic acid decarboxylase antibodies. *Eur J Neurol*. 2012;19(6):827-833. doi:10.1111/j.1468-1331.2011.03609.x

211. Sokol DK, McIntyre JA, Wagenknecht DR, et al. Antiphospholipid and glutamic acid decarboxylase antibodies in patients with focal epilepsy. *Neurology*. 2004;62(3):517-518. doi:10.1212/01.WNL.0000106821.83436.59

212. Kwan P, Sills GJ, Kelly K, Butler E, Brodie MJ. Glutamic acid decarboxylase autoantibodies in controlled and uncontrolled epilepsy: a pilot study. *Epilepsy Res*. 2000;42(2-3):191-195. http://www.ncbi.nlm.nih.gov/pubmed/11074191.

213. Vezzani A. Brain Inflammation and Seizures: Evolving Concepts and New Findings in the Last 2 Decades. *Epilepsy Curr*. 2020;20(6_suppl):40S-43S. doi:10.1177/1535759720948900

214. Ravizza T, Vezzani A. Pharmacological targeting of brain inflammation in epilepsy: Therapeutic perspectives from experimental and clinical studies. *Epilepsia Open*. 2018;3(S2):133-142. doi:10.1002/epi4.12242

215. Pauletti A, Terrone G, Shekh-Ahmad T, et al. Targeting oxidative stress improves disease outcomes in a rat model of acquired epilepsy. *Brain*. 2019;142(7):e39-e39.

doi:10.1093/brain/awz130

216. Paudel YN, Shaikh MF, Chakraborti A, et al. HMGB1: A Common Biomarker and Potential Target for TBI, Neuroinflammation, Epilepsy, and Cognitive Dysfunction. *Front Neurosci*. 2018;12. doi:10.3389/fnins.2018.00628

217. Frigerio F, Flynn C, Han Y, et al. Neuroinflammation Alters Integrative Properties of Rat Hippocampal Pyramidal Cells. *Mol Neurobiol*. 2018;55(9):7500-7511. doi:10.1007/s12035-018-0915-1

218. Vezzani A, Viviani B. Neuromodulatory properties of inflammatory cytokines and their impact on neuronal excitability. *Neuropharmacology*. 2015;96:70-82. doi:10.1016/j.neuropharm.2014.10.027

219. Hu S, Sheng WS, Ehrlich LC, Peterson PK, Chao CC. Cytokine Effects on Glutamate Uptake by Human Astrocytes. *Neuroimmunomodulation*. 2000;7(3):153-159. doi:10.1159/000026433

220. Li G, Bauer S, Nowak M, et al. Cytokines and epilepsy. *Seizure*. 2011;20(3):249-256. doi:10.1016/j.seizure.2010.12.005

221. Bauer S, Cepok S, Todorova-Rudolph A, et al. Etiology and site of temporal lobe epilepsy influence postictal cytokine release. *Epilepsy Res*. 2009;86(1):82-88. doi:10.1016/j.eplepsyres.2009.05.009

222. Kamaşak T, Dilber B, Yaman SÖ, et al. HMGB-1, TLR4, IL-1R1, TNF-**α**, and IL-1**β**: novel epilepsy markers? *Epileptic Disord*. 2020;22(2):183-193. doi:10.1684/epd.2020.1155

223. Balosso S, Ravizza T, Aronica E, Vezzani A. The dual role of TNF-**α** and its receptors in seizures. *Exp Neurol*. 2013;247:267-271. doi:10.1016/j.expneurol.2013.05.010

224. Maldonado M, Baybis M, Newman D, et al. Expression of ICAM-1, TNF-**α**, NF**κ**B, and MAP kinase in tubers of the tuberous sclerosis complex. *Neurobiol Dis*. 2003;14(2):279-290. doi:10.1016/S0969-9961(03)00127-X

225. Heinemann U, Kaufer D, Friedman A. Blood-brain barrier dysfunction, TGF**β** signaling, and astrocyte dysfunction in epilepsy. *Glia*. 2012;60(8):1251-1257. doi:10.1002/glia.22311

226. Weissberg I, Wood L, Kamintsky L, et al. Albumin induces excitatory synaptogenesis through astrocytic TGF-**β**/ALK5 signaling in a model of acquired epilepsy following blood–brain barrier dysfunction. *Neurobiol Dis*. 2015;78:115-125. doi:10.1016/j.nbd.2015.02.029

227. Aronica E, Boer K, van Vliet EA, et al. Complement activation in experimental and human temporal lobe epilepsy. *Neurobiol Dis*. 2007;26(3):497-511. doi:10.1016/j.nbd.2007.01.015

228. Xiong Z-Q, Qian W, Suzuki K, McNamara JO. Formation of Complement Membrane

Attack Complex in Mammalian Cerebral Cortex Evokes Seizures and Neurodegeneration. *J Neurosci*. 2003;23(3):955-960. doi:10.1523/JNEUROSCI.23-03-00955.2003

229. Fabene PF, Bramanti P, Constantin G. The emerging role for chemokines in epilepsy. *J Neuroimmunol*. 2010;224(1-2):22-27. doi:10.1016/j.jneuroim.2010.05.016

230. Cerri C, Genovesi S, Allegra M, et al. The Chemokine CCL2 Mediates the Seizure-enhancing Effects of Systemic Inflammation. *J Neurosci*. 2016;36(13):3777-3788. doi:10.1523/JNEUROSCI.0451-15.2016

231. de Vries EE, van den Munckhof B, Braun KPJ, van Royen-Kerkhof A, de Jager W, Jansen FE. Inflammatory mediators in human epilepsy: A systematic review and meta-analysis. *Neurosci Biobehav Rev*. 2016;63:177-190. doi:10.1016/j.neubiorev.2016.02.007

232. Sun B, Ramberger M, O'Connor KC, Bashford-Rogers RJM, Irani SR. The B cell immunobiology that underlies CNS autoantibody-mediated diseases. *Nat Rev Neurol*. 2020;16(9):481-492. doi:10.1038/s41582-020-0381-z

233. Hughes EG, Peng X, Gleichman AJ, et al. Cellular and Synaptic Mechanisms of Anti-NMDA Receptor Encephalitis. *J Neurosci*. 2010;30(17):5866-5875. doi:10.1523/JNEUROSCI.0167-10.2010

234. Ohkawa T, Fukata Y, Yamasaki M, et al. Autoantibodies to Epilepsy-Related LGI1 in Limbic Encephalitis Neutralize LGI1-ADAM22 Interaction and Reduce Synaptic AMPA Receptors. *J Neurosci*. 2013;33(46):18161-18174. doi:10.1523/JNEUROSCI.3506-13.2013

235. Petit-Pedrol M, Sell J, Planagumà J, et al. LGI1 antibodies alter Kv1.1 and AMPA receptors changing synaptic excitability, plasticity and memory. *Brain*. October 2018. doi:10.1093/brain/awy253

236. Ramberger M, Berretta A, Tan JMM, et al. Distinctive binding properties of human monoclonal LGI1 autoantibodies determine pathogenic mechanisms. *Brain*. 2020;143(6):1731-1745. doi:10.1093/brain/awaa104

237. Tanaka K, Kawamura M, Sakimura K, Kato N. Significance of Autoantibodies in Autoimmune Encephalitis in Relation to Antigen Localization: An Outline of Frequently Reported Autoantibodies with a Non-Systematic Review. *Int J Mol Sci*. 2020;21(14):4941. doi:10.3390/ijms21144941

238. Evergren E, Marcucci M, Tomilin N, et al. Amphiphysin is a Component of Clathrin Coats Formed During Synaptic Vesicle Recycling at the Lamprey Giant Synapse. *Traffic*. 2004;5(7):514-528. doi:10.1111/j.1398-9219.2004.00198.x

239. Geis C, Carreño M, Planagumà J, Graus F, Dalmau J. Autoimmune seizures and epilepsy. *J Clin Invest*. 2019;(19):1-15. doi:10.1172/jci125178

240. Werner C, Pauli M, Doose S, et al. Human autoantibodies to amphiphysin induce

defective presynaptic vesicle dynamics and composition. *Brain*. 2016;139(2):365-379. doi:10.1093/brain/awv324

241. Liimatainen S, Honnorat J, Pittock SJ, et al. GAD65 autoantibody characteristics in patients with co-occurring type 1 diabetes and epilepsy may help identify underlying epilepsy etiologies. *Orphanet J Rare Dis*. 2018;13(1):1-9. doi:10.1186/s13023-018-0787-5

242. Baekkeskov S, Landin M, Kristensen JK, et al. Antibodies to a 64,000 Mr human islet cell antigen precede the clinical onset of insulin-dependent diabetes. *J Clin Invest*. 1987;79(3):926-934. doi:10.1172/JCI112903

243. Dalakas MC, Fujii M, Li M, Lutfi B, Kyhos J, McElroy B. High-Dose Intravenous Immune Globulin for Stiff-Person Syndrome. *N Engl J Med*. 2001;345(26):1870-1876. doi:10.1056/NEJMoa01167

244. Muñoz-Lopetegi A, de Bruijn MAAM, Boukhrissi S, et al. Neurologic syndromes related to anti-GAD65. *Neurol - Neuroimmunol Neuroinflammation*. 2020;7(3):e696. doi:10.1212/NXI.0000000000000696

245. Bjork E, Velloso LA, Kampe O, Karlsson FA. GAD Autoantibodies in IDDM, Stiff-Man Syndrome, and Autoimmune Polyendocrine Syndrome Type I Recognize Different Epitopes. *Diabetes*. 1994;43(1):161-165. doi:10.2337/diab.43.1.161

246. Hansen N, Grünewald B, Weishaupt A, et al. Human Stiff person syndrome IgG-containing high-titer anti-GAD65 autoantibodies induce motor dysfunction in rats. *Exp Neurol*. 2013;239:202-209. doi:10.1016/j.expneurol.2012.10.013

247. Nemni R, Caniatti LM, Gironi M, Bazzigaluppi E, De Grandis D. Stiff person syndrome does not always occur with maternal passive transfer of GAD65 antibodies. *Neurology*. 2004;62(11):2101-2102. doi:10.1212/01.WNL.0000127446.61806.2F

248. Gresa-Arribas N, Ariño H, Martínez-Hernández E, et al. Antibodies to inhibitory synaptic proteins in neurological syndromes associated with glutamic acid decarboxylase autoimmunity. *PLoS One*. 2015;10(3):1-14. doi:10.1371/journal.pone.0121364

249. Saiz A, Blanco Y, Sabater L, et al. Spectrum of neurological syndromes associated with glutamic acid decarboxylase antibodies: Diagnostic clues for this association. *Brain*. 2008;131(10):2553-2563. doi:10.1093/brain/awn183

250. Mäkelä K-M, Hietaharju A, Brander A, Peltola J. Clinical Management of Epilepsy With Glutamic Acid Decarboxylase Antibody Positivity: The Interplay Between Immunotherapy and Anti-epileptic Drugs. *Front Neurol*. 2018;9. doi:10.3389/fneur.2018.00579

251. Stork O, Ji F-Y, Kaneko K, et al. Postnatal development of a GABA deficit and disturbance of neural functions in mice lacking GAD65. *Brain Res*. 2000;865(1):45-58. doi:10.1016/S0006-8993(00)02206-X

252. Kash SF, Johnson RS, Tecott LH, et al. Epilepsy in mice deficient in the 65-kDa isoform of glutamic acid decarboxylase. *Proc Natl Acad Sci*. 1997;94(25):14060-14065. doi:10.1073/pnas.94.25.14060

253. Farooqi MS, Lai Y, Lancaster E, Schmitt SE, Sachais BS. Therapeutic plasma exchange and immunosuppressive therapy in a patient with anti-GAD antibody-related epilepsy: Quantification of the antibody response. *J Clin Apher*. 2015;30(1):8-14. doi:10.1002/jca.21342

254. Carreño M, Bien CG, Asadi-Pooya AA, et al. Epilepsy surgery in drug resistant temporal lobe epilepsy associated with neuronal antibodies. *Epilepsy Res*. 2017;129:101-105. doi:10.1016/j.eplepsyres.2016.12.010

255. Aull-Watschinger S, Pataraia E, Czech T, Baumgartner C. Outcome predictors for surgical treatment of temporal lobe epilepsy with hippocampal sclerosis. *Epilepsia*. 2008;49(8):1308-1316. doi:10.1111/j.1528-1167.2008.01732.x

256. de Tisi J, Bell GS, Peacock JL, et al. The long-term outcome of adult epilepsy surgery, patterns of seizure remission, and relapse: a cohort study. *Lancet*. 2011;378(9800):1388-1395. doi:10.1016/S0140-6736(11)60890-8

257. Wieser HG, Blume WT, Fish D, et al. ILAE Commission Report: Proposal for a new classification of outcome with respect to epileptic seizures following epilepsy surgery. *Epilepsia*. 2001;42(2):282-286. http://www.ncbi.nlm.nih.gov/pubmed/11240604.

258. Witebsky E. Chronic thyroiditis and autoimmunization. *J Am Med Assoc*. 1957;164(13):1439. doi:10.1001/jama.1957.02980130015004

259. Rose NR, Bona C. Defining criteria for autoimmune diseases (Witebsky's postulates revisited). *Immunol Today*. 1993;14(9):426-430. doi:10.1016/0167-5699(93)90244-F

260. Irani SR. "Moonlighting" surface antigens: A paradigm for autoantibody pathogenicity in neurology? *Brain*. 2016;139(2):304-306. doi:10.1093/brain/awv364

261. Chang T, Alexopoulos H, McMenamin M, et al. Neuronal surface and glutamic acid decarboxylase autoantibodies in nonparaneoplastic stiff person syndrome. *JAMA Neurol*. 2013;70(9):1140-1149. doi:10.1001/jamaneurol.2013.3499

262. Richter W, Shi Y, Baekkeskov S. Autoreactive epitopes defined by diabetes-associated human monoclonal antibodies are localized in the middle and C-terminal domains of the smaller form of glutamate decarboxylase. *Proc Natl Acad Sci*. 1993;90(7):2832-2836. doi:10.1073/pnas.90.7.2832

263. Hampe CS, Petrosini L, De Bartolo P, et al. Monoclonal antibodies to 65kDa glutamate decarboxylase induce epitope specific effects on motor and cognitive functions in rats. *Orphanet J Rare Dis*. 2013;8(1). doi:10.1186/1750-1172-8-82

264. Fouka P, Alexopoulos H, Akrivou S, Trohatou O, Politis PK, Dalakas MC. GAD65 epitope mapping and search for novel autoantibodies in GAD-associated neurological disorders. *J Neuroimmunol*. 2015;281:73-77.

doi:10.1016/j.jneuroim.2015.03.009

265. Fisher RS, Cross JH, D'Souza C, et al. Instruction manual for the <scp>ILAE</scp> 2017 operational classification of seizure types. *Epilepsia*. 2017;58(4):531-542. doi:10.1111/epi.13671

266. NICE. *Epilepsies: Diagnosis and Management (CG137).*; 2012.

267. Shorvon SD. The etiological classification of epilepsy. *Causes Epilepsy Common Uncommon Causes Adults Child*. 2011;9780521114(6):21-23. doi:10.1017/CBO9780511921001.004

268. Balestrini S, Arzimanoglou A, Blümcke I, et al. The aetiologies of epilepsy. *Epileptic Disord*. 2021;23(1):1-16. doi:10.1684/epd.2021.1255

269. Pack AM. Epilepsy Overview and Revised Classification of Seizures and Epilepsies. *Contin Lifelong Learn Neurol*. 2019;25(2):306-321. doi:10.1212/CON.0000000000000707

270. Panayiotopoulos CP. The new ILAE report on terminology and concepts for the organization of epilepsies: Critical review and contribution. *Epilepsia*. 2012;53(3):399-404. doi:10.1111/j.1528-1167.2011.03381.x

271. Fisher RS, Cross JH, D'Souza C, et al. Instruction manual for the ILAE 2017 operational classification of seizure types. *Zeitschrift fur Epileptol*. 2018;31(4):282-295. doi:10.1007/s10309-018-0217-7

272. Lüders H, Akamatsu N, Amina S, et al. Critique of the 2017 epileptic seizure and epilepsy classifications. *Epilepsia*. March 2019:epi.14699. doi:10.1111/epi.14699

273. Loddenkemper T, Kotagal P. Lateralizing signs during seizures in focal epilepsy. *Epilepsy Behav*. 2005;7(1):1-17. doi:10.1016/j.yebeh.2005.04.004

274. Foldvary-Schaefer N, Unnwongse K. Localizing and lateralizing features of auras and seizures. *Epilepsy Behav*. 2011;20(2):160-166. doi:10.1016/j.yebeh.2010.08.034

275. Bonini F, McGonigal A, Trébuchon A, et al. Frontal lobe seizures: From clinical semiology to localization. *Epilepsia*. 2014;55(2):264-277. doi:10.1111/epi.12490

276. Rüber T, David B, Elger CE. MRI in epilepsy: clinical standard and evolution. *Curr Opin Neurol*. 2018;31(2):223-231. doi:10.1097/WCO.0000000000000539

277. Sidhu MK, Duncan JS, Sander JW. Neuroimaging in epilepsy. *Curr Opin Neurol*. 2018;31(4):371-378. doi:10.1097/WCO.0000000000000568

278. Cooper GS, Stroehla BC. The epidemiology of autoimmune diseases. *Autoimmun Rev*. 2003;2(3):119-125. doi:10.1016/S1568-9972(03)00006-5

279. Audi S, Burrage DR, Lonsdale DO, et al. The 'top 100' drugs and classes in England: an updated 'starter formulary' for trainee prescribers. *Br J Clin Pharmacol*. 2018;84(11):2562-2571. doi:10.1111/bcp.13709

280. de Bruijn MAAM, van Sonderen A, van Coevorden-Hameete MH, et al. Evaluation of seizure treatment in anti-LGI1, anti-NMDAR, and anti-GABA B R encephalitis. *Neurology*. 2019;92(19):e2185-e2196. doi:10.1212/WNL.0000000000007475

281. Brenner T, Sills GJ, Hart Y, et al. Prevalence of neurologic autoantibodies in cohorts of patients with new and established epilepsy. *Epilepsia*. 2013;54(6):1028-1035. doi:10.1111/epi.12127

282. McGinty RN, Handel A, Moloney T, et al. Clinical features which predict neuronal surface autoantibodies in new-onset focal epilepsy: implications for immunotherapies. *J Neurol Neurosurg Psychiatry*. November 2020:jnnp-2020-325011. doi:10.1136/jnnp-2020-325011

283. Dubey D, Kothapalli N, McKeon A, et al. Predictors of neural-specific autoantibodies and immunotherapy response in patients with cognitive dysfunction. *J Neuroimmunol*. 2018;323(June):62-72. doi:10.1016/j.jneuroim.2018.07.009

284. Graus F, Titulaer MJ, Balu R, et al. Position Paper A clinical approach to diagnosis of autoimmune encephalitis. *Lancet Neurol*. 2016;15(April):391-404. doi:10.1016/S1474-4422(15)00401-9

285. Irani SR, Bera K, Waters P, et al. N-methyl-d-aspartate antibody encephalitis: temporal progression of clinical and paraclinical observations in a predominantly non-paraneoplastic disorder of both sexes. *Brain*. 2010;133(6):1655-1667. doi:10.1093/brain/awq113

286. Moloney TC, Idris I, Waters P, et al. Autoantibodies to glutamic acid decarboxylase in patients with epilepsy and their relationship with type 1 diabetes: A pilot study. *J Neurol Neurosurg Psychiatry*. 2016;87(6):676-677. doi:10.1136/jnnp-2015-310512

287. Varley JA, Irani SR. Antibody-associated autoimmune neurological disease. *Med (United Kingdom)*. 2016;44(9):563-569. doi:10.1016/j.mpmed.2016.06.008

288. Nikolic L, Nobili P, Shen W, Audinat E. Role of astrocyte purinergic signaling in epilepsy. *Glia*. 2020;68(9):1677-1691. doi:10.1002/glia.23747

289. Chan F, Lax NZ, Voss CM, et al. The role of astrocytes in seizure generation: insights from a novel in vitro seizure model based on mitochondrial dysfunction. *Brain*. 2019;142(2):391-411. doi:10.1093/brain/awy320

290. Boison D, Steinhäuser C. Epilepsy and astrocyte energy metabolism. *Glia*. 2018;66(6):1235-1243. doi:10.1002/glia.23247

291. Shan F, Long Y, Qiu W. Autoimmune Glial Fibrillary Acidic Protein Astrocytopathy: A Review of the Literature. *Front Immunol*. 2018;9. doi:10.3389/fimmu.2018.02802

292. Etemadifar M, Sabeti F, Khorvash R, Mirbagheri M, Nouri H, Salari M. Seizure incidence among neuromyelitis optica spectrum disorder patients. *Rev Neurol (Paris)*. 2021;177(6):655-659. doi:10.1016/j.neurol.2020.08.011

293. Eyo UB, Murugan M, Wu LJ. Microglia–Neuron Communication in Epilepsy. *Glia*. 2017;65(1):5-18. doi:10.1002/glia.23006

294. Luo Y, Hu Q, Zhang Q, et al. Alterations in hippocampal myelin and oligodendrocyte precursor cells during epileptogenesis. *Brain Res*. 2015;1627:154-164. doi:10.1016/j.brainres.2015.09.027

295. Donkels C, Peters M, Fariña Núñez MT, et al. Oligodendrocyte lineage and myelination are compromised in the gray matter of focal cortical dysplasia type IIa. *Epilepsia*. 2020;61(1):171-184. doi:10.1111/epi.16415

296. Rose AS, Bradley AR, Valasatava Y, Duarte JM, Prlić A, Rose PW. NGL viewer: web-based molecular graphics for large complexes. Valencia A, ed. *Bioinformatics*. 2018;34(21):3755-3758. doi:10.1093/bioinformatics/bty419

297. Williams AJK, Lampasona V, Wyatt R, et al. Reactivity to N-terminally truncated GAD65(96-585) identifies GAD autoantibodies that are more closely associated with diabetes progression in relatives of patients with type 1 diabetes. *Diabetes*. 2015;64(9):3247-3252. doi:10.2337/db14-1694

298. Leite MI, Jacob S, Viegas S, et al. IgG1 antibodies to acetylcholine receptors in 'seronegative' myasthenia gravis†. *Brain*. 2008;131(7):1940-1952. doi:10.1093/brain/awn092

299. Waters P, Jarius S, Littleton E, et al. Aquaporin-4 Antibodies in Neuromyelitis Optica and Longitudinally Extensive Transverse Myelitis. *Arch Neurol*. 2008;65(7). doi:10.1001/archneur.65.7.913

300. Lang B, Makuch M, Moloney T, et al. Intracellular and non-neuronal targets of voltage-gated potassium channel complex antibodies. *J Neurol Neurosurg Psychiatry*. 2017;88(4):353-361. doi:10.1136/jnnp-2016-314758

301. Pettingill P, Kramer HB, Coebergh JA, et al. Antibodies to GABAA receptor **α**1 and **γ**2 subunits. *Neurology*. 2015;84:1-9. doi:10.1016/j.tecto.2013.10.012

302. Ruiz-García R, Martínez-Hernández E, García-Ormaechea M, et al. Caveats and Pitfalls of SOX1 Autoantibody Testing With a Commercial Line Blot Assay in Paraneoplastic Neurological Investigations. *Front Immunol*. 2019;10. doi:10.3389/fimmu.2019.00769

303. Höltje M, Mertens R, Schou MB, et al. Synapsin-antibodies in psychiatric and neurological disorders: Prevalence and clinical findings. *Brain Behav Immun*. 2017;66:125-134. doi:10.1016/j.bbi.2017.07.011

304. Tora M, Graus F, de Bolos C, Real FX. Cell surface expression of paraneoplastic encephalomyelitis/sensory neuronopathy-associated Hu antigens in small-cell lung cancers and neuroblastomas. *Neurology*. 1997;48(3):735-741. doi:10.1212/WNL.48.3.735

305. Prüss H, Finke C, Höltje M, et al. N-methyl- <scp>D</scp> -aspartate receptor

antibodies in herpes simplex encephalitis. *Ann Neurol*. 2012;72(6):902-911. doi:10.1002/ana.23689

306. Makuch M, Wilson R, Al-Diwani A, et al. N-methyl-D-aspartate receptor antibody production from germinal center reactions: Therapeutic implications. *Ann Neurol*. 2018;83(3):553-561. doi:10.1002/ana.25173

307. Castillo-Gómez E, Oliveira B, Tapken D, et al. All naturally occurring autoantibodies against the NMDA receptor subunit NR1 have pathogenic potential irrespective of epitope and immunoglobulin class. *Mol Psychiatry*. 2017;22(12):1776-1784. doi:10.1038/mp.2016.125

308. Jarius S, Franciotta D, Bergamaschi R, Wildemann B, Wandinger K-P. Immunoglobulin M antibodies to aquaporin-4 in neuromyelitis optica and related disorders. *Clin Chem Lab Med*. 2010;48(5). doi:10.1515/CCLM.2010.127

309. Pettingill P, Kramer HB, Coebergh JA, et al. Antibodies to GABAA receptor 1 and 2 subunits: Clinical and serologic characterization. *Neurology*. 2015;84(12):1233-1241. doi:10.1212/WNL.0000000000001326

310. Makuch M, Wilson R, Al-Diwani A, et al. N-methyl-D-aspartate receptor antibody production from germinal center reactions: Therapeutic implications. *Ann Neurol*. 2018;83(3):553-561. doi:10.1002/ana.25173

311. Dubey D, Alqallaf A, Hays R, et al. Neurological autoantibody prevalence in epilepsy of unknown etiology. *JAMA Neurol*. 2017;74(4):397-402. doi:10.1001/jamaneurol.2016.5429

312. Vincent A, Bien CG, Irani SR, Waters P. Autoantibodies associated with diseases of the CNS: new developments and future challenges. *Lancet Neurol*. 2011;10(8):759-772. doi:10.1016/S1474-4422(11)70096-5

313. Liu T, Li S, Ying S, et al. The IL-23/IL-17 Pathway in Inflammatory Skin Diseases: From Bench to Bedside. *Front Immunol*. 2020;11. doi:10.3389/fimmu.2020.594735

314. Mahil SK, Smith CH. Psoriasis biologics: a new era of choice. *Lancet*. 2019;394(10201):807-808. doi:10.1016/S0140-6736(19)31772-6

315. Mertens M, Singh JA. Anakinra for rheumatoid arthritis. *Cochrane Database Syst Rev*. January 2009. doi:10.1002/14651858.CD005121.pub3

316. Wang Y, Wang D, Guo D. Interictal cytokine levels were correlated to seizure severity of epileptic patients: a retrospective study on 1218 epileptic patients. *J Transl Med*. 2015;13(1):378. doi:10.1186/s12967-015-0742-3

317. Kanemoto K, Kawasaki J, Miyamoto T, Obayashi H, Nishimura M. Interleukin (IL)1beta, IL-1alpha, and IL-1 receptor antagonist gene polymorphisms in patients with temporal lobe epilepsy. *Ann Neurol*. 2000;47(5):571-574. http://www.ncbi.nlm.nih.gov/pubmed/10805326.

318. Shi Y, Zhang L, Teng J, Miao W. HMGB1 mediates microglia activation via the TLR4/NF-κB pathway in coriaria lactone induced epilepsy. *Mol Med Rep*. January 2018. doi:10.3892/mmr.2018.8485

319. Plata-Salamán CR, Ilyin SE, Turrin NP, et al. Kindling modulates the IL-1β system, TNF-α, TGF-β1, and neuropeptide mRNAs in specific brain regions. *Mol Brain Res*. 2000;75(2):248-258. doi:10.1016/S0169-328X(99)00306-X

320. Gouveia TLF, Vieira de Sousa PV, de Almeida SS, et al. High serum levels of proinflammatory markers during epileptogenesis. Can omega-3 fatty acid administration reduce this process? *Epilepsy Behav*. 2015;51:300-305. doi:10.1016/j.yebeh.2015.07.021

321. Mazumder AG, Patial V, Singh D. Mycophenolate mofetil contributes to downregulation of the hippocampal interleukin type 2 and 1β mediated PI3K/AKT/mTOR pathway hyperactivation and attenuates neurobehavioral comorbidities in a rat model of temporal lobe epilepsy. *Brain Behav Immun*. 2019;75:84-93. doi:10.1016/j.bbi.2018.09.020

322. Sinha S, Patil SA, Jayalekshmy V, Satishchandra P. Do cytokines have any role in epilepsy? *Epilepsy Res*. 2008;82(2-3):171-176. doi:10.1016/j.eplepsyres.2008.07.018

323. Strauss KI, Elisevich K V. Brain region and epilepsy-associated differences in inflammatory mediator levels in medically refractory mesial temporal lobe epilepsy. *J Neuroinflammation*. 2016;13(1):270. doi:10.1186/s12974-016-0727-z

324. Thaler FS, Thaller AL, Biljecki M, et al. Abundant glutamic acid decarboxylase (GAD)-reactive B cells in gad-antibody-associated neurological disorders. *Ann Neurol*. 2019;85(3):448-454. doi:10.1002/ana.25414

325. Rosa DV, Rezende VB, Costa BS, et al. Circulating CD4 and CD8 T cells expressing pro-inflammatory cytokines in a cohort of mesial temporal lobe epilepsy patients with hippocampal sclerosis. *Epilepsy Res*. 2016;120:1-6. doi:10.1016/j.eplepsyres.2015.11.011

326. Ethemoglu O, Ay H, Koyuncu I, Gönel A. Comparison of cytokines and prooxidants/antioxidants markers among adults with refractory versus well-controlled epilepsy: A cross-sectional study. *Seizure*. 2018;60(April):105-109. doi:10.1016/j.seizure.2018.06.009

327. Peltola J, Palmio J, Korhonen L, et al. Interleukin-6 and Interleukin-1 receptor antagonist in cerebrospinal fluid from patients with recent tonic–clonic seizures. *Epilepsy Res*. 2000;41(3):205-211. doi:10.1016/S0920-1211(00)00140-6

328. Gao F, Gao Y, Zhang S -j., et al. Alteration of plasma cytokines in patients with active epilepsy. *Acta Neurol Scand*. 2017;135(6):663-669. doi:10.1111/ane.12665

329. Liimatainen S, Fallah M, Kharazmi E, Peltola M, Peltola J. Interleukin-6 levels are increased in temporal lobe epilepsy but not in extra-temporal lobe epilepsy. *J Neurol*. 2009;256(5):796-802. doi:10.1007/s00415-009-5021-x

330. Lehtimäki K., Keränen T, Huhtala H, et al. Regulation of IL-6 system in cerebrospinal fluid and serum compartments by seizures: the effect of seizure type and duration. *J Neuroimmunol*. 2004;152(1-2):121-125. doi:10.1016/j.jneuroim.2004.01.024

331. Peltola J, Hurme M, Miettinen A, Keränen T. Elevated levels of interleukin-6 may occur in cerebrospinal fluid from patients with recent epileptic seizures. *Epilepsy Res*. 1998;31(2):129-133. doi:10.1016/S0920-1211(98)00024-2

332. Alapirtti T, Lehtimäki K, Nieminen R, et al. The production of IL-6 in acute epileptic seizure: A video-EEG study. *J Neuroimmunol*. 2018;316(December):50-55. doi:10.1016/j.jneuroim.2017.12.008

333. Morin-Brureau M, Milior G, Royer J, et al. Microglial phenotypes in the human epileptic temporal lobe. *Brain*. 2018;141(12):3343-3360. doi:10.1093/brain/awy276

334. Taalab YM, Fathi Mohammed W, Helmy MA, et al. Cannabis Influences the Putative Cytokines-Related Pathway of Epilepsy among Egyptian Epileptic Patients. *Brain Sci*. 2019;9(12):332. doi:10.3390/brainsci9120332

335. Bernasconi NL, Traggiai E, Lanzavecchia A. Maintenance of serological memory by polyclonal activation of human memory B cells. *Science (80-)*. 2002;298(5601):2199-2202. doi:10.1126/science.1076071

336. Mao LY, Ding J, Peng WF, et al. Interictal interleukin-17A levels are elevated and correlate with seizure severity of epilepsy patients. *Epilepsia*. 2013;54(9):142-145. doi:10.1111/epi.12337

337. Kumar P, Shih DCW, Lim A, et al. Proinflammatory IL-17 pathways dominate the architecture of the immunome in pediatric refractory epilepsy. *JCI Insight*. 2019;4(8). doi:10.1172/jci.insight.126337

338. Friedman LK, Mancuso J, Patel A, et al. Transcriptome profiling of hippocampal CA1 after early-life seizure-induced preconditioning may elucidate new genetic therapies for epilepsy. *Eur J Neurosci*. 2013;38(1):2139-2152. doi:10.1111/ejn.12168

339. Langrish CL, Chen Y, Blumenschein WM, et al. IL-23 drives a pathogenic T cell population that induces autoimmune inflammation. *J Exp Med*. 2005;201(2):233-240. doi:10.1084/jem.20041257

340. Kothur K, Wienholt L, Brilot F, Dale RC. CSF cytokines/chemokines as biomarkers in neuroinflammatory CNS disorders: A systematic review. *Cytokine*. 2016;77:227-237. doi:10.1016/j.cyto.2015.10.001

341. Modvig S, Degn M, Horwitz H, et al. Relationship between Cerebrospinal Fluid Biomarkers for Inflammation, Demyelination and Neurodegeneration in Acute Optic Neuritis. Reindl M, ed. *PLoS One*. 2013;8(10):e77163. doi:10.1371/journal.pone.0077163

342. Russell SE, Moore AC, Fallon PG, Walsh PT. Soluble IL-2R**α** (sCD25) Exacerbates Autoimmunity and Enhances the Development of Th17 Responses in Mice.

Pietropaolo M, ed. *PLoS One*. 2012;7(10):e47748. doi:10.1371/journal.pone.0047748

343. Buhelt S, Søndergaard HB, Oturai A, Ullum H, von Essen MR, Sellebjerg F. Relationship between Multiple Sclerosis-Associated IL2RA Risk Allele Variants and Circulating T Cell Phenotypes in Healthy Genotype-Selected Controls. *Cells*. 2019;8(6):634. doi:10.3390/cells8060634

344. Karnell JL, Albulescu M, Drabic S, et al. A CD40L-targeting protein reduces autoantibodies and improves disease activity in patients with autoimmunity. *Sci Transl Med*. 2019;11(489):eaar6584. doi:10.1126/scitranslmed.aar6584

345. Gardell JL, Parker DC. CD40L is transferred to antigen-presenting B cells during delivery of T-cell help. *Eur J Immunol*. 2017;47(1):41-50. doi:10.1002/eji.201646504

346. Fluidigm. Helios User Guide 2018. https://www.fluidigm.com/binaries/content/documents/fluidigm/resources/helios-user-guide0400250/helios-user-guide0400250/fluidigm%3Afile. Published 2018. Accessed September 16, 2020.

347. Maecker HT, Harari A. Immune monitoring technology primer: flow and mass cytometry. *J Immunother Cancer*. 2015;3(1):44. doi:10.1186/s40425-015-0085-x

348. Rao DA, Gurish MF, Marshall JL, et al. Pathologically expanded peripheral T helper cell subset drives B cells in rheumatoid arthritis. *Nature*. 2017;542(7639):110-114. doi:10.1038/nature20810

349. Fluidigm. Human Immune Monitoring. https://www.fluidigm.com/articles/him. Published 2018. Accessed September 16, 2020.

350. Fluidigm. Cell-ID 20-Plex Pd Barcoding Kit. https://www.fluidigm.com/binaries/content/documents/fluidigm/search/hippo%3Aresultset/cell-id-20-plex-pd-barcoding-kit-ug-prd023/fluidigm%3Afile. Published 2019. Accessed September 16, 2020.

351. Van Gassen S, Gaudilliere B, Angst MS, Saeys Y, Aghaeepour N. CytoNorm: A Normalization Algorithm for Cytometry Data. *Cytom Part A*. 2020;97(3):268-278. doi:10.1002/cyto.a.23904

352. Ansari B, Etemadifar M, Najafi M, Nasri M, Meamar R. Neuronal autoantibodies in focal epilepsy with or without mesial temporal sclerosis. *Iran J Neurol*. 2019;18(1):13-18. http://www.ncbi.nlm.nih.gov/pubmed/31316731.

353. Bien CG, Urbach H, Schramm J, et al. Limbic encephalitis as a precipitating event in adult-onset temporal lobe epilepsy. *Neurology*. 2007;69(12):1236-1244. doi:10.1212/01.wnl.0000276946.08412.ef

354. Tecellioglu M, Kamisli O, Kamisli S, Yucel FE, Ozcan C. Neurological autoantibodies in drug-resistant epilepsy of unknown cause. *Irish J Med Sci (1971 -)*. March 2018. doi:10.1007/s11845-018-1777-2

355. Marin GG, Cardiel MH, Cornejo H, Viveros ME. Prevalence of Antinuclear Antibodies in 3 Groups of Healthy Individuals. *JCR J Clin Rheumatol*. 2009;15(7):325-329. doi:10.1097/RHU.0b013e3181bb971b

356. Abeles AM, Abeles M. The Clinical Utility of a Positive Antinuclear Antibody Test Result. *Am J Med*. 2013;126(4):342-348. doi:10.1016/j.amjmed.2012.09.014

357. Lacroix-Desmazes S, Kaveri S V, Mouthon L, et al. Self-reactive antibodies (natural autoantibodies) in healthy individuals. *J Immunol Methods*. 1998;216(1-2):117-137. doi:10.1016/S0022-1759(98)00074-X

358. Vincent A, Crino PB. Systemic and neurologic autoimmune disorders associated with seizures or epilepsy. *Epilepsia*. 2011;52(SUPPL. 3):12-17. doi:10.1111/j.1528-1167.2011.03030.x

359. Ranua J, Luoma K, Peltola J, et al. Anticardiolipin and antinuclear antibodies in epilepsy—a population-based cross-sectional study. *Epilepsy Res*. 2004;58(1):13-18. doi:10.1016/j.eplepsyres.2003.12.004

360. Zelano J, Axelsson M, Constantinescu R, Malmeström C, Kumlien E. Neuronal antibodies in adult patients with new-onset seizures: A prospective study. *Brain Behav*. 2019;9(11). doi:10.1002/brb3.1442

361. McKnight K, Jiang Y, Hart Y, et al. Serum antibodies in epilepsy and seizure-associated disorders. *Neurology*. 2005;65(11):1730-1736. doi:10.1212/01.wnl.0000187129.66353.13

362. Waldmann TA. Disorders of Immunoglobulin Metabolism. Sherwood LM, Parris EE, eds. *N Engl J Med*. 1969;281(21):1170-1177. doi:10.1056/NEJM196911202812107

363. Wilson R, Makuch M, Kienzler A-K, et al. Condition-dependent generation of aquaporin-4 antibodies from circulating B cells in neuromyelitis optica. *Brain*. 2018;141(4):1063-1074. doi:10.1093/brain/awy010

364. Berridge G, Menassa DA, Moloney T, et al. Glutamate receptor **δ**2 serum antibodies in pediatric opsoclonus myoclonus ataxia syndrome. *Neurology*. 2018;91(8):e714-e723. doi:10.1212/WNL.0000000000006035

365. Dubey D, Pittock SJ, McKeon A. Antibody Prevalence in Epilepsy and Encephalopathy score: Increased specificity and applicability. *Epilepsia*. 2019;60(2):367-369. doi:10.1111/epi.14649

366. Belbezier A, Joubert B, Montero-Martin G, et al. Multiplex family with GAD65-Abs neurologic syndromes. *Neurol Neuroimmunol NeuroInflammation*. 2018;5(1):1-5. doi:10.1212/NXI.0000000000000416

367. Falip M, Rodriguez-Bel L, Castañer S, et al. Musicogenic reflex seizures in epilepsy with glutamic acid decarbocylase antibodies. *Acta Neurol Scand*. 2018;137(2):272-276. doi:10.1111/ane.12799

368. Altan-Bonnet G, Mukherjee R. Cytokine-mediated communication: a quantitative appraisal of immune complexity. *Nat Rev Immunol*. 2019;19(4):205-217. doi:10.1038/s41577-019-0131-x

369. Bartee E, McFadden G. Cytokine synergy: An underappreciated contributor to innate anti-viral immunity. *Cytokine*. 2013;63(3):237-240. doi:10.1016/j.cyto.2013.04.036

370. Ozaki K, Leonard WJ. Cytokine and Cytokine Receptor Pleiotropy and Redundancy. *J Biol Chem*. 2002;277(33):29355-29358. doi:10.1074/jbc.R200003200

371. Holbrook J, Lara-Reyna S, Jarosz-Griffiths H, McDermott MF. Tumour necrosis factor signalling in health and disease. *F1000Research*. 2019;8:111. doi:10.12688/f1000research.17023.1

372. Vazquez MI, Catalan-Dibene J, Zlotnik A. B cells responses and cytokine production are regulated by their immune microenvironment. *Cytokine*. 2015;74(2):318-326. doi:10.1016/j.cyto.2015.02.007

373. Raphael I, Nalawade S, Eagar TN, Forsthuber TG. T cell subsets and their signature cytokines in autoimmune and inflammatory diseases. *Cytokine*. 2015;74(1):5-17. doi:10.1016/j.cyto.2014.09.011

374. Moens L, Tangye SG. Cytokine-Mediated Regulation of Plasma Cell Generation: IL-21 Takes Center Stage. *Front Immunol*. 2014;5. doi:10.3389/fimmu.2014.00065

375. Martinez-Sanchez ME, Huerta L, Alvarez-Buylla ER, Villarreal Luján C. Role of Cytokine Combinations on CD4+ T Cell Differentiation, Partial Polarization, and Plasticity: Continuous Network Modeling Approach. *Front Physiol*. 2018;9. doi:10.3389/fphys.2018.00877

376. Jabri B, Abadie V. IL-15 functions as a danger signal to regulate tissue-resident T cells and tissue destruction. *Nat Rev Immunol*. 2015;15(12):771-783. doi:10.1038/nri3919

377. Saraiva M, O'Garra A. The regulation of IL-10 production by immune cells. *Nat Rev Immunol*. 2010;10(3):170-181. doi:10.1038/nri2711

378. Pacifici R, Paris L, Carlo S, Bacosi A, Pichini S, Zuccaro P. Cytokine Production in Blood Mononuclear Cells from Epileptic Patients. *Epilepsia*. 1995;36(4):384-387. doi:10.1111/j.1528-1157.1995.tb01013.x

379. Mao L-Y, Ding J, Peng W-F, et al. Interictal interleukin-17A levels are elevated and correlate with seizure severity of epilepsy patients. *Epilepsia*. 2013;54(9):e142-e145. doi:10.1111/epi.12337

380. Cavalli G, Dinarello CA. Treating rheumatological diseases and co-morbidities with interleukin-1 blocking therapies. *Rheumatology*. July 2015:kev269. doi:10.1093/rheumatology/kev269

381. Kau AL, Korenblat PE. Anti-interleukin 4 and 13 for asthma treatment in the era of

endotypes. *Curr Opin Allergy Clin Immunol*. 2014;14(6):570-575. doi:10.1097/ACI.0000000000000108

382. Mitoma H, Horiuchi T, Tsukamoto H, Ueda N. Molecular mechanisms of action of anti-TNF-**α** agents – Comparison among therapeutic TNF-**α** antagonists. *Cytokine*. 2018;101:56-63. doi:10.1016/j.cyto.2016.08.014

383. Rivas JR, Liu Y, Alhakeem SS, et al. Interleukin-10 suppression enhances T-cell antitumor immunity and responses to checkpoint blockade in chronic lymphocytic leukemia. *Leukemia*. March 2021. doi:10.1038/s41375-021-01217-1

384. Zhao L, Hu B, Zhang Y, et al. An activation-induced IL-15 isoform is a natural antagonist for IL-15 function. *Sci Rep*. 2016;6(1):25822. doi:10.1038/srep25822

385. Mochol M, Taubøll E, Aukrust P, Ueland T, Andreassen OA, Svalheim S. Interleukin 18 (IL-18) and its binding protein (IL-18BP) are increased in patients with epilepsy suggesting low-grade systemic inflammation. *Seizure*. 2020;80:221-225. doi:10.1016/j.seizure.2020.05.018

386. Basnyat P, Pesu M, Söderqvist M, et al. Chronically reduced IL-10 plasma levels are associated with hippocampal sclerosis in temporal lobe epilepsy patients. *BMC Neurol*. 2020;20(1):241. doi:10.1186/s12883-020-01825-x

387. Nowak M, Bauer S, Haag A, et al. Interictal alterations of cytokines and leukocytes in patients with active epilepsy. *Brain Behav Immun*. 2011;25(3):423-428. doi:10.1016/j.bbi.2010.10.022

388. Hulkkonen J, Koskikallio E, Rainesalo S, Keränen T, Hurme M, Peltola J. The balance of inhibitory and excitatory cytokines is differently regulated in vivo and in vitro among therapy resistant epilepsy patients. *Epilepsy Res*. 2004;59(2-3):199-205. doi:10.1016/j.eplepsyres.2004.04.007

389. Berzero G, Psimaras D. Neurological paraneoplastic syndromes: an update. *Curr Opin Oncol*. 2018;30(6):359-367. doi:10.1097/CCO.0000000000000479

390. Geng G, Yu X, Jiang J, Yu X. Aetiology and pathogenesis of paraneoplastic autoimmune disorders. *Autoimmun Rev*. 2020;19(1):102422. doi:10.1016/j.autrev.2019.102422

391. Pignolet BS, Gebauer CM, Liblau RS. Immunopathogenesis of paraneoplastic neurological syndromes associated with anti-Hu antibodies. *Oncoimmunology*. 2013;2(12):e27384. doi:10.4161/onci.27384

392. Voltz R, Dalmau J, Posner JB, Rosenfeld MR. T-cell receptor analysis in anti-Hu associated paraneoplastic encephalomyelitis. *Neurology*. 1998;51(4):1146-1150. doi:10.1212/WNL.51.4.1146

393. Vieira ÉLM, de Oliveira GNM, Lessa JMK, et al. Peripheral leukocyte profile in people with temporal lobe epilepsy reflects the associated proinflammatory state. *Brain Behav Immun*. 2016;53:123-130. doi:10.1016/j.bbi.2015.11.016

394. Beniczky S, Arbune AA, Jeppesen J, Ryvlin P. Biomarkers of seizure severity derived from wearable devices. *Epilepsia*. June 2020:epi.16492. doi:10.1111/epi.16492

395. Fisher RS, Afra P, Macken M, et al. Automatic Vagus Nerve Stimulation Triggered by Ictal Tachycardia: Clinical Outcomes and Device Performance—The U.S. E-37 Trial. *Neuromodulation Technol Neural Interface*. 2016;19(2):188-195. doi:10.1111/ner.12376

396. Zhao X, Lhatoo SD. Seizure detection: do current devices work? And when can they be useful? *Curr Neurol Neurosci Rep*. 2018;18(7):40. doi:10.1007/s11910-018-0849-z

397. Kurada A V., Srinivasan T, Hammond S, Ulate-Campos A, Bidwell J. Seizure detection devices for use in antiseizure medication clinical trials: A systematic review. *Seizure*. 2019;66:61-69. doi:10.1016/j.seizure.2019.02.007

398. Brown LM, Clark JW, Neuland CY, et al. Cryopreservation and long-term liquid nitrogen storage of peripheral blood mononuclear cells for flow cytometry analysis effects on cell subset proportions and fluorescence intensity. *J Clin Lab Anal*. 1991;5(4):255-261. doi:10.1002/jcla.1860050406

399. Valeri C, Pivacek L. Effects of the temperature, the duration of frozen storage, and the freezing container on in vitro measurements in human peripheral blood mononuclear cells. *Transfusion*. 1996;36(4):303-308. doi:10.1046/j.1537-2995.1996.36496226141.x

400. Havenar-Daughton C, Lindqvist M, Heit A, et al. CXCL13 is a plasma biomarker of germinal center activity. *Proc Natl Acad Sci*. 2016;113(10):2702-2707. doi:10.1073/pnas.1520112113

401. Ravizza T, Terrone G, Salamone A, et al. High Mobility Group Box 1 is a novel pathogenic factor and a mechanistic biomarker for epilepsy. *Brain Behav Immun*. 2018;72:14-21. doi:10.1016/j.bbi.2017.10.008

402. Bagwell CB, Inokuma M, Hunsberger B, et al. Automated Data Cleanup for Mass Cytometry. *Cytom Part A*. 2020;97(2):184-198. doi:10.1002/cyto.a.23926

403. Ogishi M, Yang R, Gruber C, et al. Multibatch Cytometry Data Integration for Optimal Immunophenotyping. *J Immunol*. 2021;206(1):206-213. doi:10.4049/jimmunol.2000854

404. Pettingill P, Kramer HB, Coebergh JA, et al. Antibodies to GABAA receptor alpha1 and gamma2 subunits: clinical and serologic characterization. *Neurology*. 2015;84(12):1233-1241. doi:10.1212/WNL.0000000000001326

405. Binks S, Varley J, Lee W, et al. Distinct HLA associations of LGI1 and CASPR2-antibody diseases. *Brain*. 2018;141(8):2263-2271. doi:10.1093/brain/awy109

406. Kopczynska M, Zelek WM, Vespa S, et al. Complement system biomarkers in epilepsy. *Seizure*. 2018;60:1-7. doi:10.1016/j.seizure.2018.05.016

407. Bonaz B, Sinniger V, Hoffmann D, et al. Chronic vagus nerve stimulation in Crohn's disease: a 6-month follow-up pilot study. *Neurogastroenterol Motil*. 2016;28(6):948-953. doi:10.1111/nmo.12792

408. Koopman FA, Chavan SS, Miljko S, et al. Vagus nerve stimulation inhibits cytokine production and attenuates disease severity in rheumatoid arthritis. *Proc Natl Acad Sci*. 2016;113(29):8284-8289. doi:10.1073/pnas.1605635113

409. Toffa DH, Touma L, El Meskine T, Bouthillier A, Nguyen DK. Learnings from 30 years of reported efficacy and safety of vagus nerve stimulation (VNS) for epilepsy treatment: A critical review. *Seizure*. 2020;83:104-123. doi:10.1016/j.seizure.2020.09.027